ABSTRACT

MORRIS, AMANDA JEAN. Phosphate Binding to Fe and Al in Organic Matter as Affected by Redox Potential and pH. (Under the direction of Dr. Dean L. Hesterberg.)

Mobilization of phosphorus from land to surface waters frequently results in the nutrient enrichment of aquatic ecosystems, which leads to enhanced primary productivity and water quality degradation. Mobilization of inorganic orthophosphate (PO_4) in soils depends on pH, redox potential, dissolved organic carbon (DOC), and concentrations and forms of accessible Fe and Al. Because the roles of these parameters on PO_4 retention in soil organic matter (OM) are largely undefined, my goal was to identify and quantify their roles on PO_4 retention in soil OM. My research objectives were to: 1. Determine the molecular coordination environment of Fe(III) bound to OM by direct addition of Fe(III), and addition of Fe(II) followed by oxidation, 2. Identify and separate pH and DOC effects on PO_4 retention by OM, 3. Model the relative effects of pH and DOC on PO_4 retention by OM, 4. Determine the impact of different peat/metal ratios on the microbial reduction rate of Fe(III) bound to peat, and 5. Determine the impacts of bound Fe and Al proportions on mobilization rates of PO_4 from OM. Phosphate sorption may vary with the molecular bonding environment of Fe(III) in seasonally inundated organic soils.

In Pahokee peat with 1200 mmol Fe kg^{-1} peat, extended X-Ray absorption fine structure (EXAFS) spectroscopy indicated the presence of mixed Fe species ranging from mononuclear Fe-NOM to polymeric Fe(III) clusters. The bonding environment of Fe(III) and the PO_4 sorption capacity of Fe(III) bound to OM were indistinguishable between samples where Fe(III) was added directly (as Fe_3Cl), and where Fe(II) (as Fe_2Cl) was added followed by an oxidation period of 39 h. The pH dependent sorption of PO_4 to OM was characterized

by envelopes analogous to adsorption envelopes for Fe- and Al-oxide minerals, with maximum PO_4 sorption of 420 and 380 mmol PO_4 kg^{-1} peat in Fe and Al systems, respectively. At pH 6.0, dissolved PO_4 increased at a rate of 0.36 µmol PO_4 mg^{-1} DOC, suggesting that although pH dominantly controlled PO_4 sorption, DOC also played a role. The resultant PO_4 sorption to Fe-OM was successfully modeled using a surface complexation model in Visual MINTEQ. No trends in Fe(III) reduction rates were observed as OM concentrations were increased from 0 to 3,330 g OM mol^{-1} Fe. However, as peat increased from 0 to 833 g OM mol^{-1} Fe, the proportion of dissolved Fe(II) to bound Fe(II) decreased, and as peat increased from 833 to 3,330 g OM mol^{-1}, the proportion of dissolved Fe(II) to bound Fe(II) increased. Phosphate mobilization from organic matter was also correlated with Fe(III) reduction ($P< 0.001$), and the Pseudo first-order rate coefficients of PO_4 dissolution increased as Fe/Al ratio increased. Overall, PO_4 sorption to OM occurred, and was dominantly controlled by pH. Results suggested that maintaining organic soils between pH 4.0 and 5.0 would maximize PO_4 sorption in aerobic organic soils. At any given pH, PO_4 sorption was influenced by bound Fe and Al, DOC, and redox state. Iron(III) reduction was closely tied to PO_4 mobilization, and the mobility of Fe(II) depended on total bound Fe(III) concentration. Maximum PO_4 mobilized during Fe(III) reduction decreased as bound Al(III) increased, suggesting Al addition would enhance PO_4 sorption to organic soils. Overall, the interdependent roles of pH, redox potential, DOC, and bound Fe and Al controlled PO_4 sorption to Fe- and Al- bound to OM.

Phosphate Binding to Fe and Al in Organic Matter as Affected by Redox Potential and pH

by
Amanda J. Morris

A dissertation submitted to the Graduate Faculty of
North Carolina State University
in partial fulfillment of the
requirements for the degree of
Doctor of Philosophy

Soil Science

Raleigh, North Carolina

2011

APPROVED BY:

Dean Hesterberg Chair of Advisory Committee	Owen Duckworth
Wei Shi	James D. Martin

DEDICATION

"Study nature, love nature, stay close to nature. It will never fail you."

- Frank Lloyd Wright

I dedicate this work to my husband Perry. Without his humor, understanding, and constant support, I would not be here today. Undoubtedly, the past four years have been the best in my life as we have started ours together. Furthermore, I dedicate this work to my family for encouraging me to aim high, work hard, and never give up. All of you have been supportive toward my education despite your desires for me to be closer to home. Lastly, I dedicate this work to my grade school teachers Mrs. Nancy Schaefer and Mrs. Charlotte Pestka. Both instilled in me a curiosity and passion for learning that has grown stronger with time. The lessons they taught me early in life have helped to shape the person that I have become today.

BIOGRAPHY

Amanda Jean Morris, daughter of Robert and Mary Zelasko, grew up on a small family farm near DuBois Illinois. At an early age, helping out on the farm sparked her interest in soil science. In Amanda's youth she enjoyed riding in the combine during harvest season, working on her tan while mowing grass or spreading fertilizer on fields, climbing trees, riding her bike, walking through the woods, riding four-wheelers, swimming, reading books, playing with her dog Shadow and her cat Blacky, and most of all walking to grandmas to visit.

In high school, Amanda was active in the FFA, in which she won numerous awards and proudly served as section 24 president in 2001-2002. She was the most improved senior band member in which she played the French Horn, and was also a member of the varsity volleyball team. She decided that she wanted to study agriculture to help local farmers maximize their productivity while minimizing environmental degradation. Amanda was awarded several scholarships, which allowed her to follow her dream to study soil science at Southern Illinois University in Carbondale. She obtained her B.S. degree in Plant and Soil Science in May 2005.

Amanda became interested in wetlands during a wetland ecology course at SIUC, and decided to pursue her MS degree in soil science at North Carolina State University in 2005, where she studied the impacts of soil properties on Fe(III) reduction rates. During her M.S., Amanda developed her research abilities, and decided to pursue a Ph.D. in soil chemistry. Amanda's life-long goal is to contribute to the advancement of science in order to protect and preserve the natural environment for the enjoyment of future generations.

ACKNOWLEDGMENTS

Funding was provided by USDA –NRI Grant No. 2005-35107-16253 and the North Carolina State University Department of Soil Science. Sincere thanks to Dr. Dean Hesterberg who provided me with guidance throughout my research. I will always remember the patience, positive attitude and energetic enthusiasm for research and teaching that he exhibited. Further thanks to Drs. Wei Shi, Owen Duckworth, and Jim Martin for their valuable advice and contributions to my research. Thank you to Dr. Torbjoern Karlsson for advice regarding Wavelet Transform, and Jon Petter Gustafsson for advice regarding the use of a surface sorption model to model PO_4 sorption to Fe and Al bound to OM. Additionally, this work would not have been possible without the advice and company of my associates Fiona Kizewski, and Yu-Ting Liu. A special thanks goes to Kim Hutchison for answering multiple questions throughout my work and allowing me to use her previously collected peat titration data. Lastly, my work would not have been possible without the encouragement and guidance of faculty, staff and fellow students at NCSU. I have enjoyed my time at NCSU and hope to work together with many of them in the future.

TABLE OF CONTENTS

LIST OF TABLES

LIST OF FIGURES

LIST OF ABBREVIATIONS

Atomic absorption spectrometry (AAS); bidentate (BD); bidentate-bridging (BD-BG); dissolved organic carbon (DOC); dissolved organic matter (DOM); extended X-ray absorption fine structure (EXAFS); fourier transform infrared spectroscopy (FTIR); humic acid (HA); inductively coupled plasma spectroscopy optical emission spectrometry (ICP-OES); molecular weight cut-off (MWC); organic carbon (OC), organic matter (OM); unidentate (UD); wavelet transform (WT); X-ray absorption near structure (XANES)

CHAPTER 1: INTRODUCTION

Environmental Problem - Eutrophication

In freshwaters systems, phosphorus concentrations exceeding 0.05 mg L^{-1} often lead to eutrophication, which is the process of nutrient enrichment that leads to enhanced primary productivity and degradation of water quality (Hinesly and Jones, 1990; Khan and Ansari, 2005). Although nutrient enrichment can occur naturally, humans strongly influence almost every major aquatic ecosystem, and their activities have dramatically altered the fluxes of growth-limiting nutrients from land to receiving waters (Smith, 2003). For example, von Gunten et al. (2009) analyzed lake sediments and found that increases in primary productivity and resulting eutrophication in several Chilean lakes occurred after 1980, which corresponded to increased anthropogenic nutrient inputs. Most water bodies are oligotrophic (nutrient poor), and are projected to require thousands of years to become eutrophic (nutrient rich) under natural conditions (Khan and Ansari, 2005).

Land-use models have identified agriculture as a leading source of excess P and N in surface waters, accounting for 56% of the pollution load into the Neuse River estuary, and 76% into the Tar-Pamlico River in North Carolina (Marks and Knuffke, 1998). In 2008, North Carolina produced 19% of the nation's pork and was the second leading state in swine production (National Pork Producers Council 2008a, 2008b). Associated with the large scale production of swine and other livestock is the large scale use of animal wastes rich in P as agricultural fertilizer. Sorption of P in soils minimizes P movement through the soil matrix, however, dissolution of P and transport to open water bodies potentially leads to

eutrophication. In addition, increasing soil temperatures often result in the acceleration of chemical and microbial reactions that lead to soil reduction under water-saturated conditions (Vaughan et al., 2009), which often increases the dissolution and mobilization of PO_4 (Ajmone-Marsan et al., 2006; Ann et al., 2000; Holford and Patrick, 1979; Macrae et al., 2005; Newman and Pietro, 2001; Sposito, 1989). Mobilization is used to refer to any chemical or physical mechanism resulting in PO_4 transitioning from the solid to solution phase, while dissolution specifically refers to the solubilization of PO_4 precipitates (Reddy et al., 2005). Rising temperatures can also enhance breakdown of soil organic matter (SOM), potentially mobilizing organic phosphorus, which represents > 40% of the total soil P (Pant, 2007). Thus, global climate change could enhance PO_4 mobilization and transport into open water bodies.

Despite our current knowledge and the use of management techniques (such as riparian buffers) that decrease PO_4 inputs into open water bodies, additional knowledge is needed in order to strengthen management techniques to prevent eutrophication. Determining and quantifying the mechanisms of PO_4 mobilization from soils is needed to build a framework for accurately modeling PO_4 mobilization from soils ranging in chemical properties. With accurate models, the management techniques used to prevent dissolution and transport into open water bodies can be tailored to fit specific environmental conditions.

Wetlands and PO_4 Retention

Phosphorous retention has traditionally been considered one of the most important attributes of natural and constructed wetlands, particularly those that receive non-point source pollution or wastewater (Mitsch and Gosselink, 2000). Hence, characterization of PO_4

sorption in soils is of great importance from both agronomic and environmental perspectives (Brand-Klibanski et al., 2007). In North Carolina, wetlands and deepwater habitats total an estimated 7,440 acres (NRCS, 2004). Nationally, between 1997 and 2001 there was an estimated annual net gain of 33,000 acres of wetland resulting from restoration of agricultural lands (NRCS, 2004). This conversion of previously fertilized land to wetlands often leads to the mobilization and movement of PO_4 to open water bodies (Dangelo and Reddy, 1994; Olila and Reddy, 1997; Zak et al., 2008). For example, Zak et al. (2008) observed net P mobilization rates as high as 1288 μmol m^{-2} day^{-1} in rewetted fens that had been drained for agricultural use. Clearly, the mobilization of PO_4 from restored wetlands poses a threat to environmental quality. A comprehensive understanding of PO_4 mobilization mechanisms in saturated soils would aid in predicting and preventing the transport of PO_4 to open water bodies.

Mechanisms of PO_4 Dissolution

Phosphorus mobilization from soils depends in part on the amount and form of Fe- and Al- oxides and organic matter (OM), and has previously been correlated to soil redox potential, dissolution of Fe(III)-oxides, dissolved organic carbon, and various indices of acid ammonium oxalate Fe- and Al-oxide extractions (Holford and Patrick, 1981; Hutchison and Hesterberg, 2004; Patrick and Khalid, 1974; Phillips, 1998; Sallade and Sims, 1997). Proposed mobilization mechanisms are depicted in Figure 1.1 and include: (1) erosion, (2) the co-dissolution of PO_4 bound to Fe(III) as Fe(III) is reduced during anaerobic soil conditions, (3) mineralization of organic P, (4) increasing pH causing increased PO_4 mobilization, (5) competitive sorption of DOC with PO_4, and (6) formation of either PO_4-

Fe/Al or ternary PO_4 – Fe/Al – DOM colloids > 0.2 µm (Hutchison and Hesterberg, 2004; Patrick and Khalid, 1974; Patrick, 1974; Roden and Edmonds, 1997). Historically, the majority of PO_4 mobilization from saturated soils has been hypothesized to occur through the soil erosion, organic P mineralization, and the co-dissolution of Fe(III) and PO_4.

Microbial Reduction of Fe(III) and PO_4 dissolution

When soils are water saturated for extended periods, anaerobic conditions develop as O_2 becomes depleted during the microbial oxidation of OM, and alternative electron acceptors such as NO_3^-, Mn(IV), Fe(III), and SO_4^{2-} are used. Because of the binding affinity of PO_4 to Fe(III), reduction of Fe(III) to Fe(II) can lead to PO_4 mobilization and transport through groundwater into nearby water sources, resulting in water quality degradation. In fact, several studies have indicated that when soils undergo water saturated anaerobic conditions, the dissolved phosphorus concentration in the pore water increases (Ajmone-Marsan et al., 2006; Ann et al., 2000; Holford and Patrick, 1979; Macrae et al., 2005; Newman and Pietro, 2001).

The presence of Fe(II) in anoxic and sub-oxic environments is typically attributed to the activity of dissimilatory iron reducing bacteria (DIRB) and Archaea, a diverse group of microorganisms that are able to couple the oxidation of organic compounds or molecular hydrogen to the reduction of Fe(III) to Fe(II) (O'Loughlin et al., 2007). Microbial reduction of Fe(III) oxides is expected to be influenced by PO_4, organic ligands, and reactions that alter the speciation of Fe(III) (Fredrickson et al., 2003; Fredrickson et al., 1998; Roden, 2003). *Shewanella putrefaciens* species have been widely used in Fe(III) reduction experiments as a representative of bacterial Fe(III) reduction, although their metabolism is expected to be a

minor pathway for carbon and electron flow in Fe(III) reducing soil environments (Lovley, 1993),. *Shewanella* species are a phylogenetically diverse group of bacteria that have been isolated from a wide range of aquatic and terrestrial environments and exhibit a broad versatility regarding anaerobic respiration (Bowman, 2005; O'Loughlin et al., 2007). *Shewanella putrefaciens* is a facultative anaerobe of terrestrial origin capable of coupling the oxidation of a variety of organic compounds (including formate, lactate, and pyruvate) to Fe(III) and Mn(IV) reduction (Lovley, 1991).

Repetitions of reduction oxidation cycles have been shown to alter soil Fe minerals, which potentially impacts P sorption and mobilization. Although most research has found that Fe-oxide crystallinity decreases when subjected to several redox cycles, recent research has also indicated increasing crystallinity with consecutive cycles (Thompson et al., 2006). Research by Hansel et al. (2004) showed that the reactions of Fe(II) with ferrihydrite in a carefully controlled anaerobic setting formed goethite, lepidocrocite, and magnetite, and were dependent on concentration of Fe(II) and ligand type (Cl, SO_4, CO_3). Continued microbial reduction of Fe(III) substrates is impeded by Fe(II) complexation to bacterial and/or oxide surfaces (Roden and Wetzel, 1999; Roden and Urrutia, 2002; Royer et al., 2002; Urrutia et al., 1999), which can affect secondary mineralization (Hansel et al., 2004). For example, the type of Fe-oxides formed at pH 6.0 has been shown to vary with citrate/Fe(II) ratio, with predominantly goethite and maghemite being formed at a ratio of 0, and lepidocrocite and/or X-ray amorphous oxides being formed at ratios of 0.001, 0.01, and 0.1 (Liu and Huang, 2000).

Binding Mechanisms of PO_4 to OM

Organic matter tends to accumulate in poorly-drained soils, and dissolved organic matter (DOM) serves as an energy source for microbial reduction of NO_3^-, Mn-oxides, Fe-oxides, and SO_4^{2-}. In order to fully understand PO_4 binding and mobilization from OM, the molecular environment of Fe and Al bound in OM needs to be determined. Detachment of Fe(II) from Fe(III) minerals can occur following the exchange of electrons from a reductant to a surface Fe(III) center, and can be accelerated in the presence of surface complexing agents such as oxalate, citrate, or salicylate (Stumm, 1993; Sulzberger et al., 1989). Once in solution, organic acids such as citrate and salicylate have been shown to increase Fe(II) oxidation rates (Pham and Waite, 2008). Iron(III) and Fe(II) can remain in mineral or plant residues, become dissolved and form new Fe minerals, sorb to OM or minerals, be taken up by organisms, or be leached from the soil (Lovley, 1991; Lovley, 1993; Stevenson and Fitch, 1986; Weiss et al., 2004). Given that Fe dissolution occurs from minerals by surface protonation (at low pH), complexometric dissolution by organic ligands, or reductive dissolution (Sulzberger et al., 1989), it stands to reason that Fe can be incorporated into OM as either Fe(III) or Fe(II).

Experimental evidence suggests that in OM the binding of inorganic PO_4 involves Fe(III) and Al(III) as bridging cations (ternary complexes) (Bloom, 1981; Gerke, 1992b; Hermann and Gerke, 1992; Gerke, 2010). Ultrafiltration of soil solution through 20,000 Da membranes decreased organic carbon, iron, aluminum and inorganic phosphorus concentrations by as much as 50% at pH 5.5 and as much as 10% at pH 3.5 in solution, potentially indicating the existence of ternary complexes in solution (Gerke, 1992b).

Furthermore, Gerke (1997) showed that Fe- and Al- organic complexes are important in rhizosphere soils and increased with increasing pH. Hutchison and Hesterberg (2004) observed an increase in dissolved PO_4 with increasing DOC, which suggested that the formation of ternary P-Fe-OM and P-Al-OM complexes and competitive sorption were possible mechanisms. In addition, Guardado et al. (2008) found that PO_4-Fe/Al-humic acid (HA) complexes could play an important role in the dynamics of phosphorus in certain soils, and found that the binding affinity of PO_4 to Fe and Al bound in HA were similar. Recent work compiled by Gerke (2010) suggested that more than 50% of the dissolved P in natural waters is typically associated with humics, mainly through Al and Fe bridging, and that humic substances in soils increased the plant availability of P.

The form of Fe-oxide minerals in soils can also alter the mobilization of PO_4 from soils and transport into water bodies. The thermodynamic stability of Fe-oxides is a function of crystal structure and particle size, and generally increases from ferrihydrite to goethite to hematite (Cornell and Schwertmann, 1993; Hansel et al., 2004). More recently, the thermodynamic properties of Fe-oxides were found to have only a secondary control on Fe(III) reduction rates by *Shewanella putrefaciens* (CN32), with surface area being the primary control of reduction rates (Roden, 2003). In addition, Neal et al. (2005) suggested that the electrostatic interactions between S*hewanella oneidensis* and Fe-oxides depend on the oxide surface, and should be considered when comparing reactivity of different iron oxides towards dissimilatory iron reduction. For example, total Fe(III) reduction was higher for ferrihydrite than for goethite or hematite in a study by Hansel et al. (2004). Because of its high surface area and intrinsic reactivity, ferrihydrite serves as a dominant sink for numerous

metals and nutrients, including P (Hansel et al., 2004). Because Fe(III)-(hydr)oxides account for a large portion of PO_4 sorption in soils, their intrinsic reactivity could directly impact the mobilization of PO_4 from soils during Fe(III) reduction.

Organic Matter impacts on PO_4 sorption to Fe- and Al- (hydr)oxide minerals

The influence of soil OM on PO_4 sorption in mineral soils has been studied extensively, whether by the use of bulk OM, OM fractions, or specific organic compounds used to model OM (Bhatti et al., 1998; Borggaard et al., 1990; Borggaard et al., 2005; Easterwood and J.B. Sartain, 1990; Gerke, 1993b; Gjettermann et al., 2007; Guppy et al., 2005a; Hiemstra et al., 2010; Masscheleyn et al., 1992). Organic matter can modify PO_4 sorption in soils via several mechanisms; (1) binding of humics to Fe or Al surfaces, blocking P binding sites (Moshi et al., 1974); (2) inhibiting the crystallization of Fe- and Al-oxides (Schwertmann, 1966); and (3) enhancing Fe and Al mobilization by complexometric dissolution of bound Fe and Al (Gerke, 1993a). While mechanism 1 potentially decreases PO_4 sorption in soils, mechanisms 2 and 3 potentially increase PO_4 sorption. Humic substances bound to Fe- and Al-oxide surfaces can block PO_4 binding sites (Schwertmann, 1966), decreasing P sorption, and inhibit the crystallization of Fe- and Al-oxides (Schwertmann, 1966), leading to higher concentrations of poorly crystalline Fe-oxides that increase P sorption.

In addition, PO_4 and DOC can compete for sorption sites in soil. Macrae et al. (2005) found that dissolved PO_4 in an organic soil was more than two-fold greater than in a mineral soil. Several authors observed an increase in DOC following the addition of PO_4 to soil, and attributed this increase to competitive sorption of PO_4, which displaces DOC into solution

(Arbestain et al., 2002; Beck et al., 1999; Bhatti et al., 1998; Giesler et al., 2005; Kaiser and Zech, 1996). Conversely, ligand exchange between bound PO_4 and oxalate led to increased dissolved PO_4 in a Florida spodisol (Bhatti et al., 1998). Similarly, organic acids formed from the decomposition of clover were able to increase plant availability of PO_4 (Easterwood and Sartain, 1990). Arbestain et al. (2002) found that Fe and Al concentrations, along with organic C concentrations, explained PO_4 sorption to soils, and that DOC increased with increasing PO_4 sorption. Fulvic acid competition with PO_4 binding to goethite was greater than that of humic acid (HA), which was hypothesized to result from electrostatic interactions (Weng et al., 2008). Shuai and Zinati (2009) utilized Weng's (Weng et al., 2008) model and determined that the proposed electrostatic interactions did explain the sorption of PO_4 and HA on goethite. In contrast, increases in dissolved PO_4 from soils have been attributed to an underestimation of PO_4 mobilization from decomposition of OM (Guppy et al., 2005a; Guppy et al., 2005b). Despite past research detailing OM effects on PO_4 retention and mobilization in mineral soils, relative contributions of specific PO_4 mobilization mechanisms remain uncertain in organic soils.

Iron(III) Reduction and Dissolution Impacted by Organic Matter

Soil OM has also been shown to impact the microbial reduction rate of Fe(III) (Lovley et al., 1996; Zelasko, 2007), as well as Fe mobility (Rakshit et al., 2009; Royer et al., 2002), and Fe mineral formation (Cornell and Schwertmann, 1993). Organic matter potentially plays a role in microbial Fe(III) reduction by; (1) the enhancement of Fe(III) reduction by electron shuttling (Jiang and Kappler, 2008; Rakshit et al., 2009; Scott et al., 1998b), (2) altering the structure of Fe minerals by sorption, complexiметric dissolution, or

impeding crystallization (Cornell and Schwertmann, 1993), (3) serving as the electron donor (Fredrickson et al., 1998; Urrutia et al., 1998), and (4) influencing microbial activity (Paul and Clark, 1996). It is generally accepted that humic substances can serve as electron shuttles in environmentally important reduction processes that occur in soils and sediments, although the occurrence of these processes in the environment is still debatable (Jiang and Kappler, 2008; Kappler and Haderlein, 2003; Rakshit et al., 2009). Limiting the amount of electron donor (such as humic substances) in soils can inhibit microbial reduction of Fe(III) to Fe(II), in turn inhibiting the co-dissolution of PO_4 with Fe(II)

Reducing Capacity of OM

Natural organic matter (NOM) is known to be redox active and capable of reducing Mn(IV), NO_3^-, Fe(III), and SO_4^{2-} in soils. Certain anaerobic microorganisms (including *Shewanella putrefaciens*) can reduce OM, which can result in the reduction of Fe(III) coupled to OM oxidation (Kizewski, 2011; Lovley et al., 1996). Quinone moieties are known to be redox active (Scott et al., 1998a; Scott et al., 1998b); however, they are not the sole functional groups responsible for OM mediated Fe(III) reduction (Ratasuk and Nanny, 2007). The chemical composition and electron-carrying capacity of humic substances depends upon the source material and the environmental conditions under which it was produced (Lovley et al., 1996). Structural transformations during aging can lead to a decrease in the number of aliphatic and carboxylic functional groups in humic acids, and to an increased number of polyphenolic and quinine groups (Jerzykiewicz et al., 2002). Thus, the variability in OM with landscape position likely impacts Fe(III) reduction, which potentially impacts PO_4 mobilization.

Several organic acids and soil OM have been directly shown to participate in electron shuttling (Jiang and Kappler, 2008; Scott et al., 1998b), with resulting enhancement of Fe(III) reduction rates (Rakshit et al., 2009; Scott et al., 1998b). Various humic substances including International Humic Substances Society (IHSS) standards Leonardite, soil, and reference peat (Peretyazhko and Sposito, 2005), Elliot soil humic acid, Pahokee peat, and Suwannee River natural organic matter (Rakshit et al., 2009) have been characterized by their reducing capacity as an estimate of electron shuttling capacity. Reduction of Fe(III) has also been observed by reduced humic substances in aerobic environments (Jiang and Kappler, 2008; Kappler and Haderlein, 2003; Peretyazhko and Sposito, 2005). It has been hypothesized that these humic compounds contain reducing equivalents that are stable against oxidation with O_2, or that during incubation with Fe(III) compounds, the humic molecules change their 3-dimensional structure exposing reduced redox-active functional groups (Jiang and Kappler, 2008). Kizewski (2011) determined that organics served as a remote rather than direct electron shuttle, because the reduction of both organic functional groups and Fe(III) occurred simultaneously regardless of the potential for electron transfer from OM to Fe(III).

Mineralization of Soil Phosphorus

Phosphorus is an essential component of nucleic acids and many intermediary metabolites such as sugar phosphates and adenosine phosphates, which are an integral part of the metabolism of all life forms (Correll, 1998). Several studies have suggested that the initial flux of dissolved PO_4 following saturation of a soil results, in part, from mineralization of organic P (D'angelo and Reddy, 1994; Fellman and D'Amore, 2007 Noe, 2011). For

example, 65% of the variability in P mobilized in a restored marsh in central Florida was accounted for by relating dissolved inorganic PO_4 to dissolved inorganic carbon and CH_4 production, which are released during OM decomposition (D'angelo and Reddy, 1994). Phosphorus mineralization potentials calculated by monitoring changes in soil P ranged from 4 to 48 µg P kg $soil^{-1}$ day^{-1} in three wetland types (a bog, a forested wetland, and a riparian wetland), with no apparent dependency on wetland type (Fellman and D'Amore, 2007). Mineralization rates of 10 µmol P m^{-1} d^{-1} were observed in a floodplain soils in Virginia using a modified resin-core technique, and were 18 x greater than mineralization rates measured using the polyethylene bag method used by Fellman and D'Amore (2007) (Noa, 2011).

pH Effects on PO_4 Sorption

Other studies have looked at the pH dependency of PO_4 binding and dissolution in soils (Giesler et al., 2005; Borggaard et al., 2005; Gerke, 1993a; Gjettermann et al., 2007). Gjettermann et al. (2007) found that increasing pH resulted in decreased organic P and DOC sorption. Gerke (1993b) observed increased PO_4 sorption at pH 4.0, which was correlated with greater bound Fe. Giesler et al. (2005) showed pH dependency on PO_4 sorption to soil humus, with a maximum sorption at approximately pH 6.0. Overall, PO_4 sorption varies between organic soils and potentially depends on several variables, which include; (1) pH, (2) Fe and Al speciation and concentration, (3) OM content, (4) DOC concentration, and (5) redox potential.

Research Objectives

The goal of this research was to identify and quantify the roles of pH, redox potential, DOC, and bound Fe and Al on PO_4 sorption to organic soils. Determining, quantifying, and modeling the mechanisms of PO_4 binding and dissolution from soil OM could aid in reducing PO_4 inputs into open water bodies from soils, thus preventing further water quality degradation. Because PO_4 sorption in OM depends in part on Fe(III), the molecular binding environment of Fe(III) to OM could impact PO_4 sorption. Two mechanisms in which Fe(III) could bind to OM in soils are (1) the complexiметric dissolution of mineral phase Fe(III) with OM, and (2) the binding of Fe(II) to OM followed by oxidation. The first objective of this research was to determine the differences in the molecular coordination environment of Fe(III) bound to OM and resulting PO_4 sorption between OM in which Fe(III) was added directly as $FeCl_3$, and OM in which Fe(III) was added by addition of Fe(II) followed by oxidation.

To date, the impacts of pH, DOC, and bound metal concentration on PO_4 sorption to OM have not been observed separately. The second objective of this research was to determine the relative effects of pH and dissolved organic matter (DOC) on the retention of inorganic PO_4 by soil OM. My third objective was to model these relative effects on the retention of inorganic PO_4 by soil OM using Visual MINTEQ. Phosphate bound to Fe(III) in OM may also become mobilized in OM as Fe(III) becomes reduced to Fe(II). As such, the kinetics of Fe(III) reduction may impact PO_4 mobilization from OM. My fourth research objective was to determine the microbial reduction rate of Fe(III) bound to peat as impacted by the bound Fe(III) concentration. In addition, the specific roles that DOC, Fe(III), and Al

play in PO_4 dissolution from anaerobic organic soils remain unclear. Thus, my last objective was to determine the impact of the relative proportions of Fe and Al bound to OM on the mobilization of PO_4 from soil OM during microbial reduction. The experimental outcomes of these objectives will identify the roles of pH, redox potential, DOC, and Fe and Al speciation and concentration on PO_4 retention by soil OM.

BIBLIOGRAPHY

Ajmone-Marsan F., D. Cote, R.R. Simard. 2006. Phosphorus transformations under reduction in long-term manured soils. Plant Soil 282:239-250.

Arbestain M.C., M.E. Barreal, F. Macias. 2002. Phosphate and sulfate sorption in spodosols with albic horizon from Northern Spain. Soil Sci. Soc. Am. J. 66:464-473.

Beck M.A., W.P. Robarge, S.W. Buol. 1999. Phosphorus retention and release of anions and organic carbon by two Andisols. Eur. J. Soil. Sci. 50:157-164.

Bhatti J.S., N.B. Comerford, C.T. Johnston. 1998. Influence of oxalate and soil organic matter on sorption and desorption of phosphate onto a spodic horizon. Soil Sci. Soc. Am. J. 62:1089-1095.

Bloom P.R., 1981. Phosphorus adsorption by an aluminum-peat complex. Soil Sci. Soc. Am. J. 45:267-272.

Borggaard O.K., S.S. Jorgensen, J.P. Moberg, B. Rabenlange. 1990. Influence or organic-matter on phosphate adsorption by aluminum and iron-oxides in sandy soils. J. Soil. Sci. 41:443-449.

Borggaard O.K., B. Raben-Lange, A.L. Gimsing, B.W. Strobel. 2005. Influence of humic substances on phosphate adsorption by aluminium and iron oxides. Geoderma 127:270-279.

Bowman J.P., 2005. Genus XIII. Shewanella., in: N. R. K. D.J. Brenner, J.T. Stanley, and G.M. Garrity (Ed.), Bergey's manual of systematic bacteriology, Springer, NY.

Brand-Klibanski S., M.I. Litaor, M. Shenker. 2007. Overestimation of phosphorus adsorption capacity in reduced soils: An artifact of typical batch adsorption experiments. Soil Science Society of America Journal 71:1128-1136.

Cornell R.M., U. Schwertmann. 1993. The iron oxides: structure, properties, reactions, occurrence and uses VCH.

Correll D.L., 1998. The role of phosphorus in the eutrophication of receiving waters: A review. J. Environ. Qual. 27:261-266.

Dangelo E.M., K.R. Reddy. 1994. Diagenesis of organic-matter in a wetland recieving hypereutrophic lake water. 1. distribution of dissolved nutrients in the soil and water column. . Journal of Environmental Quality 23:928-936.

Easterwood G.W., J.B. Sartain. 1990. Clover residue effectivness in reducing orthophosphate sorption on ferric hydroxide coated soil. Soil Sci. Soc. Am. J. 54:1345-1350.

Fellman J.B., D.V. D'Amore. 2007. Nitrogen and phosphorus mineralization in three wetland types in Southeast Alaska, USA. Wetlands 27:44-53.

Fredrickson J.K., S. Kota, R.K. Kukkadapu, C.X. Liu, J.M. Zachara. 2003. Influence of electron donor/acceptor concentrations on hydrous ferric oxide (HFO) bioreduction. Biodegradation 14:91-103.

Fredrickson J.K., J.M. Zachara, D.W. Kennedy, H. Dong, T.C. Onstott, N.W. Hinman, S. Li. 1998. Biogenic iron mineralization accompanying the dissimilatory reduction of hydrous ferric oxide by a groundwater bacterium. Geochim. Cosmochim. Acta 62: 3239-3257.

Gerke J., 1992a. Orthophosphate and organic phosphate in the soil solution of 4 sand soil solution in relation to pH-evidence for humic-Fe-(Al-) phosphate complexes. Commun. Soil Sci. Plant Anal. 23:601-612.

Gerke J., 1992b. Phosphate, aluminum and iron in the soil solution of 3 different soils in relation to varying concentrations of citric-acid. Z. Pflanzenernahr. Bodenkd. 155: 339-343.

Gerke J., 1993a. Solubilization of Fe(III) from humic-Fe complexes, humic Fe-oxide mixtures and from poorly ordered Fe-oxide by organic-acids - consequences for P-adsorption. Z. Pflanzenernahr. Bodenkd. 156:253-257.

Gerke J., 1993b. Phosphate adsorption by humic/Fe-oxide mixtures aged at pH-4 and pH-7 and by poorly ordered Fe-oxide. Geoderma 59:279-288.

Gerke J., 1997. Aluminum and iron(III) species in the soil solution including organic complexes with citrate and humic substances. Z. Pflanzenernahr. Bodenkd. 160:427-432.

Gerke, J. 2010. Humic (Organic Matter)-Al(Fe)-Phosphate complexes: An underestimated phosphate form in soils and source of plant-available phosphate. Soil Sci. 175:417-425.

Gerke J., R. Hermann. 1992. Adsorption of orthophosphate to humic-Fe complexes and to amorphous Fe-oxide Z. Pflanzenernahr. Bodenkd. 15:233-236.

Giesler R., T. Andersson, L. Lovgren, P. Persson. 2005. Phosphate sorption in aluminum- and iron-rich humus soils. Soil Sci. Soc. Am. J. 69:77-86.

Gjettermann B., M. Styczen, S. Hansen, O.K. Borggaard, H.C.B. Hansen. 2007. Sorption and fractionation of dissolved organic matter and associated phosphorus in agricultural soil. J. Env. Qual. 36:753-763.

Guardado I., O. Urrutia, and J.M. Garcia-Mina. 2008. Some structural and electronic features of the interactions of phosphate with Metal-humic Complexes. J. Agric. Food. Chem. 56:1035-1042.

Guppy C.N., N.W. Menzies, P.W. Moody, F.P.C. Blamey. 2005a. Competitive sorption reactions between phosphorus and organic matter in soil: a review. Aust. J. Soil Res. 43:189-202.

Guppy C.N., N.W. Menzies, F.P.C. Blamey, P.W. Moody, Py. 2005b. Do decomposing organic matter residues reduce phosphorus sorption in highly weathered soils? Soil Sci. Soc. Am. J. 69:1405-1411.

Gustafsson J.P., I. Persson, D.B. Kleja, J.W.J. Van Schaik. 2007. Binding of iron(III) to organic soils: EXAFS spectroscopy and chemical equilibrium modeling. Environ. Sci. Technol. 41:1232-1237.

Hansel C.M., S.G. Benner, P. Nico, S. Fendorf. 2003. Structural constraints of ferric (hydr)oxides on dissimilatory iron reduction and the fate of Fe(II). Geochim. Cosmochim. Acta 68:3217-3229.

Hansel C.M., S.G. Benner, P. Nico, S. Fendorf. 2004. Structural constraints of ferric (hydr)oxides on dissimilatory iron reduction and the fate of Fe(II). Geochimica Et Cosmochimica Acta 68:3217-3229.

Hermann R., J. Gerke. 1992. Complexation of iron(III) to humic substances of a humic podzol at pH 2.5-6.4 - quantification of the organically complexed iron by pyrophosphate extraction. Z. Pflanzenernahr. Bodenkd. 155:229-232.

Hiemstra T., J. Antelo, A.M.D. van Rotterdam, W.H. van Riemsdijk. 2010. Nanoparticles in natural systems II: The natural oxide fraction at interaction with natural organic matter and phosphate. Geochim. Cosmochim. Acta. 74:59-69.

Hinesly T.D., R.L. Jones. 1990. Phosphorus in waters from sewage-sludge amended lysimeters. Environ. Pollut. 65:293-309.

Holford I.C.R., W.H. Patrick. 1979. Effects of reduction and pH changes on phosphate sorption and mobility in an acid soil. Soil Sci. Soc. Am. J. 43:292-297.

Holford I.C.R., W.H. Patrick. 1981. Effects of duration of anaerobiosis and reoxidation on phosphate sorption characteristics of an acid soil Aust. J. Soil Res. 19:69-78.

Hue N.V., 1991. Effects of organic-acids anions on P-sorption and phytoavailability in soils with different mineralogies. Soil Sci. 152:463-471.

Hunt J.F., T. Ohno, Z.Q. He, C.W. Honeycutt, and D.B. Dail. 2007. Inhibition of phosphorus sorption to goethite, gibbsite, and kaolin by fresh and decomposed organic matter. Biology Fert. Soils. 44:277-288.

Hutchison K.J., D. Hesterberg. 2004. Dissolution of phosphate in a phosphorus-enriched ultisol as affected by microbial reduction. J. Environ. Qual. 33:1793-1802.

Jansen B., K.G.J. Nierop, and J.M. Verstraten. 2002. Influence of pH and metal/carbon ratios on soluble organic complexation of Fe(II), Fe(III) and Al(III) in soil solutions determined by diffusive gradiens in thin films. Anal. Chim. Acta 454:259-270.

Jansen B., K.G.J. Nierop, and J.M. Verstraten. 2005. Mechanisms controlling the mobility of dissolved organic matter, aluminium and iron in podzol B horizons. Eur. J. Soil Sci. 56:537-550.

Jerzykiewicz M., A. Jezierski, F. Czechowski, J. Drozd. 2002. Influence of metal ions binding on free radical concentration in humic acids. A quantitative electron paramagnetic resonance study. Org. Geochem. 33:265-268.

Jiang J., A. Kappler. 2008. Kinetics of microbial and chemical reduction of humic substances: Implications for electron shuttling. Env. Sci. Tech. 42:3563-3569.

Kaiser K., W. Zech. 1996. Nitrate, sulfate, and biphosphate retention in acid forest soils affected by natural dissolved organic carbon. J. Environ. Qual. 25:1325-1331.

Kappler A., S.B. Haderlein. 2003. Natural organic matter as reductant for chlorinated aliphatic pollutants. Env. Sci. Tech. 37:2714-2719.

Karlsson T., P. Persson. 2010. Coordination chemistry and hydrolysis of Fe(III) in a peat humic acid studied by X-ray absorption spectroscopy. Geochim. Cosmochim. Acta. 74:30-40.

Karlsson T., P. Persson, U. Skyllberg, C.M. Morth, and R. Giesler. 2008. Characterization of iron(III) in organic soils using extended X-ray absorption fine structure spectroscopy. Environ. Sci. Technol. 42:5449-5454.

Khan F.A., A.A. Ansari. 2005. Eutrophication: An ecological vision. Bot. Rev. 71:449-482.

Kizewski, F.R.2011. Phosphate Binding and Fe(III) Reduction as Affected by Fe(III)

and Organic Matter Interactions. Ph.D. Dissertation. North Carolina State University, Raleigh, NC

Lindsay W.L., 1979. Chemical equilibria in soils John Wiley & Sons, New York, NY.

Liu C., P.M. Huang. 2000. Kinetics of phosphate adsorption on iron oxides formed under the influence of citrate. Can. J. Soil Sci. 80:445-454.

Lovley D.R., 1991. Dissimilatory Fe(III) and Mn(IV) reduction. Microbiol. Rev. 55:259-287.

Lovley D.R., 1993. Dissimilatory metal reduction. Annu. Rev. Microbiol. 47:263-290.

Lovley D.R., J.D. Coates, E.L. Blunt-Harris, E.J.P. Phillips, J.C. Woodward. 1996. Humic substances as electron acceptros for microbial respiration. Nature 38:445-448.

Macrae M.L., T.E. Redding, I.F. Creed, W.R. Bell, K.J. Devito. 2005. Soil, surface water and ground water phosphorus relationships in a partially harvested Boreal Plain aspen catchment. For. Ecol. Manage. 206:315-329.

Marks R., R. Knuffke. 1998. Americas animal factories: How states fail to prevent pollution from livestock waste, Natural resources defense council and Clean Water Network.

Masscheleyn P.H., J.H. Pardue, R.D. Delaune, W.H. Patrick. 1992. Phosphorus release and assimilatory capacity of 2 lower Mississippi valley fresh-water wetland soils Water Resour. Bull. 28:763-773.

Mitsch W.J., J.G. Gosselink. 2000. Wetlands. 3rd ed. John Wiley & Sons, New York.

Moshi A.O., A. Wild, Greenlan.Dj. 1974. Effect of organic-matter on charge and phosphate adsorption characteristics of kikuyu red clay from Kenya. . Geoderma 11:275-285.

National Pork Producers Council N.C.P., 2008a. http://www.ncpork.org.

National Pork Producers Council N.C.P., 2008b. http://www.nppc.org.

Neal, A.L., T.L. Bank, M. F. Hochella, and K. M. Rosso. 2005. Cell adhesion of Shewanella oneidensis to iron oxide minerals: Effect of different single crystal faces. Geochem. Trans. 6:77-84

Noe G.B., 2011. Measurement of Net Nitrogen and Phosphorus Mineralization in Wetland Soils Using a Modification of the Resin-Core Technique. Soil Sci. Soc. Am. J. 75:760-770.

NRCS. 2004. National Resources Inventory 2002 annual NRI. Wetlands, http://www.nrcs.usda.gov/technical/land/nri02/wetlands.pdf.

O'Loughlin E.J., P. Larese-Casanova, M. Scherer, R. Cook. 2007. Green rust formation from the bioreduction of gamma-FeOOH (lepidocrocite): Comparison of several Shewanella species. Geomicrobiology J. 24:211-230.

Pant H.K., 2007. Nonlinear effects of climate change on phosphorus stability in wetlands: Concept and estimation. J. Food, Ag., Environ. 5:295-301

Patrick W.H., R.A. Khalid. 1974. Phosphate release and sorption b soils and sediments-effects of aerobic and anaerobic conditions Science 186:53-55.

Paul E.A., F.E. Clark. 1996. Soil Microbiology and biochemistry Academic Press, San Diego, CA. USA.

Peretyazhko T., G. Sposito. 2005. Iron(III) reduction and phosphorous solubilization in humid tropical forest soils. Geochim. Cosmochim. Acta. 69:3643-3652.

Pham A.N., T.D. Waite. 2008. Oxygenation of Fe(II) in the presence of citrate in aqeous solutions at pH 6.0-8.0 and 25^0C: Interpretation from an Fe(II)/citrate speciation prespective. J. Phys. Chem. 112:643-651.

Phillips I.R., 1998. Phosphorus availability and sorption under alternating waterlogged and drying conditions. Commun. Soil Sci. Plant Anal. 29:3045-3059.

Rakshit S., M. Uchimiya, G. Sposito. 2009. Iron(III) bioreduction in soil in the presence of added humic substances. Soil Sci. Soc. Am. J. 73:65-71.

Ratasuk N., M.A. Nanny. 2007. Characterization and quantification of reversible redox sites in humic substances. Environ. Sci. Tech. 41:7844-7850.

Reddy, K.R., R.G. Wetzel, and R.H. Kadlec. 2005. Biogeochemistry of phosphorus in wetlands. p. 263-316 *In.* J.T. Sims and A.N. Sharpley ed. Phosphorus: Agriculture and the Environment. ASA, Madison, WI.

Roden E.E., 2003. Fe(III) oxide reactivity toward biological versus chemical reduction. Environ. Sci. Tech. 37:1319-1324.

Roden E.E., R.G. Wetzel. 1999. Humic substances accelerate microbial reduction of amorphous Fe(III) oxide in aquatic sediments. Abstracts of the General Meeting of the Am. Soc. Microbiol. 99: 452.

Roden E.E., M.M. Urrutia. 2002. Influence of biogenic Fe(II) on bacterial crystalline Fe(III) oxide reduction. Geomicrobiology J. 19:209-251.

Rose J., A. Vilge, G. Olivia-Lauquet, A. Masion, C. Frechou, J. Bottero. 1998. Iron speciation in natural organic matter colloids. Colloids Surf., A 136:11-19.

Rose A.L., and T.D. Waite. 2003. Kinetics of iron complexation by dissolved natural organic matter in coastal waters. Mar. Chem. 84:85-103.

Royer R.A., W.D. Burgos, A.S. Fisher, R.F. Unz, B.A. Dempsey. 2002. Enhancement of biological reduction of hematite by electron shuttling and Fe(II) complexation. Env. Sci. Tech. 36:1939-1946.

Sallade Y.E., J.T. Sims. 1997. Phosphorus transformations in the sediments of Delaware's agricultural drainageways: II. Effect of reducing conditions on phosphorus release. Journal of Environmental Quality 26:1579-1588.

Santana-Casiano J.M., M. Gonzalez-Davila, M.J. Rodriguez, F.J. Millero. 2000. The effect of organic compounds in the oxidation kinetics of Fe(II). ar. Chem. 70:211-222.

Schwertmann U., 1966. Inhibitory effect of soil organic matter on crystalization of amorphours ferric hydroxide. Nature. 212:645-646.

Scott D.T., D.M. McKnight, E.L. Blunt-Harris, S.E. Kolesar, D.R. Lovley. 1998a. Quinone moieties act as electron acceptors in the reduction of humic substances by humics-reducing microorganisms. . Env. Sci. Tech. 32:2984-2989.

Scott D.T., D.M. McKnight, E.L. Blunt-Harris, D.R. Lovley, S.E. Kolesar. 1998b. Quinone groups in humic substances as electron acceptors by humic-reducing microorganisms. Abstracts of Papers American Chemical Society 216, ENVR 74.

Shuai X.F., G. Zinati. 2009. Proton Charge and Adsorption of Humic Acid and Phosphate on Goethite. Soil Sci. Soc. Am. J. 73:2013-2020.

Smith V.H., 2003. Eutrophication of freshwater and coastal marine ecosystems - A global problem. Environ. Sci. Pollut. Res. 10:126-139.

Sposito G., 1989. The chemistry of soils Oxford University Press, New York, NY. USA.

Stevenson F.J., A. Fitch. 1986. Chemistry of complexation of metal ions with soil solution organics, Interactions of soil minerals with natural organics and microbes, SSSA, Madison WI.

Stumm W., 1993. From surface acidity to surface reactivity: inhibition of oxide dissolution. Aquat. Sci. 55:1015-1621.

Sulzberger B., D. Suter, C. Siffert, S. Banwart, W. Stumm. 1989. Dissolution of Fe(III) (hydr)oxides in natural waters: laboratory assessment on the kinetics controlled by surface coordination. Mar. Chem. 28:127-144.

Taiz L., E. Zeiger. 2002. Assimilation of Mineral Nutrients, Plant Physiology, Sinauer Associates, Inc., Sunderland, MA.

Thompson A., O.A. Chadwick, D.G. Rancourt, J. Chorover. 2006. Iron-oxide crystallinity increases during soil redox oscillations. Geochimica Et Cosmochimica Acta 70:1710-1727.

Urrutia M.M., E.E. Roden, J.M. Zachara. 1999. Influence of aqueous and solid-phase Fe(II) complexants on microbial reduction of crystalline iron(III) oxides. Environmental Science & Technology 33:4022-4028.

Urrutia M.M., E.E. Roden, J.K. Fredrickson, J.M. Zachara. 1998. Microbial and surface chemistry controls on reduciton of synthetic Fe(III) oxide minerals by the dissimilatory iron-reducing bacterium Shewanella alga. Geomicrobiol. 15:269-291.

Van Schaik J.W.J., I. Persson, D.B. Kleja, J.P. Gustafsson. 2008. EXAFS study on the reactions between iron and fulvic acid in acid aqueous solutions. Environ. Sci. Technol. 42:2367-2373.

Vaughan K.L., M.C. Rabenhorst, B.A. Needelman. 2009. Saturation and temperature effects on the development of reducing conditions in soils. Soil Sci. Soc. Am. J. 73: 663-667.

von Gunten L., M. Grosjean, U. Eggenberger, P. Grob, R. Urrutia, A. Morales. 2009. Pollution and eutrophication history AD 1800-2005 as recorded in sediments from five lakes in Central Chile. Global and Planetary Change 68:198-208.

Weiss J.V., D. Emerson, J.P. Megonigal. 2004. Geochemical control of microbial Fe(III) reduction potential in wetlands: comparison of the rhizosphere to non-rhizosphere soil. FEMS Microbiol. Ecol. 48:89-100.

Weng L.P., W.H. Van Riemsdijk, T. Hiemstra. 2008. Humic Nanoparticles at the Oxide-Water Interface: Interactions with Phosphate Ion Adsorption. Environ. Sci. Technol. 42:8747-8752.

Zak D., J. Gelbrecht, C. Wagner, C.E.W. Steinberg. 2008. Evaluation of phosphorus mobilization potential in rewetted fens by an improved sequential chemical extraction procedure. European Journal of Soil Science 59:1191-1201.

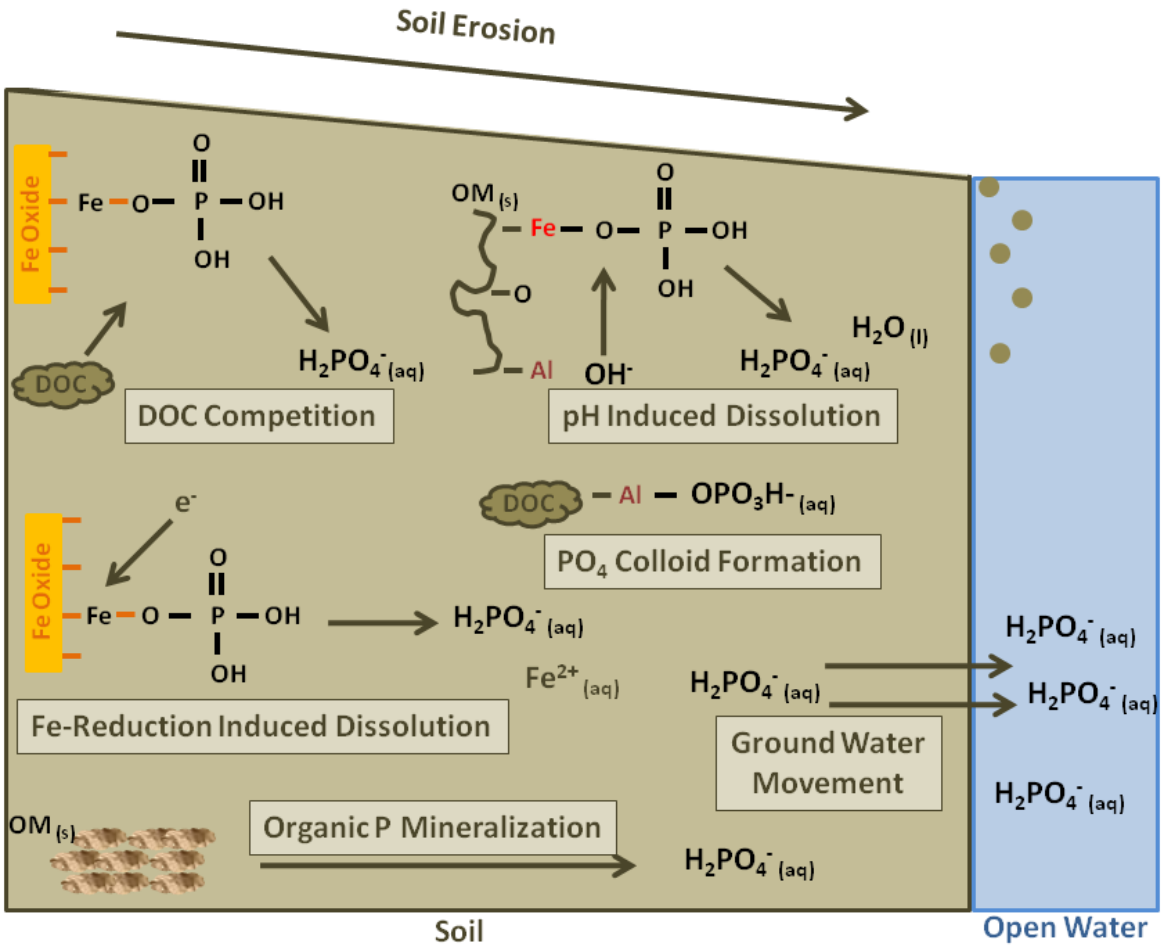

Figure 1.1. Schematic illustrating the potential PO_4 mobilization mechanisms from soil and transport into open water bodies. Mechanisms of mobilization shown include: DOC competition, pH induced PO_4 dissolution, PO_4-Fe-OM colloid formation, Fe-reduction induced PO_4 dissolution, organic P mineralization, and soil erosion.

CHAPTER 2: ORGANIC-MATTER BOUND IRON SPECIATION FROM Fe(III) ADDITION OR Fe(II) OXIDATION

ABSTRACT

Iron retention by soil organic matter (OM), Fe reducibility and mobility, and binding of anions to Fe in OM potentially depend on the bonding configuration of Fe(III)-OM complexes. The molecular bonding environment of Fe(III) associated with soil OM in seasonally saturated soils has not been identified. The coordination of Fe(III) with OM in aerobic and anaerobic soils may differ depending on how Fe(III) is incorporated into OM. My objectives were to determine if the molecular coordination environment of Fe(III) bound to OM differed between direct addition of Fe(III) and addition of Fe(II) followed by oxidation to Fe(III), and to quantify the resultant effects on PO_4 binding to OM. Aqueous solutions of Fe(II) and Fe(III) were reacted with Pahokee peat at 300, 900, and 1200 mmol Fe kg^{-1} peat at pH 2.5, prior to adjusting the pH to 6.8 and introducing oxygen to induce Fe(II) oxidation. Extended X-ray absorption fine structure (EXAFS) and Wavelet Transform (WT) analysis indicated the presence of mixed Fe species, ranging from mononuclear Fe-NOM to polynuclear Fe(III) complexes in samples from both addition methods. No significant differences were found in the bonding environment of Fe(III) to OM or the PO_4 sorption capacity between Fe addition methods. Overall, my results suggested that when Fe binds to OM as oxidized Fe(III) or during Fe(II) oxidation, neither the molecular coordination environment of Fe(III) bound to OM or the anion sorption capacity differs.

INTRODUCTION

Dissolution and transport of certain oxyanions such as $H_2PO_4^-$, NO_3^-, and $H_2AsO_4^-$ to open water bodies causes water quality degradation and is a potential hazard to human and ecosystem health (Carpenter et al., 1998, Islam et al., 2004). For example, excess $H_2PO_4^-$ and NO_3^- in surface waters causes excessive algal growth that leads to low oxygen levels and decreased aquatic biodiversity, a process known as eutrophication (Carpenter et al., 1998). Similarly, the mobilization of $H_2AsO_4^-$ from soils and transport into surface and groundwater is a threat to human health, because As(III) is toxic (Islam et al., 2004). Although oxyanion binding in soils is typically attributed to Fe- and Al- oxides, soil OM can potentially bind oxyanions in organic rich soils and soil horizons.

Iron and Al bound to OM play a role in the retention and dissolution of anions such as PO_4 (Bloom, 1981; Gerke and Hermann, 1992). For example, the molar ratio of P/Fe in Fe-added to humic substances was 6 to 7 x greater than in poorly crystalline Fe-oxides, which suggested a greater accessibility of Fe bound to OM (Gerke and Hermann, 1992). From such data it is hypothesized that the formation of ternary complexes between the Fe-humic substances and PO_4 or other anions occurs. Consequently, the molecular coordination environment of organically bound Fe(III) could alter oxyanion binding and dissolution mechanisms in soils.

Migration of Fe(II) from Fe(III) minerals can be generated by the exchange of electrons from a reductant to a surface Fe(III) center, and may be accelerated in the presence of surface complexing agents such as oxalate, citrate, or salicylate (Stumm, 1993; Sulzberger et al., 1989). Organic acids such as citrate and salicylate have been shown to increase Fe(II)

oxidation rates (Pham and Waite, 2008). Iron dissolved from minerals or plant residues can form new Fe-oxides, sorb to OM or minerals, be taken up by organisms, or be leached from the soil (Lovley, 1991; Lovley, 1993; Stevenson and Fitch, 1986; Weiss et al., 2004).

In nature, Fe(III) can become solubilized from minerals and incorporated into OM by: (1) reductive dissolution of Fe(III) from minerals and re-oxidation of the Fe(II) within the OM matrix (Jansen et al., 2002; Lindsay, 1979), (2) direct incorporation of residual biological Fe [dominantly as Fe(III)] into OM during biodegradation (Taiz and Zeiger, 2002); or (3) complexometric or acid dissolution of minerals and chelation of Fe(III) by OM (Jansen et al., 2005; Lundstrom, 1993). Given that Fe dissolution occurs from minerals by surface protonation (at low pH), complexometric dissolution by organic ligands, or reductive dissolution (Sulzberger et al., 1989), it stands to reason that Fe can be incorporated into OM as either Fe(III) or Fe(II). Although the same coordination sites in OM have been shown to be responsible for both Fe(II) and Fe(III) binding to OM (Rose and Waite, 2003), Fe(II)-NOM can undergo oxidation-reduction cycles, which potentially alters the partitioning of Fe(III) among OM functional groups (Santana-Casiano et al., 2000). Consequently, the molecular bonding environment of Fe(III) that partitions into OM following complexometric dissolution may differ considerably from that of Fe(III) derived from oxidation of OM-bound Fe(II).

Several models based on Fe- K edge EXAFS data have been developed for the binding of Fe(III) to OM under various conditions. The first Fe-O distance was consistently at 2.00 Å (Gustafsson et al., 2007; Karlsson et al., 2008; Rose et al., 1998; van Schaik et al., 2008; Karlsson and Persson, 2010), consistent with Fe(III) in octahedral configuration. As

Fe(II) becomes reduced the Fe-O bond length increases by as much as 0.11 Å (van Schaik et al., 2008). Additionally, several EXAFS models have included an Fe-C shell between 2.7 to 3 Å which indicated Fe(III) binding to OM functional groups (Gustafsson et al., 2007; Karlsson et al., 2008; Rose et al., 1998; van Schaik et al., 2008). Previous studies found that Fe-C distances around 2.95 Å were similar to the binding of Fe to carboxylate or phenolate complexes (van Schaik et al., 2008), while shorter Fe-C distances were similar to Fe binding to oxalate (Karlsson et al., 2008). Several Fe-Fe distances ranged from 2.8 Å to 3.01 Å and up to 4 Å, which are similar to Fe-Fe distances found in goethite, ferrihydrite, and hydrolyzed Fe respectively (Gustafsson et al., 2007; Karlsson et al., 2008). Moreover, Wavelet Transform (WT) has recently been applied as a way to visualize k and R space data, which allows for distinction between heavy and light backscattering atoms (Karlsson and Persson, 2010; Karlsson et al., 2008). Karlsson and Persson (2010) found that $Fe(NO_3)_3$ added to Pahokee peat humic acid yielded monomeric Fe(III) bound to several nearest neighbor C/O/N atoms as determined by both EXAFS data fitting and WT qualitative analysis. Among these studies, different methods in sample preparation and data analysis potentially resulted in the various models and conclusions involving the bonding environment of Fe in OM.

The objectives of this research were to, (1) determine the molecular coordination environment of Fe(III) bound to OM by two methods of Fe addition, direct addition of Fe(III), or addition of Fe(II) followed by oxidation, and (2) compare PO_4 retention in Fe-OM complexes derived from these methods.

MATERIALS AND METHODS

Pahokee peat, an organic soil material from Florida supplied by the International Humic Substances Society (IHSS Bulk Solid Material #2BS103P) was used in these experiments. Care was taken throughout all experiments to exclude oxygen by purging samples with $N_{2(g)}$ and working in a glove box when possible. Hydration of the peat was conducted using CO_2 – free H_2O at a H_2O:peat ratio of $\geq$ 20 at pH 7.5. The pH was raised to 11 and equilibrated for 1 hour to induce hydration. The peat was then equilibrated with pH adjustments to pH 7.5 twice a day for 4 to 5 days, or until pH was stabilized. Finally, the peat was washed 3 times in 200 mL of 0.1 M HCl, followed by 3 washes in 200 mL of 0.1 M KCl. Solid concentrations were determined by oven drying 4 replications of 1 mL sample at 70˚C for 24 h and correcting for background KCl salts.

Binding of Fe to Peat

Peat was initially suspended in 0.1 M KCl and brought to pH 2.5. Solutions of Fe(II) (as $FeCl_2$) or Fe(III) (as $FeCl_3$) were added in 1 mL increments, followed by immediate pH adjustments back to 2.5 using 0.1 M KOH until a total of 300, 900, or 1200 mmol Fe kg^{-1} peat were added. Following addition of Fe, the sample pH was slowly increased to pH 6.8 over 30 min. Solutions were equilibrated for 16 h by shaking at 150 oscillations min^{-1} on a reciprocating water bath shaker at 25°C, and were adjusted to pH 6.8 (as needed) after 2 and 15 h using 0.1 M HCl or 0.1 M KOH. After equilibration, all samples were aerated by bubbling scientific laboratory grade air containing N_2, a maximum of 215000 ppm O_2, $\leq$ 5 ppm H_2O, $\leq$ 0.1 ppm total hydrocarbons, $\leq$ 1 ppm CO, and $\leq$ 1 ppm CO_2 (National Welders

Supply Co. Raleigh, NC. # 020541) while continuously stirring for 3 h. The pH was measured and adjusted to 6.8 every 30 min during the oxidation process.

Sample headspaces was purged with laboratory grade air and allowed to equilibrate for an additional 36 h at 25˚C with pH adjustments at 2, 16, 22 and 34 h. Samples were centrifuged at 20 000 x g for 20 minutes, and the supernatants filtered through 0.2 µm Isopore polycarbonate filter membranes prior to analysis (Millipore Corp., Bedford, MA). The colorimetric 1,10 phenanthroline method (Loeppert and Inskeep, 1996) was used to measure dissolved Fe(II) immediately after Fe addition, and in final supernatant solutions. Total dissolved Fe was measured by flame atomic absorption spectrometry (FAAS) (Model 3100; Perkin Elmer, Wellesey, MA) and by inductively coupled plasma optical emission spectrometry (ICP-OES) (Perkin-Elmer ICP-OES 2000DV, Elmer, Germany). Total dissolved Al and P were measured by ICP-OES. Dissolved reactive P (DRP) was analyzed by the Murphy-Riley colorimetric method (Olsen and Sommers, 1982), and DOC was measured using a Shmadzu TOC-5050 TOC analyzer.

EXAFS Analysis

Following centrifugation, the remaining moist solids were mixed thoroughly and mounted into 380 µm thick teflon sample holders and covered with one layer of Kaptan tape (1 mil, Budnick Converting, Inc., Columbia, IL) for EXAFS analysis. All samples were maintained in an anaerobic moist environment for no more than 3 days (N_2-purged, sealed canning jars) after sample preparation and prior to analysis. Standards including siderite (Wards Scientific), goethite [synthesized following Cornell and Schwertmann (1993)], and ferrihydrite [synthesized following the hydrolysis method in Cornell and Schwertmann

(1993)] were obtained and prepared for analysis. Iron K-edge XANES and EXAFS spectra were obtained at Beamline X-11B at the National Synchrotron Light Source, Upton, NY. The beamline was equipped with a Si(1 1 1) monochromator, which was detuned by > 30% and calibrated to an elemental Fe reference foil placed after the sample. Reference spectra on the foil were collected simultaneously with each sample spectrum for energy calibration. Both transmission and fluorescence were measured simultaneously using ion chambers filled with $N_{2(g)}$ and a Lytle detector, respectively. Sample spectra were collected in the energy range from 200 eV before the edge, to 800 eV after the edge, with a step size of 5 eV from 200 eV to 50 eV below the edge, 0.3 eV from 50 eV below the edge to 50 eV above the edge, and increasing from 1.14 to 5.33 eV from 50 eV to 800 eV above the edge. Each sample spectra represents the average of 3 to 8 scans, and were collected in a randomized chronological order to reduce any systematic trend effects resulting from beamline optics or changing current between storage-ring fills.

Transmission data were analyzed for all samples except for the 300 mmol Fe kg^{-1} peat, for which fluorescence spectra were merged for analysis. Data alignment, merging, normalization, background removal, and Fourier transformation were performed as described in Kelly et al. (2008), employing the data analysis program Athena, an interface of IFEFFIT (version 1.2.10) (Ravel and Newville, 2005). Energy-calibrated spectra were normalized using a linear pre-edge function from -200 to -30 eV and a linear or quadratic baseline function between 80 and 730 eV (Kelly et al., 2008). A cubic function with nodes defined by the AUTOBKG function in IFEFFIT was used to remove backgrounds (Newville, 2001). The

k^3-weighted spectra were Fourier transformed (FT) over the range of k = 3.2 - 9.8 $Å^{-1}$ using a Hanning window function.

Wavelet transform (WT) analysis was performed to distinguish between light and heavy backscattering in the higher coordination shells (Karlsson and Persson, 2010). The qualitative nature of the backscattering atoms in higher coordination shells was compared using the WT method as implemented in the Igor Pro script developed by Funke et al. (2005). The contributions from different backscattering atoms at specific regions in k and R space are visualized in these plots as ridges, and the location of the ridges helps to differentiate between light and heavy backscattering in higher coordination shells (Karlsson and Persson, 2010). The WT's of the Fe bound to Pahokee peat were compared to the WT's of goethite, ferrihydrite and siderite standards in order to visualize differences in the coordination environment of Fe. All spectra were analyzed by means of the Morlet-wavelet, and different ή and σ values were used to obtain an overview and high-resolution plots as denoted in figure captions.

The EXAFS spectra were fit using Artimis (Ravel and Newville, 2005), and theoretical EXAFS paths from goethite (Gualtieri and Venturelli, 1999) and PO_4-Fe(III)-oxalate (Kizewski et al., 2010) were generated using FEFF 6 (Zabinsky et al., 1995) for a cluster size of 5 Å. The coordination number (N) of the first oxygen shell was set to 6, while values of N, ΔR, and σ^2 were fitted. All final values are listed in Table 1, and are discussed below. Several previously conducted fits, including those from Karlsson and Persson (2010), Gustafsson et al. (2007), and Karlsson et al. (2008) were used as first approximations to fit data. Only paths that significantly contributed to overall goodness of fit were included in the

final fit. Parameters that were the same within uncertainties between sample fits were constrained to be equal across multiple samples in the final fits to decrease the number of fitting variables.

P Sorption Isotherm

Additional samples containing 1200 mmol Fe kg^{-1} were prepared using the two methods of Fe addition described above. Following the 36 h equilibration phase with Fe, PO_4 was added at twelve different concentrations and allowed to equilibrate for 36 h. The pH was maintained at 6.8 by adjusting (as needed) at 12, 24 and 34 h following P addition. Samples were centrifuged at 20,000 x g, and the supernatant solutions were decanted, filtered, and analyzed as above for total dissolved Fe(III), Al(III), DRP, total dissolved P and DOC. Bound PO_4 values used to generate P-sorption isotherms were calculated by subtracting DRP from total P.

RESULTS AND DISCUSSION

Oxidation of Fe(II) to Fe(III)

No significant differences in total bound Fe(III) were distinguishable between Fe addition methods (Figure 2.1). As added Fe increased from 300 to 1200 mmol Fe kg^{-1} peat, the bound Fe(III) increased from 130 $\pm$ 9.0 to 860 $\pm$ 72 µmol kg^{-1} peat, while total dissolved Fe increased from 170 $\pm$ 27 to 340 $\pm$ 38 µmol L^{-1} respectively (Figure 2.1). Furthermore, total bound Fe(III) increased as the added Fe concentration increased and dissolved organic carbon concentration decreased (Figure 2.1). Overall, results indicated that method of addition did not alter total bound Fe(III) concentration.

Stacked, normalized K-edge Fe-XANES, and first derivative XANES spectra from both methods of Fe(III) addition, along with standard spectra from siderite, goethite, and ferrihydrite are presented in Figure 2.2. All XANES data exhibited a white line peak at approximately 7132 eV, comparable to that of ferrihydrite at 7132.8 (Figure 2.2 A and B). Typically Fe(II) compounds have lower white line energy positions than Fe(III) compounds (Prietzel et al., 2007). In addition, first derivative absorbance peaks of sample data corresponded to peak positions in goethite and ferrihydrite standards, whereas the peak position of the Fe(II) siderite standard was shifted to lower energy by approximately 5 eV (Figure 2.1 C and D). Two peaks were visible in the ferrihydrite and goethite spectra between 7120 and 7130 eV, while only one broad peak was distinguishable in the sample spectra (Figure 2.2). The broadness of the peak in the sample spectra increased with Fe(III) concentration, indicating the potential development of a doublet as Fe(III) concentration increased (Figure 2.2). Overall, data indicated that sample spectra were most similar to the

ferrihydrite standard, and that peak positions indicated the presence of Fe(III), rather than Fe(II), following both methods of addition.

Chemical analysis of dissolved Fe(II) indicated that less than 5% of total Fe was reduced by the peat, which was equivalent to 40 $\pm$ 2 mmol Fe(II) kg^{-1} peat prior to aeration in the Fe(III) addition method. Moreover, further reduction or oxidation of Fe did not take place during the 36 h equilibration period in the oxidized Fe(III) addition samples, because no significant differences were found between dissolved Fe(II) concentration measured immediately following the aeration period and dissolved Fe(II) levels following the subsequent 36 h equilibration period. However, 67% of the added Fe in the Fe(II) addition samples remained as Fe(II) immediately following the 3 h oxidation period, and < 5% remained after 36 h of equilibration. Even though XANES first derivative peak positions indicated the dominant presence of Fe(III), a 1 eV blue shift with decreasing added Fe concentration in the Fe(III) addition method occurred, potentially indicating that the ratio of Fe(II)/Fe(III) increased as total Fe(III) decreased (Figure 2.1 C). A shift was also found for the Fe(II) addition method, but the peak position was 1 eV higher for the 1200 mmol Fe kg^{-1} treatment compared to the 900 mmol Fe kg^{-1} peat treatment.

EXAFS Results

No differences were found between stacked k^3-weighted EXAFS spectra and sample spectra of Fe, and that data quality decreased with decreasing Fe concentration (Figure 2.3). A visual comparison between the stacked k^3-weighted spectra of Fe bound to OM with standards indicated that Fe bound to OM was not in the form of ferrihydrite, goethite, or siderite, consistent with XANES results. The Fe-peat spectra most resembled the ferrihydrite

standard, however, an oscillation occurring near 7.5 Å in the ferrihydrite spectra was absent in the Fe-peat samples. As Fe(III) concentration increased, a small oscillation near 7.2 Å developed from both addition methods. These differences show that the dominant form of Fe in OM was unique compared with crystalline or poorly crystalline Fe(III)-(hydr)oxides. In addition, as Fe(III) concentration increased, the form of Fe(III) transitioned toward the formation of a poorly crystalline Fe(III)-(hydr)oxides.

Fourier transform (FT) magnitudes of EXAFS spectra for samples and standards are presented in Figure 2.4. Fourier transform magnitude and real spectra revealed that the first Fe-Fe shell at approximately 2.8 Å in standard spectra (Figure 2.4) weakly grew in sample spectra as Fe concentration increased, and in the case of the 300 mmol Fe kg^{-1}peat, was indiscernible. Furthermore, the appearance of a peak between 2.2 and 2.3 Å occurred in sample spectra, which corresponded to previously observed peaks attributed to Fe-C/N distances in aqueous solutions of iron(III) desferrioxamine B and trisoxalatoiron(III) (Karlsson and Persson, 2010; Edwards and Myneni, 2005).

Wavelet Transform Analysis

The WT analysis provides the ability to easily differentiate between two types of atoms within one shell (Karlsson et al., 2008). Generally, WT analysis of Fe K-edge EXAFS data showed different high-shell backscatters between my samples and standards (Figure 2.5). The overview of the low-resolution wavelets reveals a strong visible feature between R = 1 and 2 Å for all samples, which corresponds to the first oxygen shell of Fe(III) (Figure 2.5 D, E, F, G, H, and I). Additionally, a strong feature between R = 2 and 4 Å in the standards corresponds to the second peak in the FT (Figure 2.5 A, B, and C). The feature between R =

2 and 4 Å occurs at higher wavenumber (k = 5.5 – 9 $Å^{-1}$) compared to the WT modulus of the first shell (k = < 3.0 – 8.0 $Å^{-1}$), and is nearly identical to data presented in Karlsson and Persson (2010). The location of the feature between R = 2 and 4 Å at higher wavenumber indicates heavy backscattering, which corresponds to the nearest Fe neighbors of the goethite structure. Likewise, a somewhat weaker feature appears between R = 2.5 and 3 Å, corresponding to the nearest Fe neighbors in ferrihydrite. Distinction between Fe-Fe distances such as those in goethite at 3.03, 3.26, and 3.43 Å were not resolved in the low-resolution wavelets of the standards. The strong second shell Fe feature, visible in the standard wavelets is weakly visible in the wavelets for 1200 and 900 mmol Fe kg^{-1} peat samples, and nearly disappears in the 300 mmol Fe kg^{-1} peat samples, indicating minimal backscattering contributions from nearest neighbor Fe atoms.

The same features corresponding to second shell Fe in standards and samples are visible in high resolution wavelets (Figure 2.6), but more detailed information is gained. Along with the visible features resulting from nearest neighbor Fe backscattering in samples (Figure 2.5), additional features are evident between k = 2 and 2.5$Å^{-1}$, which corresponds to the first shell oxygen, and between k = 2.9 and 3.5 $Å^{-1}$, which corresponds to the second shell C/O. These features are similar to those found in Fe(III)-desferrioxamine B and Pahokee peat humic acid by Karlsson and Persson (2010). Despite these similarities, Fe-C paths present in Fe(III)-desferrioxamine at k = 3 and 4 $Å^{-1}$ were less distinct in my samples. These features are evident at lower wavenumber, indicating that they are caused by lighter atoms such as C or O in the second and third coordination shells. Features between k = 2.5 and 3.5 $Å^{-1}$ and between k = 5.5 and 8 $Å^{-1}$ are present and resemble the second shell Fe

backscattering feature in ferrihydrite. Wavelet features that corresponded to C or O between R = 3 and 3.5 Å became more prominent as Fe(III) concentration decreased in samples. In addition, the Fe(III) contribution from k = 6 to 7 $Å^{-1}$ shifted from between R = 2.5 to 3.0 Å to between 3.0 to 3.5 Å as total Fe concentration decreased, suggesting that the proportion of Fe(II) to Fe(III) increased with decreasing total Fe concentration. This trend corresponded to XANES data that suggests an increased Fe(II)/Fe(III) with decreasing Fe concentration. However, the sensitivity of XANES for detection of Fe species is typically greater than the 5% Fe(II) detected by chemical analysis in my samples, thus we cannot say with certainty that the shift in R from 3.0 to 3.5 between R = 2.5 and 3.0 corresponded to changing Fe(II)/Fe(III) ratios. Furthermore, although the previous trends were evident in samples from both methods of Fe addition, the Fe contribution was stronger in samples were Fe(III) was added directly. Overall, no visible differences in the location of wavelets between addition methods were found, which indicated that the method of Fe addition did not impact the coordination environment of Fe(III) bound to peat.

EXAFS Fitting Results

EXAFS fitting of peat sample data with an Fe coordination of 6 O atoms in the first shell resulted in a mean Fe-O bond distance of 1.99 $\pm$ 0.004 Å (were $\pm$ indicates calculated uncertainty) (Table 2.1). In all cases the existence of an Fe-C bond at 2.90 $\pm$ 0.04 Å indicated the presence of organic groups bound to Fe(III) (Table 2.1, Figure 2.4). The Fe-C bond distance of 2.90 Å is comparable to Fe-C distances in oxalate (2.82 Å), malonate (2.97 Å) (Persson and Axe, 2005), organic soil horizons taken from Spodisols (3-3.02 Å) (Gustafsson et al., 2007), soils (2.72-2.86 Å) (Karlsson et al., 2008), and different Fe concentrations

added to Pahokee peat humic acid between 90 and 880 mmol kg^{-1} peat (2.87-2.91 Å) (Karlsson and Persson, 2010). The comparable distances between Fe-C distances suggested that the binding of Fe to OM was similar to that of Fe bound to oxalate, malonate, and soils, and corresponded with previous results that identified the Fe-C distances for Fe bound to Pahokee peat. Furthermore, a multi-scattering Fe-O-C contribution was fit at 4.07 $\pm$ 0.05, 4.01 $\pm$ 0.05, and 4.19 $\pm$ 0.03 Å in the 1200, 900, and 300 mmol Fe kg^{-1} peat samples respectively. The Fe-O-C fit at 4.19 Å in the 300 mmol Fe kg^{-1} peat sample was comparable to the Fe-C-C/O multi-scattering path found by Karlsson et al. (2008) at 4.20 Å in Fe bound to Pahokee peat humic acid. The fit with a Fe-O-C multi-scattering path at 4.19 Å suggests that this signal may actually be due to Fe-C-C multi-scattering. However, EXAFS cannot readily distinguish between C and O backscatters (Kelly et al., 2008), and as a result, it is unclear if the paths at 4.01 to 4.19 correspond to Fe-O-C or to Fe-C-C multi-scattering.

The Fe-Fe distances fit at 3.04 $\pm$ 0.02 Å and 3.44 $\pm$ 0.04 Å for all three Fe addition concentrations were similar to Fe-Fe distances for edge sharing and double corner geometries in Fe(III) (hydr)oxides minerals such as ferrihydrite, goethite and akaganeite (Karlsson and Persson, 2010; Manceau and Drits, 1993; O'Day et al., 2004). The Fe-Fe distance at 3.28 Å present in these mineral phases was absent in my sample spectra, which suggests that Fe in the peat was in polynuclear Fe(III)-OM clusters rather than crystalline or poorly-crystalline Fe(III)-(hdry)oxides. Overall, spectra from Fe-OM were consistent with those reported previously for Fe(III) bound in organic soils, fulvic acid, oxalate, malonate, and ligneous materials (Guillon et al., 2003; Gustafsson et al., 2007; Karlsson et al., 2008; Persson and Axe, 2005; van Schaik et al., 2008). No differences in the molecular binding environment of

Fe between Fe addition methods were determined by EXAFS data fitting. These data indicated Fe-Fe edge and corner sharing, consistent with the formation of Fe(III)-OM clusters. We conclude that my samples contained a mixture of mononuclear Fe(III)-OM (Persson and Axe, 2004; Karlsson et al., 2008; van Schaik et al., 2008) and polynuclear Fe(III)-OM clusters.

P Sorption Isotherms

Because bound Fe(III) also varied across treatments, the bound PO_4 to Fe(III) ratio was used instead of bound PO_4 (Figure 2.7). Generally, bound PO_4 /Fe increased with increasing dissolved PO_4 up to 0.15 mol mol^{-1} (Figure 2.7). Comparisons of PO_4 sorption isotherms for bound PO_4 and bound PO_4 to Fe(III) ratio showed typical L-type isotherms, which were fit with Freundlich-models (Figure 2.7, Figure A1.1). Trends in PO_4/Fe were consistent when the bound PO_4/Fe ratio was < 0.1 mol mol^{-1}, but became variable as the bound PO_4/Fe ratio was > 0.1 mol mol^{-1} (Figure 2.7). Although the fitted Freundlich models suggested that the addition of Fe(III) imparted a greater PO_4 sorption capacity (Fig. 2.7), the high variability of the data at bound PO_4/ bound Fe ratios of > 0.1 mol mol^{-1} resulted in overleaping standard error bars in PO_4 sorption for the two methods of Fe addition.

Separate tests were performed to determine the impact of DOC on the colorimetric measurement of dissolved PO_4. In each case, the background absorbance was subtracted from the sample absorbance prior to correlating the absorbance to the standard curve in order to account for any differences in absorbance due to DOC. The absorbance of samples in the absence of the colorimetric reagents was $\leq$ 0.007, which corresponded to < 2 % of total PO_4.

Thus, DOC was unable to explain the variability in the bound PO_4 to bound Fe ratios above > 0.1 mol mol^{-1}.

CONCLUSIONS

EXAFS analysis indicated that the coordination environment of Fe(III) bound to OM was the same from the direct addition of Fe(III) to OM and the addition of Fe(II) prior to oxidation. Wavelet transform analysis confirmed the presence of Fe-Fe and Fe-C/O distances, and in all cases, > 95% of added Fe was oxidized (chemical analysis), and bound as either mononuclear Fe(III)-OM or polynuclear Fe(III)-OM clusters (EXAFS analysis). In addition, colorimetric measurements of dissolved PO_4 suggested that PO_4 sorption to Fe(III) bound to OM was no different between samples where Fe(III) was added directly and where Fe(II) was added to OM prior to oxidation. Iron(II) is as much as 9 x more soluble than Fe(III), and as such, the incorporation of Fe(III) into OM was hypothesized to predominantly occur from the partitioning of Fe(II) into OM before or during oxidation. EXAFS, WT, and chemical speciation results suggested that the partitioning of Fe(III) into organic matter as Fe(II) was identical to the partitioning of Fe(III) into organic matter as Fe(III). Because no differences were determined between the direct addition of Fe(III) and the addition of Fe(II) prior to oxidation, the quicker method in which Fe(III) was added directly to OM was used in all remaining experiments.

BIBLIOGRAPHY

Bloom P.R., 1981. Phosphorus adsorption by an aluminum-peat complex. Soil Sci. Soc. Am. J. 45:267-272.

Carpenter S.R., N.F. Caraco, D.L. Correl, R.W. Howarth, A.N. Sharpley, and V.H. Smith. 1998. Nonpoint pollution of surface waters with phophorus and nitrogen. Ecol. Appl. 8:559-568.

Edwards, D.C., and S.C.B. Myneni. 2005. Hard and soft X-ray absorption spectroscopic investigation of aqueous Fe(III)-Hydroxamate siderophore complexes. J. Phys. Chem. A. 109:10249-10256.

Funke H., A.C. Scheinost, and M. Chukalina. 2005. Wavlet analysis of extended X-ray absorption fine structure data. Phys. Rev. B 71:1-7.

Gerke J., and R. Hermann. 1992. Adsorption of orthophosphate to humic-Fe complexes and to amorphous Fe-oxide J. Plant Nutr. Soil Sci. 155:233-236.

Gualtieri A.F., and P. Venturelli. 1999. In situ study of the goethite-hematite phase transformation by real time synchrotron powder diffraction. Am. Mineral. 84:895-904.

Guillon E., P. Merdy, and M. Aplincourt. 2003. Molecular scale speciation of first-row transition elements bound to ligneous materials by using X-ray absoprtion spectroscopy. Chem. Eur. J. 9:4479-4484.

Gustafsson J.P., I. Persson, D.B. Kleja, and J.W.J. Van Schaik. 2007. Binding of iron(III) to organic soils: EXAFS spectroscopy and chemical equilibrium modeling. Environ. Sci. Technol. 41:1232-1237.

Islam F.S., A.G. Gault, C. Boothman, D.A. Polya, J.M. Chamock, D. Chatteriee, and J.R. Lloyd. 2004. Role of metal-reducing bacteria in arsenic release from Bengal delta sediments. Nature 430:68-71.

Jansen B., K.G.J. Nierop, and J.M. Verstraten. 2002. Influence of pH and metal/carbon ratios on soluble organic complexation of Fe(II), Fe(III) and Al(III) in soil solutions determined by diffusive gradiens in thin films. Anal. Chim. Acta 454:259-270.

Jansen B., K.G.J. Nierop, and J.M. Verstraten. 2005. Mechanisms controlling the mobility of dissolved organic matter, aluminium and iron in podzol B horizons. Eur. J. Soil Sci. 56:537-550.

Jiao Y., Hendershot W.H., Whalen J.K., 2008. Modeling phosphate adsorption by agricultural and natural soils. Soil Science Society of America Journal 72, 1078-1084.

Jin X.C., Wang S.R., Pang Y., Zhao H.C., Zhou X.N., 2005. The adsorption of phosphate on different trophic lake sediments. Colloids and Surfaces a-Physicochemical and Engineering Aspects 254, 241-248.

Karlsson T., and P. Persson. 2010. Coordination chemistry and hydrolysis of Fe(III) in a peat humic acid studied by X-ray absorption spectroscopy. Geochim. Cosmochim. Acta 74:30-40.

Karlsson T., P. Persson, U. Skyllberg, C.M. Morth, and R. Giesler. 2008. Characterization of iron(III) in organic soils using extended X-ray absorption fine structure spectroscopy. Environ. Sci. Technol. 42:5449-5454.

Kelly S., D. Hesterberg, and B. Ravel. 2008. Analysis of soils and minerals using X-ray absorption spectroscopy, 387-464 *In*. A. L. Ulery and R. Drees (Ed.) Methods of Soil Analysis Part 5. Mineralogical Methods. ASA and SSSA, Madison, WI.

Kizewski F.R., P. Boyle, D.L. Hesterberg, and J.D. Martin. 2010. Mixed anion (phophate/oxalate) bonding ot iron(III) materials. J. Am. Chem. Soc. 132:2301-2308.

Lindsay W.L., 1979. Chemical equilibria in soils John Wiley & Sons, New York, NY.

Loeppert R.H., and W.P. Inskeep. 1996. Iron. pp. 639-664. *In* S. L. Sparks (Ed.), Methods of soil analysis, part 3. Chemical methods, ASA and SSSA, Madison WI.

Lovley D.R., 1991. Dissimilatory Fe(III) and Mn(IV) reduction. Microbiol. Rev. 55:259-287

Lovley D.R., 1993. Dissimilatory metal reduction. Annu. Rev. Microbiol. 47:263-290.

Lundstrom U., 1993. The role of organic-acids in the soil solution chemistry of a podzolized soil. J. Soil Sci. 44:121-133.

Manceau A., and V.A. Drits. 1993. Local-structure of ferrihydrite and feroxyhite by EXAFS spectroscopy. Clay Miner. 28:165-184.

Murray G.C., Hesterberg D., 2006. Iron and phosphate dissolution during abiotic reduction of ferrihydrite-boehmite mixtures. Soil Sci. Soc. Am. J. 70, 1318-1327.

O'Day P.A., N. Rivera, R. Root, and S.A. Carroll. 2004. X-ray absorption spectroscopic study of Fe reference compounds for the analysis of natural sediments. Am. Mineral. 89:572-585.

Olsen S.R., and L.E. Sommers. 1982. Phosphorus. p. 403-427 *In* A. L. Pate (Ed.) Methods of Soil Analysis Part 2: Chemical and Microbiological Properties. ASA and SSSA Madison, WI.

Persson P., and K. Axe. 2005. Adsorption of oxalate and malonate at the water-goethite interface: molecular surface speciation from IR spectroscopy. Geochim. Cosmochim. Acta. 69:541-552.

Pham A.N., and T.D. Waite. 2008. Oxygenation of fe(II) in the presence of citrate in aqeous solutions at pH 6.0-8.0 and 25^0C: Interpritation from an Fe(II)/citrate speciation prespective. J. Phys. Chem. 112:643-651.

Prietzel J., J. Thieme, K. Eusterhues, and D. Eichert. 2007. Iron speciation in soils and soil aggregates by synchrotron based X-ray microspectroscopy (XANES, μ-XANES). Eur. J. Soil Sci. 58:1027-1041.

Ravel B., and M. Newville. 2005. ATHENA, ARTEMIS, HEPHAESTUS. Data analysis for X-ray absorption spectroscopy using IFEFFIT. J. Synchrotron Radiat. 12:537-541.

Rose A.L., and T.D. Waite. 2003. Kinetics of iron complexation by dissolved natural organic matter in coastal waters. Mar. Chem. 84:85-103.

Rose J., A. Vilge, G. Olivia-Lauquet, A. Masion, C. Frechou, and J. Bottero. 1998. Iron speciation in natural organic matter colloids. Colloids Surf. 136:11-19.

Santana-Casiano J.M., M. Gonzalez-Davila, M.J. Rodriguez, and F.J. Millero. 2000. The effect of organic compounds in the oxidation kinetics of Fe(II). Mar. Chem. 70:211-222.

Stevenson F.J., and A. Fitch. 1986. Chemistry of complexation of metal ions with soil solution organics p 29-58 *In.* Interactions of soil minerals with natural organics and microbes. ASA and SSSA, Madison WI.

Stumm W., 1993. From surface acidity to surface reactivity: inhibition of oxide dissolution. Aquat. Sci. 55:1015-1621.

Sulzberger B., D. Suter, C. Siffert, S. Banwart, and W. Stumm. 1989. Dissolution of Fe(III) (hydr)oxides in natural waters: laboratory assessment on the kinetics controlled by surface coordination. Mar. Chem. 28:127-144.

Taiz L., and E. Zeiger. 2002. Assimilation of Mineral Nutrients, Plant Physiology, Sinauer Associates, Inc., Sunderland, MA.

van Schaik J.W.J., I. Persson, D.B. Kleja, and J.P. Gustafsson, 2008. EXAFS study on the reactions between iron and fulvic acid in acid aqueous solutions. Environ. Sci. Technol. 42:2367-2373.

Weiss J.V., D. Emerson, and J.P. Megonigal, 2004. Geochemical control of microbial Fe(III) reduction potential in wetlands: comparison of the rhizosphere to non-rhizosphere soil. FEMS Microbiol. Ecol. 48:89-100.

Table 2.1. Extended X-ray absorption fine structure fitting results for peat with 300, 900, and 1200 mmol kg^{-1} Fe added as Fe(III) or Fe(II). The amplitude reduction factor was fixed to 0.84. The bond distances (R), coordination numbers (CN), and Debye-Waller factors (σ^2) were allowed to vary except where specified. Uncertainties are indicated in parenthesis. Individual R-factors were as follows: Fe(III) 1200 = 0.003, Fe (II) 1200 = 0.002, Fe(III) 900 = 0.005, Fe(II) 900 = 0.005, Fe(III) 300 = 0.02, Fe(II) 300 = 0.01.

	Fe-O(1)	**Fe-C**	**Fe-Fe1**	**Fe-Fe2**	**Fe-O-C**	**Fe-O3**	**Fe-Fe3**		**Fe-Fe4**	
	N=6†, R =1.99 (0.004)‡ Å	**R=2.90 (0.04) Å‡, σ^2 =0.007 (0.007) ‡ Å²**	**R= 3.04 (0.02) ‡, σ^2 =0.008 (0.008) ‡ Å²**	**R= 3.44 (0.04), σ^2 =0.0006(0.007) ‡ Å²**	**$N_{Fe\text{-}OC}$ = 2 X $N_{Fe\text{-}C}$, σ^2 =0.009 (0.007) ‡ Å²**	**R = 4.39 (0.02) ‡, σ^2 =0.002 (0.005) ‡ Å²**	**σ^2 = 0.001 (0.01) ‡ Å²**		**σ^2 = 0.007 (0.02) ‡ Å²**	
	σ^2	**CN**	**CN**	**CN**	**R(Å)**	**CN**	**CN**	**R(Å)#**	**CN**	**R(Å)**
Sample										
Fe(III) 1200	0.009 (0.0003)	1.35 (0.75)	0.75 (0.59)	0.46 (0.48)	4.07‡ (0.05)	2.27 (1.92)	0.00 (0.43)	4.87 (0.03)	1.14 (2.19)	5.23‡ (0.03)
Fe(II) 1200	0.009 (0.0003)	1.28 (0.76)	0.37 (0.37)	0.71 (0.62)	4.07‡ (0.05)	4.01 (2.22)	0.25 (0.40)	4.68‡ (0.03)	1.02 (2.21)	5.23‡ (0.03)
Fe(III) 900	0.008 (0.0004)	1.47 (0.78)	0.03 (0.33)	0.80 (0.65)	4.01§ (0.05)	5.02 (2.34)	0.52 (0.66)	4.68‡ (0.03)	0.84 (1.76)	5.31§ (0.06)
Fe(II) 900	0.008 (0.0004)	1.20 (0.69)	0.08 (0.33)	0.62 (0.54)	4.01§ (0.05)	5.1 (2.33)	0.32 (0.43)	4.68‡ (0.03)	1.25 (2.46)	5.31§ (0.06)
Fe(III) 300	0.009 (0.0008)	3.56 (2.11)	0.19 (0.37)	0.11 (0.51)	4.19¶ (0.03)	0.00 (2.82)	0.14 (0.45)	4.64§ (0.05)	1.52 (3.25)	5.23‡ (0.03)
Fe(II) 300	0.01 (0.0006)	0.76 (0.94)	0.19 (0.33)	0.37 (0.43)	4.19¶ (0.03)	3.28 (2.27)	0.34 (0.53)	4.64§ (0.05)	1.46 (3.06)	5.23‡ (0.03)

† – indicates values were set

‡, §, or ¶ within columns indicate that values were defined to equal each other during the fit

#- Two different Fe-Fe3 paths were used in the fits. One at 4.7699 for the 1200 mmol Fe kg^{-1} peat sample, and one at 4.58 for the other samples

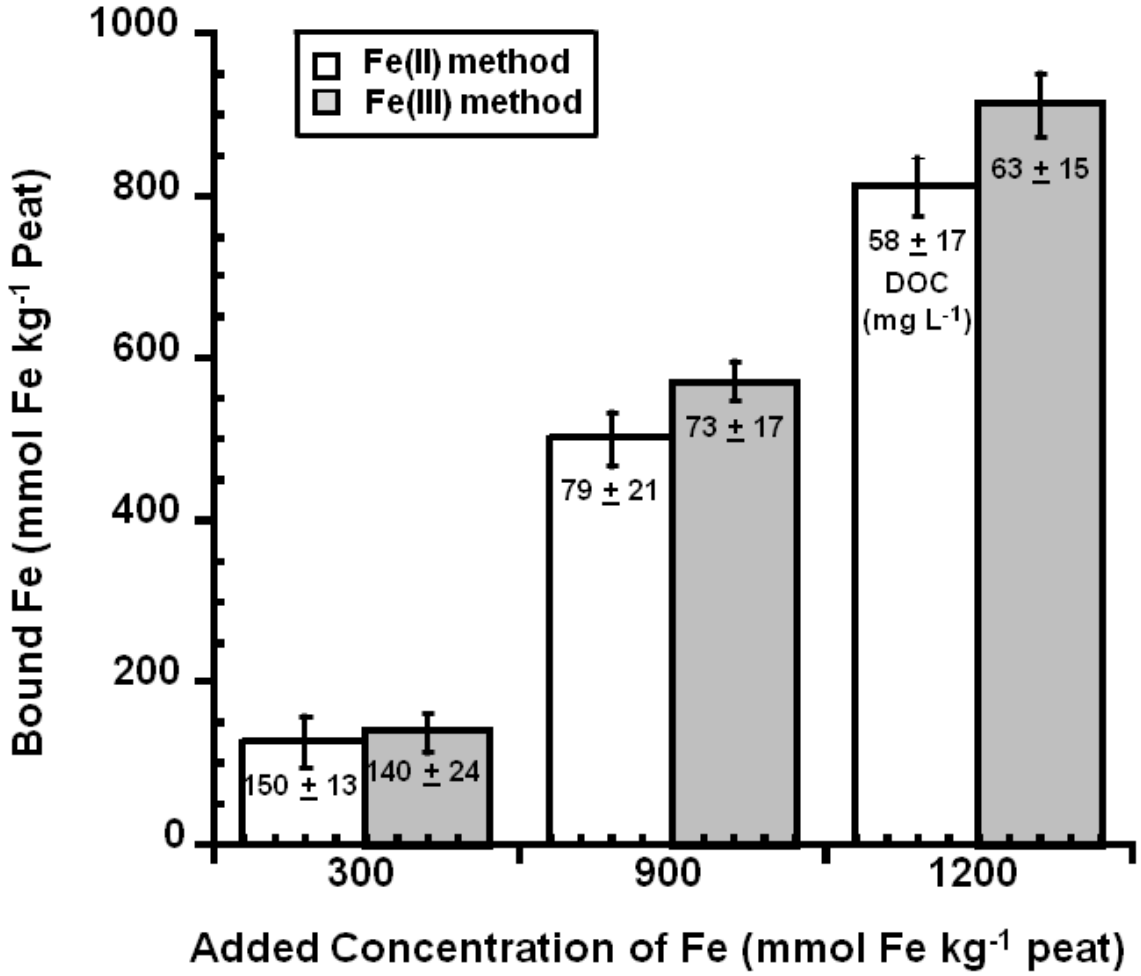

Figure 2.1. Bound Fe(III) (mmol kg^{-1} peat) for Fe(II) and Fe(III) addition methods. Error bars indicate no significant differences in bound Fe(III) between addition methods at pH 6.8. Dissolved organic carbon (DOC) concentration are indicated in mg L^{-1} and decreased with increasing Fe addition.

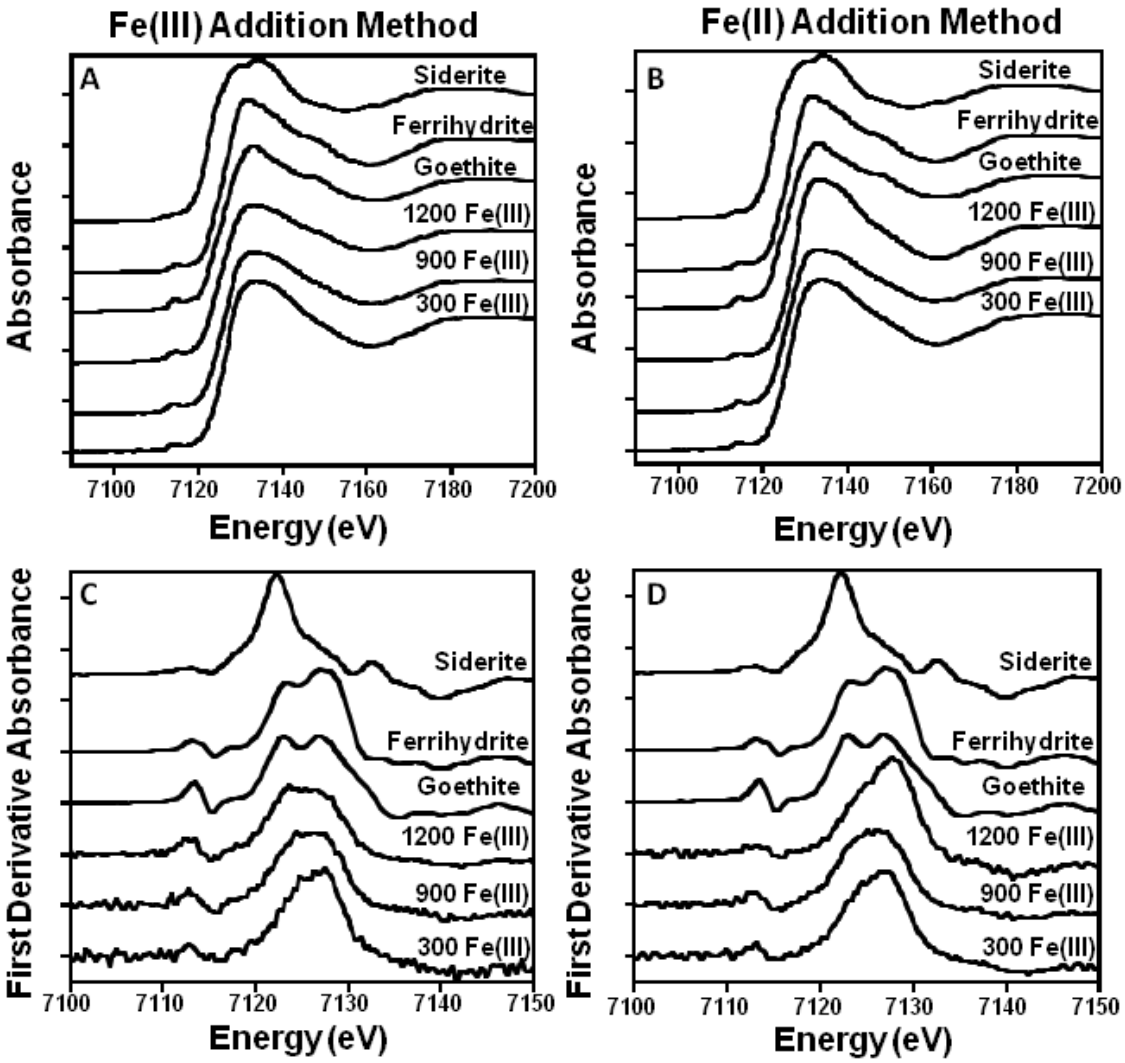

Figure 2.2. Stacked normalized K-edge Fe-XANES (A and B) and first derivative XANES spectra (C and D) from Fe(III) (A and C) and Fe(II) (B and D) methods of Fe(III) binding. Data shown are siderite, goethite, ferrihydrite, and Pahokee peat with 1200 mmol Fe kg^{-1}, 900 mmol Fe kg^{-1}, or 300 mmol Fe kg^{-1}.

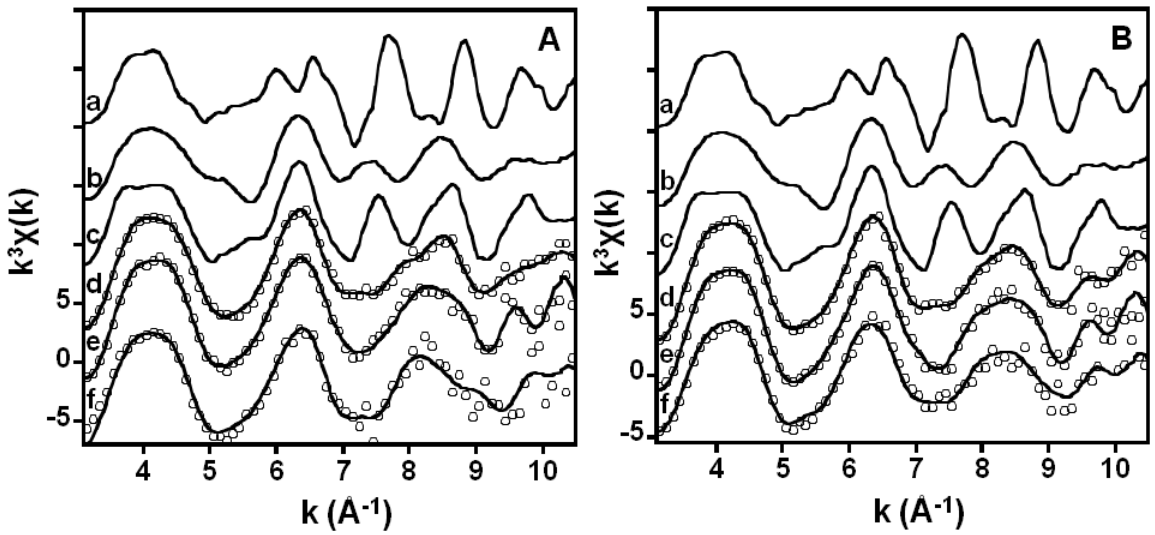

Figure 2.3. Stacked k^3-weighted Fe-EXAFS spectra (circles) for (A) Fe(III) addition and (B) Fe(II) addition for (a) siderite, (b) ferrihydrite, (c) goethite, (d) 1200 mmol Fe kg^{-1} peat, (e) 900 mmol Fe kg^{-1} peat, and (f) 300 mmol Fe kg^{-1} peat. Solid lines overlaid on peat samples are EXAFS fitting models. Standards are presented as solid lines.

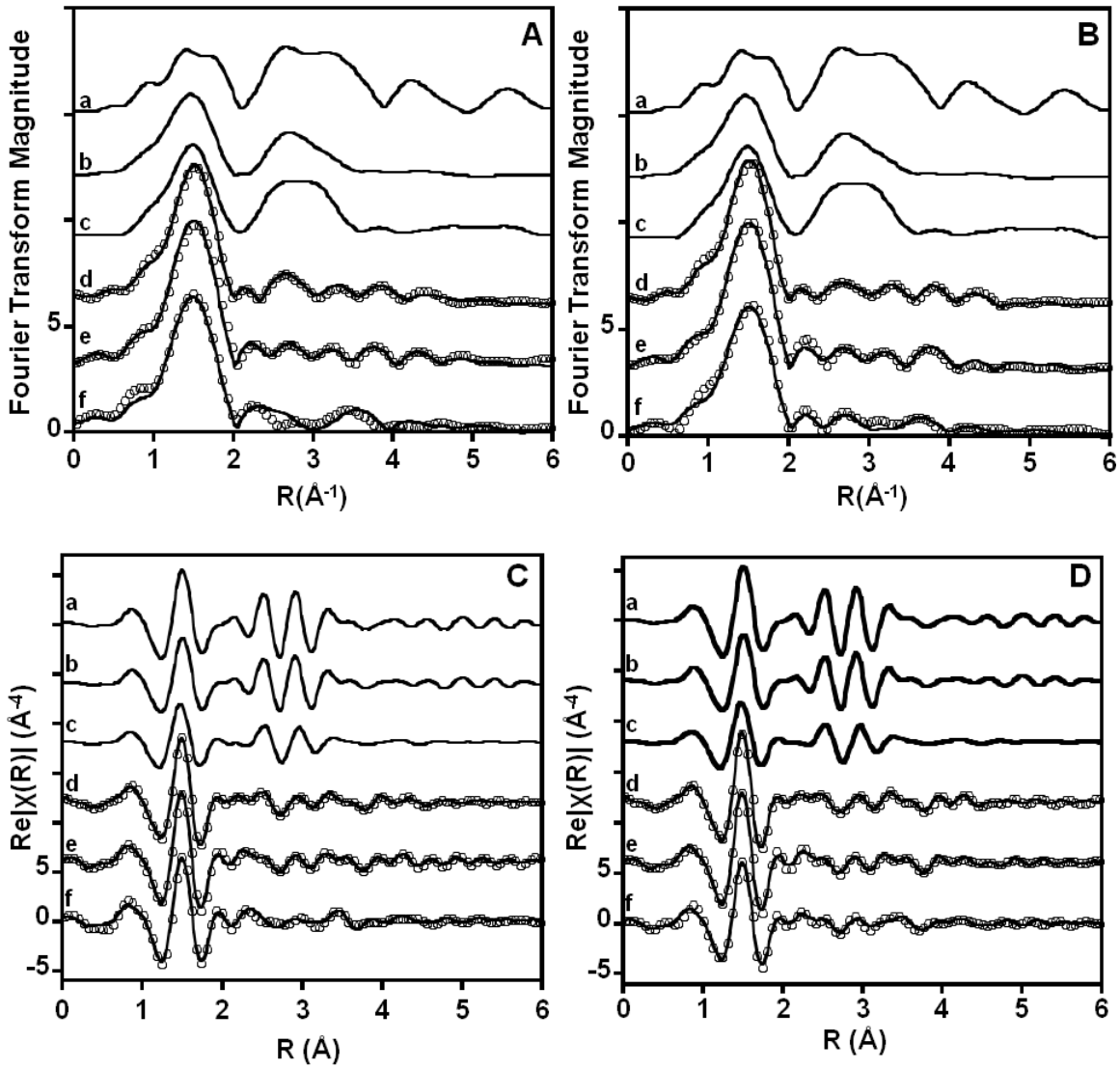

Figure 2.4. Stacked k^3-weighted Fourier transform magnitude (A and B) and real data (C and D) for the Fe(III) addition method (A and D) and the Fe(II) addition method (B and D) for (a) siderite, (b) ferrihydrite, (c) goethite, (d) 1200 mmol Fe kg^{-1} peat, (e) 900 mmol Fe kg^{-1} peat, and (f) 300 mmol Fe kg^{-1}. Solid lines overlaid on peat samples (circles) are EXAFS fitting models. Standards are represented by solid lines. Distances are not corrected for phase shift.

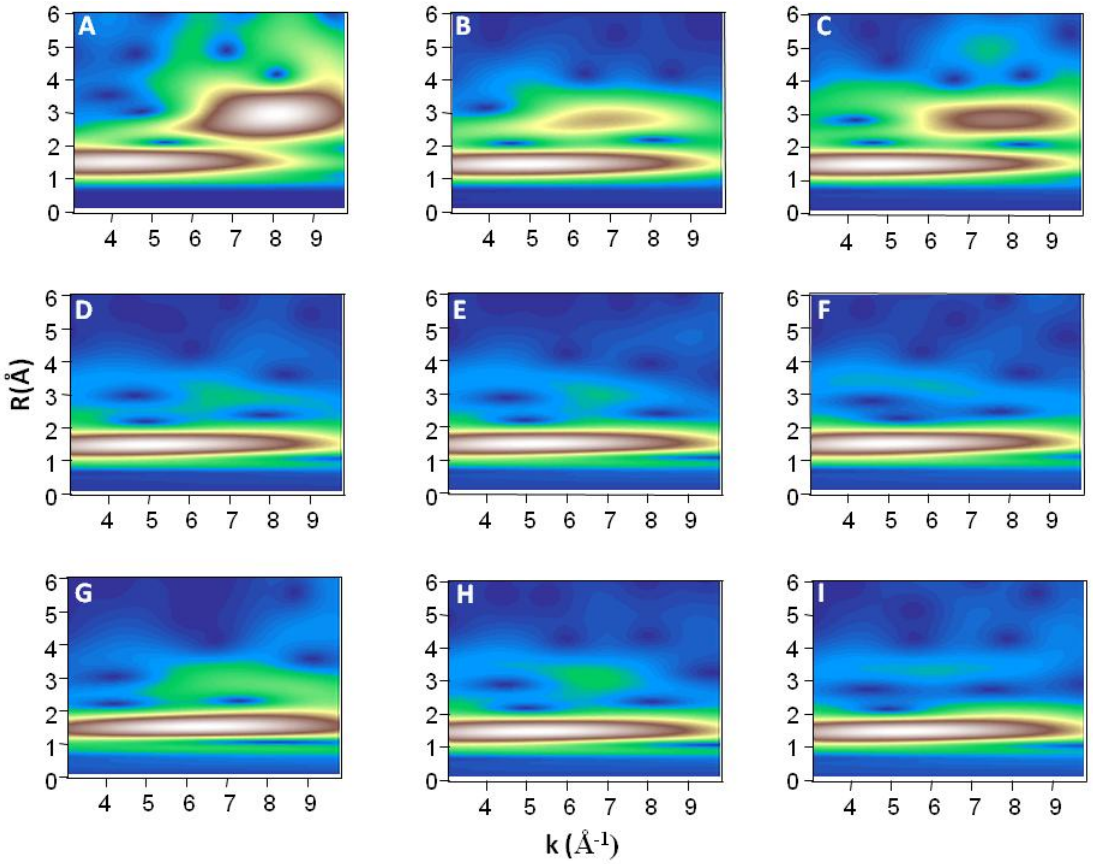

Figure 2.5. Low-resolution Wavelet Transform (WT) modulus (ή = 13, σ = 0.6) displaying the second and third coordination shells for (A) siderite, (B) ferrihydrite, (C) goethite, (D) 1200, (E) 900, and (F) 300 mmol Fe(III) kg^{-1} peat by the Fe(II) addition method, and (G) 1200, (H) 900, and (I) 300 mmol Fe(III) kg^{-1} peat by the Fe(III) addition method.

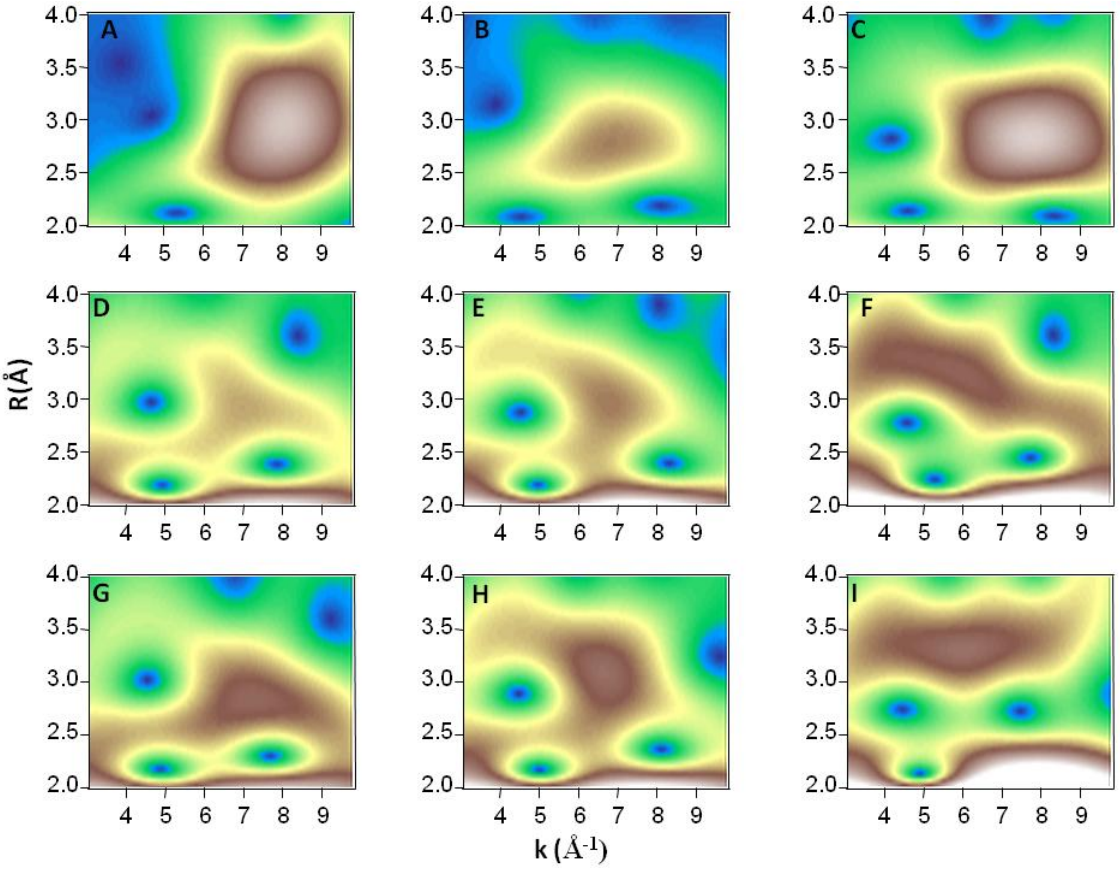

Figure 2.6. High-resolution WT modulus (ή = 8, σ = 1) displaying the second and third coordination shells for (A) siderite, (B) ferrihydrite, (C) goethite, (D) 1200, (E) 900, and (F) 300 mmol Fe(III) kg^{-1} peat by the Fe(II) addition method, and (G) 1200, (H) 900, and (I) 300 mmol Fe(III) kg^{-1} peat by the Fe(III) addition method. Contrast for sample plots was adjusted relative to standard plots to aid in visualization of second and third coordination shells.

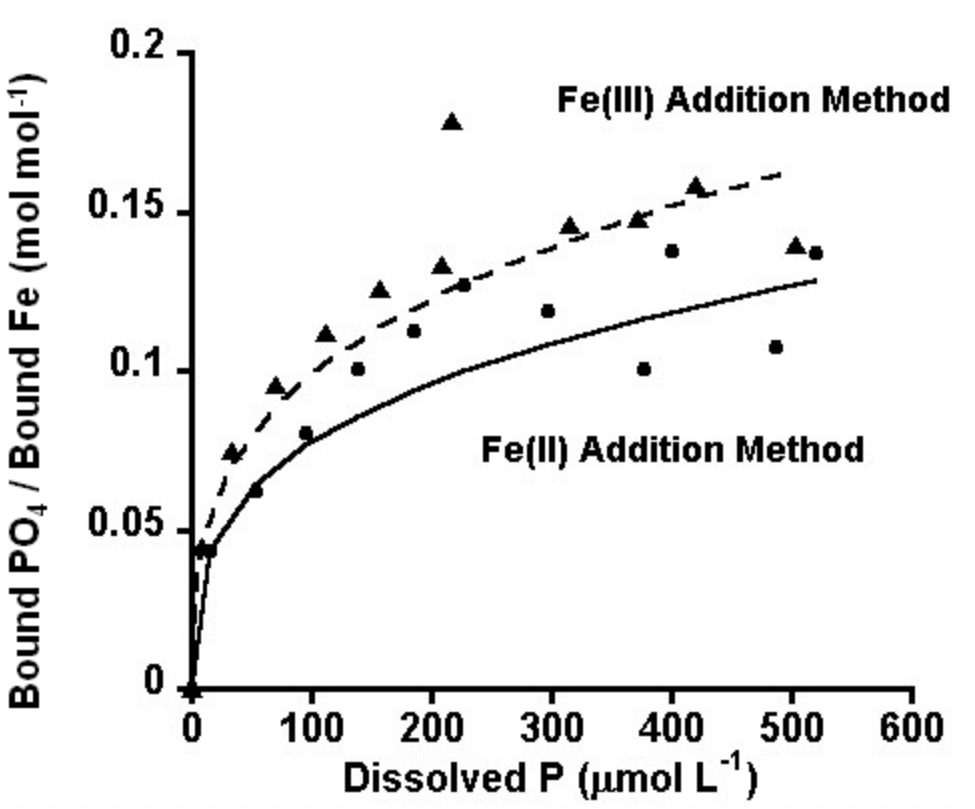

Figure 2.7. Phosphate sorption isotherms conducted at pH 6.8 and 25˚C for Fe(III) and Fe(II) addition methods. Data were fit using the Freundlich model with models of y = 2.5078c*^0.31 r2 = 0.87 for the Fe(II) addition method; and y = 2.01*c^0.31 r2 = 0.90 for the Fe(III) addition method. Since the logarithm of any positive number < 1.0 is negative, the bound PO_4 to bound Fe ratios were multiplied by 100 prior to log transformation and divided by 100 following back-transformation. Models were not statistically different between Fe(III) addition methods.

CHAPTER 3: DISSOLVED ORGANIC CARBON AND pH INFLUENCE PHOSPHATE SORPTION TO ORGANIC MATTER

ABSTRACT

Mobilization of phosphorus from land to surface waters frequently results in eutrophication, which is the nutrient enrichment of aquatic ecosystems that leads to enhanced primary productivity and water quality degradation. Iron(III) reduction, dissolved organic carbon (DOC), and pH potentially impact PO_4 sorption to soils. Organic matter (OM) is often a significant component in soils near surface waters, yet little research has been conducted regarding PO_4 sorption to OM. My objective was to determine the relative effects of pH and DOC on the sorption of PO_4 by soil OM. Phosphate sorption between pH 3 and 8.5 was measured on Pahokee peat containing 1200 mmol kg^1 of pre-sorbed Fe(III) or Al(III), with PO_4 added at 300 or 600 mmol kg^{-1} peat. The pH dependent sorption of PO_4 (mass basis) was characterized by envelopes analogous to adsorption envelopes for Fe- and Al-oxide minerals. Between pH 3 and 8.5, PO_4 sorption decreased from 280 (low P input) or 420 mmol kg^{-1} peat (high P input) to 50 mmol kg^{-1} peat. Phosphate bound to Al-OM showed similar trends, but with maximum sorbed PO_4 of 260 (low P input) and 380 mmol kg^{-1} (high P input) between pH 4.0 and 6.0. The molar ratio of sorbed PO_4 to sorbed Fe or Al decreased from pH 3.0 to 3.5 (from 0.36 to 0.21 or 0.39 to 0.37 in the Fe- and Al-OM high P input systems respectively), and then increased at pH > 6.0 (from 0.20 to 0.24 or 0.38 to 0.58 in Fe- and Al-OM high P input systems respectively). When DOC was kept at < 5 mg L^{-1}, the molar ratios of sorbed PO_4 to sorbed Fe or Al were again analogous to PO_4 sorption

envelopes on Fe- or Al- oxide minerals. These differences were explained by increases in DOC (from 10 to 200 mg L^{-1} between pH 5 and 8.5), and sorbed Fe or Al (maximized at pH 4.5 and from pH 4.0 to 5.0, respectively). Overall, PO_4 sorption was dominantly controlled by pH, with limited influence from DOC at pH > 5.0. These results indicate that pH effects on PO_4 mobilization are more important than DOC effects, however at any given pH, DOC and bound Fe or Al play important roles.

INTRODUCTION

The impacts of soil reduction on PO_4 mobilization from soils are variable. Although enhanced PO_4 mobilization has been documented in a number of anaerobic soils (Ajmone-Marsan et al., 2006; Ann et al., 2000; Holford and Patrick, 1979; Macrae et al., 2005; Newman and Pietro, 2001; Niedermeier and Robinson, 2007; Pant and Reddy, 2001; Young and Ross, 2001), in other soils PO_4 mobilization decreased following soil reduction (Holford and Patrick, 1981; Patrick and Khalid, 1974; Vadas and Sims, 1998; Zhang et al., 2010). For example, in a bottomland hardwood forest, net PO_4 uptake occurred, while in a freshwater marsh, net mobilization occurred following reduction (Masscheleyn et al., 1992). Both Newman and Pietro (2001) and Roden and Edmonds (1997) found that reducing conditions led to P mobilization from soils (and sediments). In contrast, Patrick and Khalid (1974) and Zhang et al. (2010) found increased PO_4 sorption following soil reduction. Heiberg et al. (2010) observed increased or decreased PO_4 sorption after establishment of anoxic conditions, depending on soil type, and hypothesized that increased sorption resulted from the formation of Fe(II)-phosphate minerals such as vivianite. In one study, enhanced P mobilization in rewetted fens only occurred when the surface soil layers consist of highly decomposed peat with an Fe/P molar ratio < 10 (Zak et al., 2010). These contrasting results highlight the need for further research addressing the underlying mechanisms of PO_4 mobilization.

Retention and mobilization of PO_4 in soils is controlled by a number of factors. Generally, PO_4 sorption capacity increases when crystalline Fe(III)-hydroxides are converted to poorly-crystalline Fe(III) hydroxides, which occur in soils that experience reduction-

oxidation cycles (Holford and Patrick, 1981; Patrick and Khalid, 1974; Zhang et al., 2010). However, formation of Fe(II)-phosphates like vivianite also occurs, a process which is easily mistaken for PO_4 adsorption (Brand-Klibanski et al., 2007; Heiberg et al., 2010). Increased PO_4 dissolution during soil reduction has been attributed to (i) mobilization of PO_4 bound to Fe(III) as Fe(III) is reduced and mobilized as Fe(II); (ii) competitive sorption of dissolved organic matter (DOM) displacing PO_4 from soil components by ligand exchange; (iii) increased PO_4 dissolution with a redox-coupled increase in pH, and (iv) formation of ternary DOM-Fe-PO_4 or DOM-Al-PO_4 complexes (Patrick and Khalid, 1974; Roden and Edmonds, 1997; Willett and Cunningham, 1983). Of these mechanisms, the most common explanation for increased P mobilization during anaerobic conditions is the mobilization of Fe(II) from Fe(III)-(hdry)oxide or Fe(III)-PO_4 minerals, with concomitant dissolution of associated PO_4. Nevertheless, the competitive sorption of DOM (Bhatti et al., 1998; Guppy et al., 2005a), the formation of aqueous ternary DOM-Fe-PO_4 or DOM-Al-PO_4 complexes (Guardado, 2008; De Hann, 1990; Shaw et al., 2000), and pH-dependent desorption are also important (Giesler et al., 2005; Guardado et al., 2007; Guardado, 2008).

Organic matter (OM) tends to accumulate in poorly drained soils, and plays a significant role in the cycling of nutrients such as P (Collins and Kuehl, 2001; Stevenson and Cole, 1999). In addition to serving as an energy source for microbial reduction of NO_3^-, Mn-oxides, Fe-oxides, and SO_4^{2-}, OM contains organic phosphorus and sorbs inorganic metal cations, and oxyanions such as $H_2PO_4^-$ (Stevenson and Cole, 1999). The influence of OM on PO_4 sorption in mineral soils has been studied extensively, both by humic substances and humic acids (Bhatti et al., 1998; Borggaard et al., 1990; Borggaard et al., 2005; Easterwood

and Sartain, 1990; Gerke, 1993a; Gjettermann et al., 2007; Guppy et al., 2005a; Hiemstra et al., 2010; Masscheleyn et al., 1992). Macrae et al. (2005) found that dissolved PO_4 concentration was 2 x higher in groundwater from organic soils compared to mineral soils. Several authors observed increased DOC following PO_4 additions to soil, and attributed this increase to competitive sorption of PO_4, which displaces OM into solution (Arbestain et al., 2002; Beck et al., 1999; Bhatti et al., 1998; Giesler et al., 2005; Kaiser et al., 1996). Conversely, competition between DOC and PO_4 sorption sites can enhance PO_4 mobilization. For example, ligand exchange between bound PO_4 and oxalate led to increased PO_4 dissolution in a Florida Spodisol (Bhatti et al., 1998). Similarly, organic acids formed from the decomposition of clover increased the plant availability of PO_4 (Easterwood and Sartain, 1990). In model systems, fulvic acid (FA) competition with PO_4 binding to goethite was greater than that of humic acid (HA), which was hypothesized to result from electrostatic interactions (Weng et al., 2008). Shuai and Zinati (2009) used Weng's (2008) model and determined that the proposed electrostatic interactions did explain the sorption of P and HA on goethite. In contrast, increases in dissolved P in surface and porewater from soils have been attributed to an underestimation of organic P mobilized from decomposition of OM (Guppy et al., 2005a; Guppy et al., 2005b). Despite past research detailing OM effects on PO_4 retention and dissolution in mineral soils, relative contributions of specific PO_4 mobilization mechanisms remain uncertain in organic soils.

Experimental evidence suggests that the formation of PO_4-Fe/Al-OM ternary complexes may occur in soils and surface waters (Bloom, 1981; Gerke, 1992; Gerke and Hermann, 1992). Gerke (1997) showed that Fe- and Al- organic complexes are important in

rhizosphere porewater, and increased with increasing pH. Ultra-filtration of soil porewater solution through 20,000 Da membranes decreased organic carbon, iron, aluminum and inorganic phosphorus concentrations by as much as 50% at pH 5.5 and as much as 10% at pH 3.5 in filtrates, suggesting the existence of aqueous colloidal ternary complexes (Gerke, 1992). Although indirect evidence for the formation of PO_4-Fe-OM or PO_4-Al-OM in soil porewater and surface waters has been documented, indisputable evidence that proves their existence has not.

Several other studies analyzed the pH dependency of PO_4 binding and dissolution in soils (Borggaard et al., 2005; Gerke, 1993a; Gjettermann et al., 2007; Liang et al., 2010). For example, Gerke (1993) found that the maximum PO_4 sorption to humic/Fe-oxide mixtures was higher at pH 4 than 7, which was explained by a higher amount of organically complexed Fe at pH 4.0. Similarly, a decrease in PO_4 sorption to soils at pH $\geq$ 6.0 was attributed to dissolution of organic coatings and increasing electrostatic repulsion by Liang et al (2010). Gjettermann et al. (2007) found that both DOC and dissolved organic phosphorus increased with increasing pH. Overall, previous research suggested that the impacts of pH on PO_4 mobilization are complicated by OM and DOC effects.

Although research has indicated that PO_4 sorption to soils depends in part on pH and DOC, the effects of pH and DOC on PO_4 sorption to soil OM have not been separated previously. The objective of this research was to determine and separate the relative effects of pH and DOM on PO_4 sorption to OM. Quantitative and mechanistic details regarding the binding and dissolution of PO_4 from OM will aid in predicting the effects of soil OM on the PO_4 sorption capacity of both mineral and organic soils.

MATERIALS AND METHODS

Organic Matter Preparation

Details of Pahokee peat preparation are presented in Chapter 2. Prior to use, the hydrated peat was stored at pH 3.0 and 5°C for no more than 5 days. Additionally, DOC was collected from hydrated Pahokee peat for one experiment by bringing the peat to pH 6.0, equilibrating for 24 h, and centrifuging at 1600 x g for 10 min. The supernatant solution was filtered through 0.2 µm Isopore polycarbonate filter membranes (Millipore Corp., Bedford, MA) and DOC was measured.

Phosphate Sorption Envelopes

Peat was suspended in 0.05 M KCl at pH 2.5 prior to Fe(III) or Al(III) additions to achieve hydration. Iron Fe(III) (as $FeCl_3$) or Al(III) (as $AlCl_3$) were added to 1200 mmol metal kg^{-1} peat followed by immediate pH adjustments back to 2.5 using 0.05 M KOH. Samples were sub-divided gravimetrically into 50 mL centrifuge tubes. The pH of each sub-divided sample was then adjusted between 3 and 8.5. To equilibrate samples, tubes were continuously shaken (150 oscillations min^{-1}) for 48 h at 25°C. The pH was adjusted twice daily and at 2 h prior to PO_4 addition by addition of 0.05 M HCl or 0.05 M KOH. Following equilibration, PO_4 (as KH_2PO_4) was added to samples at a level corresponding to 300 or 600 mmol kg^{-1} peat. Samples were then allowed to equilibrate for an additional 48 h, with pH adjustments twice each day and 2 h prior to sample collection. Henceforth, treatments will be referred to as PO_4-Fe-OM or PO_4-Al-OM.

Following the final equilibration, samples were centrifuged at 50,000 x g for 20 minutes. The supernatant solutions were filtered through 0.2µm Isopore polycarbonate filter

membranes (Millipore Corp., Bedford, MA) and aqueous samples were stored in 30 mL polycarbonate bottles for later analysis. Solids were freeze dried for later analysis. Total dissolved Fe in filtered samples was measured by flame atomic absorption spectrometry (FAAS) (Model 3100; Perkin Elmer, Wellesey, MA), and total dissolved Al was measured by ICP spectrometry (Perkin-Elmer ICP-OES 2000DV, Elmer, Germany). Dissolved reactive P (DRP) was analyzed by utilizing the Murphy-Riley colorimetric method (Olsen & Sommers, 1982) with a Shimadzu UV-2101PC scanning UV-visible spectrophotometer at λ=840 nm, and DOC was measured using a Shmadzu TOC-5050 TOC analyzer. Background absorbance of DOC was accounted for in DRP measurements by subtracting the absorbance of a blank sample in which the colorimetric reagents were not added. In all cases, the absorbance of the background was < 10% of the sample absorbance. The total concentrations of Fe, Al, and P bound to peat were determined by subtraction of measured dissolved concentrations from the initially added total concentrations of Fe(III), Al(III) or P.

Competitive DOC Sorption

Six sub-samples each of PO_4-Fe-OM and PO_4-Al-OM, prepared as described above, were spiked with DOC solutions to achieve DOC concentrations from 0 to 200 mg DOC L^{-1}. Samples were equilibrated for 48 hours, and supernatant solutions were analyzed as above for total dissolved Al, total dissolved Fe, dissolved reactive PO_4, and DOC.

pH Effects

In order to study pH effects separate of DOC effects, Pahokee peat was washed with 2,000 mL of 0.05 M KCl in 200 mL increments at pH 8.5. Following these washes, the peat was suspended in 0.05 M KCl and adjusted to pH 3.0. Less than 10% of the total peat was

removed during the washing procedure. Sorption envelopes were then conducted on 1200 Fe mmol Fe kg^{-1} peat and 1200 mmol Al kg^{-1} peat with both 300 and 600 mmol P kg^{-1} peat. Dissolved PO_4, dissolved Fe/Al and DOC were measured as above.

Size Fractionation

Selected filtrates (< 0.02µm) from the third replicate of PO_4 sorption envelope experiments were filtered again to separate non-colloidal PO_4 from colloidal PO_4-DOM complexes. Here we classify the non-colloidal fraction in filtrates as < 5,000 Da and the colloidal fraction in filtrates as > 100,000 Da. Samples chosen consisted of PO_4-Fe-OM with 600 mmol P kg^{-1} peat at pH 3.0, 4.0, 5.0, 6.0, 7.0, and 8.0, and PO_4-Al-OM with 600 mmol P kg^{-1}peat at pH 3.0, 3.5, 4.0, 5.0, 6.5, and 8.0, respectively. Following 0.2 µm filtration, samples were separated by using 15 mL Vivaspin centrifugal concentrators with 5,000, 10,000 and 100,000 Da molecular weight cut-off polyethersulfone membranes (Sartorius VS0413, VS0403, VS0443). All membranes were washed by centrifuging at 1080 x g for 30 min with 0.5 M NaOH / 250 ppm NaOCl, followed by DI water (Wu et al., 2006). Filters were kept moist in DI water until used. Filtrates were then analyzed as above for dissolved PO_4, DOC, and total Fe and Al.

FTIR

The freeze-dried M-OM and PO_4–M-OM complexes were prepared for Fourier transformed infrared spectroscopy (FTIR) spectroscopy by mixing 0.2 mg sample with 500 mg of KBr dried for 2 h. at 70˚C, and pressing the mixture into a pellet. Infrared spectra (32 scans) were recorded on pellets with a Nicolet Nexus 470 FTIR spectrometer over the 4000 – 400 cm^{-1} range.

RESULTS AND DISCUSSION

Phosphate Sorption Envelopes

The pH-dependent sorption of PO_4 added at 300 and 600 mmol PO_4 kg^{-1} to Fe(III)- and Al(III)-OM is shown in Figure 1, along with a control in which no PO_4 was added. Phosphate bound to Fe-OM (Figure 3.1 A) decreased between pH 3.5 and 8.5 from 280 mmol kg^{-1} peat (low PO_4 input) and 420 mmol kg^{-1} peat (high PO_4 input) to 50 mmol kg^{-1} peat. In the Al-OM system, PO_4 sorption showed similar trends, but with a maximum sorbed PO_4 concentration between pH 4.0 to 6.0 of 260 mmol kg^{-1} peat (low PO_4 input) and 380 mmol kg^{-1} peat (high PO_4 input) (Figure 3.1 B). Dissolved P from control experiments indicated a maximum residual PO_4 contribution from the peat of 6% and 3% of total dissolved P in the 300 and 600 mmol P kg^{-1} OM systems respectively. Overall, trends indicated that PO_4 sorption in Fe and Al bound to OM was pH dependent, similar to sorption envelopes on Fe and Al (hydr)oxides (Huang, 1975; Huang, 2009). For example, Huang et al. (2009) found that adsorption of PO_4 on aluminum oxides gave maximum adsorption at pH 4 while PO_4 adsorption on an Fe-oxide (hematite) was maximized at pH < 3.0. Despite these similarities, PO_4 sorption to Fe and Al bound to OM is expected to be more complex due to changes in bound Fe and Al and DOC with pH.

Dissolved organic carbon increased with increasing pH in both Fe and Al treatments, from a nearly-constant concentration of 10 mg L^{-1} between pH 3 and 5, up to 200 mg L^{-1} at pH 8.5 (Figure 3.1 C and D). No significant differences in DOC were determined between Fe and Al treatments, or between treatments with different PO_4 concentrations. These results suggested that PO_4 sorption depended on both pH and DOC. Because DOC is constant at pH

$\leq$ 5.0, DOC impacts are expected to be minimal at pH $\leq$ 5.0. At pH > 5.0, however, both pH and DOC effects potentially contribute to decreasing PO_4 sorption with increasing pH. Because DOC concentration is also pH-dependent, the interactions between pH and DOC complicate the interpretation of the PO_4 sorption envelopes.

Bound metal concentration potentially contributed to trends in PO_4 sorption as well. Bound Fe was maximized at 1200 mmol Fe kg^{-1} peat at pH 4.5 and decreased by 130 mmol kg^{-1} peat at pH < 4.5 (Figure 3.1 E). Similarly, bound Al was maximized between pH 4.0 and 5.0, and decreased by 600 mmol Al kg^{-1} peat from pH 4.5 to 3.0 (Figure 3.1 F). Dissolved Fe and Al also increased linearly with increasing DOC (Figure A3.1), indicating a potential interrelated impact on PO_4 sorption. Because PO_4 sorption decreased at pH < 4.5 in the PO_4-Al-OM treatments, and DOC was minimum at pH < 4.5 (< 10 mg L^{-1}), results suggested that pH effects on OM and Al chemical speciation caused the decrease in PO_4 sorption at pH < 4.5. In contrast, PO_4 sorption continued to increase at pH < 4.5 in the PO_4-Fe-OM treatments, indicating that, despite the decrease in bound Fe (130 mmol kg^{-1} peat), the net resultant pH effects on PO_4 and Fe chemical speciation at pH < 4.5 enhanced PO_4 sorption.

The molar ratio of bound P/Al and bound P/Fe are shown in Figure 3.2. The ratios of bound P/Fe were between 0.12 and 0.40 mol P mol^{-1} Fe higher than the ratios of bound P/Al. The Fe samples showed greater increase in bound PO_4/Fe ratio at pH > 6.0 than the Al samples, increasing from a molar P/Fe ratio of 0.26 to 0.43 (low PO_4 input) and 0.39 to 0.58 (high PO_4 input). Conversely, the Al samples showed a greater decrease in bound PO_4/Al ratio at pH 3.0 to 4.0, decreasing from a molar P/Al ratio of 0.28 to 0.15 (low PO_4 input) and 0.36 to 0.21 (high PO_4 input). Overall, these data show that PO_4 sorption per mol Fe and Al

increased as pH increased > 6.0 and decreased < 4.0. In comparison, bound Fe, Al, and PO_4 all decreased at pH > 6.0, and bound Al and PO_4 decreased at pH < 4.0 (Figure 3.1). Equation 3.1 displays an example of the complexation of PO_4^{3-} by an $–FeOH^{1/2-}$ surface (modified from Gustafsson, 2006). Here, the pH dependency of this reaction indicates that PO_4 sorption to Fe would decrease with increasing pH. Conversely, according to chemical equilibrium principles, an increase in dissolved PO_4 relative to solid phase Fe would alter the reaction equilibrium toward the formation of complexed PO_4.

$$-FeOH^{1/2-}_{(s)} + 3H^{+}_{(aq)} + PO_4^{3-}_{(aq)} \leftrightarrow -FeOPO_3H_2^{1/2-}_{(s)} + H_2O_{(l)}$$

$$\text{Log } K = 32.51 \qquad \text{Equation 3.1}$$

Thus, the increase in P/Fe ratio at pH > 6.0 was potentially due to higher dissolved PO_4 relative to Fe-OM sorption sites. Dissolved OC also increased at pH > 6.0, but would be expected to decrease rather than increase PO_4 sorption.

Overall, three main parameters potentially contributed to the trends in PO_4 sorption across pH, including; (i) pH induced electrostatic interactions, (ii) DOC, and (iii) bound Fe and Al concentration. These effects are interrelated, and as such that they cannot be easily separated to determine the relative contributions of each effect. For example, increasing pH can impact the solubility of Fe and Al and increase DOC. Equation 3.1 shows the equilibrium reaction for amorphous $Fe(OH)_3$ dissolution in the absence of OM.

$$Fe(OH)_3 + 3H^{+} \leftrightarrow Fe^{3+} + 3H_2O \qquad \log K = 3.54 \qquad \text{Equation 3.1}$$

Here, as pH decreases, the reaction equilibrium is driven toward product formation (dissolved Fe^{3+}). In fact, as pH decreases from 6 to 3, the solubility of $Fe(OH)_3$ increases up to 9 fold. In addition, the hydrolysis species of Fe is expected to transition from $Fe(OH)^{+2}$ to $Fe(OH)_2^+$ to $Fe(OH)_4^-$ as pH increases from 3 to 8, which would impact Fe sorption to OM. Here, because the formation of Fe or Al (hydr)oxides is not expected, it is unclear to what extent increasing pH plays in the coordination environment of Fe-OM or Al-OM. Despite these limitations, pH, DOC, and bound Fe and Al effects may be separated by experiments which hold DOC, pH or bound Fe and Al constant.

DOC, pH, and bound Fe and Al Effects on PO_4 Sorption

Dissolved PO_4 increased with DOC across both Fe and Al treatments (Figure 3.3). The increase in dissolved PO_4 with DOC was 2-fold higher in the 600 mmol P kg^{-1} OM treatments than in the 300 mmol P kg^{-1} treatments, highlighting PO_4 concentration effects on sorption in the presence of DOC. Between pH 6 and 8.5, where DOC increased from approximately 10 to 200 mg L^{-1}, dissolved PO_4 increased linearly with DOC in both Fe and Al systems (average $r^2 = 0.97$). In the Fe systems, dissolved PO_4 was also increased with DOC from pH 3 to 6 (average $r^2 = 0.88$), however in the Al systems increase was found from pH 4 to 6 (average $r^2 = 0.05$). These trends indicated the potential dependence of sorbed PO_4 on DOC.

To determine the impacts of pH on PO_4 sorption in the absence of DOC, the experiment on extensively washed peat in which DOC was minimized to < 5 mg L^{-1} was used. Figure 3.4 displays sorption envelopes for Fe and Al treatments with either 600 or 300

mmol P kg^{-1} peat. In the Al treatments, P sorption was identical regardless of pH and DOC, indicating that pH effects, which controlled the chemical speciation of Al and PO_4 and the bound concentration of Al, controlled PO_4 sorption (Figure 3.4). In the Fe treatments, PO_4 sorption was up to 140 mmol P kg^{-1} peat lower in experiments were DOC was minimized, which suggested that DOC enhanced PO_4 sorption (Figure 3.4). One way that DOC could potentially decreased PO_4 sorption is by inhibiting the formation of Fe-oxides above pH 5.0 (Schwertmann, 1966). Chapter 2 showed that Fe bound to OM was in the form of mononuclear Fe-OM or polynuclear Fe-OM clusters. In the absence of DOC, the formation of Fe-oxides would potentially decrease availability of PO_4 sorption sites. It is not clear, however, based on existing data, if the formation of Fe-(hydr)oxides contributed to the decrease in PO_4 sorption in these experiments. Overall, the trend in PO_4 sorption did not change in the absence of DOC, indicating that pH effects on PO_4 sorption dominated over DOC effects.

In addition, at pH < 5.0, bound Fe and Al concentrations were similar to those in experiments with DOC present (Figure 3.5), however at pH $\geq$ 5, bound Fe and Al did not decrease in the absence of DOC. Thus DOC rather than pH had controlled Fe and Al binding at pH $\geq$ 5.0, (Figure 3.5). As suggested earlier in equation 3.1, decreasing pH leads to increased solubility of Fe and Al. At pH < 5.0 trends in bound metal and PO_4 concentrations in the absence of DOC were the same, thus both bound Fe or Al and pH influenced PO_4 sorption. Despite the dominant pH effects on PO_4 sorption, changing total Fe(III) or Al(III) concentration at any given pH would be expected to alter PO_4 sorption. This effect, however, is not demonstrated here.

In experiments were DOC was minimized, as pH and dissolved PO_4 increased, the ratio of bound P/Fe decreased (Figure 3.6). Figure 3.6 depicts the decreasing Fe/P and Al/P ratios from 0.21 and 0.50 to 0.04 and 0.11 respectively. These data contrast those from PO_4 sorption envelopes in which DOC was present because the P/Fe ratio decreases consistently across pH. Because bound Fe or Al concentrations were constant at pH > 4.0, the decrease in bound P/Fe and P/Al ratios with increasing pH results solely from dissolved PO_4 concentration and chemical speciation transitions across pH. This data supports the previous conclusion that increasing dissolved PO_4 relative to solid Fe/Al phase resulted in higher P/Fe ratios at pH $\geq$ 6.0 in the Fe systems and pH $\leq$ 4.0 in the Al systems.

In a separate experiment at pH 6.0, dissolved PO_4 (added at 600 and 300 mmol P kg^{-1} peat) increased with added DOC in both Fe and Al treatments (Figure 3.7). Although the rate of increasing dissolved PO_4 with DOC was identical between Fe(III) and Al(III) treatments at pH 6.0, the intercept was 80 µmol L^{-1} lower for the Al(III) peat treatment. Additionally, the positive slope between dissolved PO_4 and DOC was 1.3-fold higher for the 600 mmol P kg^{-1} peat treatments relative to the 300 mmol P kg^{-1} peat treatments. The greater slope of the regression model for the 600 mmol P kg^{-1} peat treatment indicates that DOC had a greater impact at the higher bound PO_4 concentration, consistent with competitive sorption mechanisms between PO_4 and DOM.

The slope of increasing PO_4 sorption with DOC in initial PO_4 sorption experiments (Figure 3.3) was higher, compared to the slope of increasing PO_4 sorption with DOC in pH 6.0 experiments where DOC was added (Figure 3.7). By comparing the slopes between the initial PO_4 sorption envelopes and the experiment where DOC was added, it was estimated

that at maximum, 26 and 44% of PO_4 dissolution resulted from increasing DOC rather than pH in the 600 and 300 mmol P kg^{-1} systems respectively. These results support the previous conclusion that PO_4 sorption was predominantly controlled by pH. The experiment in which DOC was minimized to < 5 mg L^{-1}, however, indicated no difference in PO_4 sorption at high pH, which suggests that adding DOC at pH 6.0 overestimated the impact of DOC on PO_4 sorption. In any case, increasing DOC and pH led to decreased PO_4 sorption. Another factor that potentially contributes to decreased PO_4 sorption at pH $\geq$ 5.0 is the formation of colloidal PO_4< 0.2µm.

Beyond competitive sorption mechanisms, the formation of PO_4-Fe/Al-DOM complexes could also lead to decreased PO_4 sorption with increasing DOC. Separation of colloidal (> 100,000 Da) from non-colloidal (< 5,000 Da) PO_4, DOC, and dissolved Fe and Al showed that 94.5 $\pm$ 10% of Fe and 81 $\pm$ 9.5% of OC passing through a 0.2 µm filter was colloidal (Figure 3.8). Similarly, 87 $\pm$ 17% of Al and 90 $\pm$ 1.0% of DOC passing through a 0.2 µm filter was colloidal (Figure 3.8 F and D). In contrast, colloidal PO_4 accounted for only 16 $\pm$ 5.9% of total PO_4 that passed through a 0.2 µm filter in the PO_4-Fe-OM system (Figure 3.8 A) and 10 $\pm$ 4% in the PO_4-Al-OM system (Figure 3.8 B) at pH > 4. Overall, > 75% of PO_4 (< 0.2µm) was not associated with Fe, Al, and DOC in the colloidal fraction. Furthermore, as DOC increased, the formation of colloidal PO_4 complexes was observed. Although the formation of Fe/Al-PO_4 or ternary PO_4-Fe/Al-OM complexes was a potential mechanism for increasing PO_4 mobilization at pH > 5.0, the majority of PO_4 was in the non-colloidal form. In addition, Figure A3.2 shows the partitioning of dissolved and colloidal PO_4 in DOC addition experiments. Here, it is evident that PO_4 mobilization due to the addition of

DOC was nearly 100% in the colloidal fraction > 10,000 Da. These results are in agreement with previous studies that provided evidence for the formation of ternary PO_4 complexes in environmental systems, however direct proof was not obtained (Guardado et al., 2007; De Hann et al., 1990; Gerke, 2010).

FTIR

To determine if Fe(III) and Al(III) were bound to carboxylic functional groups in the OM and if the formation of PO_4-Fe/Al-OM ternary complexes occurred FTIR was used (Appendix 2). Although the binding of Fe(III) or Al(III) to carboxylic functional groups was evident in all samples, no significant trends were identified between Fe/Al-OM and PO_4-Fe/Al-OM systems. A peak at 1033 cm^{-1} increased with addition of PO_4, corresponding to the ν_{as} of P-O. Although in certain cases the position of this peak shifted to higher wavenumber (e.g. From 1033 to 1096 cm^{-1}) data were not consistent enough to determine the bonding environment of P in OM. Thus, although the presence of ternary complexes was suggested based on solution chemistry, direct proof was not obtained by FTIR spectroscopy.

Combined pH, DOC Impacts on PO_4 and Fe/Al Speciation

Overall, as pH increased, PO_4 sorption decreased due to changes in the protonation states of Fe/Al and PO_4. In addition, at pH $\geq$ 5.0, the pH induced production of DOC resulted in decreased bound Fe and Al, in turn decreasing the number of PO_4 sorption sites. Although the increase in DOC led to additional PO_4 mobilization by competitive sorption reactions and < 0.2µm colloidal PO_4 complex formation, pH effects predominantly controlled PO_4 sorption. In contrast, DOC controlled bound Fe and Al concentrations at pH $\geq$ 5.0.

Figure 3.9 depicts the partitioning of Fe/Al and PO_4 between potential dissolved and solid phases in a PO_4 sorption experiment at pH 6.0. Here, 50% of PO_4 was dissolved, with only 5% present as complexed PO_4 colloidal complexes (potentially as PO_4-Fe/Al-OM or PO_4-Fe/Al). In addition, 90% of Fe(III) or Al(III) was bound at pH 6.0, with the remaining 10% in the form of Fe(III) and Al(III) colloidal complexes. The proportion of PO_4 present in PO_4 colloidal complexes increases with increasing pH along with increasing colloidal Fe(III) and DOC.

CONCLUSIONS

Overall, changes in PO_4 sorption across pH were attributed to a combination of three predominant mechanisms: (i) changes in Fe, Al, and PO_4 protonation and resulting binding affinity (ii) changes in bound Fe and Al concentration, and (iii) pH induced DOC production at pH > 5.0. In the absence of DOC, PO_4 sorption at pH $\geq$ 5.0 was lower than, or equivalent to PO_4 sorption in the presence of DOC, indicating that PO_4 sorption was predominantly controlled by changes in Fe, Al, and PO_4 protonation with pH. Dissolved OC induced dissolution of PO_4 was 1.3-fold lower at pH 6.0 than the combined DOC and pH effects, providing further evidence that pH effects predominantly controlled PO_4 sorption. Although PO_4 sorption tended to decrease with decreasing bound Fe and Al at pH > 5.0, a comparison with experiments where DOC was excluded and Fe and Al remained constant at pH 5.0 indicated that bound Fe/Al had little effect on total PO_4 sorption at pH > 5.0. In contrast, results showed that bound Fe and Al at pH $\geq$ 5.0 decreased as DOC increased. As DOC was added to PO_4-OM, additional colloidal PO_4 < 0.2 µm and > 5,000 Da was mobilized, indicating that the formation of colloidal PO_4 potentially contributed to PO_4 mobilization. Combined effects of pH, DOM, and bound Fe or Al on organic-matter bound inorganic PO_4 need to be considered in order to quantitatively predict and prevent PO_4 dissolution from organic soils, and transport into open water bodies. Although pH effects were dominant, DOM and bound Fe/Al concentrations also impact PO_4 sorption at any given pH.

BIBLIOGRAPHY

Ajmone-Marsan F., D. Cote, and R.R. Simard. 2006. Phosphorus transformations under reduction in long-term manured soils. Plant Soil. 282:239-250.

Ann Y., K.R. Reddy, and J.J. Delfino. 2000. Influence of redox potential on phosphorus solubility in chemically amended wetland organic soils. Ecol. Eng. 14:169-180.

Arbestain M.C., M.E. Barreal, and F. Macias. 2002. Phosphate and sulfate sorption in spodosols with albic horizon from Northern Spain. Soil Sci. Soc. Am. J. 66:464-473.

Bauer M., C. Blodau. 2009. Arsenic distribution in the dissolved, colloidal and particulate size fraction of experimental solutions rich in dissolved organic matter and ferric iron. Geochimica Et Cosmochimica Acta 73, 529-542.

Beck M.A., W.P. Robarge, and S.W. Buol. 1999. Phosphorus retention and release of anions and organic carbon by two Andisols. Eur. J. Soil Sci. 50:157-164.

Bhatti J.S., N.B. Comerford, and C.T. Johnston. 1998. Influence of oxalate and soil organic matter on sorption and desorption of phosphate onto a spodic horizon. Soil Sci. Soc. Am. J. 62:1089-1095.

Bloom P.R. 1981. Phosphorus adsorption by an aluminum-peat complex. Soil Sci. Soc. Am. J. 45:267-272.

Borggaard O.K., S.S. Jorgensen. J.P. Moberg, and B. Rabenlange. 1990. Influence or organic-matter on phosphate adsorption by aluminum and iron-oxides in sandy soils. J. Soil Sci. 41:443-449.

Borggaard O.K., B. Raben-Lange, A.L. Gimsing, and B.W. Strobel. 2005. Influence of humic substances on phosphate adsorption by aluminium and iron oxides. Geoderma. 127:270-279.

Brand-Klibanski S., M.I. Litaor, and M. Shenker. 2007. Overestimation of phosphorus adsorption capacity in reduced soils: An artifact of typical batch adsorption experiments. Soil Sci. Soc. Am. J. 71:1128-1136.

Buffle, J., K.J. Wilkinson, S. Stoll, M. Filella, and J.W. Zhang. 1998. A generalized description of aquatic colloidal interactions: the three-colloidal component approach. Enviorn. Sci. Technol. 32:2887-2899.

Collins M.E., and R.J. Kuehl. 2001. Organic matter accumulation and organic soils. pp. 137-162. *In.* J. L. Richardson and M. J. Vepraskas (Eds.), Wetland Soils: Genesis, hydrology, landscapes, and classification. Lewis Publishers, Washington D.C.

De Haan, H., R.I. Jones, and K. Salonen. 1990. Abiotic interactions of iron and phosphate in humic lake water revealed by double-isotope labelling and gel filtration. Limnol. Oceanogr. 35:491-497.

Djafer, M., R.K. Khanda, and M. Terce. 1991. Interactions between different anions and the goethite surface as seen by different methods. Colloid Surf. 54:209-218.

Easterwood G.W., and J.B. Sartain. 1990. Clover residue effectivness in reducing orthophosphate sorption on ferric hydroxide coated soil. Soil Sci. Soc. Am. J. 54:1345-1350.

Gerke J. 1992. Orthophosphate and organic phosphate in the soil solution of 4 sand soil solution in relation to pH-evidence for humic-Fe-(Al-) phosphate complexes. Commun. Soil Sci. Plant Anal. 23:601-612.

Gerke J. 1993a. Phosphate adsorption by humic/Fe-oxide mixtures aged at pH-4 and pH-7 and by poorly ordered Fe-oxide. Geoderma 59:279-288.

Gerke J. 1993b. Solubilization of Fe(III) from humic-Fe complexes, humic Fe-oxide mixtures and from poorly ordered Fe-oxide by organic-acids - consequences for P-adsorption. Z. Pflanzenernahr. Bodenkd. 156:253-257.

Gerke J. 1997. Aluminum and iron(III) species in the soil solution including organic complexes with citrate and humic substances. Z. Pflanzenernahr. Bodenkd. 160:427-432.

Gerke J., and R. Hermann. 1992. Adsorption of orthophosphate to humic-Fe complexes and to amorphous Fe-oxide. Z. Pflanzenernahr. Bodenkd. 155:233-236.

Giesler R., T. Andersson, L. Lovgren, and P. Persson. 2005. Phosphate sorption in aluminum- and iron-rich humus soils. Soil Sci. Soc. Am. J. 69:77-86.

Gjettermann B., M. Styczen, S. Hansen, O.K. Borggaard, and H.C.B. Hansen. 2007. Sorption and fractionation of dissolved organic matter and associated phosphorus in agricultural soil. J. Environ. Qual. 36:753-763.

Guardado I., O. Urrutia, and J.M. Garcia-Mina. 2007. Size distribution, complexing capacity, and stability of phosphate-metal-humic complexes. J. Agric. Food. Chem. 55:408-413.

Guardado I., O. Urrutia, and J.M. Garcia-Mina. 2008. Some structural and electronic features of the interactions of phosphate with Metal-humic Complexes. J. Agric. Food. Chem. 56:1035-1042.

Guppy C.N., N.W. Menzies, P.W. Moody, and F.P.C. Blamey. 2005a. Competitive sorption reactions between phosphorus and organic matter in soil: a review. Aust. J. Soil Res. 43:189-202.

Guppy C.N., N.W. Menzies, F.P.C. Blamey, and P.W. Moody. 2005b. Do decomposing organic matter residues reduce phosphorus sorption in highly weathered soils? Soil Sci. Soc. Am. J. 69:1405-1411.

Heiberg L., T.V. Pedersen, H.S. Jensen, C. Kjaergaard, and H.C.B. Hansen. 2010. A comparative study of phosphate sorption in lowland soils under oxic and anoxic conditions. J. Environ. Qual. 39:734-743.

Hiemstra T., J. Antelo, A.M.D. van Rotterdam, and W.H. van Riemsdijk. 2010. Nanoparticles in natural systems II: The natural oxide fraction at interaction with natural organic matter and phosphate. Geochim. Cosmochim. Acta. 74:59-69.

Holford I.C.R., and W.H. Patrick. 1979. Effects of reduction and pH changes on phosphate sorption and mobility in an acid soil. Soil Sci. Soc. Am. J. 43:292-297.

Holford I.C.R., and W.H. Patrick. 1981. Effects of duration of anaerobiosis and reoxidation on phosphate sorption characteristics of an acid soil. Aust. J. Soil Res. 19:69-78.

Huang C.P. 1975. Adsorption of phosphate at the hydrous ψ-Al_2O_3-Electrolyte interface. J. Colloid Interface Sci. 53:178-186

Huang X., G.D. Foster, R. V. Honeychuck, and J.A. Schreifels. 2009. The maximum of phosphate adsorption at pH 4.0: why it appears on aluminum oxides but not on iron oxides. Langmuir 25:4450-4461.

Hutchison K.J., and D. Hesterberg. 2004. Dissolution of phosphate in a phosphorus-enriched ultisol as affected by microbial reduction. J. Environ. Qual. 33:1793-1802.

Jones, R.I., P.J. Shaw, and H. De Haan. 1993. Effects of dissolved humic substances on the speciation of iron and phosphate at different pH and ionic strenght. Environ. Sci. Technol. 27:1052-1059.

Kaiser K., G. Guggenberger, and W. Zech. 1996. Sorption of DOM and DOM fractions to forest soils. Geoderma 74:281-303.

Lead, J.R. and K.J. Wilkinson. 2007. Environmental colloids and particles: current knowledge and future developments. p. 1-16 *In*. Environmental Colloids and Particles, vol. 10. K.J. Wilkinson and J.R. Lead ed. John Wiley and Sons. New York. NY.

Liang, X.Q., J. Liu, Y.X. Chen, H. Li, Y.S. Ye, Z.Y. Nie, .M.M. Su, and Z.H. Xu. 2010. Effect of pH on the release of soil colloidal phosphorus. J. of Soil and Sediments. 10:1548-1556.

Macrae M.L., T.E. Redding, I.F. Creed, W.R. Bell, and K.J. Devito. 2005. Soil, surface water and ground water phosphorus relationships in a partially harvested Boreal Plain aspen catchment. For. Ecol. Manage. 206:315-329.

Masscheleyn P.H., J.H. Pardue, R.D. Delaune, and W.H. Patrick. 1992. Phosphorus release and assimilatory capacity of 2 lower Mississippi valley fresh-water wetland soils. Water Resour. Bull. 28:763-773.

Newman S., and K. Pietro. 2001. Phosphorus storage and release in response to flooding: implications for Everglades stormwater treatment areas. Ecol. Eng. 18:23-38.

Niedermeier A., and J.S. Robinson. 2007. Hydrological controls on soil redox dynamics in a peat-based, restored wetland. Geoderma 137:318-326.

Olsen S.R., L.E. Sommers. 1982. Phosphorus, in: A. L. Pate (Ed.), Methods of soil analysis. Part 2. 2nd ed., ASA and SSSA, Madison, WI.

Pant H.K., and K.R. Reddy. 2001. Phosphorus sorption characteristics of estuarine sediments under different redox conditions. J. Environ. Qual. 30:1474-1480.

Patrick W.H., and R.A. Khalid. 1974. Phosphate release and sorption by soils and sediments-effects of aerobic and anaerobic conditions. Science 186:53-55.

Roden E.E., and J.W. Edmonds. 1997. Phosphate mobilization in iron-rich anaerobic sediments: Microbial Fe(III) oxide reduction versus iron-sulfide formation. Archiv Fur Hydrobiologie 139:347-378.

Schwertmann U., 1966. Inhibitory effect of soil organic matter on crystalization of amorphours ferric hydroxide. Nature. 212:645-646.

Schwertmann, U., and R.M. Taylor. 1977. Iron Oxides. pp. 145-193. *In.* Dixon, J.B. and S.B. Weed (Ed.), Minerals in soil environements. SSSA, Madison WI. USA.

Shaw P.J., R.I. Jones, and H. De Haan. 2000. The influence of humic substances on the molecular weight distributions of phosphate and iron in epilimnetic lake waters. Freshwater Biol. 45:383-393.

Shuai X.F., and G. Zinati. 2009. Proton Charge and Adsorption of Humic Acid and Phosphate on Goethite. Soil Sci. Soc. Am. J. 73:2013-2020.

Stevenson, F.J., and M.A. Cole. 1999. Cycles of Soil: Carbon, Nitrogen, Phosphorus, Sulfur, Micronutrients. John Wiley & Sons. New York.

Stevenson F.J., and G.F. Vance, 1989. Naturally occurring aluminum-organic complexes, pp. 118-142.*Iin*: G. Sposito (Ed.), The environmental chemistry of aluminum, CRC Press Inc New York, NY.

Vadas P.A., and J.T. Sims. 1998. Redox status, poultry litter, and phosphorus solubility in Atlantic Coastal plain soils. Soil Sci. Soc. Am. J. 62:1025-1034.

Weng L.P., W.H. Van Riemsdijk, and T. Hiemstra. 2008. Humic Nanoparticles at the Oxide-Water Interface: Interactions with Phosphate Ion Adsorption. Environ. Sci. Technol. 42:8747-8752.

Willett, I.R., and R.B. Cunningham. 1983. Influence of sorbed phosphate on the stability of ferric hydrous oxide under controlled pH and Eh conditoins. Aus. J. Soil Res. 21:301-308.

Wu Y., A. Ahmed, R. Waghmare, and D. Kahn. 2006. Cleaning polyethersulfone membranes after ultrafiltration-diafiltration in monoclonal antibody production. BioPharm International 19.

Young E.O., and D.S. Ross. 2001. Phosphate release from seasonally flooded soils: A laboratory microcosm study. J. Environ. Qual. 30:91-101.

Zabinsky, S.L., J.J. Rehr, A. Ankundinov, R. Albers, and M.J. Eller. 1995. Multiple scatterinc calculations of X-ray absorption spectra. Phys. Rev. B 52:2995-3009.

Zak D., C. Wagner, B. Payer, J. Augustin, and J. Gelbrecht. 2010. Phosphorus mobilization in rewetted fens: the effect of altered peat properties and implications for their restoration. col. Appl. 20:1336-1349.

Zhang W., J.W. Faulkner, S.K. Giri, L.D. Geohring, and T.S. Steenhuis. 2010. Effect of Soil Reduction on Phosphorus Sorption of an Organic-Rich Silt Loam. Soil Sci. Soc. Am. J. 74:240-249.

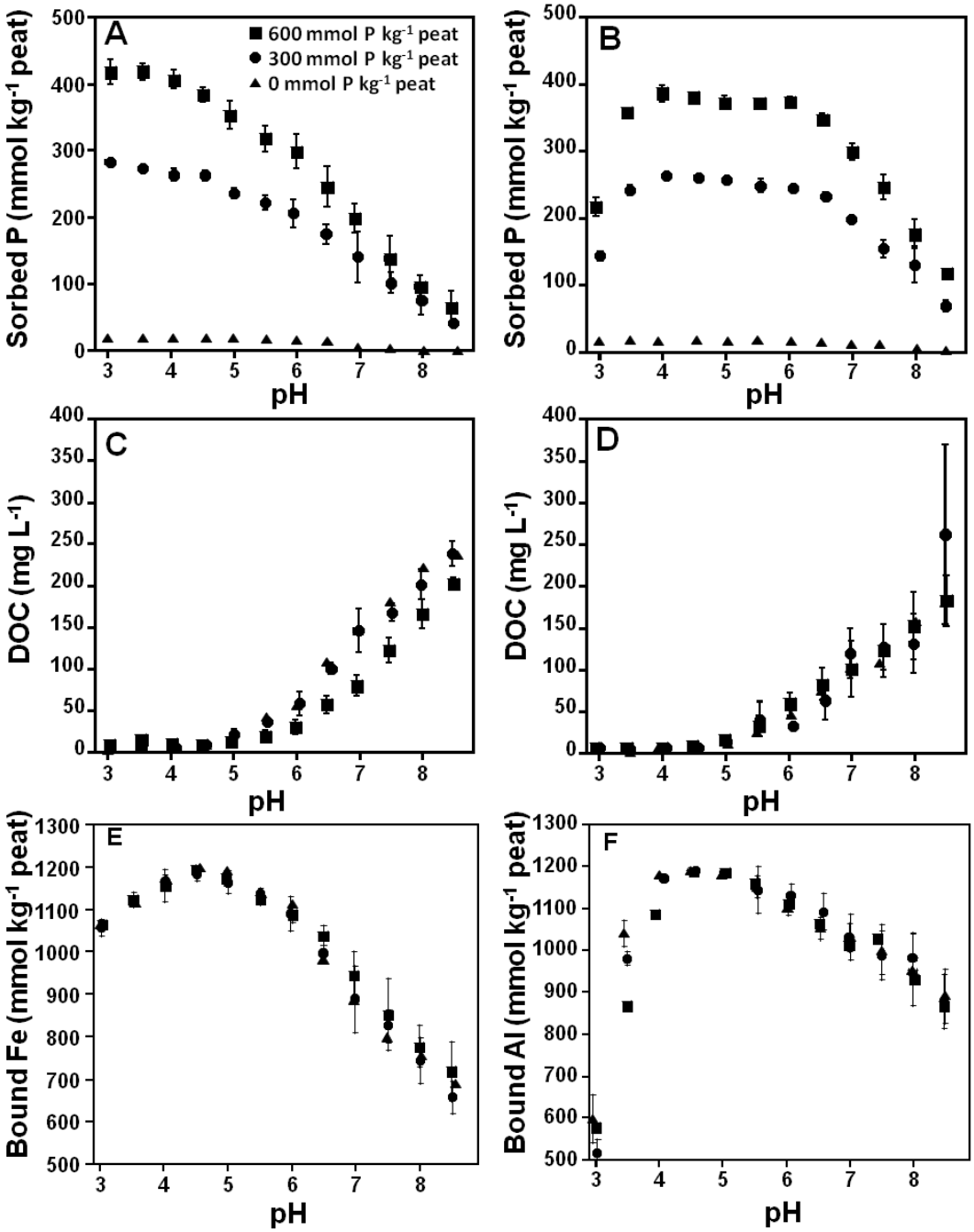

Figure 3.1. Phosphorus sorption (A and B), Dissolved Organic Carbon (DOC) (C and D), and bound metal (E and F) with increasing pH for Fe (left) and Al (right) treatments. Data are presented along with the control in with 0 mmol P kg^{-1} peat.

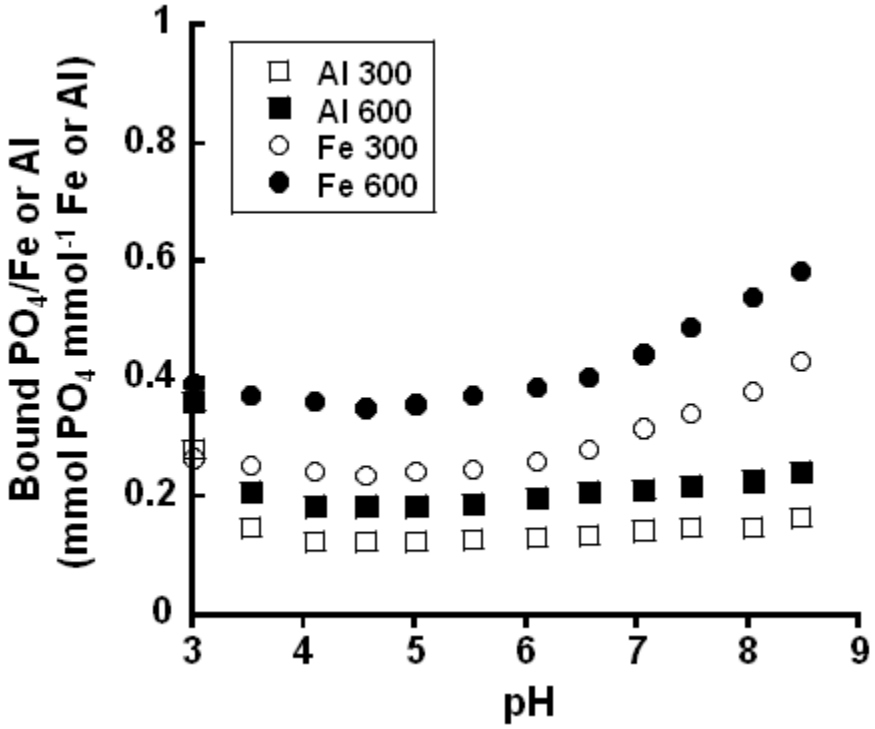

Figure 3.2. pH-dependent sorption of PO_4 in Pahokee peat suspensions of 1 g kg^{-1} containing 1200 mmol Fe or Al, and KH_2PO_4 added at 300 or 600 mmol kg^{-1} peat.

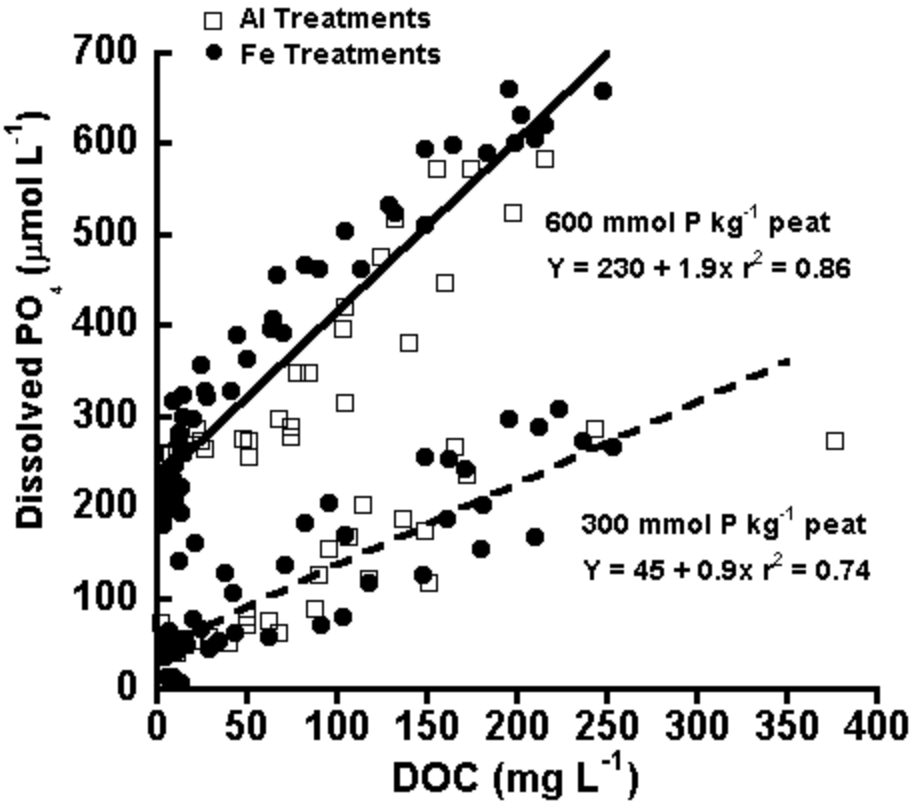

Figure 3.3. Linear models display increasing dissolved PO_4 with dissolved organic carbon (DOC) in both 1200 mmol Fe kg^{-1} peat and 1200 mmol Al kg^{-1} peat.

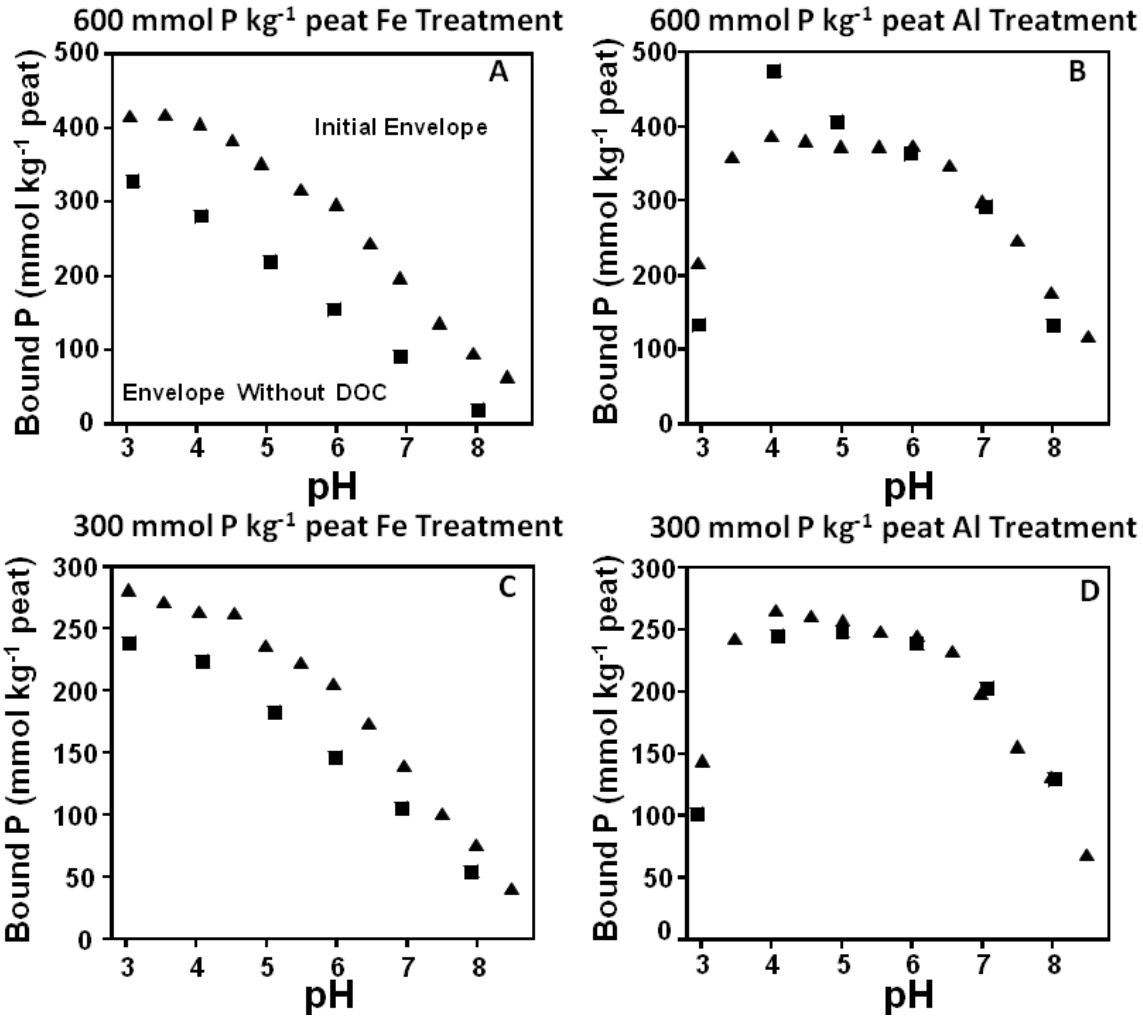

Figure 3.4. Phosphorus sorption in DOC depleted experiments where DOC was reduced to < 5 mg L^{-1} by washing peat prior to Fe, Al and PO_4 addition are compared to P sorption of initial envelope experiments containing DOC in the Fe-OM (A and C), and the Al-OM (B and D) treatments.

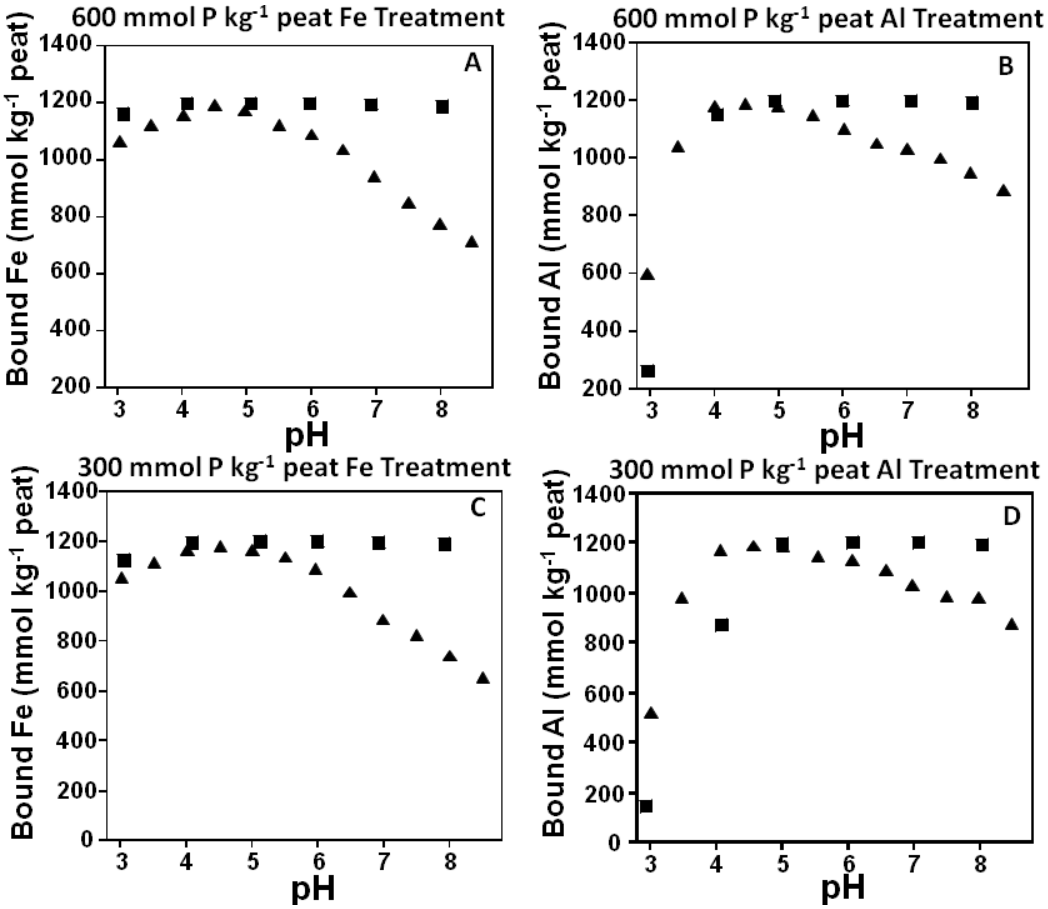

Figure 3.5. Fe (A and C) and Al (B and D) sorption to peat in DOC depleted experiments were DOC was < 5 mg L^{-1} compared to Fe and Al sorption to peat in initial envelope experiments containing DOC.

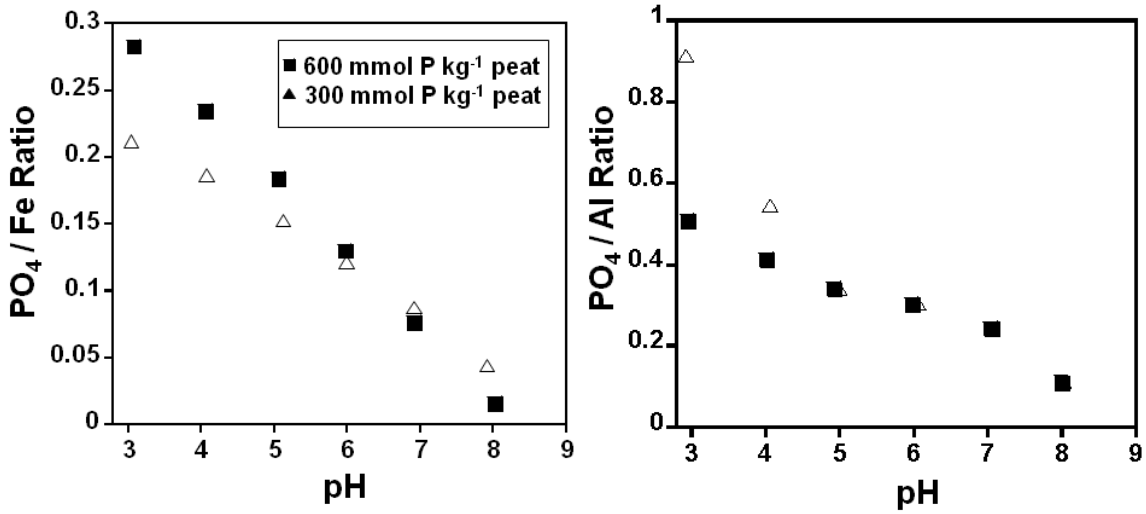

Figure 3.6. Ratio of bound P to bound Fe (left) or Al (right) across pH in DOC depleted experiments containing < 5.0 mg DOC L^{-1} was minimized for 600 mmol P kg^{-1} peat and 300 mmol P kg^{-1} peat treatments.

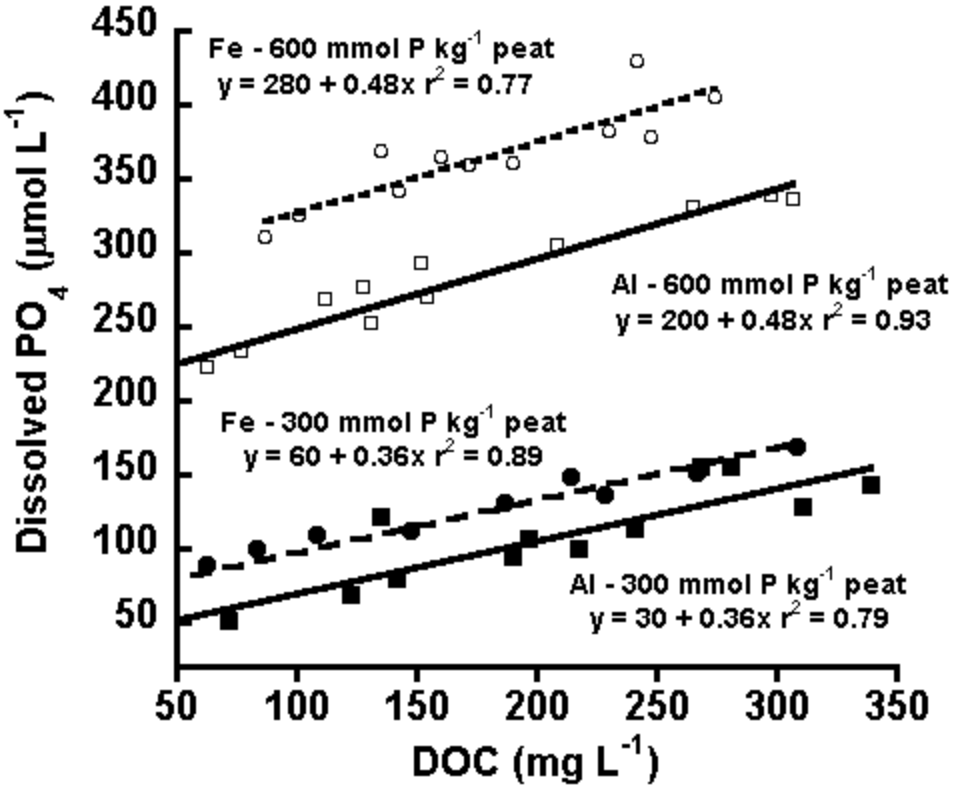

Figure 3.7. Dissolved PO_4 increased with dissolved organic carbon when the DOC was added to both Fe and Al treatments of peat with added PO_4 at 300 and 600 mmol PO_4 kg^{-1} peat at pH 6.0.

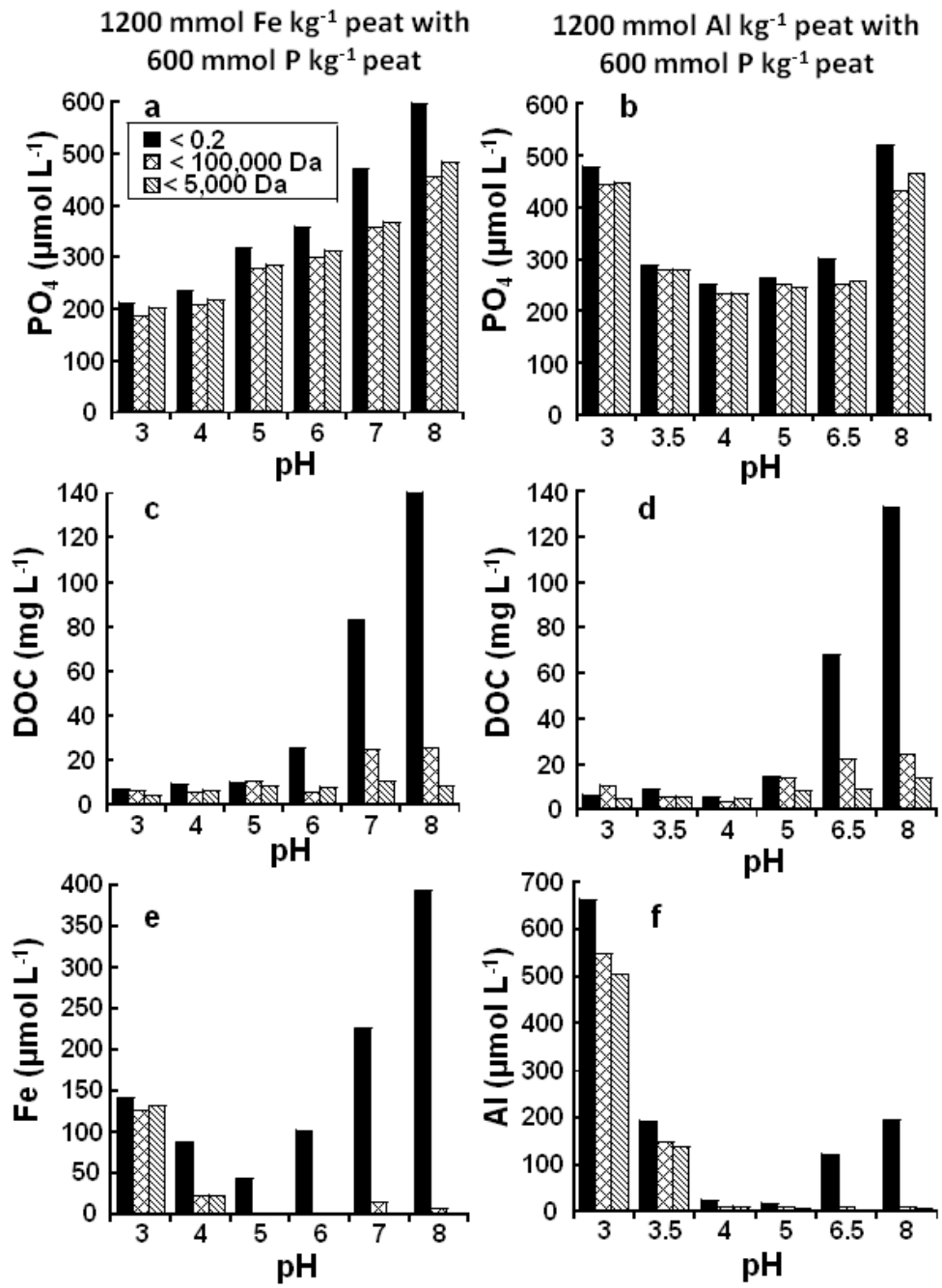

Figure 3.8. Dissolved PO_4, DOC, and Fe or Al after filtration through 0.2 µm, 100,000 Da and 5,000 Da filters across pH.

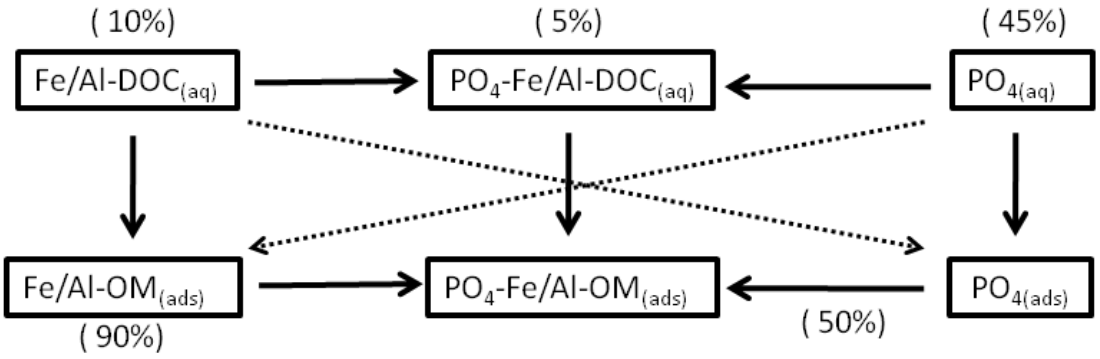

Figure 3.9. Schematic representation of speciation of PO_4 and bound metal at pH 6.0 in systems containing 1200 mmol Fe/Al kg^{-1} peat, and 600 mmol PO_4 kg^{-1} peat. Here, 50% of PO_4 was aqueous (< 0.2 µm) with 5% bound in ternary complexes while the remaining 50% was bound to OM. Similarly, 90% of Fe and Al were bound to OM with only 10% in the < 0.2 µm fraction.

CHAPTER 4: MODELING PO_4 BINDING TO Fe AND Al LADEN ORGANIC MATTER

ABSTRACT

Mobilization of inorganic orthophosphate (PO_4) from soils and transport to open water bodies often leads to water quality degradation. Organic soils are often near open water bodies and wetlands, thus predicting PO_4 mobilization from organic soils will aid in quantifying potential threats to water quality. The objective of this research was to determine if the Three-Plane CD-MUSIC (TPCD) model in Visual MINTEQ could accurately model the impacts of pH and dissolved organic matter (DOM) on the retention of inorganic PO_4 by soil organic matter (OM). Two different models were used here, Model 1 - the Stockholm Humic Model (SHM) to model Fe and Al binding to peat, and Model 2 - the TPCD to model PO_4 sorption to Fe and Al in OM. The SHM model accurately predicted Fe and Al sorption to Pahokee peat across all pH values (root mean square error (rmse) < 36 µmol Fe kg^{-1} peat). The TPCD model along with a sorbed RO^- component to simulate competition between DOM and PO_4 for Fe/Al sorption sites was used to model PO_4 sorption to Fe/Al-OM. The TPCD model was able to accurately predict PO_4 sorption to Fe-OM, but not to Al-OM. Overall, results indicated that the TPCD model within Visual MINTEQ was capable of modelling PO_4 sorption to Fe bound to OM. Overall, results demonstrated the potential for using the TCPD model in Visual MINTEQ to accurately predict and manage PO_4 sorption and dissolution in soil OM.

INTRODUCTION

Predicting phosphorus mobilization from soils remains a significant challenge despite recent research advances. To accurately predict and define mechanisms of P retention across variable soil types, an understanding of P retention to various components of soils, including specific mineral and organic components is needed. Although several studies have modeled inorganic PO_4 sorption to soils (Abou Nohra, 2007; Jiao, 2008; Devau, 2009; Gustafsson, 2001; Goldberg and Sposito 1984b) and inorganic PO_4 sorption to a variety of minerals (Hiemstra, 1996; Frau, 2008; Goldberg and Sposito, 1984a), the applicability of these models to soils containing high concentrations of OM remains remain unknown. Retention of both organic and inorganic PO_4 by organic matter (OM) is generally accepted to be a result of a combination of mechanisms, including; 1. Remnants of residual bound PO_4 remaining from un-decomposed organic materials (Fellman, 2007; Wang, 2010; Fisher, 2010), 2. Organic matter association serving as peptizing agents for inorganic colloids containing iron and PO_4 (Shapiro, 1967), and 3. The formation of Fe and Al bridges between the organic functional groups and PO_4 (Bloom, 1981; Schnitzer M., 1972; Gerke, 1992; Buschmann, 2006; Shaw, 2000). Despite our current knowledge, quantitatively predicting the retention of inorganic PO_4 by OM remains a challenge. Modeling PO_4 sorption to OM will improve our knowledge regarding mechanisms of PO_4 binding to OM, as well as aid in predicting the PO_4 sorption capacity of organic soils.

Phosphate binding to soils has been shown to depend on pH (Wisawapipat, 2009), amount and form of Fe and Al (Strahm, 2007; Igwe, 2010), oxidation state (Newman, 2001; Roden, 1997; Zhang, 2010; Heiberg, 2010), and amount and form of OM (Zhang, 2010;

Negassa, 2008; Hua, 2008; Groenenberg, 2010). The predominant ion binding groups found in humic acid (HA) and fulvic acid (FA) are phenolic and carboxylic functional groups, although nitrogen and sulfur groups can also play a role in binding Fe and Al (Koopal, 2005). Several models have been used to predict metal sorption onto OM, including: the nonideal competitive adsorption model (NICA) (Koopal, 1994), the NICA-Donnan model (Kinniburgh, 1999), Model V (Tipping, 1994), Model VI (Tipping, 1998), the Stockholm Humic Model (SHM) (Gustafsson, 2001b), the Windermere Humic Aqueous Model for soils and sediments (WHAM-S - which contains Model V) (Tipping, 1994), and the Ligand and Charge Distribution model (LCD) (Weng, 2008). Both Model VI and the NICA-Donnan models were successfully used by Weber et al., (2006) to describe pH and concentration dependence of Fe sorption to insoluble humic acid. Conversely, Groenenberg et al., (2010) found that variability in binding properties of humic substances (HS) and DOM lead to great uncertainties when modeling metal binding to HS with the NICA-Donnan and Model VI models. The WHAM-S model was used to model solution pH and Al in organic and mineral soil horizons from forested sites in Norway, Germany, and Spain (Lofts, 2001). The SHM model has also shown great promise when applied to cation binding to humic substances, and has been used to model both Fe and Al to OM, (Gustafsson, 2003;Gustafsson, 2007).

In regards to anion binding to soils, the constant capacitance model (Stumm et al., 1980) was successfully used by Goldberg and Sposito (1984b) to model PO_4 adsorption to non-calcareous soils using PO_4 packing parameters adapted from reference hydrous oxide minerals. Furthermore, both Jiao et al. (2008) and Abou Nohra et al. (2007) successfully modeled PO_4 binding to agricultural and natural soils using the NICA model. Devau et al.

(2009) employed the NICA 1-pK Triple Plane, ion-exchange, and NICA-Donnan models using an additive approach to determine the plant availability of PO_4 in the surface horizon of a Cambisol. The potential for inorganic PO_4 mobilization from highly organic soils, however, has not been successfully modeled, despite the frequent occurrence of organic soils in close proximity to open water bodies.

Gustafsson (2006) accurately predicted DOM competition with AsO_4 sorption to soils by using an irreversibly sorbed component (RO), which represented bound OM, into the Three-Plane CD-MUSIC model. It remains to be determined if the incorporation of the RO^- factor may be successfully applied to other systems, such as that of PO_4 binding to Fe/Al-OM complexes. Using Visual MINTEQ to model PO_4 sorption to soil OM containing Fe and Al with an emphasis on both DOC and pH effects has not been conducted previously. A successful model would identify possible chemical properties that could be altered to diminish PO_4 dissolution and transport from organic soils to surface waters, and guide experimental research to determine mechanisms affecting PO_4 binding to and mobilization from soil OM. The objective of this study was to determine if the TPCD model could accurately predict the impacts of pH and DOM on the retention of inorganic PO_4 by soil OM.

MATERIALS AND METHODS

Adsorption Envelopes

The preparation and analysis of PO_4 sorption envelopes of Fe- and Al- bound to OM were obtained from Chapter 3, and are not described here.

Peat Titration

Titration of acid-washed Pahokee peat stock suspension (unpublished) was conducted by K. Hutchison. Titrations were performed in triplicate on 25 mg of peat while stirring under $N_{2(g)}$. Standardized 0.1 M KOH was added to bring the suspension to pH 11.0 and 0.1 M KCl was added to bring the suspension to a total of 20 mL. Stepwise additions of 0.1 M HCl were used to bring the pH to 3.0. A forward titration was then performed with 0.1M KOH to pH 11.0, followed by a backward titration to pH 3.0. After each stepwise acid or base addition, samples were allowed to equilibrate for a minimum of 20 s before recording pH. Blank titrations were also performed in triplicate on 0.1 M KCl solutions. Total acidity (-Z) in $mmol_c\ g^{-1}$ at any given titration point was calculated using forward titrations based on equation 4.1, where V_s and V_b correspond to volume of sample and blank, M_b corresponds to molarity of base, and W_s corresponds to the solid mass of peat (g).

$$\text{Total acidity } (mmol_c\ g^{-1}) = (V_s - V_b) \times M_b/W_s(g) \qquad \text{Equation 4.1}$$

Modeling

Acid - Base Modeling

In order to utilize the TPCD model, first the amount of bound Fe and Al in OM needs to be quantified or predicted. Although bound Fe and Al were measured, we also tested the use of the SHM for predicting Fe and Al sorption to OM. The SHM is an integrated part of the chemical equilibrium model Visual MINTEQ version 3.0 (Gustafsson et al., 2005; Gustrafsson, 2010). Briefly, the SHM is a discrete-ligand model with seven adjustable parameters in which the HA or FA is assumed to have eight proton-binding sites with different acid-base characteristics (Gustafsson, 2003). A summary of SHM parameters is presented in Table 4.1. As a first approximation in modeling the proton binding properties of Pahokee peat, titration data were used to optimize the SHM parameters. Average model parameters were adjusted by minimizing the root-mean-square error (*rmse*) between modeled and actual data through trial and error (Gustafsson 2003; Gustafsson, 2001b). Specifically, Pahokee peat titration data were used to adjust the amount of proton-dissociating sites (mol g^{-1}) (n), log K values for type A and B sites along with their respective distribution terms ΔpK_A and ΔpK_B, and the gel fraction parameter g_f (Table 4.1). Activity corrections in the model were made using the Davies equation. The input DOC and solid OM concentrations were adjusted at each pH according to actual measured DOC, and solid concentrations were calculated by equation 4.2 (Collins, 2001). A known concentration of 1 g L^{-1} of Pahokee peat was used, thus solid phase OM was calculated by subtracting DOM from added OM.

$$\% \text{ Soil DOM} = 1.724\% * \text{DOC} \qquad \text{Equation 4.2}$$

Initial and final model parameters are listed in Table 4.2. The default "typicalFA" database was used to represent the dissolved active OM content (Gustafsson, 2010). The ratio of active DOM to DOC was kept at the default value of 1.4 (Bryan, 2002), with the percent of active DOC that was FA was set to 75% (Gustafsson, 2005).

Bound Fe and Al

Because the bound metal concentrations at any given pH were nearly identical between 300 and 600 mmol P kg^{-1} peat treatments, they were averaged prior to modeling data. To account for aqueous and solid phase complexation, solution speciation was calculated using the thermodynamic data in the Visual MINTEQ database, which is largely derived from the NIST Critical Stability constants (Table 4.3) (Smith et al., 2003; Gustafsson 2006). The constants of the default Visual MINTEQ database (typicalFA and typicalHA) were used along with the adjusted SHM parameters (above). While these parameters provided a good fit for Fe binding, a new complex, $HA_2Al(OH)_2^-{}_{(s)}$ was needed to adequately describe Al binding across pH (Table 4.3). The new Al log K value was adjusted by trial and error to minimize the *rmse.* For an accurate model, the log K value had to be adjusted to 13.5, which was higher than the previously determined log K values shown in Tables 4.4 and 4.5.

Dissolved organic carbon and solid OM were set at measured values at each pH, while total (dissolved + bound) metal concentration was held constant at the added concentration of 1200 µmol L^{-1}. Although speciation calculations indicated that the systems were supersaturated with respect to ferrihydrite and goethite at pH $\geq$ 3 for the Fe system and

$Al(OH)_3$ at pH > 4 for the Al system, no specified mineral phases were allowed to precipitate in Visual MINTEQ beyond complexation to OM.

Surface Complexation modeling

The 1pK Three-Plane (TP) model with the CD-MUSIC option (CD) (collectively called TPCD) was used here because of its successful application in modeling AsO_4 sorption to soils containing OM and DOC (Gustafsson, 2006) and PO_4 sorption to goethite (Hiemstra and Van Riemsdijk, 1996). The TPCD model is a sub-model of the chemical equilibrium program Visual MINTEQ (Gustafsson, 2005; Gustafsson 2006). A detailed description of the TPCD model may be found in Hiemstra and van Riemsdijk (2006), and is briefly described here. In the TP model, three electrostatic planes (0, 1, and 2 or *d*-pane) separate inner-sphere and outer-sphere complexes, which enclose two empty layers in terms of charge, each with its own electrostatic capacitance (Figure 4.1) (Hiemstra and van Riemsdijk, 2006). Classically, ion adsorption has been based on the solution side of the interface in which ions are treated as point charges (Hiemstra and van Riemsdijk, 1996). The classical Gouy-Chapman treatment of the diffuse double layer is an example of this. In contrast, on the interface side, the concept of charge distribution introduced by Pauling in 1929 (Pauling, 1929) is used. The CD MUSIC model combines both of these concepts (Hiemstra and Riemsdijk, 1996). The CD-MUSIC model (Figure 4.1) treats outer sphere complex formation of oxyanions as point charges and inner sphere complex formation of oxyanions using a charge distribution concept (Hiemstra and Van Riemsdijk, 2006). The acid-base characteristics of each surface site are described with only one reaction, and adsorbing ions

can be positioned on any of the three different surface planes, while allowing their valence to be spread over two adjacent planes (Gustafsson 2006).

Here, several assumptions are used in the TPCD model, which need to be carefully considered prior to forming detailed models and drawing conclusions. Generally, the binding of orthophosphate anions to Al- or Fe-OM is hypothesized to be similar to the binding of PO_4 to Fe/Al (hydr)oxides where H_2PO_4 or HPO_4^{2-} anions exchange with metal-bound OH^- or H_2O via ligand exchange (Gerke, 1992). In fact, here Fe(III) bound to peat potentially varied from mononuclear Fe(III) to polynuclear Fe(III)-OM clusters (Chapter 2). The well-defined planar surface used in the TPCD model, however (Fig 4.1), is likely different than the Fe/Al surfaces in my PO_4-Fe/Al-OM systems (Figure 4.2). Figure 4.2 depicts one hypothesized model for Fe/Al binding to OM. In this case, the Fe/Al surface is not continuous and is rather heterogeneous in its distribution across OM. Thus, the use of a continuous surface would not correctly represent the PO_4 binding environment to Fe/Al-OM. Furthermore, OM properties are altered by pH, which in turn potentially alters Fe/Al binding to OM and PO_4 sorption. The use of the TPCD model to predict PO_4 complexation to Fe/Al-OM disregards these potential pH effects on the OM, because the geometry of binding sites is treated like a plane in an Fe- or Al- (hydr)oxide. Despite these limitations, the use of the TPCD model to model PO_4 sorption to OM remains a potentially useful *semi-empirical* first approximation toward developing more accurate models.

Several parameters are outlined in Table 4.6, and are needed to account for differences between the (hydr)oxide model and the Fe/Al-OM model. Instead of calculating surface area (g L^{-1}), the site density was optimized to 0.7 $mmol_c$ $mmol^{-1}$ Fe kg^{-1} suspension

and 0.9 $mmol_c$ $mmol^{-1}$ Al kg^{-1} suspension by trial and error. Surface complexation reactions of PO_4 with Fe- and Al-OM were obtained from Gustafsson (2001a, 2006), and are presented in Table 4.8. These parameters were obtained from ferrihydrite and allophane with a more comprehensive list presented in Table 4.9. The Log K parameters were fit to data from pH 3.0 – 5.0 in the Fe 600 mmol PO_4 kg^{-1} peat treatment of my experiments, and from pH 3.0-5.0 in the Al 300 mmol PO_4 kg^{-1} peat treatment.

In surface complexation models the competition of PO_4 with DOC is generally not accounted for. Recently, a new component, RO^-, was introduced by Gustafsson (2006) that described the competitive sorption of AsO_4 and DOC to soils. This RO^- component is designed to serve as a surrogate to any dissolved organic functional groups that may compete with PO_4 for Fe and Al binding sites. This component does not correctly describe the partitioning of OM between solution and the absorbed phase, but only simulates the competitive effects that dissolved OM may have on the adsorption of anions. Here we use this RO^- component to describe the competition between DOC and OM with PO_4 for sorption sites (Table 4.4). Again, this technique does not account for changes in the partitioning of OM into solid phase or aqueous phase (DOC) across pH, which likely greatly impacts competitive sorption of PO_4. In order to maximize RO^- sorption in the model, the log K value was set to 25 (Gustafsson, 2006). To determine the RO^- concentrations, RO^- was adjusted for the best fit from pH 3.0 to 5.0. Resultant RO^- values were compared with DOC to determine the ratio of DOC to RO^- competition. Here, 1 mg DOC L^{-1} was equivalent to 1 µmol RO^- L^{-1}.

Overall, the advantages of using the surface complexation method with the RO^- factor rather than a method where ternary PO_4-Fe/Al-OM complexes are formed include; (1) the

formation of ternary complexes has not been proven, and no complexation constants have been determined, which makes surface complexation more reasonable than forcing the formation of ternary complexes, (2) PO_4 sorption isotherms can be used to determine the actual number of sorption sites in any given soil or soil organic matter sample, instead of relying on Fe or Al concentrations, and (3) the use of a surface model calibrated with sorption isotherms could be easily used on soils ranging in Fe, Al, and OM content.

Methods Summary

In summary, two different models were used here, Model 1 - the SHM to model Fe and Al binding to peat, and Model 2 - the CD-MUSIC surface complexation model to model PO_4 sorption to Fe and Al in OM. For both models a general summary of methods is presented below.

Model I:

1. Organic matter model parameters including; the amount of proton-dissociating sites (mol g^{-1}) (n), log K values for type A and B sites along with their respective distribution terms ΔpK_A and ΔpK_B, and the gel fraction parameter g_f, were adjusted using peat titration data. Data fitting was carried out by minimizing the *rmse* of the humic charge –Z (mol kg^{-1} HS) by trial and error as described by Gustafsson (2001b).

2. Bound metal to peat was modeled by utilizing default parameters in the "typicalFA" and "typicalHA" databases of Visual MINTEQ. The addition of a new Al complex was used to describe Al binding with the corresponding Log K value adjusted by minimizing *rmse* values by trial and error.

Model II:

1. Surface complexation parameters were assumed to be most similar to those of ferrihydrite and allophone (Gustafsson, 2006) (Table 4.7). The site density was set at 0.7 mmol $mmol^{-1}$ Fe kg suspension and 0.9 mmol $mmol^{-1}$ Al kg suspension.

2. The suspension concentration of RO^- was optimized by trial and error at each pH in the calibration region. Trends between DOC and RO^- were used to predict the suspension concentrations of RO^- needed to optimize the model, which was that 1 mg DOC L^{-1} was equivalent to 1 µmol RO^- L^{-1}.

RESULTS AND DISCUSSION

Modeling the titration data to set SHM parameters

Optimized SHM model parameters for Pahokee peat are presented in Table 4.2 along with the default parameters used by Gustafsson (2001b) in the AvgHA database. Some parameters needed significant adjustment. For example, the number of proton-dissociating sites (n) was lower for Pahokee peat at 4.5 relative to the average SHM value of 5.3. This value was reasonable, however, compared to best fits to the Tongbersven humic acid, which had an even lower n at 3.8 in a data set used by Gustafsson (2001b) to determine default SHM parameters. Other parameters only needed minor adjustments, such as the proton dissociation constant (log K_A and log K_B) adjustments from -4.1 and -8.95 to -3.9 and -9 respectively. Although best fit parameters differed from the average SHM model parameters found by Gustafsson (2001b), they were within the range of previous individual humic acid fits.

Figure 4.3 shows peat titration data along with the default and optimized SHM models. The trend in proton binding to peat ($mmol_c\ H^+$) with pH was linear up to pH 6.0, and decreased from pH 6.0 – 8.0. The default model followed data closely from pH 3.0 to 4.0, but overestimated the amount of H^+ needed to increase pH from 4.0-8.0. The optimized SHM model followed data closely across all pH values with an *rmse* of 0.04. The close fit between optimized SHM model parameters and the peat titration data indicated that the SHM model was adequate for describing proton binding to Pahokee peat from pH 3 to 8.

Fe and Al binding to peat

Parameters used in modeling Fe and Al binding to peat are presented in Table 4.3. Default database parameters were successful in describing Fe binding. For optimization of Al models, log K values were adjusted to minimize deviation in the final fits. All initial and adjusted values were consistent with previously determined values for Al- and Fe- binding to OM, or OM components such as humic and fulvic acid. Comparable values, such as those determined by Cabaniss (2008; 2009) are summarized in Table 4.4. Similarly, constants previously proposed for Al binding to OM in the SHM and WinHumic V models are presented in Table 4.5.

Optimized models of Fe and Al sorption to peat are shown in Figure 4.4. Bound Al decreased sharply from 1200 to 550 mmol kg^{-1} peat between pH 4 and 3, and from 1200 to 880 mmol kg^{-1} peat between pH 5 and 8.5. Likewise, bound Fe decreased from 1200 to1000 mmol kg^{-1} peat between pH 4 and 3, and from 1200 to 680 mmol kg^{-1} between pH 5 and 8.5. Overall, optimized models followed data closely, with *rmse* values indicating < 3% error. Previous data suggested that the decrease in Fe and Al sorption at low pH was predominantly due to the competitive binding of protons with Fe and Al, while the decrease in Fe and Al sorption at high pH was due to a combination of proton effect and increasing DOC (Chapter 3). In the SHM model, changes in DOC, pH, and solid phase OM were accounted for with model parameters, which confirmed that proton competition with Fe and Al sorption occurred at pH < 6.0, and that a combination of proton effect and increasing DOC controlled Fe and Al sorption at pH $\geq$ 6.0. Although the model accurately accounted for bound Fe and Al to OM, the model represents only potential, not proven mechanisms of Fe and Al sorption

to OM. Overall, the SHM in Visual MINTEQ provided an accurate, albeit semi-empirical, method to predict both Fe and Al binding to soil OM following calibration.

Phosphate binding to peat

P Sorption Envelopes

Phosphate sorption envelopes, and trends in DOC across pH are discussed in detail in Chapter 3 and are not shown here.

Modeling PO_4 Sorption

A summary of defined parameters used in the TPCD model is shown in Table 4.6. Generally, previously defined surface complexation parameters for ferrihydrite were used to model PO_4 sorption to Fe-OM (Gustafsson, 2006) (Table 4.7). From my comprehensive literature review, surface parameters for modeling an amorphous Al (hydr)oxide in Visual MINTEQ were not found. Thus, previously defined surface complexation parameters for allophone were used as a starting point to model PO_4 sorption to Al-OM.

Figure 4.5 A depicts the modeled PO_4 sorption along with the actual bound PO_4 calculated by loss from solution. Generally, modeled PO_4 sorption decreased with increasing pH in both 300 and 600 mmol P kg^{-1} peat treatments, corresponding to actual measurements. Overall, the model fit to PO_4 sorption on Fe-peat had *rmse* values of 20 and 17 for the 300 and 600 mmol P kg^{-1} peat envelopes respectively (Figure 4.5 A). Modeling PO_4 sorption to Al-OM was less successful, with *rmse* values of 30 and 67 for the 300 and 600 mmol P kg^{-1} peat respectively (Figure 4.5 B), with most deviation at pH > 5.0 . Thus, the use of a surface complexation model in Visual MINTEQ was able to accurately model PO_4 sorption to Fe-

OM, but was less accurate for PO_4 sorption to Al-OM. In order to accurately model PO_4 sorption to Al-OM using Visual MINTEQ, further data is needed regarding the chemical complexation constants of PO_4 for Al.

Dissolved organic carbon has been shown to play a part in PO_4 sorption to minerals (Hiemstra et al., 2010; Borggaard et al., 2005; Kaiser and Zech 1996). The degree that DOC impacts PO_4 sorption to OM was determined in Chapter 3. Despite quantification of DOC impacts, it was not clear to what extent the individual mechanisms of PO_4-Fe/Al-DOM complex formation or DOC competition impacted PO_4 sorption. The use of the RO^- factor simulates competition mechanisms but ignores aqueous PO_4-Fe/Al-OM complex formation. Thus, the use of RO^- is simply a semi-empirical approach to modeling these data and provides no detailed information regarding the actual reaction mechanisms between DOC and PO_4 for sorption to Fe/Al-OM.

Regardless of unknown parameters or mechanisms, final results demonstrated a quantitatively accurate model of PO_4 sorption to Fe-OM. Although the SHM model was successful in practice, it should be understood that metal and PO_4 binding to humics is complex, and involves numerous parameters and assumptions that are simplifications of reality. These limitations however, do not diminish the need for quantitatively modeling PO_4 binding to OM with variable pH and DOC, nor for the need to successfully model DOC competition with PO_4 for sorption to OM.

CONCLUSIONS

The TPCD model was able to accurately model the binding of both Fe and Al to OM. The TPCD model along with a parameter to account for DOM (RO^-) gave a better fit of PO_4 sorption data on Fe-SOM compared with on Al-OM. Although the DOC competition factor was needed to accurately predict PO_4 sorption to Fe and Al bound in OM, the potential formation of aqueous DOM-Fe/Al-PO_4 complexes was ignored. Thus, using the RO^- factor to accurately model PO_4 sorption to Fe-OM did not account for specific mechanisms of DOC induced PO_4 mobilization, but rather the net mobilization effect. However, previous results (Chapter 3) indicated that pH and resultant bound Fe and Al concentrations were more important for determining PO_4 sorption to OM, which corresponded with the predominant dependence of this model on pH and bound Fe and Al concentrations. Coupling a model (such as the SHM) that predicts the sorption of Fe and Al to OM with one that predicts PO_4 sorption could be used to accurately predict PO_4 sorption in organic soils. Overall, the successful application of the TPCD model for describing PO_4 sorption to OM suggests that this model may be used for organic soils, or incorporated into more comprehensive models that describe PO_4 sorption to mineral soils.

BIBLIOGRAPHY

Abou Nohra J.S., C.A. Madramootoo, and W.H. Hendershot. 2007. Modelling phosphate adsorption to the soil: Application of the non-ideal competitive adsorption model. Environ. Pollut. 149:1-9.

Bloom P.R. 1981. Phosphorus adsorption by an aluminum-peat complex. Soil Sci. Soc. Am. J. 45:267-272.

Borggaard O.K., B. Raben-Lange, A.L. Gimsing, and B.W. Strobel. 2005. Influence of humic substances on phosphate adsorption by aluminium and iron oxides. Geoderma. 127, 270-279.

Bryan S.E., E. Tipping, and J. Hamilton-Taylor. 2002. Comparison of measured and modelled copper binding by natural organic matter in freshwaters. Comp. Biochem. Phys. C. 133:37-49.

Buschmann J., A. Kappeler, U. Lindauer, D. Kistler, M. Berg, and L. Sigg. 2006. Arsenite and Arsenate Binding to Dissolved Humic Acids: Influence of pH, Type of Humic Acid, and Aluminum. Environ. Sci. Tech. 40:6015-6020.

Cabaniss S.E. 2008. Quantitative structure-property relationships for predicting metal binding by organic ligands. Environ. Sci. Tech. 42:5210-5216.

Cabaniss S.E. 2009. Forward Modeling of Metal Complexation by NOM: I. A priori Prediction of Conditional Constants and Speciation. Environ. Sci. Tech. 43:2838-2844.

Collins M.E., and R.J. Kuehl. 2001. Organic matter accumulation and organic soils. pp. 137-162. *In.* J. L. Richardson and M. J. Vepraskas (Eds.), Wetland Soils: Genesis, hydrology, landscapes, and classification. Lewis Publishers, Washington D.C.

De Wit H.A., M. Kotowski, and J. Mulder. 1999. Modeling aluminum and organic matter solubility in the forest floor using WHAM. Soil Sci. Soc. Am. J. 63:1141-1148.

Devau N., E. Le Cadre, P. Hinsinger, B. Jaillard, and F. Gerard. 2009. Soil pH controls the environmental availability of phosphorus: Experimental and mechanistic modelling approaches. Appl. Geochem. 24:2163-2174.

Fellman J.B., and D.V. D'Amore. 2007. Nitrogen and phosphorus mineralization in three wetland types in Southeast Alaska, USA. Wetlands. 27:44-53.

Fisher M.M., and K.R. Reddy. 2010. Estimating the Stability of Organic Phosphorus in Wetland Soils. Soil Sci. Soc. Am. J. 74:1398-1405.

Frau F., R. Biddau, and L. Fanfani. 2008. Effect of major anions on arsenate desorption from ferrihydrite-bearing natural samples. Appl. Geochem. 23:1451-1466.

Gerke J., 1992. Phosphate, aluminum and iron in the soil solution of 3 different soils in relation to varying concentrations of citric-acid. Z. Pflanzenernahr. Bodenkd. 155, 339-343.

Gerke J., and R. Hermann. 1992. Adsorption of orthophosphate to humic-Fe complexes and to amorphous Fe-oxide. Z. Pflanz. Bodenkunde**.** 155:233-236.

Goldberg, S. and G. Sposito. 1984a. A chemical model of phosphate adsorption by soils: I. Reference oxide minerals. Soil Sci. Soc. Am. J. 48:772-778.

Goldberg, S. and G. Sposito. 1984b. A chemical model of phosphate adsorption by soils II. Noncalcareous soils. Soil Sci. Soc. Am. J. 48:779-783.

Groenenberg J.E., G.F. Koopmans, and R.N.J. Comans. 2010. Uncertainty Analysis of the Nonideal Competitive Adsorption-Donnan Model: Effects of Dissolved Organic Matter Variability on Predicted Metal Speciation in Soil Solution. Environ. Sci. Tech. 44:1340-1346.

Gustafsson J.P. 2001a. Modelling competitive anion adsorption on oxide minerals and an allophane-containing soil. Eur. J. Soil Sci. 52:639-653.

Gustafsson J.P. 2001b. Modeling the acid-base properties and metal complexation of humic substances with the Stockholm Humic Model. J. Colloid Interf. Sci. 244:102-112.

Gustafsson J.P. 2006. Arsenate adsorption to soils: Modelling the competition from humic substances. Geoderma. 136:320-330.

Gustafsson J.P. 2010. Visual MINTEQ Version 3.0, Department of Land and Water Resources, Stockholm, Sweden.

Gustafsson J.P., and J.W. J. van Schaik 2003. Cation binding in a mor layer: batch experiments and modelling. Eur. J. Soil Sci. 54:295-310.

Gustafsson J.P., and D.B. Kleja. 2005. Modeling salt-dependent proton binding by organic soils with the MICA-Donnan and Stockholm Humic models. Environ. Sci. Tech. 39:5372-5377.

Gustafsson J.P., P. Pechova, and D. Berggren. 2003. Modeling metal binding to soils: The role of natural organic matter. Environ. Sci. Tech. 37:2767-2774.

Gustafsson J.P., I. Persson, D.B. Kleja, and J.W.J. Van Schaik. 2007. Binding of iron(III) to organic soils: EXAFS spectroscopy and chemical equilibrium modeling. Environ. Sci. Tech. 41:1232-1237.

Huang X., G.D. Foster, R. V. Honeychuck, and J.A. Schreifels. 2009. The maximum of phosphate adsorption at pH 4.0: why it appears on aluminum oxides but not on iron oxides. Langmuir. 25:4450-4461.

Heiberg L., T.V. Pedersen, H.S. Jensen, C. Kjaergaard, and H.C.B. Hansen. 2010. A Comparative Study of Phosphate Sorption in Lowland Soils under Oxic and Anoxic Conditions. J. Environ. Qual. 39:734-743.

Hiemstra T., J. Antelo, A.M.D. van Rotterdam, and W.H. van Riemsdijk. 2010. Nanoparticles in natural systems II: The natural oxide fraction at interaction with natural organic matter and phosphate. Geochim. Cosmochim. Acta. 74, 59-69.

Hiemstra T., and W.H. VanRiemsdijk. 1996. A surface structural approach to ion adsorption: The charge distribution (CD) model. J. Colloid Interf. Sci. 179:488-508.

Hiemstra T., and W.H. Van Riemsdijk. 1999. Surface structural ion adsorption modeling of competitive binding of oxyanions by metal (hydr)oxides. J. Colloid Interf. Sci. 210:182-193.

Hua Q.X., J.Y. Li, J.M. Zhou, H.Y. Wang, C.W. Du, and X.Q. Chen. 2008. Enhancement of phosphorus solubility by humic substances in ferrosols. Pedosphere. 18:533-538.

Igwe C.A., M. Zarei, and K. Stahr. 2010. Fe and Al oxides distribution in some ultisols and inceptisols of southeastern Nigeria in relation to soil total phosphorus. Environ. Earth Sci. 60:1103-1111.

Jansen B., J. Mulder, and J.M. Verstraten. 2003. Organic complexation of Al and Fe in acidic soil solutions - Comparison of diffusive gradients in thin films analyses with Models V and VI predictions. Analytica Chimica Acta. 498, 105-117.

Jiao Y., W.H. Hendershot, and J.K. Whalen. 2008. Modeling phosphate adsorption by agricultural and natural soils. Soil Sci. Soc. Am. J. 72:1078-1084.

Kaiser K., and W. Zech. 1996. Nitrate, sulfate, and biphosphate retention in acid forest soils affected by natural dissolved organic carbon. J. Environ. Qual. 25, 1325-1331.

Kinniburgh D.G., W.H. van Riemsdijk, L.K. Koopal, M. Borkovec, M.F. Benedetti, and M.J. Avena. 1999. Ion binding to natural organic matter: competition, heterogeneity, stoichiometry and thermodynamic consistency. Colloid Surface A. 151:147-166.

Koopal L.K., W.H. Vanriemsdijk, J.C.M. Dewit, and M.F. Benedetti. 1994. Analytical Isotherm Equations for Multicomponent Adsorption to Heterogeneous Surfaces. J. Colloid Interf. Sci. 166:51-60.

L.G. Sillen, and A.E. Martell. 1971. Stability Constants of Metal-Ion Complexes. The Chemical Society, London, UK.

Lofts S., C. Woof, E. Tipping, N. Clarke, and J. Mulder. 2001. Modelling pH buffering and aluminium solubility in European forest soils. Eur. J. Soil Sci. 52:189-204.

Manning B.A., and S. Goldberg. 1996. Modelling competitive adsorption of arsenate with phosphate and molybdate on oxide minerals. . Soil Sci. Soc. Am. J. 60:121-131.

McBride, M.B. 1994. Environemental Chemistry of Soils. Oxford University Press, Oxford NY. USA.

Negassa W., S. Dultz, A. Schlichting, and P. Leinweber. 2008. Influence of specific organic compounds on phosphorus sorption and distribution in a tropical soil. Soil Sci. 173:587-601.

Newman S., and K. Pietro. 2001. Phosphorus storage and release in response to flooding: implications for Everglades stormwater treatment areas. Ecol. Eng. 18:23-38.

Roden E.E., and J.W. Edmonds. 1997. Phosphate mobilization in iron-rich anaerobic sediments: Microbial Fe(III) oxide reduction versus iron-sulfide formation. Arch. Hydrobiol.139:347-378.

S.D. Young and B.W. Bache 1985. Aluminum-organic complexation: formation constants and a speciation model for the soil solution. J. Soil. Sci. 36:261-269.

Schnitzer M. S.U.Khan. 1972. Humic Substances in the Environment, Dekker, NY.

Shapiro J. 1967. Yellow organic acids of lake water: differences in their composition and behaviour. pp. 202-216 *In.* H.L Golterman and R.S. Clymo (Ed.) NV Noord-Hollandsche Uitgevers Maatschappij, Amsterdam.

Shaw P.J., R.I. Jones, and H. De Haan. 2000. The influence of humic substances on the molecular weight distributions of phosphate and iron in epilimnetic lake waters. Freshwater Biol. 45:383-393.

Sillen L.G., Martell. A.E., 1971. Stability Constants of Metal-Ion Complexes. The Chemical Society, London, UK.

Smith, R.M., A.E. Martell, and R.J. Motekaitis. 2003. NIST Critically Selected Stability Constants of Metal Complexes Database.Version 7.0. *In*. Van Reeuwijk, L.P., 1995. NIST Standard Reference Database 46. US Department of Commerce, National Institute of Standards and Technology, Gaithersburg.

Sparks, D.L. 2003. Soil Chemistry. Elsevier Science, Orlando, FL. USA.

Stevenson F.J., and G.F. Vance, 1989. Naturally occurring aluminum-organic complexes, in: G. Sposito (Ed.), The environmental chemistry of aluminum, CRC Press Inc New York, NY. pp. 118-142.

Strahm B.D., and R.B. Harrison. 2007. Mineral and organic matter controls on the sorption of macronutrient anions in variable-charge soils. Soil Sci. Soc. Am. J. 71:1926-1933.

Tipping E. 1994. WHAM - A chemical equilibrium model and computer code for waters, sediments, and soils incorporating a discrete site/electrostatic model of ion-binding by humic substances. Comput. Geosci 20:973-1023.

Tipping E., A.J. Lawlor, S. Lofts, and L. Shotbolt,. 1998. Simulating the long-term chemistry of an upland UK catchment: Heavy metals. Environ. Pollut. 141:139-150.

Wang Y.P., R.M. Law, and B. Pak. 2010. A global model of carbon, nitrogen and phosphorus cycles for the terrestrial biosphere. Biogeosciences 7:2261-2282.

Weber T., T. Allard, E. Tipping, and M.F. Benedetti. 2006. Modeling iron binding to organic matter. Environ. Sci. Tech. 40:7488-7493.

Weng L.P., W.H. Van Riemsdijk, and T. Hiemstra. 2008. Humic Nanoparticles at the Oxide-Water Interface: Interactions with Phosphate Ion Adsorption. Environ. Sci. Tech. 42:8747-8752.

Wisawapipat W., I. Kheoruenromne, A. Suddhiprakarn, and R.J. Gilkes. 2009. Phosphate sorption and desorption by Thai upland soils. Geoderma 153:408-415.

Young, S.D., and B.W. Bache. 1985. Aluminum-organic complexation: formation constants and a speciation model for the soil solution. J. Soil Sci. 36:261-269.

Zhang M.K., and H.M. Zhang. 2010. Co-transport of dissolved organic matter and heavy metals in soils induced by excessive phosphorus applications. J. Environ. Sci. China. 22:598-606.

Zhang W., J.W. Faulkner, S.K. Giri, L.D. Geohring, and T.S. Steenhuis. 2010. Effect of Soil Reduction on Phosphorus Sorption of an Organic-Rich Silt Loam. Soil Sci. Soc. Am. J. 74:240-249.

Table 4.1. Summary of parameters used in SHM model (Gustafsson 2001).

Parameter	Description (Gustafsson 2001)	How Determined
n	Amount of proton-dissociation sites (mol g^{-1})	Fitted from experimental data
n_B	Amount of type B sites (mol g^{-1})	0.5 x n_A (humic acid) 0.3 x n_A (fulvic acid)
Log K_A	Intrinsic proton dissociation constant for type A sites	Fitted from experimental data
Log K_B	Intrinsic proton dissociation constant for type B sites	Fitted from experimental data
$\Delta_p K_B$	Distribution term that modifies log K_A	Fitted from experimental data
$\Delta_p K_A$	Distribution term that modifies log K_B	Fitted from experimental data
Log K_{Mb}	Intrinsic equilibrium constant for bidentate complexation of metal M	Obtained from Gustafsson, 2001
ΔLK_2	Distribution term that modifies the strengths of complexation sites	Obtained from Gustafsson, 2001
g_f	Gel fraction parameters	Fitted from experimental data

Table 4.2. Visual MINTEQ SHM AvgHA model parameters along with the best fit modeled parameters to Pahokee Peat titration data in 0.1M M KCl background.

Data	n (mmol g^{-1})	log K_A	ΔpK_A	log K_B	ΔpK_B	g_f	rmse
AvgHA	5.3	-4.1	3.1	-8.95	2.5	0.78	0.4591
Best Fit	4.5	-3.9	3.1	-9	2.45	0.5	0.0449

*Ratio of active DOM to DOC 1.4, % of active DOM that is FA = 75

Table 4.3. Parameters for the cation complexation used in the SHM model. The ratio of active DOM to DOC was 1.4, and the % of active DOM that was FA was 75%

Speciation Equations	Log K_{Mb}	ΔLK_2*
Humic Acid		
$2HAH_{(s)} + Al^{3+}_{(aq)} + OH^-_{(aq)} \leftrightarrow HA_2AlOH_{(s)} + 2H^+_{(aq)}$	-6.8	1
$2HAH_{(s)} + Al^{3+}_{(aq)} \leftrightarrow HA_2Al^+_{(s)} + 2H^+_{(aq)}$	-2.6	1
$2HAH_{(s)} + Al^{3+}_{(aq)} + 2OH^- \leftrightarrow HA_2Al(OH)_2^-{}_{(s)} + 2H^+_{(aq)}$	-13.5*	1
$2HAH_{(s)} + 2Fe^{3+}_{(aq)} \leftrightarrow HA_2Fe_2O^+_{(s)}$	-5.15	1.8
Fulvic Acid		
$2FAH_{(s)} + Al^{3+}_{(aq)} + OH^-_{(aq)} \leftrightarrow FA_2AlOH_{(s)} + 2H^+_{(aq)}$	-6.55	1
$2FAH_{(s)} + Al^{3+}_{(aq)} \leftrightarrow FA2Al^+_{(s)} + 2H^+_{(aq)}$	-3.9	1
$2FAH_{(s)} + Fe^{3+}_{(aq)} + 2OH^-_{(aq)} \leftrightarrow FA_2Fe(OH)_2^-{}_{(s)} + 2H^+_{(aq)}$	-5.8	1
$2FAH_{(s)} + Fe^{3+} \leftrightarrow /FA_2Fe^+_{(s)} + 2H^+_{(aq)}$	-2	1

* New complex generated to model Al binding to OM. Log K value (-13.5) was adjusted to maximize fits to actual data.

Table 4.4. Complexation constants of Fe and Al to various organic ligands.

Ligand	Ligands per metal ion	Complexation constant Fe^{3+}	Complexation Constant Al^{3+}	Reference
Formic Acid	1	3.10 (1.0)	1.36 (1.0)[a]	(Stevenson and Vance, 1989)
Acetic acid	1	3.38 (0.1)	1.51 (1.0)	(Stevenson and Vance, 1989)
	2	6.50 (0.1)	3.76 (0.3)[b]	(Stevenson and Vance, 1989; Young and Bache)
Propionic acid	1	3.40 (0.1)	1.69(1.0)	(Stevenson and Vance, 1989)
Oxalic Acid	1	7.53 (0.1)	6.10 (1.0)	(Stevenson and Vance, 1989)
	2	13.64 (0.1)	11.09 (1.0)	(Stevenson and Vance, 1989)
	3	18.49 (0.1)	15.12 (1.0)	(Stevenson and Vance, 1989)
Citric Acid	1	1.20 (0.1)	8.32 (0.25)	(Stevenson and Vance, 1989; Sillen and Martell, 1971)
Catechol	1	20.00 (0.1)	16.30 (0.1)	(Stevenson and Vance, 1989)
	2	34.70 (0.1)	29.30 (0.1)	(Stevenson and Vance, 1989)
	3	43.80 (0.1)	37.60 (0.1)	(Stevenson and Vance, 1989)
COOH			1.31 (0.1) [0.44]	(Cabaniss, 2008)
Amines			1.59 (0.1) [0.45]	(Cabaniss, 2008)
Phenols			3.07 (0.1) [0.22]	(Cabaniss, 2008)
Humic Acid			0.90	(de Wit et al., 1999)
Fulvic Acid			1.58	(de Wit et al., 1999)

(a) numbers in parenthesis represent ionic strength (in mol L^{-1}) at which the stability constant was determined while [] indicate standard deviations.

Table 4.5. Complexation constants for Al binding to NOM as modeled and predicted in previous literature.

SHM (Al)	**Log K_{Mb}**	**LK_2**	**Reference**
SHM (HA and FA)	3.4 (0.001-5)	1.5	(Gustafsson, 2001a)
SHM (HA and FA)	-3.9	1	(Gustafsson and van Schaik, 2003)
SHM HA and FA	-4.1 (-3.9 revised)	1	(Gustafsson and van Schaik, 2003)
WinHumicV HA	-1.3	1	(Gustafsson and van Schaik, 2003)
WinHumic V FA	-0.6	1	(Gustafsson and van Schaik, 2003)
Soil mean	2.47		(Cabaniss, 2009)
Water mean	3.02		(Cabaniss, 2008)

Table 4.6 Summary of parameters used in TPCD model (Hiemstra and VanRiemsdijk, 2006; Gustafsson 2006). All values were obtained from Gustafsson, 2006 except were indicated

Parameter	**Description**	
Δz_o	Charge of o-plane	
Δz_1	Charge of 1-plane	
Δz_2	Charge of 2- or d-plane	
A/m^2g^{-1}	Specific Surface Area	-Adjusted for Al-OM to match Ferrihydrite
N_s/sites nm^{-2}	Site Density	-Adjusted to fit experimental data
C_1/F m^{-2}	Inner capacitance	
C_2/F m^{-2}	Outer capacitance	

Table 4.7. Parameters used in surface charging models of PO_4 sorption

Parameter	**Fe-peat**	**Al-peat**
A/m^2g^{-1}	750*	750
N_s/sites nm^{-2}	5.5	5.5
$C_1/F\ m^{-2}$	1.3*	1.1*
$C_2/F\ m^{-2}$	5*	5*

*Parameters obtained from Gustafsson (2006)

Table 4.8. Surface complexation reactions for modeling PO_4 binding to Fe and Al peat

Reaction	**Δz_1**	**Log K[*] Fe**	**Log K[*] Al**
$2SOH^{1/2-} + 2H^+ + PO_4^{3-} \leftrightarrow$ $S_2O_2PO_2^{2-} + 2\ H_2O$	-1.5	28.29	28.73
$2SOH^{1/2-} + 3H^+ + PO_4^{3-} \leftrightarrow$ $S_2O_2POOH^- + 2\ H_2O$	-1	36.16	36.16
$SOH^{1/2-} + 3H^+ + PO_4^{3-} \leftrightarrow$ $SOPO_3H_2^{1/2-} + H_2O$	-0.5	32.31	32.00
$SOH^{1/2-} + H^+ \leftrightarrow SOH_2^{1/2+}$	0.5	8.1	10
$SOH^{1/2-} + H^+ + RO^- \leftrightarrow$ $SOR^{1/2-} + H_2O$	0.5	25	25

[*] All reactions taken from Gustafsson (2006)
[a] Value adjusted to fit data

Table 4.10. Thermodynamic equilibrium constants of PO4 surface complexes for minerals

Complex	Goethite	Ferrihydrite	Gibbsite	Reference
$=SOPO_3^{-2.5}$	20.8	19.7		(Devau et al., 2009)
$=SO_2PO_2^{-2}$	25.59	26.01	25.45	(Devau et al., 2009)
$=SO_2POOH^{-}$	31.79	32.61	33.05	(Devau et al., 2009)
$=SOPO_3H_2^{-0.5}$			32.5	(Devau et al., 2009)
$Al_2O_2PO_4^{-2}$			28.5	(Manning and Goldberg, 1996; Gustafsson, 2001b)
$Al_2O_2POOH^{-1}$			36.1	(Manning and Goldberg, 1996; Gustafsson, 2001b)
$AlOPO_3H_2^{-0.5}$			32.5	(Manning and Goldberg, 1996; Gustafsson, 2001b)
$FeOPO_3^{-2.5}$	20.8			(Gustafsson, 200b;Hiemstra and Van Riemsdijk, 1999)
$Fe_2O_2PO_2^{-2}$	29.2			(Gustafsson, 200b;Hiemstra and Van Riemsdijk, 1999)
$Fe_2O_2POOH^{-1}$	35.4			(Gustafsson, 200b;Hiemstra and Van Riemsdijk, 1999)
$FeOPO_3H_2^{-0.5}$	32.1			(Gustafsson, 2001b)

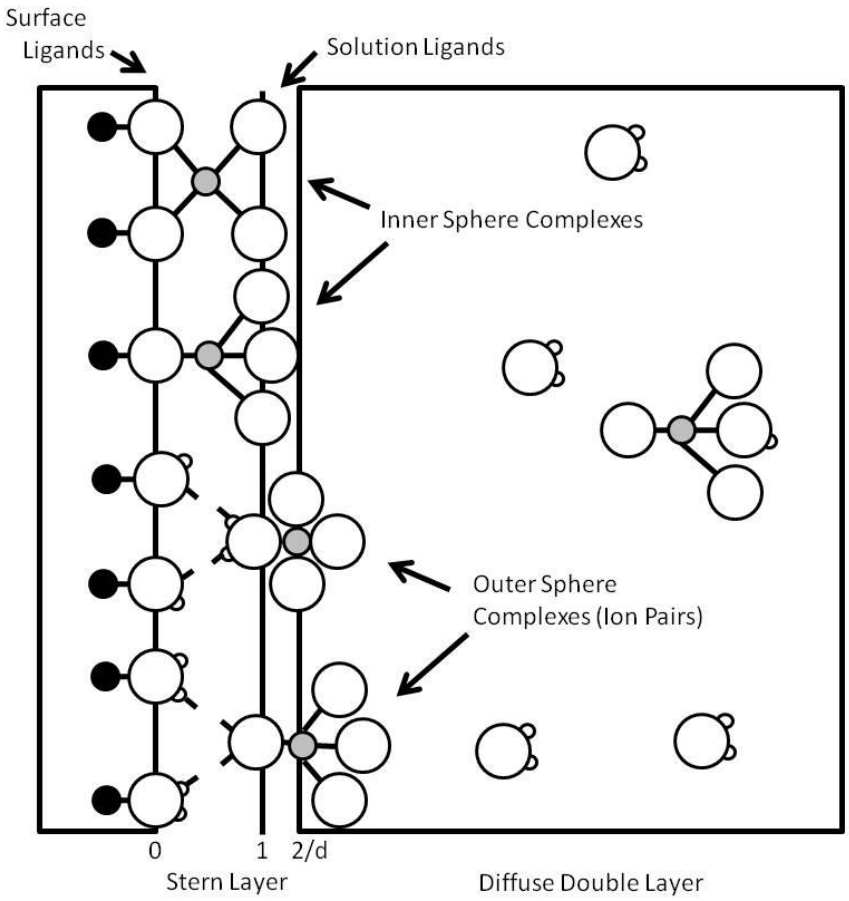

Figure 4.1. A. Schematic representation of the Three-Plane CD-MUSIC model showing location of outer sphere and inner sphere PO_4 complexes at the solid-solution interface (Hiemstra and Van Riemsdijk, 1996). The position of outer sphere complexes is determined by the minimum distance of hydrated ions to a closely packed (hydr)oxide surface and are treated as point charges in the CD model. Inner sphere complexes are close to the hydr(oxide) surface and penetrate the Stern layer. In the MUSIC model, inner sphere complexes are treated as a distribution of charge rather than points. (Figure modeled after Hiemstra and Van Riemsdijk, 1996; and Devau et al., 2009).

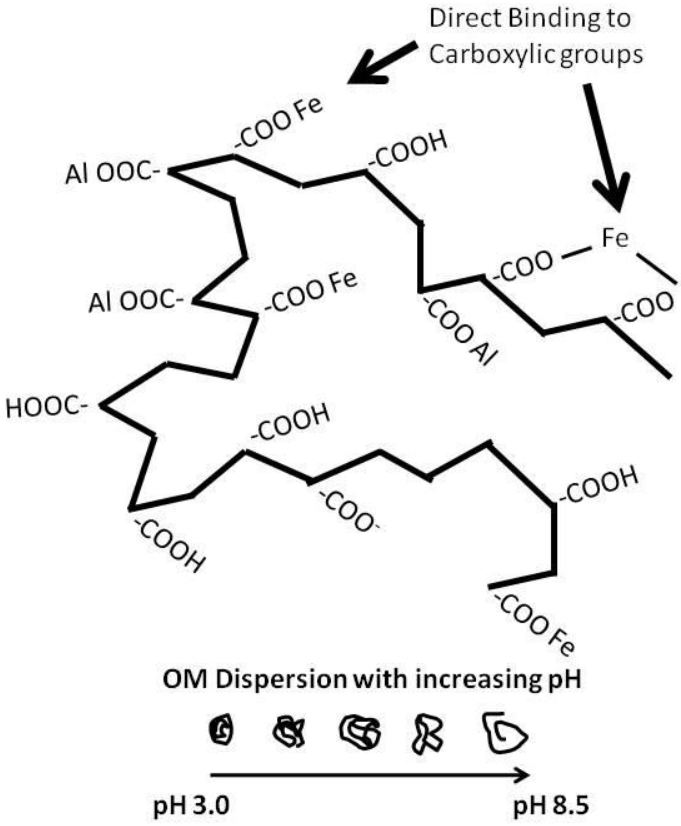

Figure 4.2. A schematic representation (based on McBride, 1994) of potential Fe and Al binding to organic matter (OM) (top). Here mono-nuclear and poly-nuclear Fe/Al (hydr)oxides are expected to bind to OM through carboxylic and phenolic functional groups. Metal binding to OM may also depend on the un-coiling of OM with increasing pH (bottom) (based on Sparks, 2003).

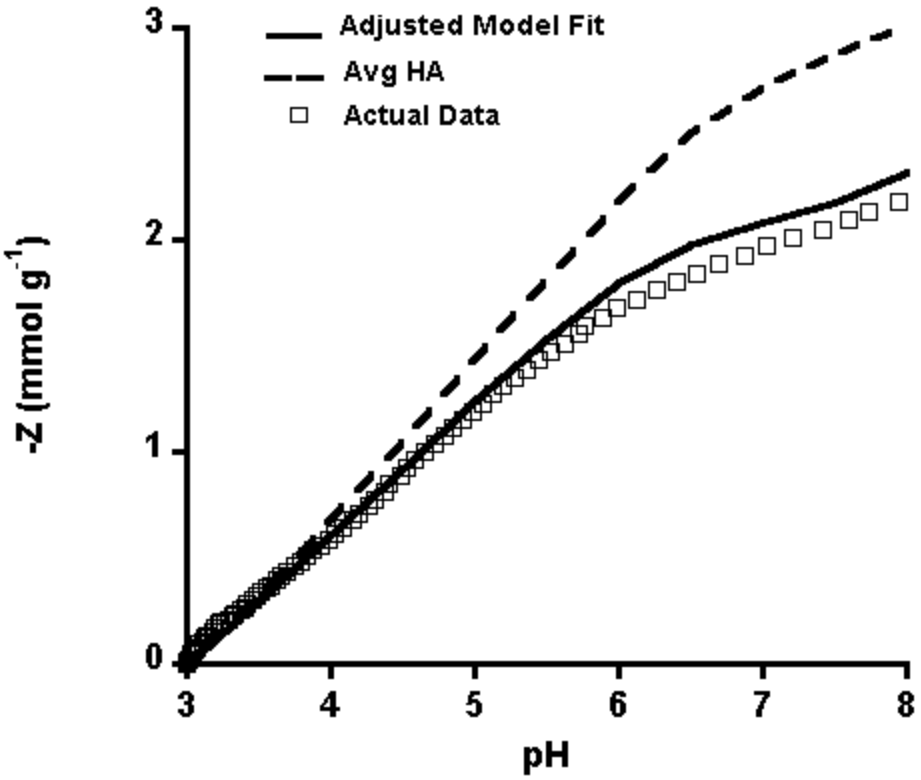

Figure 4.3. Proton titration of Pahokee Peat in a 0.1 M KCl background (unpublished data from K. Hutchison) compared to default (dashed line) and optimized (solid line) SHM fits.

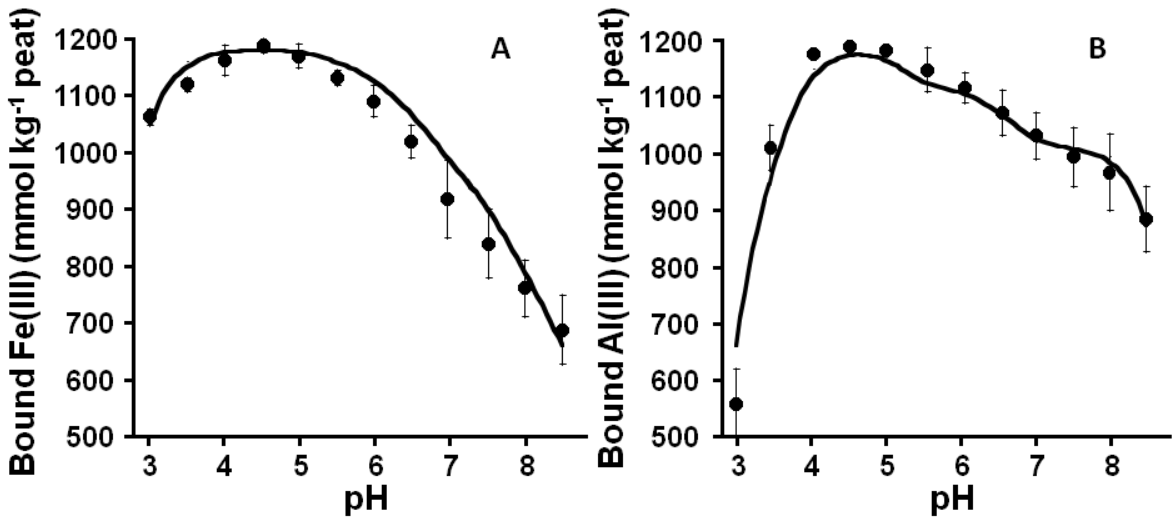

Figure 4.4. Average bound Fe (A) and Al (B) plotted along with the best fit modeled bound Fe and Al data generated from the Stockholm Humic Model (SHM) in Visual MINTEQ. Fit parameters are shown in Table 2. Error bars representing standard deviations are shown for actual bound Fe and Al and the *rmse* values of the fits were 38.6 and 35.6 for Fe and Al respectively.

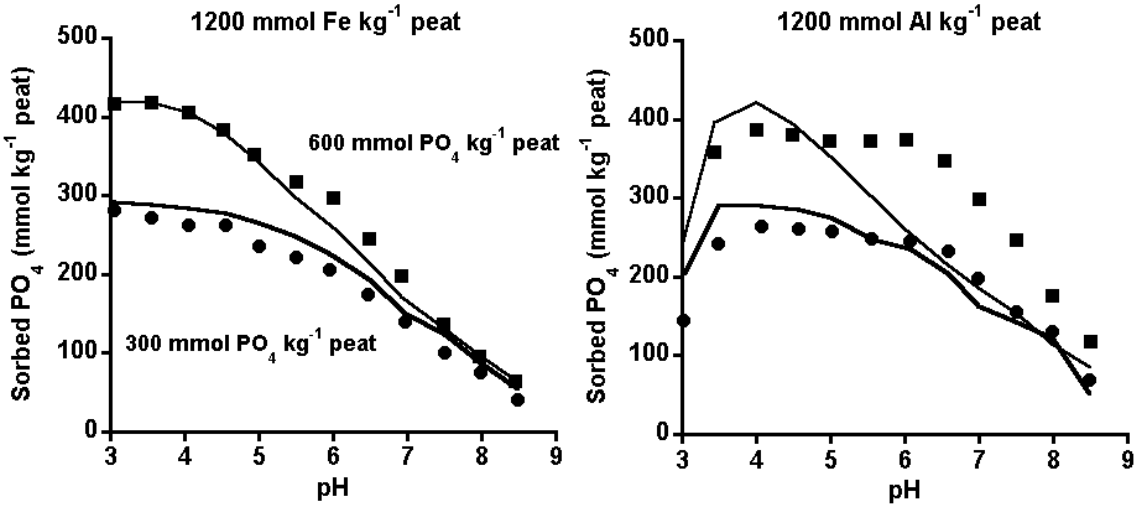

Figure 4.5. Phosphate sorption envelope to 1200 mmol Fe kg^{-1} peat (left) and 1200 mmol Al kg^{-1}peat (right) modeled using Visual MINTEQ surface complexation model. The points represent actual data while fits are shown as solid lines. RMSE values were 20 and 17 mmol PO_4 kg^{-1} peat for the 600 and 300 mmol Fe P kg^{-1} peat treatments and 30 and 68 mmol PO_4 kg^{-1} peat for the 600 and 300 mmol Al P kg^{-1} peat treatments respectively.

CHAPTER 5. MICROBIAL REDUCTION OF Fe(III) BOUND TO PAHOKEE PEAT

ABSTRACT

The reduction rate of Fe(III) potentially impacts a host of soil processes, including the retention and mobilization of nutrients and contaminants, formation of redoximorphic features that are used in wetland delineation, and plant availability of Fe. Organic matter (OM) is the main reducing agent for reduction of Fe(III)-oxides in reduced soils, but the mechanisms and kinetics of OM-bound Fe(III) reduction are poorly defined. The objective of this research was to quantify the impacts of soil OM on the microbial reduction rates of Fe(III). Aqueous suspensions containing 1200 mmol Fe(III) L^{-1} were continuously stirred at 25°C and pH 6.0 with varying concentrations of Pahokee peat to achieve bound Fe(III) concentrations between 300 and 3600 mmol Fe kg^{-1} peat. Iron(III) reduction was induced using *Shewanella putrefaciens* strain CN32 bacteria, and bubbling $H_{2(g)}$ as an electron donor through the suspensions, which were sampled between 0 and 48 h. Electron shuttling was minimal in all incubations, and bound Fe(III) concentration did not significantly alter the reduction rate of Fe(III) bound to OM. However, the ratio of total dissolved Fe(II) to total bound Fe(II) decreased with increasing peat addition from 37 to 0.7 up to 1 g peat L^{-1}, and then increased by as much as 0.6 from 1 to 4 g peat L^{-1}, suggesting that Fe(II) dissolution was enhanced by association with DOC. Although the concentration of Fe(III) bound to peat did not alter Fe(III) reduction rates, bound Fe(III) concentrations controlled DOC concentrations that were shown previously (above) to impact Fe(II), Fe(III), Al(III), and PO_4 mobilization.

INTRODUCTION

Iron(III) is one of the most abundant potential electron acceptors (below O_2) in the heterotrophic decomposition of soil organic matter (OM), and dissimilatory Fe(III) reduction as has been researched extensively (Jiang and Kappler, 2008; Lovley, 1991; Lovley, 1993; Lovley and Anderson, 2000; O'Loughlin et al., 2007; Rakshit et al., 2009; Zelasko, 2007). Quantifying how the concentration of OM and speciation of Fe and other soil minerals alters Fe(III) reduction and Fe(II) dissolution kinetics is important for predicting soil processes such as contaminant mobility and the formation of redoximorphic features. Redoximorphic features formed by Fe and Mn reduction are key in hydric soil identification and wetland delineation (Richardson and Vepraskas, 2001). Furthermore, nutrients, contaminants, and organic materials bound to Fe(III) are potentially mobilized during reduction of Fe(III) (Ajmone-Marsan et al., 2006; Gerke and Hermann, 1992; Hutchison and Hesterberg, 2004; Ponnamperuma, 1972; Scharer et al., 2009).

Soil OM has been shown to impact the rate of dissimilatory microbial reduction of Fe(III) (Lovley et al., 1996; Zelasko, 2007), the mobility of Fe(III) and Fe(II) (Rakshit et al., 2009; Royer et al., 2002), and Fe(III) and Fe(II) mineral formation (Cornell and Schwertmann, 1993). For example, humic substances can modify Fe(III)-oxides by several mechanisms including: 1. binding of OM to Fe/Al - oxide surfaces (Hunt et al., 2007); 2. inhibiting the crystallization of Fe-oxides; and 3. complexiметric dissolution of Fe(III) (Gerke, 1993). Surface area of Fe- and Al- oxides has been shown to play a large role in the amount of Fe(III) reduction, with higher surface area leading to a greater extent of reduction

(Hansel et al., 2003). In organic soils, Fe(III) is expected to be highly accessible to microbial populations as an electron acceptor.

Shewanella species are a phylogenetically diverse group of bacteria that have been isolated from a wide range of aquatic and terrestrial environments and exhibit a broad versatility regarding anaerobic respiration (Bowman, 2005). Although the metabolism by *Shewanella putrefaciens* is expected to be a minor pathway for electron flow in Fe(III) reducing soil environments (Lovley, 1993), this bacteria has been widely used in Fe(III) reduction experiments as a surrogate for bacterial reduction of soil Fe(III) (O'Loughlin et al., 2007). *Shewanella putrefaciens* are facultative anaerobes of terrestrial origin capable of coupling the oxidation of a variety of organic compounds (including formate, lactate, and pyruvate) to Fe(III) and Mn(IV) reduction (Lovley, 1991). A recent study indicated that solid phase humic substances may serve as an electron shuttle between *Shewanella putrefaciens* and Fe(III)-oxides in soils (Roden et al., 2010).

It is known that the addition of OM and DOC generally enhances Fe(III) reduction rates in mineral soils (Fredrickson et al., 2003), but it is not known how changes in the bound Fe(III) concentrations in peat impact Fe(III) reduction rate. In this study, *Shewanella putrefaciens* (strain CN32) was used with excess H_2 as the electron donor to remove effects of OM oxidation. My objective was to quantify the rate of Fe(III) reduction by Shewanella putrefaciens, CN32 as affected by the concentration of Fe(III) bound in peat.

MATERIALS AND METHODS

Soil Organic Mater (OM)

The IHSS standard soil, Pahokee peat was used in this study. Hydration of the Pahokee peat was conducted as described in Chapter 3.

Fe Reduction Kinetics

All incubations were performed in a randomized sequence and are outlined in Table 5.1. For all treatments, 1200 µmol of Fe L^{-1} were added (as an $FeCl_3$ solution) to 1 L suspensions containing between 0.33 and 4 g of pre-hydrated peat adjusted to pH 2.5. The incubation system consists of a 3 L cylindrical, indented, jacketed, Flat Flange reaction vessel (LG-8084 Wilmad-LabGlass) with stir plate (Corning Model PC-410), stir bar, a gas flow system, and a monitoring system (Figure 5.1). While continuously stirring the suspension, pH and Eh were monitored using electrodes inserted through the top of the incubation vessel. The Eh was measured at each sampling time using a platinum combination electrode (cat no. 476516 Corning) each time that the suspension was sampled, and pH was recorded every 2.9 min with an Accumet AccuFlow double junction pH combination electrode (13-600-109 Fisher Scientific) connected to a potentiometric titration workstation (TIM856 titralab, Radiometer Analytical). The titration workstation was equipped with two burettes containing 0.05 M HCl and 0.05 M KOH used to maintain the suspension at pH 6.0. Amounts of added acid and base were recorded every 2.9 min. A constant flow of either $N_{2(g)}$ or 0.05 % $H_{2(g)}$, (balanced by N_2) entered the incubation suspensions through a Pyrex gas dispersion tube (89091-596 Corning). Gas flow was

controlled at 60 mL min^{-1} throughout the incubations using a 65 mm Barnant Gilmont Industrial Flowmeter (GF 8321-2009). Temperature was maintained at 25˚C with an Isotemp water circulator (Isotemp 1016S, Fisher Scientific) and the reaction vessel was wrapped in Al-foil to exclude light.

This process was conducted in the following steps: (1) 0.05 M of KCl was placed in the reaction vessel, (2) the stir plate was turned on to circulate the suspension, (3) the calculated mass of hydrated Pahokee peat was added, (4) the pH was brought to 2.5 using the titration workstation with 0.05 M HCl, (5) 17 mM $FeCl_3$ solution was added to achieve1200 µmol L^{-1} in the final suspension, (6) $N_{2(g)}$ flow through the suspension was started, (7) the pH was increased to pH 6.0 by adding 0.05 M KOH at a rate of 1 mL KOH min^{-1} for up to 2 h, and (8) the suspension was brought to a final volume of 900 mL (calculated based on input volumes) with 0.05 M KCl.

The cell density of a stock suspension of a freshly prepared *Shewanella putrefaciens* CN32 was determined by measuring its optical density at 420 nm in relation to a calibration curve generated from direct plate counts (Royer et al., 2002). After equilibrating the continuously stirred Fe-peat suspension for 48 h, CN32 cells were added to the reaction vessels to achieve a concentration of 1 X 10^8 cells mL^{-1}, and the final incubation volume was brought to 1 L. A time 0 h sample was collected at this point, and the $N_{2(g)}$ was switched to 0.5% $H_{2(g)}$. A syringe was used to extract 20 mL samples at approximately 4, 8, 12, 24, 30, 38, 48, and 72 h. The total volume of sample removed during the course of an experiment was less than 20% of the suspension volume.

Sample Analyses

Immediately following sample collection, serum bottles were placed in a $N_{2(g)}$ filled glove box for filtration, and Fe(II) analysis. Total HCl extractable Fe was measured by adding 5 mL of unfiltered sample to 5 mL of 1 M HCl in a 25 mL amber serum bottle and reacting for 24 h in a $N_{2(g)}$ filled quiescent jar (Fredrickson et al., 1998). The remaining 15 mL of solution, were immediately filtered through a 0.2 µm filter (Millipore Corp., Bedford, MA) in the glove box. Ferrous Fe was measured using the 1,10-phenatnthroline method for both dissolved and HCl extractable [total Fe(II)] samples (Loeppert and Inskeep, 1996). The remaining sample was stored at 5°C for further analysis, including; total Fe with flame atomic absorption spectrometry (FAAS) (Model 3100, Perkin Elmer, Wellesey, MA) and DOC using a TOC analyzer (Shmadzu TOC-5050 TOC).

Microbial Reduction Capacity

To determine if Pahokee peat served as an electron acceptor or shuttle between CN32 and Fe(III), a microbial reduction incubation (as described above) containing 4 g of peat L^{-1} and no added Fe was conducted. Three replications of 10 mL of sample were collected at time 0, 4, 8, 12 and 24 h after microbial reduction. Working in a glove box as described above, HCl-extractable Fe(II) was measured using 5 mL of each sample. In order to evaluate the transfer of electrons from reduced peat to Fe(III) in the absence of microbial Fe(III) reduction the remaining 5 mL of sample were added to 5 mL of a fresh 4 mmol L^{-1} $FeCl_3$ solution (Peretyazhko and Sposito, 2006), sealed in a nitrogen purged crimp cap vile, and allowed to equilibrate for 24 h prior to total Fe(II) determination.

Reduction Rates

Rate coefficients for total and dissolved Fe(II) production were determined by two methods: (1) The slope of a regression fit through the linear data of Fe(II) production with time across the first 12 h of reduction (k_1) (Equation 5.1) and (2) A pseudo-first-order model with rate coefficient (k_2) (Equation 5.2). All linear regressions were conducted using the Graphpad InStat Prism version 5.0 (GraphPad Software Inc., San Diego CA).

$$Fe(II) = k_1 t + b \qquad \text{Equation 5.1}$$

$$Fe(II) = A_o(1-e^{(-k_2 t)}) \qquad \text{Equation 5.2}$$

For these calculations, b represents the concentration of Fe(II) at 0 h, k_1 and k_2 are the respective rate coefficients, and A_0 corresponds to maximum Fe(II).

RESULTS AND DISCUSSION

Microbial Reduction of Fe(III)

Iron(III) reduction began immediately upon introduction of CN32 and $H_{2(g)}$. Figure 5.2 shows an example of Fe(III) reduction with decreasing Eh in a 1200 mmol Fe kg^{-1} peat treatment over the course of 70 h. Total HCl extractable Fe(II) increased linearly with time up to 30 h, while Eh decreased (Figure 5.2). Following 30 h, both Eh and Fe(II) concentration came to a plateau, and remained constant for up to 70 h. Similar trends were exhibited among all treatments, except that with increasing bound Fe(III) concentration [decreasing peat addition for the same Fe(III) concentration], maximum dissolved Fe(II) concentration increased from 600 to as much as 1000 μmol kg^{-1} suspension. In the absence of CN32 (Control 1) no Fe(III) reduction took place within the time frame of my experiments, which shows the role of CN32 as a catalyst for Fe(III) reduction. Remaining treatments were only carried out until maximum Fe(III) reduction was achieved at 48 h.

Changes in pH During Fe(III) Reduction

Regardless of treatment, H^+ addition increased linearly with Fe(III) reduction (r^2 = 0.86) during the 48 h of microbial reduction (Figure 5.3). Overall, an average of 0.56 moles of H^+ were produced per mole of Fe(III) reduced during microbial reduction. The net H^+ consumption potentially resulted from a combination of Fe(III) reduction reactions, because the form of electron acceptor was likely variable. For example, Fe(III) reduction reactions for different hydrolysis states of bound Fe(III) show different stoichiometries of H^+ or OH^- production (Equations 5.3 – 5.4).

$RCOOFe^{2+}_{(s)} + ½\ H_{2(g)} \leftrightarrow RCOO^{-}_{(s)} + H^{+}_{(aq)} + Fe^{2+}_{(aq)}$ Equation 5.3

$RCOOFeOH^{+}_{(s)} + ½\ H_{2(g)} \leftrightarrow RCOO^{-}_{(s)} + Fe^{2+}_{(aq)} + H_2O_{(l)}$ Equation 5.4

$RCOOFe(OH)_{2(s)} + ½\ H_{2(g)} \leftrightarrow RCOO^{-}_{(s)} + Fe^{2+}_{(aq)} + OH^{-}_{(aq)} + H_2O_{(l)}$ Equation 5.5

In these chemical reactions the production of H^+ depends on the initial hydrolysis state of Fe(III) reduction and results in decreased, unchanged, or increased pH for the $RCOOFe^{2+}_{(s)}$, $RCOOFeOH^{+}_{(s)}$, and $RCOOFe(OH)_{2(s)}$ species, respectively. Thus, a combination of these reactions would be needed to achieve the 0.55 moles of H^+ consumption per mol Fe(III) reduced shown in this research.

Acid addition continued following maximum Fe(III) reduction in the > 1 g peat kg^{-1} suspension treatments (Figure A5.1). In a similar study, Kizewski (2010) determined that the microbial reduction of organic functional groups in peat occurred during microbial reduction with CN32, which resulted in proton consumption regardless of Fe(III) reduction. In addition, Roden et al. (2010) found that solid phase humic substances were capable of accepting electrons from CN32. Here, H^+ consumption continued to occur after maximum Fe(III) reduction was reached, indicating that the reduction of peat potentially occurred (Figure A5.1). Overall, at least two processes potentially contributed to changing pH during microbial Fe(III) reduction, (1) Fe(III) reduction, and (2) OM reduction. Because these processes occurred simultaneously, no quantitative information could be gained regarding the actual mechanisms responsible for H^+ consumption in these systems.

Electron Shuttling by OM

The impacts of electron shuttling by OM were negligible in comparison to direct reduction of Fe(III) by CN32 in this study. After reducing Pahokee peat with CN32, and flushing $H_{2(g)}$ from the system with N_2 to inhibit microbial reduction of Fe(III), the amount of subsequently added $FeCl_3$ that was reduced should result from the transfer of electrons from peat to Fe(III). Figure 5.4 shows the total amount of Fe(III) reduced following microbial reduction of peat for up to 25 h. Included is the Fe(II) that could be attributed to reduction of the original (residual) Fe(III) in the peat – 130 mmol kg^{-1} peat – before adding $FeCl_3$. A maximum Fe(II) concentration of 340 mmol kg^{-1} peat occurred from peat that had been reduced for 25 h (Figure 5.4). Of the total Fe(III) reduction, up to 270 mmol Fe(II) kg^{-1} peat was attributed to the reduction of residual Fe(III) because it was measured in the suspensions before adding $FeCl_3$. Consequently, only a maximum of 70 mmol Fe(II) kg^{-1} peat was attributed directly to the transport of electrons from reduced peat to oxidized Fe(III) (Figure 5.4).

In contrast, several studies have indicated that reduction of Fe(III) is enhanced by humic substances due to electron shuttling (Jiang and Kappler, 2008; Kappler and Haderlein, 2003; Rakshit et al., 2009; Scott et al., 1998). For example, Jiang and Kappler (2008) found that the transfer of electrons to humic substances from *Geobacter sulfurreducens* was 27 fold faster than the direct transfer to Fe(III)hydroxides. Similarly, Roden et al. (2010) indicated that solid humic substances were capable of serving as electron acceptors from CN32, which potentially contributed to Fe(III) reduction by way of electron shuttling. In my microbial reduction experiments the need for electron shuttling was limited since (1) the incubation

was continuously stirred, and (2) Fe(III) was presumably in an easily usable form relative to Fe(III) in minerals. In a similar study, Kizewski (2010) found that although the reduction of both OM and Fe(III) occurred, the two process occurred simultaneously, indicating that OM served as a remote, rather than active electron shuttle. It is likely, however, that increasing solid phase OM in systems where Fe(III) is bound directly to OM would inhibit rather than facilitate Fe(III) reduction because the transfer of electrons from CN32 to Fe(III) could be blocked by OM.

Initial Fe(II) Reduction

Iron(III) reduction took place prior to imposing microbial reduction, which is referred to here as the reducing capacity of the peat. Figure 5.5 shows total Fe(II) concentrations measured at time 0h, before $H_{2(g)}$ flow started, in relation to the concentrations of added Fe(III). The Fe(II) concentration at time 0 increased linearly ($r^2 = 0.90$) with added peat from 7 to 320 $\pm$ 72 mmol Fe kg^{-1} suspension (where $\pm$ indicates 95% confidence interval). These results translate to a reduction capacity of 100 $\pm$ 50 mmol Fe(III) kg^{-1} peat before microbial reduction began, which was comparable to the native reducing capacity of Pahokee peat humic acid of 120 mmol kg^{-1} peat found by Peretyazhko and Sposito (2006). Thus, prior to any microbial Fe(III) reduction, the presence of OM impacted Fe(III) reduction.

Fe(III) Reduction Rates

Because electron shuttling was not a dominant mechanism in these experiments, we were able to directly investigate if changes in the binding of Fe(III) in OM due to Fe concentration impacted Fe(III) reduction rate. Time 0 Fe(II) concentrations varied across

peat addition treatments, therefore, the initial Fe(II) was subtracted from the Fe(II) at each time prior to calculating Fe(III) reduction or dissolution rates.

From chemical kinetics, the change in concentration (denoted by brackets) of a chemical component over time (t) is related to the concentration of the reactant, where n is the reaction order (e.g., n = 0, 1, 2 for a zero, first, or second order reaction) (Equation 5.6).

$$d[Fe(III)]/dt = -k_1[Fe(III)]^n \qquad \text{Equation 5.6}$$

When Fe(III) is abundant, the rate of Fe(II) reduction is independent of Fe(III). Given that the data in Figure 5.2 showed a linear trend in Fe(III) reduction up to 20 h, indicative of zero-order kinetics, the slopes of the linear regressions up to12 h were used to represent the zero-order rate coefficients (k_1). The k_1 for the disappearance of Fe(III) under these conditions is shown in Equation 5.7. Here, final Fe(II) concentrations are denoted with brackets.

$$[Fe(II)] = k_1 t \qquad \text{Equation 5.7}$$

The k_1 was designated $k_{1(tot)}$ for total Fe(III) reduction rate and $k_{1(dis)}$ for dissolved Fe(III) dissolution rate and was obtained by monitoring the production of Fe(II), because the disappearance of $[Fe(III)] = [Fe(III)]_0 - [Fe(II)]$. In addition, since the starting concentration of Fe(II) was background subtracted to be 0, the Y intercept of linear fits were also set to 0.

Iron(III) reduction rates in soils have also been shown to follow first-order kinetics (e.g. Roden and Wetzel 2002). The pseudo-first-order kinetic equation is expressed as:

$$dA_t/dt = k_2 ([Fe(II)_{max}] - [Fe(II)]) \quad \text{Equation 5.8}$$

with dissolved [Fe(II)] at time (t), maximum $[Fe(II)_{max}]$ as t goes to ∞, and k_2 as the pseudo first-order rate coefficient. After integration and applying the condition that $A_t = 0$ when t = 0, the pseudo-first-order equation becomes Equation 5.2. The pseudo-first-order rate equations and rate coefficients for total dissolved ($k_{2(dis)}$) and total Fe(II) ($k_{2(tot)}$) production are listed in Tables A5.1 and A5.2 respectively.

Figure 5.6 shows several examples in which $k_{1(tot)}$ was calculated. Here, Fe(II) increased with time up to 12 h, and varied according to treatment (Figure 5.6). All linear equations, except for that from one 1200 mmol Fe kg^{-1} peat replicate, were significant ($P < 0.05$) despite the use of only 4 data points (Table 5.2). Among all treatments, $k_{1(tot)}$ was between 33 and 66 (Table 5.2). Similarly, linear trends in dissolved Fe(II) with time were significant in all but one 300 and one 1200 mmol Fe kg^{-1} peat treatment ($P < 0.05$). The $k_{1(dis)}$ varied between 8.8 and 31 (Table 5.3).

Overall, no significant differences were determined between $k_{1(tot)}$ and peat addition (Table 5.2). Figure 5.7 depicts the trends in $k_{1(dis)}$ and $k_{1(tot)}$ with increasing peat. Similarly, changes in $k_{1(dis)}$ (Figure 5.7, Table 5.2), and the pseudo-first-order rate coefficients $k_{2(dis)}$ and $k_{2(tot)}$ with increasing peat were not significant, presumably due in part to a lack of data points for appropriate statistical analysis. Statistically significant differences between standards and samples, however, were found.

The $k_{1(tot)}$ of ferrihydrite was more than 6 X slower than that of Fe(III) added at 3600 mmol Fe kg^{-1}or in the Fe only treatment (Control 2) (Table 5.2). These results suggested that the reduction rate of Fe(III) decreases as the Fe(III) transitions from organically bound to mineral form. Furthermore, the $k_{1(tot)}$ of the peat treatments were generally higher than in the Fe(III) only control (Control 2), suggesting that overall the addition of peat enhanced Fe(III) reduction rate (Table 5.2) to its native reduction potential or above in the presence of CN32. Two possible mechanisms of enhanced Fe(III) reduction rate are, (1) a change in the speciation of Fe(III) resulting in faster Fe(III) reduction, or (2) the electron transfer from OM to Fe(III) accelerating Fe(III) reduction. Because the transfer of electrons from reduced OM to Fe(III) was negligible, data suggest that OM enhanced Fe(III) reduction rate by altering the form of Fe(III) to one more available for microbial reduction (e.g. from Fe(III)-(hydr)oxide to polynuclear Fe(III)-OM clusters).

DOC Impacts on Fe(II) Dissolution

Initial concentration of DOC also increased with increased peat addition, which potentially contributed to Fe(II) dissolution rates (Fig. A.5.2). Previously, Fe(III) added as $FeCl_3$ has been identified as a chelating agent for DOC (Lee et al., 2008). Similarly, my results suggested that the complexation of DOC with Fe(III) resulted in decreased DOC measured at time 0 (after initial equilibrium, but before the onset of microbial reduction). Conversely, increasing DOC can enhance the dissolved concentration of Fe(III) in Fe-OM systems (Chapter 3). Thus, as the initial DOC concentration increased with increasing peat addition, DOC impacted the amount of bound vs dissolved Fe(III) prior to Fe(III) reduction.

Similarly, DOC may facilitate the mobilization of dissolved Fe(II) following Fe(III) reduction.

Figure 5.7 depicts the linear trends between dissolved Fe(II) and DOC. Four treatments are shown, including: 3600 mmol Fe kg^{-1} peat, 2400 mmol kg^{-1} peat, and two replicates of 1200 mmol Fe kg^{-1} peat. An increase in DOC concentration from 0 to 25 or 40 to 110 mg L^{-1} during Fe(III) reduction occurred in the 2400 and 3600 or 1200 mmol Fe kg^{-1} peat treatments, respectively. The slope of increasing DOC with increasing dissolved Fe(II) concentration was 0.03 in treatments containing the lowest peat (3600 mmol Fe kg^{-1} peat), and increased as peat addition increased (e.g 0.10 to 0.14 in 1200 mmol Fe kg^{-1} peat) (Figure A5.3). An exception was found in the case of solid phase OM at 300 mmol Fe kg^{-1} peat samples, where DOC remained constant during microbial reduction of Fe(III) with an average of 570 $\pm$ 70 mg L^{-1}. Overall, both solid phase OM and DOC impacted the binding and dissolution of Fe(II) during microbial Fe(III) reduction. However, the concentration of DOC alone did not account for increases in dissolved Fe(II) during microbial reduction. These results suggest that the dissolution rate of Fe(II) depends on a combination of factors, including solid OM and DOC concentrations.

Impacts of OM on Maximum Dissolved and Total Fe(II) Production

Table 5.4 shows maximum HCl extractable and dissolved Fe(II) among all treatments. Maximum HCl extractable Fe(II) was between 960 and 1300 µmol L^{-1} suspension, and maximum dissolved Fe(II) was between 390 and 1000 µmol L^{-1} (Table 5.4, Figure 5.9). Figure 5.9 shows maximum dissolved and total Fe(II) concentrations across peat addition treatments. Initially, the maximum dissolved Fe(II) decreased with peat addition,

while the maximum total Fe(II) increased. Although added Fe concentration was constant between treatments (1200 mmol Fe kg^{-1} peat), the peat had a residual Fe(III) concentration of approximately 130 mmol Fe kg^{-1} peat. The percentage of total Fe(III) reduced remained constant between the peat treatments at 75 $\pm$ 7%. These results suggested that the addition of peat had no significant impact on the % of total Fe(III) reduced, and that higher total Fe(III) reduction with OM addition was a direct result of higher total Fe(III) concentration. In addition, a decrease in total Fe(III) reduction from 84 to 75 $\pm$ 7% between the Fe only control (Control 2) and the peat treatments suggested that addition of peat potentially inhibited total Fe(III) reduction.

In contrast, the % of total added Fe(III) that became dissolved following reduction increased from 33 $\pm$ 2.5 in the 300 mmol Fe kg^{-1} peat treatment to 71 $\pm$ 15 in the 3600 mmol Fe kg^{-1} peat treatment (Table 5.4). Thus, as the amount of added peat increased, the amount of Fe(II) that remained bound also increased.

Distribution of Bound and Dissolved Fe(II)

To determine the relative proportion of bound vs dissolved Fe(II) in each treatment, distribution coefficients (K_D) were determined (Equation 5.9).

$$K_D = [Fe(II)_{(aq)}]/[Fe(II)_{(s)}] \qquad \text{Equation 5.9}$$

Generally, K_D decreased from 40 to 0.5 mol mol^{-1} between the Fe-only and the 1200 mmol Fe kg^{-1} peat treatments, and then increased from 0.5 to 1 between the 1200 and 300 mmol Fe kg^{-1} peat treatments (Figure 5.10). As peat was increased from 0 to 1200 mmol Fe kg^{-1} peat,

the dissolution of Fe(II) was inhibited, most likely because Fe(II) sorption to OM increased with increasing OM. As peat increased in the1200 to 300 mmol Fe kg^{-1} peat treatments, however, Fe(II) dissolution was enhanced, but still minimal compared to the treatment containing no OM. The enhancement of Fe(II) dissolution in the presence of peat was potentially due to two mechanisms (1) the complexation of Fe(II) to DOM following Fe(III) reduction, and (2) the reduction of Fe(III) bound in the < 0.2 µm dissolved fraction, which remains dissolved following reduction.

My results in Chapter 3 suggested that the concentration of Fe(III) found in Fe(III)-DOM complexes increased with increasing DOC. Earlier, it was determined that the total Fe(III) reduced was comparable between peat treatments with > 2400 mmol Fe kg^{-1} peat. Furthermore, the addition of solid OM would increase solid phase Fe(III) and Fe(II) binding sites, which would result in retention of Fe(II) rather than dissolution. Although the addition of accessible binding sites could explain the decrease in K_D with increasing peat up to 1200 mmol Fe kg^{-1} peat, it was unable to explain the increase in K_D with increasing peat > 1200 mmol Fe kg^{-1} peat. Previous research has indicated that dissolved Fe(III) concentration increases with DOC addition, and that both persisted in the > 5,000 Da fraction (Chapter 3, Chapter 6). Thus, we hypothesize that the reduction of Fe(III) already bound to DOM in the dissolved phase caused an increase in Fe(II) dissolution during microbial reduction in systems containing > 50 mg L^{-1} DOC. Overall, DOC played an important role in Fe(II) dissolution, which enhanced total Fe(II) dissolution during microbial reduction.

CONCLUSIONS

In my experiments aimed at determining how concentrations of sorbed Fe(III) in OM affected the rate of microbial Fe(III) reduction, no differences in Fe(III) reduction rates were determined between 1200 to 300 mmol Fe kg^{-1} peat treatments. Comparisons of treatments with controls showed that (1) CN32 activity was responsible for Fe(II) production, and (2) the reduction of Fe(III) bound to peat was faster than that of ferrihydrite. Electron transport through OM to Fe(III) was negligible in continuously stirred microbial incubations. Distribution coefficients confirmed that the amount of Fe(II) remaining bound to OM following Fe(III) reduction increased with peat addition, but as Fe(III) concentrations decreased to < 1200 mmol kg^{-1} peat, an increase of DOC correspond to enhanced Fe(II) dissolution. Both the amount of OM and DOC played important roles in Fe(II) dissolution following Fe(III) reduction. Overall, these results indicated that changes in bound Fe(III) concentration to peat did not impact Fe(III) reduction rate, although OM and DOC both impacted total Fe(II) dissolution following Fe(III) reduction.

BIBLIOGRAPHY

Ajmone-Marsan F., D. Côté, and R.R. Simard. 2006. Phosphorus transformations under reduction in long-term manured soils. Plant and Soil. 282:239-250.

Bowman J.P. 2005. Genus XIII. Shewanella., in: D.J. Brenner, N.R. Krieg, J.T. Stanley, and G.M. Garrity (Ed.), Bergey's manual of systematic bacteriology, Springer, NY. Cornell R.M.

Schwertmann U. 1993. The iron oxides: Structure, properties, reactions, occurrence and uses VCH.

Ehrlich H.L. 1995. Geomicrobial processes Marcel Dekker, New York, NY. USA.

Fiedler S., and K. Kalbitz. 2003. Concentrations and properties of dissolved organic matter in forest soils as affected by the redox regime. Soil Sci. 168:793-801.

Fredrickson J.K., S. Kota, R.K. Kukkadapu, C.X. Liu, and J.M. Zachara. 2003. Influence of electron donor/acceptor concentrations on hydrous ferric oxide (HFO) bioreduction. Biodegradation. 14:91-103.

Fredrickson J.K., J.M. Zachara, D.W. Kennedy, H.L. Dong, T.C. Onstott, N.W. Hinman, and S.M. Li. 1998. Biogenic iron mineralization accompanying the dissimilatory reduction of hydrous ferric oxide by a groundwater bacterium. Geochim. Cosmochim. Acta. 62:3239-3257.

Gerke J. 1993. Solubilization of Fe(III) from humic-Fe complexes, humic Fe-oxide mixtures and from poorly ordered Fe-oxide by organic-acids - consequences for P-adsorption. Z. Pflanzenernahr. Bodenkd. 156:253-257.

Gerke J., Hermann R. 1992. Adsorption of orthophosphate to humic-Fe-complexes and to amorphous Fe-oxide. Z. Pflanzenernahr. Bodenkd. 155:233-236.

Hansel C.M., S.G. Benner, P. Nico, and S. Fendorf. 2003. Structural constraints of ferric (hydr)oxides on dissimilatory iron reduction and the fate of Fe(II). Biochim. Cosmochim. Acta. 68:3217-3229.

Hue N.V. 1991. Effects of organic-acids anions on P-sorption and phytoavailability in soils with different mineralogies. Soil Sci. 152:463-471.

Hunt J.F., T. Ohno, Z.Q. He, C.W. Honeycutt, and D.B. Dail. 2007. Inhibition of phosphorus sorption to goethite, gibbsite, and kaolin by fresh and decomposed organic matter. Biol. Fert. Soils. 44:277-288.

Hutchison K.J., and D. Hesterberg. 2004. Dissolution of phosphate in a phosphorus-enriched ultisol as affected by microbial reduction. J. Environ.Qual. 33:1793-1802.

Jeon C.O., and J.M. Park. 2000. Enhanced biological phosphorus removal in a sequencing batch reactor supplied with glucose as a sole carbon source. Water Res. 34:2160-2170.

Jiang J., and A. Kappler. 2008. Kinetics of microbial and chemical reduction of humic substances: Implications for electron shuttling. Env. Sci. Tech. 42:3563-3569.

Kappler A., and S.B. Haderlein. 2003. Natural organic matter as reductant for chlorinated aliphatic pollutants. Env. Sci. Tech. 37:2714-2719.

Kizewski, F. R. 2010. Phosphate binding and Fe(III) reduction as affected by Fe(III) and organic matter interactions. Ph.D. Dissertation. North Carolina State University, Raleigh, NC.

Lee S.J., Y.J. Lee, and S.H. Nam. 2008. Improvement in the coagulation performance by combining Al and Fe coagulants in water purification. Korean Journal of Chemical Engineering 25:505-512.

Lindsay, W.L. 1979, Chemical equilibrium in soils. John Wiley & Sons, New York, NY. USA.

Loeppert R.H., and W.P. Inskeep. 1996. Iron, in: S. L. Sparks (Ed.), Methods of soil analysis, part 3. Chemical methods, ASA and SSSA, Madison WI. pp. 639-664.

Lovley D.R. 1991. Dissimilatory Fe(III) and Mn(IV) reduction. Microbiol. Rev. 55:259-287

Lovley D.R. 1993. Dissimilatory metal reduction. Annu. Rev. Microbiol. 47:263-290.

Lovley D.R., and R.T. Anderson. 2000. Influence of dissimilatory metal reduciton on fate of organic and metal contaminants in the subsurface. Hydrogeology. J. 8:77-88.

Lovley D.R., J.D. Coates, E.L. Blunt-Harris, E.J.P. Phillips, and J.C. Woodward. 1996. Humic substances as electron acceptros for microbial respiration. Nature. 382:445-448.

Moshi A.O., A. Wild, and DJ. Greenlan. 1974. Effect of organi-matter on charge and phosphate adsorption characteristics of Kikuyu Red Clay from Kenya Geoderma. 11:275-285.

O'Loughlin E.J., P. Larese-Casanova, M. Scherer, and R. Cook. 2007. Green rust formation from the bioreduction of γ-FeOOH (Lepidocrocite): Comparison of several Shewanella species. Geomicrobiology. 24:211-230.

Peretyazhko T., and G. Sposito. 2005. Iron(III) reduction and phosphorous solubilization in humid tropical forest soils. Geochimica Et Cosmochimica Acta. 69:3643-3652.

Peretyazhko T., and G. Sposito. 2006. Reducing capacity of terrestrial humic acids. Geoderma. 137:140-146.

Ponnamperuma F.N. 1972. The chemistry of submerged soils. Adv. Agron. 24:29-96.

Rakshit S., M. Uchimiya, and G. Sposito. 2009. Iron(III) bioreduction in soil in the presence of added humic substances. Soil Sci. Soc. Am. J. 73:65-71.

Richardson J.L., and M.J. Vepraskas. 2001. Wetland Soils: genesis, hydrology, landscapes, and classification, CRC Press LLC, Boca Raton, FL.

Roden E.E. 2003. Fe(III) oxide reactivity toward biological versus chemical reduction. Environ. Sci. Tech. 37:1319-1324.

Roden, R.E., A. Kappler, I. Bauer, J. Jiang, A. Paul, R. Stoesser, H. Konishi, and H. Xu. 2010. Extracellular electron transfer through microbial reduction of solid-phase humic substances. Nature Geoscience. 3:417-421.

Royer R.A., W.D. Burgos, A.S. Fisher, R.F. Unz, and B.A. Dempsey. 2002. Enhancement of biological reduction of hematite by electron shuttling and Fe(II) complexation. Env. Sci. Tech. 36:1939-1946.

Satoh, Y, K. Kikuchi, Y. Satoh, and H. Fujimoto. 2009. Reverse process of coprecipitation of dissolved organic carbon with Fe(III) repcipitates in a lake. Limnology. 10:131-134.

Scharer M., D.D. Grave, O. Semalulu, S. Sinaj, R.E. Vandenberghe, and E. Frossard. 2009. Effect of redox conditions on phosphate exchangeability and iron forms in a soil amended with ferrous iron. Eur. J. Soil Sci. 60:386-397.

Schefe C.R., P. Kappen, L. Zuin, P.J. Pigram, and C. Christensen. 2009. Addition of carboxylic acids modifies phosphate sorption on soil and boehmite surfaces: A solution chemistry and XANES spectroscopy study. J. Colloid Inter. Sci. 330:51-59.

Scott D.T., D.M. McKnight, E.L. Blunt-Harris, S.E. Kolesar, and D.R. Lovley. 1998. Quinone moieties act as electron acceptors in the reduction of humic substances by humics-reducing microorganisms. . Environ. Sci. Tech. 32:2984-2989.

Sposito, G. 1989. The Chemistry of Soils. Oxford University Press. Oxford, NY. USA.

Violante A., C. Colombo, and A. Buondonno. 1991. Competative adsorption of phosphate and oxalate by aluminum-oxides. Soil Sci. Soc. Am. J. 55:65-70.

Zelasko A.J. 2007. Soil reduction rates under saturated conditions in relation to soil properties, Soil Science, North Carolina State University, Raleigh NC.

Table 5.1. List of microbial reduction experiments performed.

Treatment ID	Added Fe (μmol L^{-1})	Added Peat (g L^{-1})	Fe (mmol kg^{-1} Peat)	With or without CN32	Reps
300	1200	4	300	With	2
900	1200	1.33	900	With	1
1200	1200	1	1200	With	3
2400	1200	0.5	2400	With	1
3600	1200	0.33	3600	With	2
Control 1	1200	0.5	2400	Without	1
Control 2	1200	0	∞	With	1
Control 3	0	4	0	With	1
Control 4	4800	2	2400	With	1
Ferrihydrite	20000	0	∞	With	1

Table 5.2. Linear total Fe(II) reduction rates ($k_{1(tot)}$) calculated over the first 12 h of microbial Fe(III) reduction for all treatments. Time 0 Fe(II) was subtracted from total Fe(II) at each time and y-intercepts were set at 0 µmol Fe(II) kg^{-1} suspension.

Treatment ID	Equation	$k_{1(tot)}$	95% Confidence Interval		Standard Error
			Max $k_{1(tot)}$	Min $k_{1(tot)}$	
300	Y = 66x	66	82	50	5.0
300 Rep 2	Y = 40x	40	49	32	2.6
600	Y = 48x	48	70	27	6.8
1200	Y = 64s	64	78	50	4.4
1200 Rep 2	Y = 25x	25	57	13	6.9
1200 Rep 3	Y = 38s	38	40	36	0.76
2400	Y = 46x	46	50	41	1.4
3600	Y = 48x	48	52	44	1.3
3600 Rep 2	Y = 33x	33	38	29	1.4
Control 1	Y = 1.5x	1.5	12	-8.8	2.4
Control 2	Y = 34x	34	37	31	0.91
Control 3	Y = 12x	12	16	7.9	1.3
Control 4	Y = 36x	36	41	31	1.6
Ferrihydrite	Y = 5.3x	5.3	11	-0.53	1.4

Table 5.3. Linear dissolved Fe(II) production rates ($k_{1(dis)}$) calculated over the first 12 h of microbial Fe(III) reduction. Time 0 dissolved Fe(II) was subtracted from dissolved Fe(II) at each time, and y-intercepts were set at 0 µmol Fe(II) L^{-1}.

Treatment ID	Equation	$k_{1(dis)}$	95% Confidence		Standard Error
			Max $k_{1(dis)s}$	Min $k_{1(dis)}$	
300	Y = 25x	25	39	12	4.2
300 Rep 2	Y = 13x	13	17	9.4	1.2
600	Y = 18x	18	19	17	0.36
1200	Y = 21x	21	28	14	2.1
1200 Rep 2	Y = 8.8x	8.8	11	6.6	0.64
1200 Rep 3	Y = 9.1x	9.1	13	5.3	1.2
2400	Y = 26x	26	34	17	2.6
3600	Y = 31x	31	38	25	2.0
3600 Rep 2	Y = 26x	26	30	22	1.4
Control 1	Y = -0.50x	-0.50	1.5	-2.5	0.47
Control 2	Y = 29x	29	39	20	3.0
Control 3	Y = 13x	13	26	1.0	3.9
Control 4	Y = 2.2x	2.2	2.9	1.5	0.22
Ferrihydrite	Y = 3.0x	3.0	5.1	0.96	0.48

Table 5.4. Maximum dissolved and HCL extractable Fe(II) along with the percent of total Fe(III) that was reduced to Fe(II), and the percent of total Fe(III) that became dissolved.

Treatment ID	Max Dissolved Fe(II) Fe(II) (μmol L^{-1})	Time (h)	Max Total Fe(II) Fe(II) (μmol kg^{-1}susp.)	Time (h)	% Fe(III) Reduced	% Fe(III) Dissolved
300	593	47	1320	47	77	34
300 Rep 2	533	24	1190	47	70	31
600	385	48	1000	24	68	26
1200	551	30	974	24	73	41
1200 Rep 2	395	47	956	47	72	30
1200 Rep 3	416	47	989	47	74	31
2400	810	30	981	30	78	64
3600	1007	36	1130	24	91	81
3600 Rep 2	747	24	878	24	71	60
Control 1	10.5	21	122	7.5	10	0.8
Control 2	989	46	996	46	83	82
Control 3	311	48	343	24	68	60
Control 4	596	47	2250	47	44	12
Ferrihydrite	85.0	67	147	40	0.7	0.4

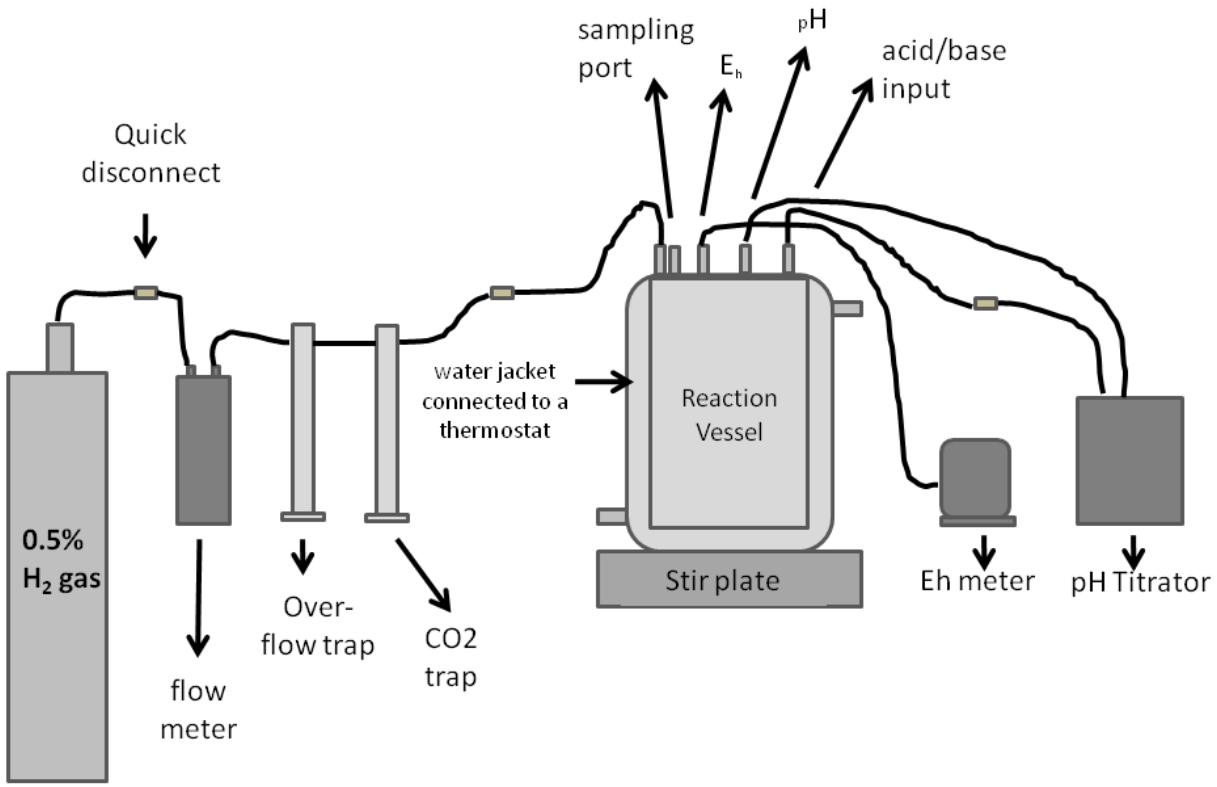

Figure 5.1. Schematic portraying microbial reduction experimental set-up. (modified from F. Kizewski, 2010)

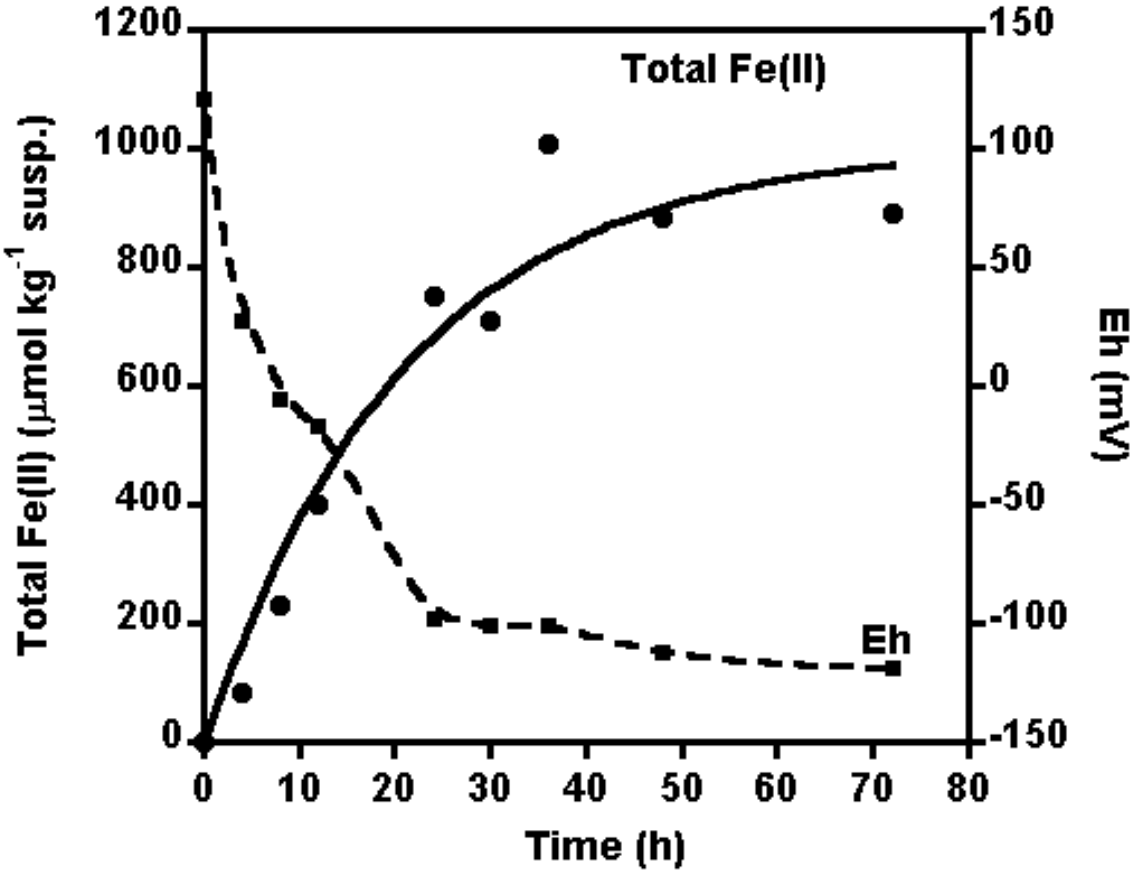

Figure 5.2. Microbial Fe(III) reduction occurred with decreasing Eh decreased over 70 h in a 1200 mmol Fe kg^{-1} peat treatment at pH 6.0.

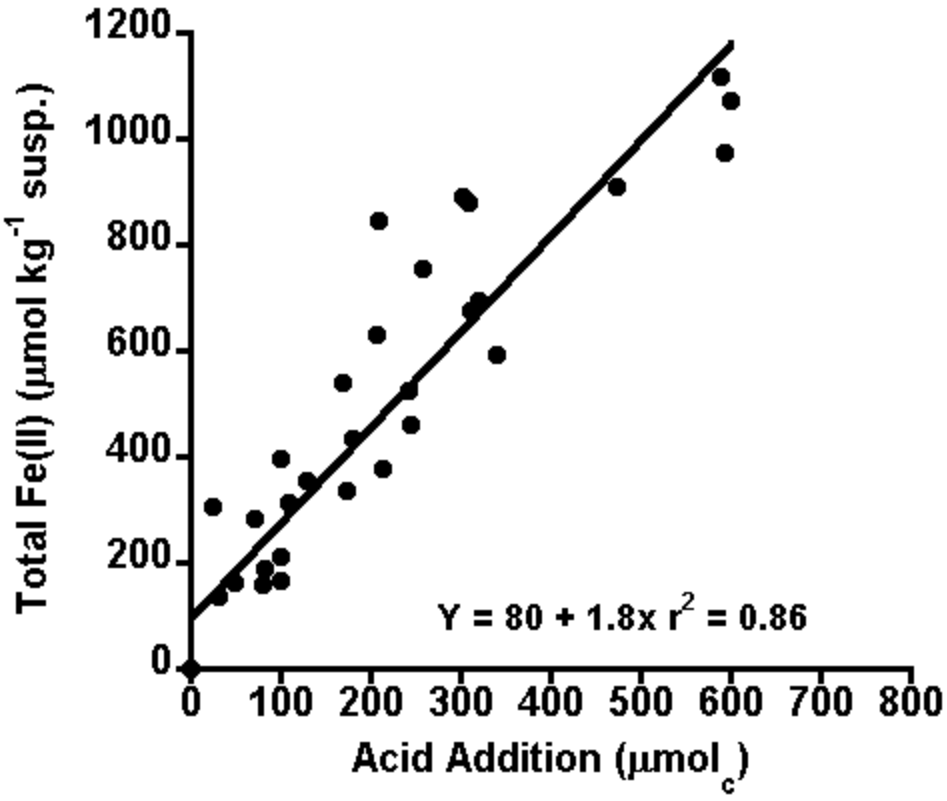

Figure 5.3. Addition of 0.05 M HCl was linearly correlated with total Fe(II) production across all treatments.

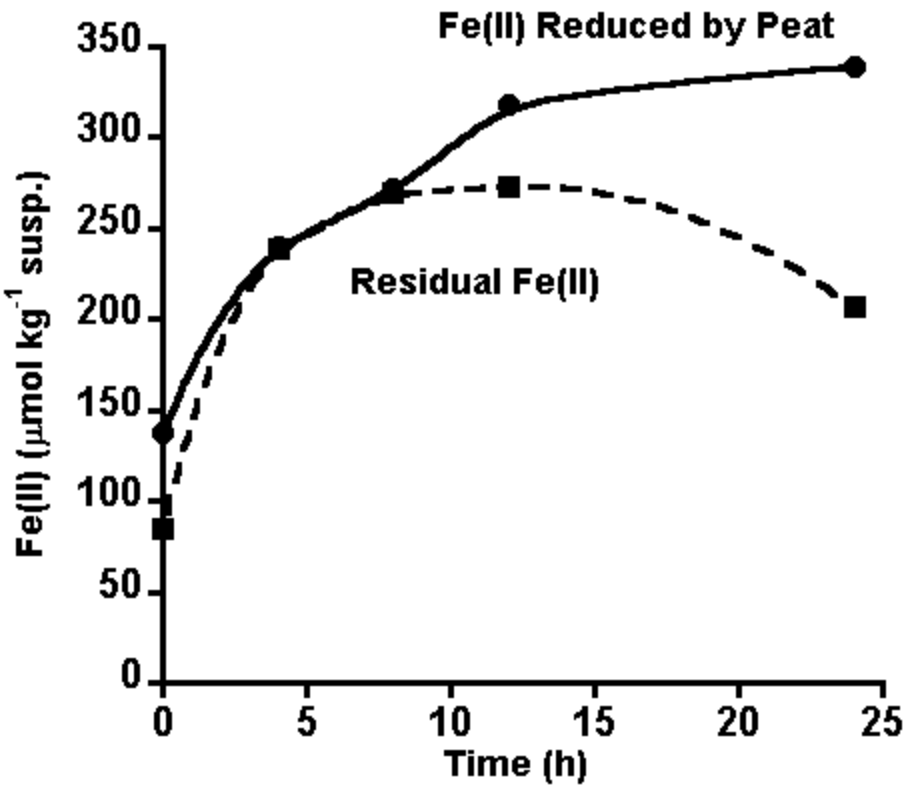

Figure 5.4. Microbial reducing capacity (solid line) and residual Fe(III) reduction (dashed line) of Pahokee peat.

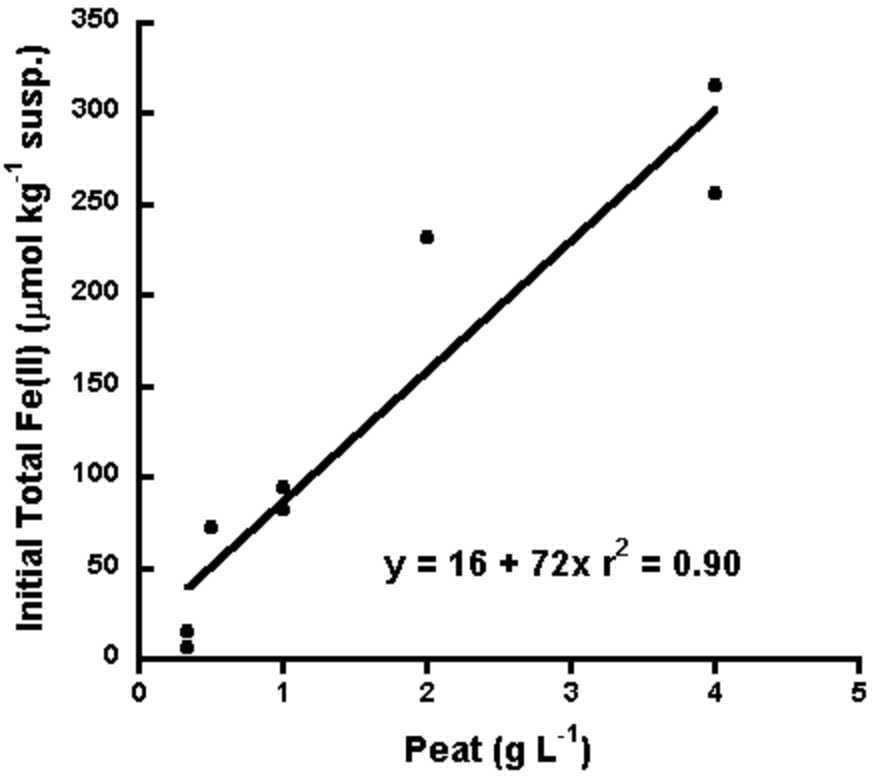

Figure 5.5. Zero hour reduced Fe(II) concentration increased with increasing peat addition. Linear trends were significant with a 95% confidence interval of $\pm$ 72 µmol Fe kg^{-1} suspension.

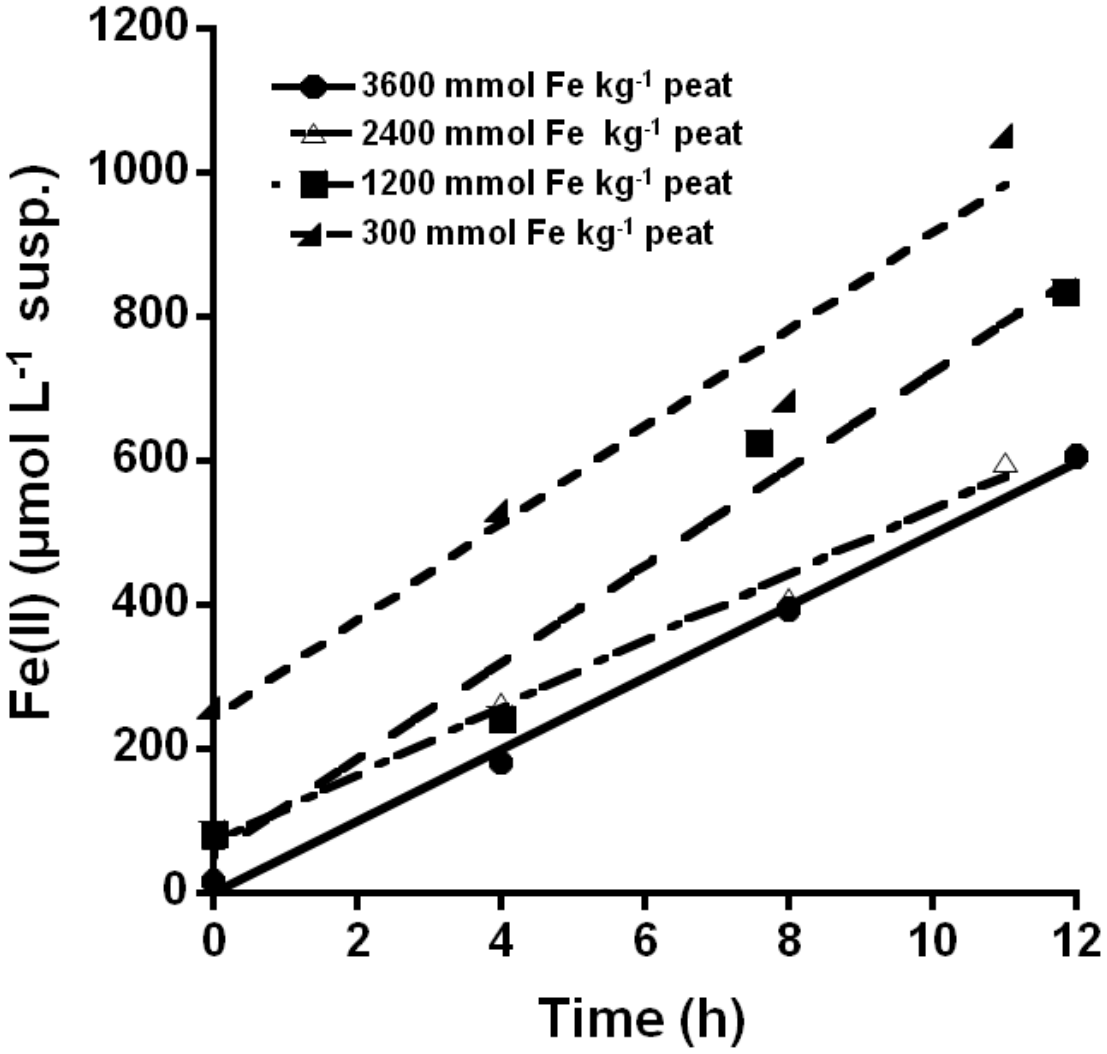

Figure 5.6. Four examples of the most linear portion of Fe(III) reduction. Zero-order rates ($k_{1(tot)}$) were calculated using the slope of the linear trend between Fe(II) (µmol Fe(II) kg^{-1} suspension) with time up to 12 h for all Fe concentrations (mmol Fe kg^{-1} peat) and controls. In this case, 3600 mmol Fe kg^{-1} peat, 2400 mmol Fe kg^{1} peat, 1200 mmol Fe kg^{-1} peat, and 300 mmol Fe kg^{-1} peat had rates of 50, 46, 67, and 68 respectively. All equations are displayed in Table 5.3.

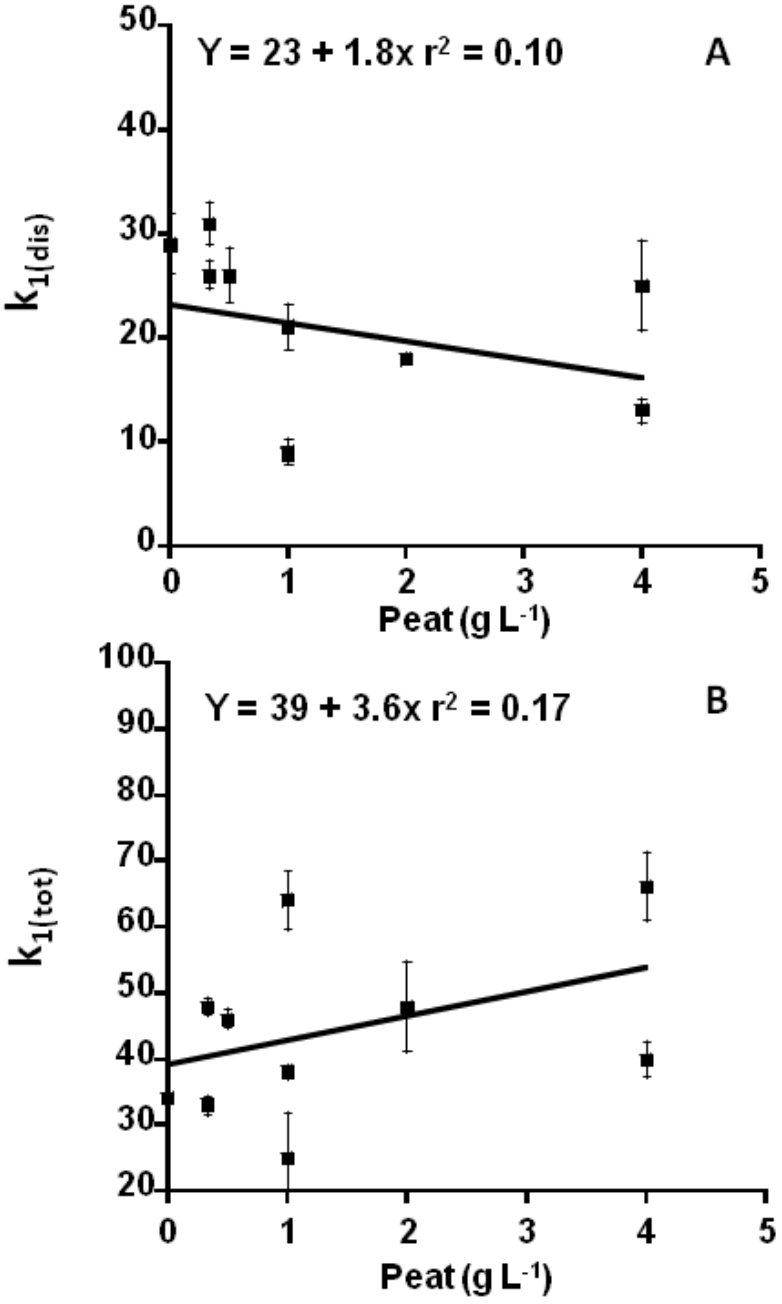

Figure 5.7. Rate coefficients ($k_{1(dis)}$ and $k_{2(tot)}$) for dissolved Fe(II) (A) and total Fe(II) (B) across peat addition. Neither the increase in total Fe(III) reduction rate nor the decrease in dissolved Fe(II) with increasing peat addition was significant. Error bars represent standard error.

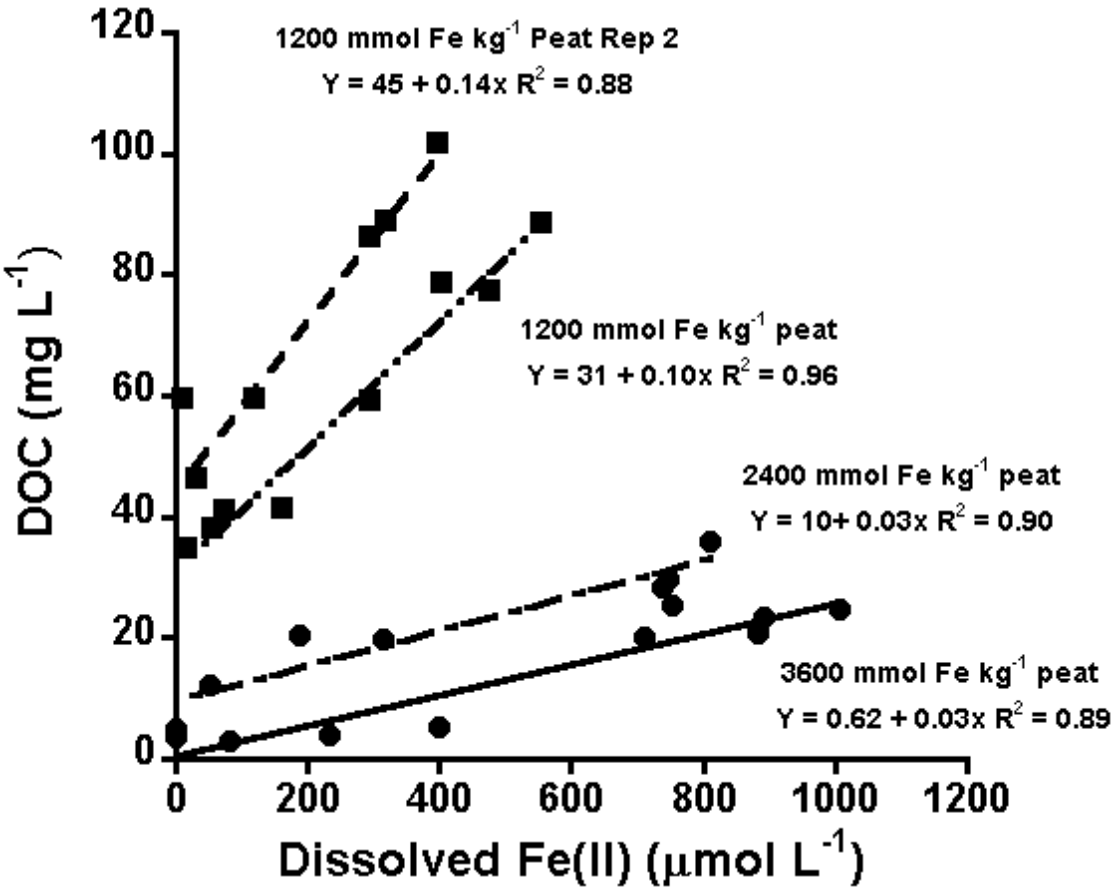

Figure 5.8. Dissolved Fe(II) increased with DOC in microbial reduction experiments containing $\geq$ 1200 mmol Fe kg^{-1} peat. All linear regressions were significant ($P < 0.05$).

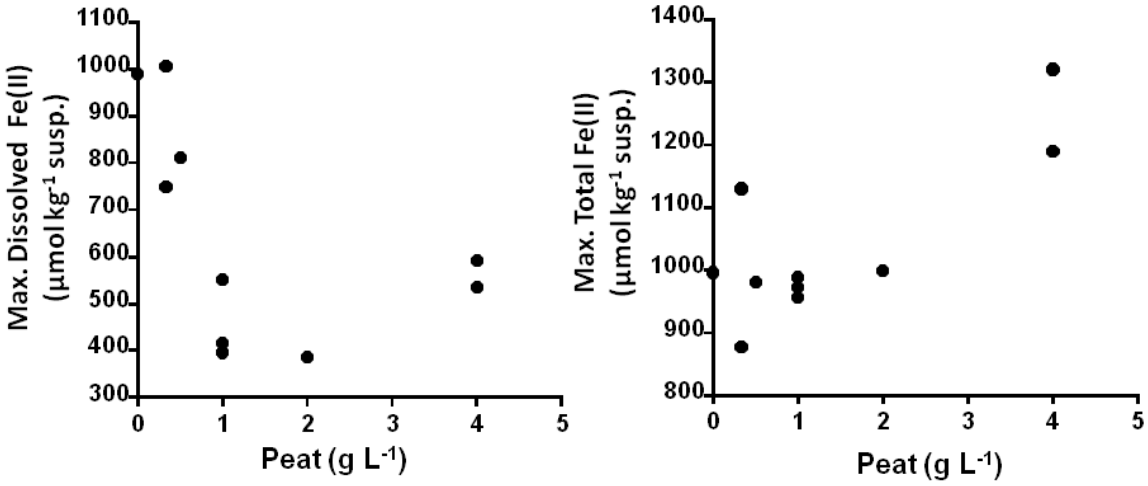

Figure 5.9. Maximum dissolved Fe(II) decreased to 2 g peat L^{-1} and then increased up to 4 g peat L^{-1}. Conversely, maximum total Fe(II) was variable at $\leq$ 1.0 g peat L^{-1}, and potentially increased at > 1.0 g peat L^{-1}.

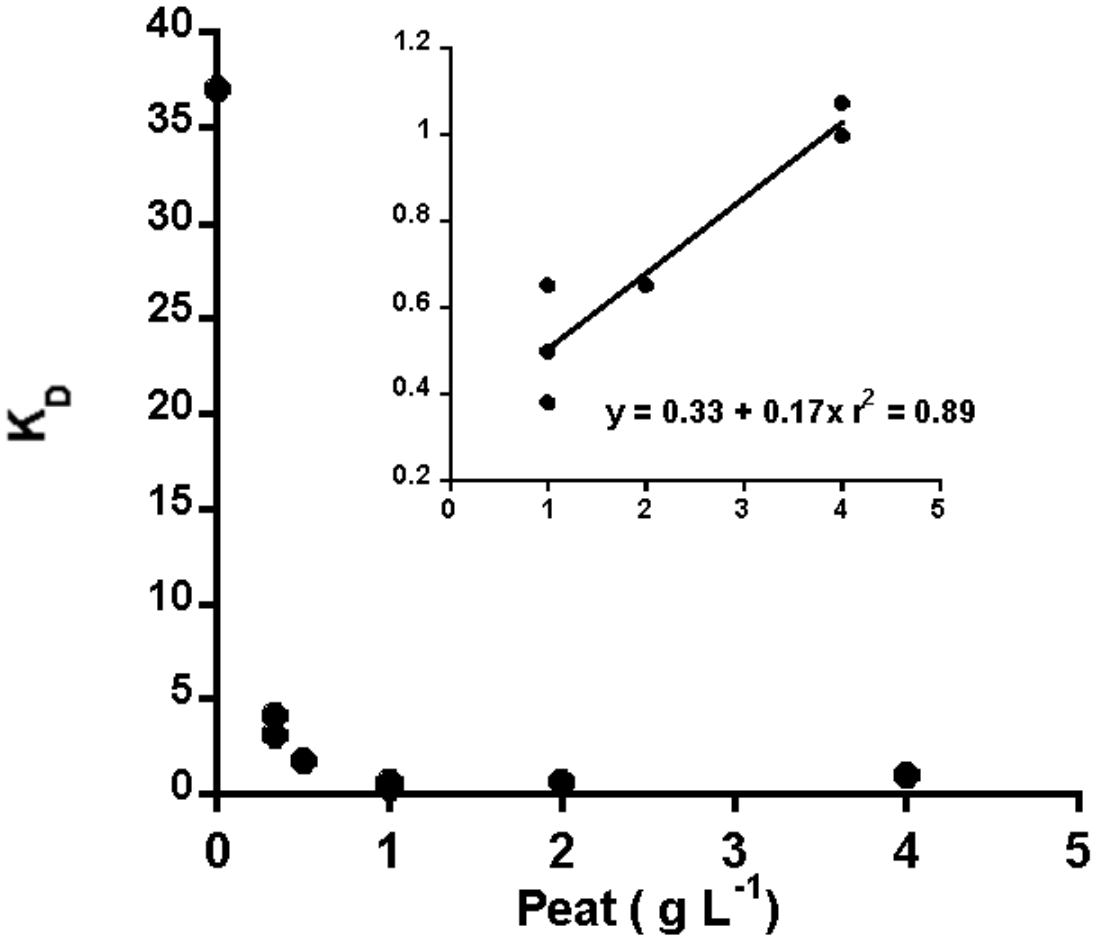

Figure 5.10. Distribution coefficient (K_D) compared with peat addition (0 to 4 g). Inset plot shows the linear relationship between amount of added peat from 1 to 4 g L^1, corresponding with 1200 to 300 mmol Fe kg^{-1} peat.

CHAPTER 6: MOBILIZATION OF PHOPHATE DURING MICROBIAL REDUCTION OF Fe AND Al BOUND TO PAHOKEE PEAT

ABSTRACT

Although PO_4 sorption to soil organic matter (OM) can occur, the impacts of OM and Fe and Al concentrations bound to OM on PO_4 mobilization during microbial reduction are currently unknown. The objective of this research was to quantify the impact of the relative proportions of bound Fe and Al on the rate of PO_4 mobilization from soil OM. Iron(III) and Al(III) were added to Pahokee peat (IHSS organic soil) at Fe/Al ratios of 0, 0.33, 2, 5, and ∞ (Fe only) to achieve a total bound metal concentration of 1200 mmol kg^{-1} peat. Peat-Fe/Al suspensions in 0.05 M KCl were continuously stirred at 25°C. Phosphate was added at 600 mmol P kg^{-1} peat, pH was maintained at 6.0, and *Shewanella putrefaciens* (CN32) were added at 1 x 10^8 cells mL^{-1} and H_2 gas (0.5% in N_2) was used as an electron donor to achieve reduction. During microbial reduction dissolved PO_4 concentration increased by as much as 260 µmol PO_4 L^{-1} between 0 and 48 h. As the Fe/Al ratio increased from 0 to ∞, the rate coefficients of PO_4 dissolution increased (e.g. from 0 to 35 mmol PO_4 kg^{-1} peat $h^{-0.5}$ as modeled by a parabolic diffusion equation), which corresponded to increases in Fe(III) reduction rates. Dissolved organic carbon (DOC) was also correlated with dissolved PO_4 concentration across all treatments during microbial reduction, and increased from 19 to 115 mg L^{-1} as the Fe/Al ratio increased from 0 to ∞. As much as 23% of PO_4 was in the > 5,000 Da colloidal fraction following Fe(III) reduction, which suggested the formation of PO_4

complexes with Fe and/or dissolved organic matter. Overall, results suggested that increasing the ratio of Fe/Al bound to OM would enhance the initial mobilization rate of PO_4 from soils.

INTRODUCTION

Phosphate mobilization from anaerobic wetland soils and associated transport to open water bodies remains a critical threat to ecosystem health, and can lead to changes in ecosystem structure, function, and services (Hagerthey et al., 2008). Although trends in PO_4 dissolution have been linked to soil properties such as pH, Fe, Al, and OC concentrations, and DOC, trends in PO_4 mobilization remain variable and difficult to predict across a range of soils. To accurately predict and control PO_4 mobilization from organic soils, specific impacts of soil properties such as Fe and Al content on PO_4 mobilization need to be determined. Ultimately, resolving specific mechanisms that lead to PO_4 mobilization during reducing conditions will aid in predicting PO_4 sorption and dissolution from soils.

Retention of PO_4 in soils depends in part on the amounts and forms of Fe- and Al-oxides and organic matter, while dissolution has been correlated to soil redox potential, Fe(III) reduction, and production of dissolved organic carbon (Holford and Patrick, 1981b; Hutchison and Hesterberg, 2004; Patrick and Khalid, 1974; Phillips, 1998). While extensive research has been conducted showing phosphorus mobilization during soil reduction (Ajmone-Marsan et al., 2006; Ann et al., 2000; Holford and Patrick, 1979), the impacts of Al and dissolved organic matter (DOM) on PO_4 have not been resolved.

Few studies have identified the impact of Al on Fe reduction and PO_4 mobilization (Murray and Hesterberg, 2006), and none have evaluated the impact of Al/Fe ratio on the mobilization of PO_4 from OM during Fe(III) reduction. Unlike Fe(III), Al(III) is not redox active in soils, and therefore, may be more important for PO_4 sorption than Fe(III) in reduced soils. In fact, non-crystalline Al-(hydr)oxides have been found to be the dominant sorbent of

P in anaerobic wetland environments (Richardson, 1985). Murray and Hesterberg (2006) found that when boehmite was added at $\geq$ 0.02 g kg^{-1} to ferrihydrite suspensions with added PO_4, PO_4 sorption increased during reduction. Other studies suggested that organically bound Al may play an important role in PO_4 sorption in wetland soils (Axt and Walbridge, 1999; Darke and Walbridge, 2000). For example, Al and soil OM were both correlated with PO_4 sorption within 6 forested wetlands in Virginia (Axt and Walbridge, 1999). To my knowledge, no one has identified how the ratio of Fe to Al bound to OM impacts PO_4 mobilization from organic soils during microbial reduction.

In addition, DOM plays a potentially important role in P dissolution (Chapter 3, Gerke, 1992b; Hutchison and Hesterberg, 2004; Gerke, 2010). For example, additions of organic amendments to soils have been shown to increase dissolved PO_4 concentrations (Chapter 3, Haynes, 1984; Schefe et al., 2009). Once PO_4, Fe, and Al are in solution, aqueous PO_4-Fe/Al-DOM complexes are hypothesized to form (Chapter 3, Gerke, 2010), which would potentially enhance PO_4 mobility (Chapter 3, Hutchison and Hesterberg, 2004).

Currently the impacts of Al on Fe reduction kinetics and associated PO_4 mobilization from soil OM are unknown. The objective of this research was to determine how the relative proportions of Fe and Al bound to OM affect the amount and rate of PO_4 dissolution.

MATERIALS AND METHODS

Microbial Reduction Incubations

All experimental treatments were performed in a randomized sequence and are outlined in Table A6.1. Iron(III) and Al were added to Pahokee peat suspended in 0.05 M KCl at Fe/Al ratios of 0, 0.33, 2, 5, and ∞ to achieve a constant added metal concentration of 1200 µmol L^{-1} at pH 2.5. The pH was adjusted to 6.0 and incubations were allowed to equilibrate in continuously stirred incubation systems for 48 h under $N_{2(g)}$ prior to imposing anaerobic conditions. Control experiments included: 1. no addition of CN32, 2. No addition of $H_{2(g)}$, 3, no addition of either Fe or Al, and 4. no addition of PO_4.

The incubation system used to determine Fe reduction and PO_4 dissolution rates is presented in chapter 5 (Figure 5.1). The set-up of each incubation was conducted in the following sequential steps: (1) 0.05 M of KCl was placed in the reaction vessel, (2) the stir plate was turned on to circulate the suspension, (3) the calculated mass of hydrated Pahokee peat was added, (4) the pH was brought to 2.5 using the titration workstation with 0.05 M HCl, (5) mixed 17 mM $FeCl_3$ and $AlCl_3$ solutions were added to achieve1200 µmol L^{-1} in the final suspension, (6) $N_{2(g)}$ flow through the suspension was started, (7) the pH was increased to pH 6.0 by adding 0.05 M KOH at a rate of 1 mL KOH min^{-1} for up to 2 h, (8) suspensions were equilibrated for 48 h while purging with $N_{2(g)}$, (9). A 50 mM KH_2PO_4 solution was added to achieve 600 mmol PO_4 kg^{-1} peat, and (10) the suspension was brought to a final volume of 900 mL (calculated based on input volumes) with 0.05 M KCl.

The cell density of a stock suspension of a freshly prepared *Shewanella putrefaciens* CN32 was determined by measuring its optical density at 420 nm in relation to a calibration

curve generated from direct plate counts (Royer et al., 2002). After equilibrating the continuously stirred Fe-peat suspension for 48 h, CN32 cells were added to the reaction vessels to achieve a concentration of 1 X 10^8 cells mL^{-1}, and the final incubation volume was brought to 1 L. A time 0 h sample was collected at this point, and the $N_{2(g)}$ was switched to 0.5% $H_{2(g)}$. A syringe was used to extract 20 mL samples at approximately 4, 8, 12, 24, 30, 38, and 48 h. The total volume of sample removed during the course of an experiment was less than 20% of the suspension volume.

Sample Analysis

Immediately following sample collection, serum bottles were placed in a $N_{2(g)}$ filled glove box for filtration, and Fe(II) analysis. Total HCl extractable Fe was measured by adding 5 mL of unfiltered sample to 5 mL of 1 M HCl in a 25 mL amber serum bottle and reacting for 24 h in a $N_{2(g)}$ filled quiescent jar (Fredrickson et al., 1998). The remaining 15 mL of solution, were immediately filtered through a 0.2 µm filter (Millipore Corp., Bedford, MA) in the glove box. Ferrous Fe was measured using the 1,10-phenatnthroline method for both dissolved and HCl extractable [total Fe(II)] samples (Loeppert and Inskeep, 1996). Dissolved reactive P (DRP) was analyzed by the Murphy-Riley colorimetric method (Olsen and Sommers, 1982). The remaining sample was stored at 5°C for further analysis, including; total Fe with flame atomic absorption spectrometry (FAAS) (Model 3100, Perkin Elmer, Wellesey, MA) and DOC using a TOC analyzer (Shmadzu TOC-5050 TOC).

Size Fractionation

A separate microbial reduction experiment containing 600 mmol P kg^{-1} peat and 1200 mmol Fe kg^{-1} peat was conducted to specifically identify the distribution of PO_4, dissolved Fe(II), and DOC between colloidal and dissolved fractions. Supernatant solutions were filtered through 15 mL Vivaspin centrifugal concentrators with 100,000, and 5,000 Da molecular weight cut-off polyethersulfone membranes (Sartorius VS0413, VS0403, and VS0443) following the 0.2µm filtration as described in Chapter 3. All filtrates were analyzed as described above for dissolved organic carbon, Fe, Al, and PO_4.

Rate Calculations

Here, three equations that have been successful used to model PO_4 dissolution from soils and phosphate minerals were used to model PO_4 mobilization during Fe(III) reduction. The time dependent dissolution of PO_4 during microbial reduction was fitted to the linear forms of the three rate equations:

Pseudo-first-order: $\ln(q_e - q_t) = \ln(q_e) - (k_a/2.303)(t)$ Equation 6.1.

Parabolic diffusion: $q_t = k_b^{(1/2)} + q_i$ Equation 6.2

Elovich: $q_t = a + b\ln t$ Equation 6.3

where q_e, q_i, and q_t correspond to maximum dissolved PO_4 concentrations, dissolved PO_4 concentration at 0 h, and dissolved PO_4 concentration at time (t), and k_1, k_2, k_3, and k_4 are the experimental rate coefficients in respect to the equation in which they appear. In the Elovich

equation, both the initial PO_4 dissolution rate (k_a) and the average PO_4 dissolution rate (k_b) were obtained.

The pseudo-first-order kinetics equation did not fit experimental Fe(III) reduction data. Instead, a zero-order Fe(III) reduction model was used (Equation 6.4), where [Fe(II)] refers to Fe(II) concentration at time (t), and k_{Fe} is the zero-order rate coefficient.

$$[Fe(II)] = k_{Fe}t \qquad \text{Equation 6.4}$$

RESULTS AND DISCUSSION

Phosphate Dissolution

Trends in PO_4 dissolution from the Fe/Al bound to peat were similar to those observed from soils (e.g. Hutchison and Hesterberg, 2004), and were attributed to the mobilization of PO_4 bound to Fe(III) during Fe(III0 reduction. Phosphate dissolution occurred during microbial Fe(III) reduction in all treatments that contained bound Fe/Al ratios > 0. Figure 6.1 shows an example of PO_4 dissolution from peat containing 600 mmol P kg^{-1} and a bound Fe/Al ratio of 5. Dissolved PO_4 increased from 230 to 300 µmol L^{-1} as Eh decreased from 150 to -200 mV during microbial reduction, and dissolved Fe(II) concentration increased linearly from 0 to 62 µmol L^{-1} from 0 to 28 h (Figure 6.1). In addition, DOC increased from 35 to 55 mg L^{-1} from 0 to 48 h. No PO_4, Fe(II), or DOC dissolution occurred in abiotic or controls in which no $H_{2(g)}$ was added, which indicated that the mobilization of PO_4 was a result of microbial, rather than abiotic processes (Fig. A6.1). These control experiments also indicated that the microbial Fe(III) reduction was coupled to H_2 oxidation rather than the oxidation of OM or DOC. Examples and a discussion of the reproducibility of microbial reduction incubations are shown in Appendix 7. Essentially, these results highlighted the potential impacts of OM on PO_4 mobilization in soils separately from the use of OM as an electron donor, or the occurrence of organic P mineralization.

Kinetics of PO_4 Mobilization

To establish if differences in PO_4 dissolution rates occurred as Fe/Al ratio changed, three kinetic equations (first-order, parabolic diffusion, and the Elovich), which are frequently used to model PO_4 mobilization from soils and PO_4 minerals, were used (He et al.,

1999; Hansen and Strawn 2003; He et al., 2005; Nafiu et al., 2008). Generally, PO_4 dissolution occurred in two phases, an initial rapid primary phase followed by a slower secondary phase. The extent of each phase depended on Fe/Al ratio with the rapid primary reaction extending longer as the Fe/Al ratio increased. In all cases, PO_4 approached equilibrium after 30 h. The pseudo-first-order equation modeled PO_4 dissolution from soil OM best during microbial Fe(III) reduction (Equation 6.1), followed by the parabolic diffusion equation (Equation 6.2), and the Elovich equation (Equation 6.3). As Fe/Al ratio increased from 0 to ∞, k_a increased from 0.001 to 0.011 h^{-1} (Table 6.1) and k_b increased from 0 to as much as 50 mmol PO_4 kg^{-1} $h^{-0.5}$ (Table 6.2). No significant increase in the initial PO_4 dissolution rate coefficient was determined from fits with the Elovich equation (a), but the average PO_4 dissolution rate coefficient (b) increased from 0 to 145 mmol PO_4 kg^{-1} peat h^{-1} (Table 6.3).

Several studies have used the Elovich equation to model PO_4 mobilization from soils (e.g. Nafiu et al., 2008; He et al., 2005; Hensen and Strawn 2003; and He et al., 1999). Typically, it has been hypothesized that PO_4 dissolution from aerobic soils is a diffusion-limited process (e.g. Nafiu et al., 2008). Although the Elovich equation was adequate to describe trends in PO_4 dissolution from OM during microbial Fe(III) reduction, the pseudo-first-order equation described the data best. It is not clear, however, based on these rate equations if PO_4 dissolution was limited by diffusion, microbial reduction, or electron transfer processes. Rather than attempting to describe specific reaction mechanisms, rate equation were used to compare rates of PO_4 dissolution across Fe/Al treatments.

Figure 6.2 shows the rate coefficients k_a, k_b, a and b across the concentrations of Fe(III) bound to peat. Variability occurred between replicates, but general trends in PO_4 dissolution and Fe(III) reduction were similar (Figure A6.2). In all cases, the individual replicates are graphed as separate data points. Because a constant metal addition of 1200 mmol Fe/Al kg^{-1} peat was used, as bound Fe(III) decreased, bound Al(III) increased. The rate coefficients of PO_4 dissolution increased with bound Fe(III) as calculated by both the first-order and parabolic diffusion equations. For the Elovich equation, no distinguishable trend was identified in model parameters between the initial PO_4 dissolution rate coefficients and Fe/Al ratio, however the average PO_4 dissolution rate coefficient increased with increasing Fe/Al ratio. Overall, each model indicated that increasing the ratio of bound Fe/Al increased the rate of PO_4 dissolution from organic matter.

Reaction 6.5 shows a possible reaction for the mobilization of PO_4 from an Fe-oxide surface (denoted with >Fe) in which both $H_2PO_4^-$ and Fe(II) are mobilized upon Fe(III) reduction.

$$>FeOPO_3H_2^{2+}{}_{(s)} + e^- \leftrightarrow Fe^{2+}{}_{(aq)} + H_2PO_4^-{}_{(aq)} \qquad \text{Equation 6.5}$$

Based on chemical equilibrium principles, the final concentration of PO_4 mobilized depends on reactant concentration. Thus, as PO_4 bound to Fe(III) increases, PO_4 mobilization during microbial reduction is predicted to increase (assuming that the Fe(III) sties binding PO_4 are reducible. Because Al(III) is not redox active in soils, PO_4 bound to Al(III) would not dissolve during reduction. Despite the influence on total PO_4 mobilization, the rate of PO_4

mobilization would be comparable between Fe/Al ratios if: (1) there was no preference for PO_4 binding to Al relative to Fe, (2) Al(III) did not impact Fe(III) reduction, and (3) Al(III) did not impact the production of DOC during Fe(III) reduction. These hypotheses suggest that one or more of these mechanisms potentially contributed to the increasing rate of PO_4 dissolution with increasing Fe/Al ratio.

Binding Affinity of PO_4 to Fe and Al bound to peat

My previous results suggested that the binding affinity of PO_4 for Al-OM was higher than that of PO_4 for Fe-OM in Pahokee peat, although the behavior of humic substances in binding Fe and Al and forming complexes with PO_4 likely varies (Chapter 3, Chapter 4). Among treatments, maximum dissolved PO_4 increased from 170 to 535 μmol L^{-1} as Fe/Al ratio increased from 0 to ∞ (Table 6.4, Figure A6.2). Dissolved PO_4 at 0 h increased from 170 to 325 μmol L^{-1}as the Fe/Al ratio was increased from 0 to ∞. Thus, an additional 155 mmol PO_4 kg^{-1} peat was retained in the Al only treatment relative to the Fe only treatment at 0 h. In a similar figure (Figure A6.3), the ratio of bound PO_4 to bound Fe/Al decreased with increasing bound Fe(III) (Chapter 3). Likewise, previous research has indicated that the binding capacity of PO_4 for Al-HA in solution was 0.04 mmol PO_4 g^{-1} HA higher than the binding capacity of PO_4 for Fe-HA in solution (Guardado et al., 2007). However, preferential binding of PO_4 to Al over Fe would potentially decrease, rather than increase PO_4 mobilization rates because the ratio of PO_4 bound to Fe(III) would be lower. Here, the rate of PO_4 mobilization increased with increasing Fe/Al ratio, suggesting that preferential binding of PO_4 to Al did not control PO_4 mobilization rate in mixed Fe/Al-OM systems.

Fe(III) Reduction

Dissolved PO_4 production also increased linearly with total Fe(III) reduction (Figure 6.3), and indicated that for each mmol of Fe(III) reduced 0.3 mmol of PO_4 was mobilized, regardless of Fe/Al ratio treatment. This trend suggests, that PO_4 dissolution was directly dependent on Fe(III) reduction across treatments, and as such any changes in Fe(III) reduction rate across Fe/Al treatments would alter the PO_4 dissolution rate. As such, Fe(III) reduction rates were investigated to determine the impact on PO_4 dissolution.

Across all treatments, total Fe(III) reduction increased as Eh decreased with time during microbial reduction. The OH production during Fe(III) reduction was balanced by the addition of H^+ as 0.05 M HCl (Figure 6.4). For each mol Fe(III) reduced, 1.7 mol of H^+ were needed to balance OH^- production. The increase in H^+ addition with Fe(III) reduction across Fe/Al ratios closely corresponded with the increase in H^+ addition with Fe(III) reduction across peat addition in Chapter 5. As such, the same reactions which led to decreased pH in Chapter 5 are expected to occur here, and are not explained in detail.

General trends in Fe(III) reduction between treatments up to 48 h are shown in Figure 6.5. Maximum Fe(III) reduction increased from 20 to 1040 μmol kg^{-1} suspension as the ratio of Fe/Al increased from 0 to ∞ (Table 6.4). Overall, the trends in Fe(III) reduction were similar to the trends in PO_4 dissolution during microbial reduction. The percent of total Fe(III) reduced after 48 h of microbial reduction was consistent between treatments at 89 $\pm$ 10% (Table 6.4).

Initially, a first-order equation comparable to Equation 6.1 was used to model Fe(III) reduction, however data were variable resulting in fits with $r^2 < 0.70$. Therefore, a zero-order

model (linear regression) was used in which the slope corresponded to the zero-order rate coefficient of Fe(III) reduction (k_{Fe}) (Equation 6.4). Here, the 0 h Fe(II) was subtracted from total Fe(II) at any given time, and the y-intercepts were set to 0. Overall, k_{Fe} increased from 2 to 39 µmol Fe(II) kg^{-1} peat h^{-1} as the Fe/Al ratio increased from 0 to ∞ (Table 6.5). Figure 6.6 shows the increase in k_{Fe} across total added Fe concentration. Here, the increase in k_{Fe} with Fe concentration was significant ($P< 0.01$), indicating that the rate of Fe(III) reduction increased with increasing Fe/Al addition.

Results indicated that although the extent of Fe(III) reduction was not impacted by the ratio of Fe/Al, the rate of Fe(III) reduction was. Both the rate of Fe(III) reduction and PO_4 dissolution decreased with decreasing Fe/Al ratios, thus the rate of PO_4 dissolution appeared to depend directly on the Fe(III) reduction rate.

Dissolved Organic Carbon Impacts on PO_4 Mobilization

My previous results showed that DOC also plays a role in PO_4 dissolution from OM (Chapter 3). Dissolved organic carbon concentrations increased linearly with dissolved PO_4 concentrations in all Fe/Al ratio treatment experiments ($P < 0.0001$) (Fig. 6.7). The two frequently proposed mechanism of increasing PO_4 resulting from DOC are (1) the competition between DOC and PO_4 for adsorption sites, and (2) the formation of colloidal OM-Fe/Al-PO_4 or Fe/Al-PO_4 in the < 0.2µm fraction (Bhatti et al., 1998; Guppy et al., 2005; Guardado, 2008; De Hann, 1990; Shaw et al., 2000). In my previous research, an increase in dissolved PO_4 concentration with increasing DOC concentration was predominantly attributed to the formation of colloidal OM-Fe/Al-PO_4 or Fe/Al-PO_4 complexes < 2 µm rather than competitive sorption (Chapter 3). Although the same mechanism potentially

contributes to PO_4 mobilization as DOC increases during microbial Fe(III) reduction, the contribution is potentially masked by the dominant PO_4 mobilization due to Fe(III) reduction.

Dissolved organic carbon concentrations also increased with total Fe(III) reduction across all treatments, and were constant in the 0 Fe/Al, abiotic, and 0 H_2 controls ($P < 0.001$). Because Fe(II) and DOC concentrations co-vary, the impacts of DOC and Fe(III) reduction on PO_4 mobilization have not been previously separated. These effects were separated by conducting an experiment in which DOC was added at pH 6.0 in the absence of microbial reduction. Comparing the combination of microbial Fe(III) reduction and co-dissolution of PO_4 and OC with DOC impacts alone, and assuming that interactions between DOC and Fe(II) did not significantly alter PO_4 dissolution kinetics, allowed us to semi-quantitatively determine the impact of each mechanism (Figure 6.8). The linear increase of PO_4 across DOC was 6.7 x greater in reduction experiments than in DOC addition experiments (Figure 6.8), which indicated that Fe(III) reduction played a larger role (as much as 6.7 x) in PO_4 dissolution than the DOC effects alone. However, Fe(III) reduction and DOC production were closely related in all experiments, which potentially impacted the combined PO_4 mobilization rate.

Filtration experiments indicated that the formation of colloidal PO_4-Fe/Al-OM or Fe/Al-PO_4 complexes > 5,000 Da occurred as PO_4 was mobilized during microbial Fe(III) reduction. Of the PO_4 mobilized during microbial reduction (170 μmol L^{-1}), up to 60% (100 μmol L^{-1}) remained bound in the > 5,000 Da fraction (Figure 6.9, Table A6.2). The majority of total PO_4 (480 μ L^{-1}) remained dissolved, passing through the < 5,000 Da filter. In contrast, 60 to 90% of DOC, and 65 to 100% of Fe remained in the colloidal fraction > 5,000

Da (Figure 6.9). Overall, although solution chemistry was dominated by dissolved PO_4 < 5,000 Da, the formation of colloidal PO_4 complexes < 0.2µm contributed to total dissolved PO_4.

Despite the relative importance of Fe(III) reduction compared to DOC competition and complexation mechanisms on PO_4 mobilization, results suggested that DOC played a key role in the rate of PO_4 dissolution from peat across the Fe/Al ratios. As Fe(III) reduction occurred, OC was mobilized. As the Fe/Al ratio increased, DOC production with time also increased, potentially enhancing PO_4 dissolution through the formation of mobile colloidal OM-Fe/Al-PO_4 complexes < 2 µm (Table 6.4, Figure A6.4). The impacts of both DOC and Fe(III) reduction on PO_4 mobilization are important for understanding and controlling PO_4 mobilization in OM.

CONCLUSIONS

Research aimed at determining the impacts of the relative proportions of Fe and Al bound to OM on the rate of PO_4 mobilization during microbial reduction showed that PO_4 mobilization from OM during reduction occurs, and that the rate of PO_4 mobilization depends on bound Fe/Al ratios and DOC. Increasing DOC co-varied with Fe(III) reduction, and PO_4 mobilization resulting from Fe(III) reduction was 6.7 x greater than PO_4 mobilization resulting from DOC alone. Additional filtration of supernatant solutions indicated that the formation of colloidal PO_4 complexes > 5,000 Da and < 0.2 μm occurred as dissolved PO_4 increased, which suggested that the formation of DOC-Fe/Al-PO_4 colloids contributed to PO_4 dissolution.

Because organic soils are often positioned near to open water bodies, the potential for PO_4 mobilization from these soils poses a possible environmental threat. Based on my research, possible approaches to minimize PO_4 dissolution from organic soils include; (1) minimizing PO_4 inputs to soils containing a high Fe/Al ratio, (2) preventing Fe(III) reduction in soils containing a high Fe/Al ratio, (3) decreasing pH to maintain low DOC and predominantly bound Fe and Al, and (4) adding Al to decrease the Fe/Al ratio.

BIBLIOGRAPHY

Ajmone-Marsan F., D. Cote, and R.R. Simard. 2006. Phosphorus transformations under reduction in long-term manured soils. Plant Soil. 282:239-250.

Ann Y., K.R. Reddy, and J.J. Delfino. 2000. Influence of redox potential on phosphorus solubility in chemically amended wetland organic soils. Ecol. Eng. 14:169-180.

Axt J.R., and M.R. Walbridge. 1999. Phosphate removal capacity of palustrine forested wetlands and adjacent uplands in Virginia. Soil Sci. Soc. Am. J. 63:1019-1031.

Bauer M., and C. Blodau. 2009. Arsenic distribution in the dissolved, colloidal and particulate size fraction of experimental solutions rich in dissolved organic matter and ferric iron. Geochimica Et Cosmochimica Acta. 73:529-542.

Bolan N.S., R. Naidu, S. Mahimairaja, and S. Baskaran. 1994. Influence of low-molecular-weight organic-acids on the solubilization of phosphates. Biol. Fertil. Soils 18:311-319.

Borch T., Y. Masue, R.K. Kukkadapu, amd S. Fendorf, 2007. Phosphate imposed limitations on biological reduction and alteration of ferrihydrite. Environ. Sci. Technol. 41:166-172.

Buffle, J., K.J. Wilkinson, S. Stoll, M. Filella, and W.J. Zhang. 1998. A generalized decription of aquatic collloidal interactions: the three-colloidal component approach. Environ. Sci. Technol. 32:2887-2899.

Darke A.K., and M.R. Walbridge. 2000. Al and Fe biogeochemistry in a floodplain forest: Implications for P retention. Biogeochem. 51:1-32.

Fredrickson J.K., J.M. Zachara, D.W. Kennedy, H. Dong, T.C. Onstott, N.W. Hinman, and S. Li. 1998. Biogenic iron mineralization accompanying the dissimilatory reduction of hydrous ferric oxide by a groundwater bacterium. Geochim. Cosmochim. Acta. 62:3239-3257.

Gerke J., 1992. Phosphate, aluminum and iron in the soil solution of 3 different soils in relation to varying concentrations of citric-acid. Z. Pflanzenernahr. Bodenkd. 155:339-343.

Gerke J., and R. Hermann. 1992. Adsorption of orthophosphate to humic-Fe complexes and to amorphous Fe-oxide Z. Pflanzenernahr. Bodenkd. 155:233-236.

Hagerthey S.E., K. Newman, E.P. Smith, and J. Godin. 2008. Multiple regime shifts in a subtropical peatland: Community-specific thresholds to eutrophication. Ecological Monographs. 78:547-565.

Hansen, J.C., and D. B. Strawn. 2003. Kinetics of phosphorus release from manure-amended alkaline soil. Soil Sci. 168:869-879.

Haynes R.J., 1984. Lime and phosphate in the soil-plant system, in: N. C. Brady (Ed.), Advances in Agronomy, Academic Press, Orlando FL. pp. 249-315.

He, Z.L., H. Yao, D.V. Calvert, P.J. Stoffella, X.E. Yang, G. Chen, and G.M. Lloyd. 2005. Dissolution characteristics of central Florida phosphate rock in an acidic sandy soil. Plant and Soil. 273:157-166.

He, Z.L., V.C. Baligar, D.C. Martens, K.D. Ritchey, and M. Elrashidi. 1999. Effect of byproduct, nitrogen fertilizer, and zeolite on phosphate rock dissolution and extractable phosphorus in acid soil. Plant and Soil. 208:199-207.

Holford I.C.R., and W.H. Patrick. 1979. Effects of reduction and pH changes on phosphate sorption and mobility in an acid soil. Soil Sci. Soc. Am. J. 43:292-297.

Holford I.C.R., and W.H. Patrick. 1981. Effects of duration of anaerobiosis and reoxidation on phosphate sorption characteristics of an acid soil Aust. J. Soil Res. 19:69-78.

Hu H.Q., J.Z. He, X.Y. Li, and F. Liu. 2001. Effect of several organic acids on phosphate adsorption by variable charge soils of central China. Environ. Int. 26:353-358.

Hue N.V., 1991. Effects of organic-acids anions on P-sorption and phytoavailability in soils with different mineralogies. Soil Sci. 152:463-471.

Hutchison K.J., and D. Hesterberg. 2004. Dissolution of phosphate in a phosphorus-enriched ultisol as affected by microbial reduction. J. Environ. Qual. 33:1793-1802.

Lead, J.R. and K.J. Wilkinson. 2007. Environmental colloids and particles: current knowledge and future developments. p. 1-16 In. Environmental Colloids and Particles, vol. 10. K.J. Wilkinson and J.R. Lead ed. John Wiley and Sons. New York. NY.

Loeppert R.H., and W.P. Inskeep. 1996. Iron. pp. 639-664. *In* S.L. Sparks (Ed.), Methods of soil analysis, part 3. Chemical methods. ASA and SSSA. Madison WI.

Martinez M.T., C. Romero, and J.M. Gavilan. 1984. Solubilization of phosphorus by humic acids from lignite. Soil Science. 138:257-261.

Moshi A.O., A. Wild, and D.J. Greenlan. 1974. Effect of organic-matter on charge and phosphate adsorption characteristics of kikuyu red clay from Kenya. . Geoderma. 11:275-285.

Murray G.C., and D. Hesterberg. 2006. Iron and phosphate dissolution during abiotic reduction of ferrihydrite-boehmite mixtures. Soil Sci. Soc. Am. J. 70:1318-1327.

Nafiu, A., J.O. Agbenin, and B.A. Raji. 2008. Kinetic desorption of native phosphorus from soils of varying lithogenic origins in the Nigerian savanna. Soil Sci. 173:937-844.

Olsen S.R., and L.E. Sommers. 1982. Phosphorus, in: A. L. Pate (Ed.), Methods of soil analysis. Part 2. 2nd ed., ASA and SSSA, Madison, WI.

Patrick W.H., and R.A. Khalid. 1974. Phosphate release and sorption b soils and sediments-effects of aerobic and anaerobic conditions Science. 186:53-55.

Phillips I.R., 1998. Phosphorus availability and sorption under alternating waterlogged and drying conditions. Communications in Soil Science and Plant Analysis 29:3045-3059.

Richardson C.J., 1985. Mechanisms controlling phosphorus retention capacity in freshwater wetlands. Soil Sci. 179:1424-1427.

Ritchie G.S.P., and P.J. Dolling. 1985. The role of organic matter in soil acidification. Aust. J. Soil Res. 23:569-576.

Schefe C.R., P. Kappen, L. Zuin, P.J. Pigram, and C. Christensen. 2009. Addition of carboxylic acids modifies phosphate sorption on soil and boehmite surfaces: A solution chemistry and XANES spectroscopy study. J. Coll. Inter. Sci.. 330:51-59.

Surridge, B.W.J., A.L. Heathwaite, and A.J. Baird. 2007. The release of phosphorus to porewater and surface water from river riparian sediments. J. Environ. Qual. 36:1534-1544.

Violante A., C. Colombo, and A. Buondonno. 1991. Competitive adsorption of phosphate and oxalate by aluminum-oxides. Soil Sci. Soc. Am. J. 55:65-70.

Willett, I.R. 1989.Causes and prediction of changes in extractable phosphorus during flooding. Aus. J. Soil Res. 27:45-54.

Wu Y., A. Ahmed, R. Waghmare, and D. Kahn. 2006. Cleaning polyethersulfone membranes after ultrafiltration-diafiltration in monoclonal antibody production. BioPharm International 19:67-71.

Table 6.1. Pseudo first-order linear rate equations of PO_4 dissolution during microbial Fe(III) reduction up to 30 h. $q_t = q_e \bullet (1-\exp(-k_a \bullet t))$ where q_t is the dissolved PO_4 at any given time (t), k_a is the pseudo first-order rate constant, and q_e is the initial dissolved PO_4 at t = 0.

Fe/Al Ratio	PO_4 Linear First Order Rate Equations*	95 % Confidence Interval		Standard Error
		Max. k_a	Min. k_a	
Fe only	$Y = 0.011x + 2.42$ $r^2 = 0.97$	0.012	0.009	0.0007
Fe only (rep 2)	$Y = 0.007x + 2.42$ $r^2 = 0.97$	0.008	0.005	0.0006
5	$Y = 0.008x + 2.41$ $r^2 = 0.97$	0.01	0.007	0.0007
2	$Y = 0.007x + 2.35$ $r^2 = 0.94$	0.009	0.005	0.0007
2 (rep 2)	$Y = 0.005x + 2.29$ $r^2 = 0.96$	0.006	0.004	0.0003
0.33	$Y = 0.004x + 2.39$ $r^2 = 0.87$	0.005	0.002	0.0005
0.33 (rep 2)	$Y = 0.004x + 2.24$ $r^2 = 0.95$	0.004	0.003	0.0003
Al only	$Y = -0.001x + 2.23$ $r^2 = 0.73$	-0.0003	-0.001	0.0002

*all equations were significant ($P < 0.05$)

Table 6.2. Parabolic diffusion rate equations of PO_4 dissolution during microbial Fe(III) reduction. $q_t = k_b^{(1/2)} + q_i$, where q_t is the dissolved PO_4 at any given time (t), k_b is the diffusion rate coefficient, and q_i is the initial dissolved PO_4 concentration at 0 h.

Fe/Al Ratio	k_b ($\mu m\ P\ L^{-1}\ h^{-0.5}$)	q_i	Standard Error		r^2
			K_1	q_i	
Fe only	50.2	211	6.65	26.2	0.88*
Fe only (rep 2)	27.1	240	3.60	14.4	0.92
5	35.8	218	5.10	18.8	0.88
2	22.2	206.09	3.31	13.3	0.87
2 (rep 2)	15.8	177	1.30	5.53	0.92
0.33	12.4	232	1.54	6.05	0.89
0.33 (rep 2)	8.91	164	0.771	2.99	0.94
Al only	-1.31	171.2	0.334	1.42	0.65

*all equations were significant ($P < 0.05$)

Table 6.3. Dissolved PO_4 fit with the Elovich equation $[PO_4] = a + b\ln t$ where (a) refers to the initial PO_4 dissolution rate, and (b) refers to the average PO_4 dissolution rate.

Fe/Al Ratio (mmol kg^{-1} peat)	a (mmol PO_4 kg^{-1} peat h^{-1})	b (mmol PO_4 kg^{-1} peat h^{-1})	r^2	Standard Error of a	Standard Error of b
Fe only	205	186	0.81*	34.6	23.0
Fe only (rep 2)	238	101	0.84	21.0	19.6
5 Fe	216	129	0.77	27.4	26.9
2Fe	205	82.6	0.83	15.1	13.9
2 (rep 2)	175	58.9	0.88	7.43	6.34
0.33	227	49.9	0.96	3.96	3.73
0.33 (rep 2)	161	33.8	0.89	4.47	4.16
Al only	171	-4.99	0.62	1.56	1.38

*all equations were significant ($P < 0.05$)

Table 6.4. Summary of dissolved PO_4, total and dissolved Fe(II) and DOC with the total % of Fe(III) reduced for each treatment.

Fe/Al Ratio	Maximum Total Fe(II) (µmol kg^{-1} susp.)	Maximum Diss. Fe(II) (µmol L^{-1})	Initial dissolved P (µmol L^{-1})	Maximum dissolved P (µmol L^{-1})	Initial DOC mg L^{-1}	Maximum DOC mg L^{-1}	Total Fe(III) Reduced (%)
Fe only	1040	450	270	535	40	110	87
Fe only (rep 2)	830	300	380	550	85	120	98
5	780	320	270	482	39	89	78
2	680	210	250	380	32	64	85
2 (rep 2)	510	125	191	286	35	68	64
0.33	330	59	230	300	35	55	100
0.33 (rep 2)	290	37	184	220	16	26	97
Al only	20	5	170	170	12	19	-

Table 6.5. Total Fe(III) reduction with time modeled by zero-order equations up to 24 h. Initial 0 h Fe(II) was subtracted from Fe(II) at any given time and the y-intercepts were set to 0.

Fe/Al Ratio	Equation	Standard Error	95% Confidence Interval	
			Max	Min
Fe only	Y = 39t	2.2	45	33
Fe only (rep 2)	Y = 31t	1.4	35	27
5	Y = 29t	1.4	32	25
2	Y = 25t	1.8	29	20
2 (rep 2)	Y = 18t	0.92	20	15
0.33Fe	Y = 8.8t	1.1	12	5.8
0.33 (rep 2)	Y = 23t	2.8	30	15
Al only	Y = 2.0t	0.33	2.9	1.0

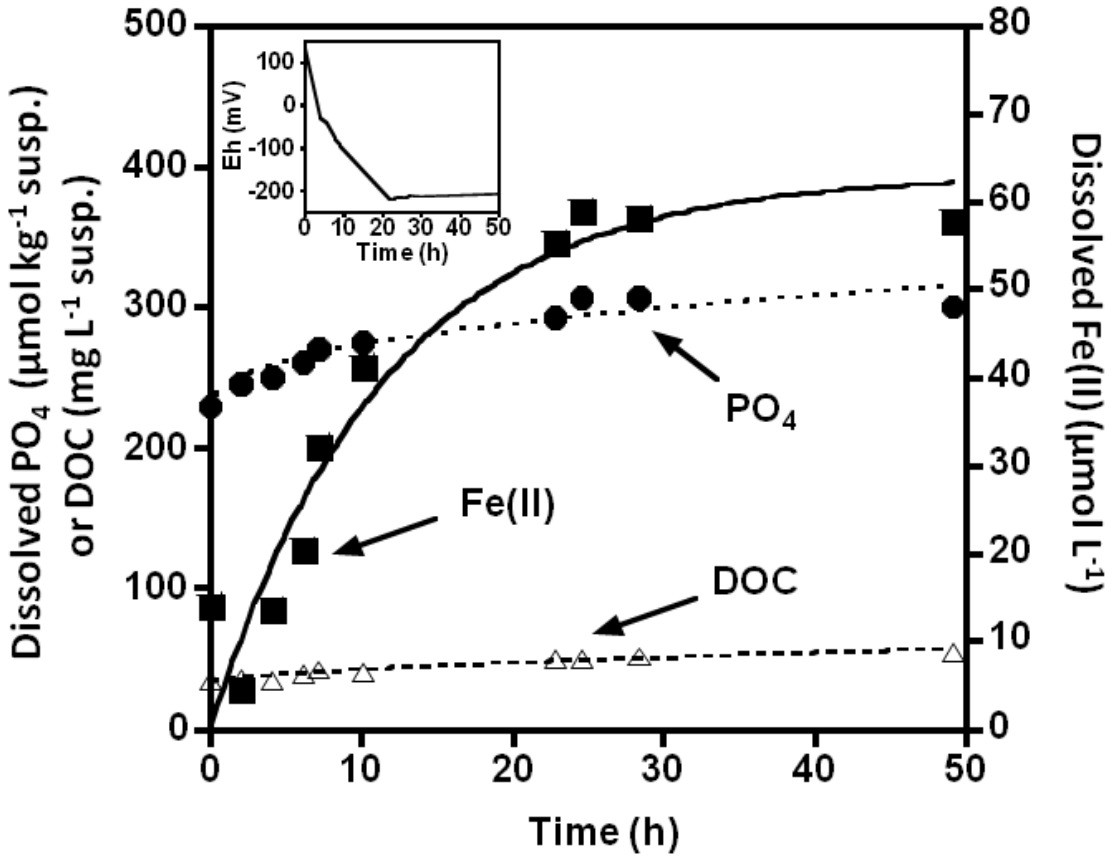

Figure 6.1. Trends in dissolved PO_4, Fe(II) reduction, and dissolved organic carbon (DOC) over 50 h during microbial reduction of peat containing Fe and Al bound at a Fe/Al ratio of 5, and 600 mmol P kg^{-1} peat. Subset (top left) shows decreasing Eh over the course of 50 h of microbial reduction.

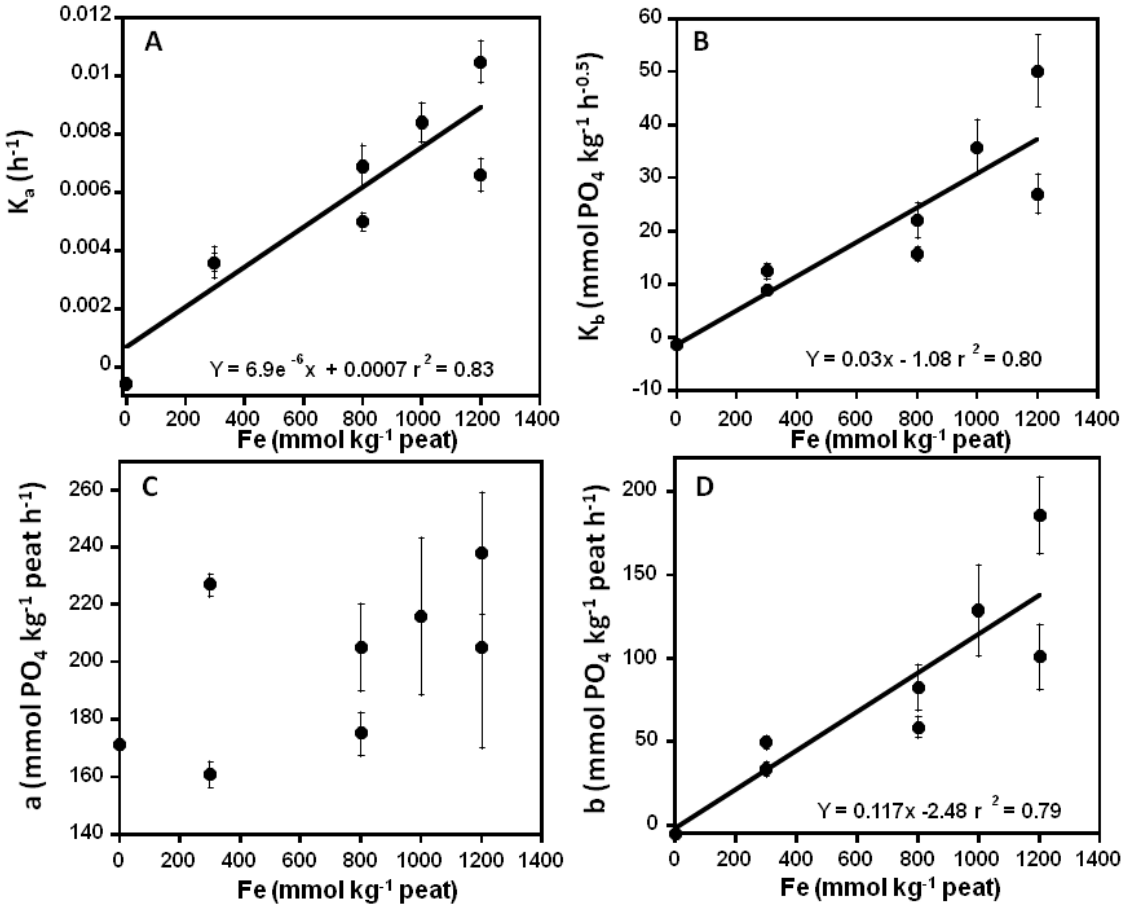

Figure 6.2. PO_4 dissolution rate model parameters for first-order (A), parabolic diffusion (B), and the Elovich equations (C and D) with respect to Fe(III) additions. Standard errors are represented by error bars.

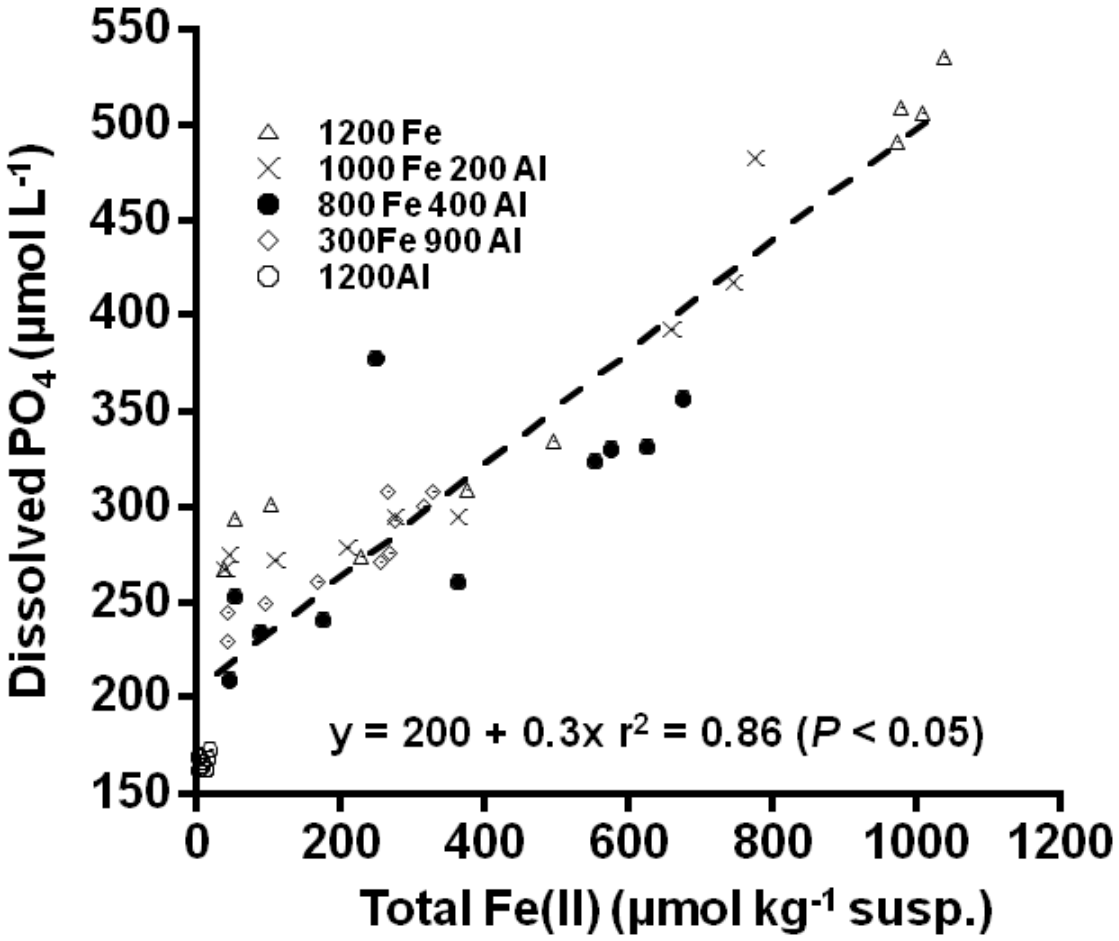

Figure 6.3. Dissolved PO_4 increased linearly with total Fe(II) production for Fe only, Al only, and Fe/Al ratios of 5, 2, and 0.33. Regression was significant with $P < 0.0001$.

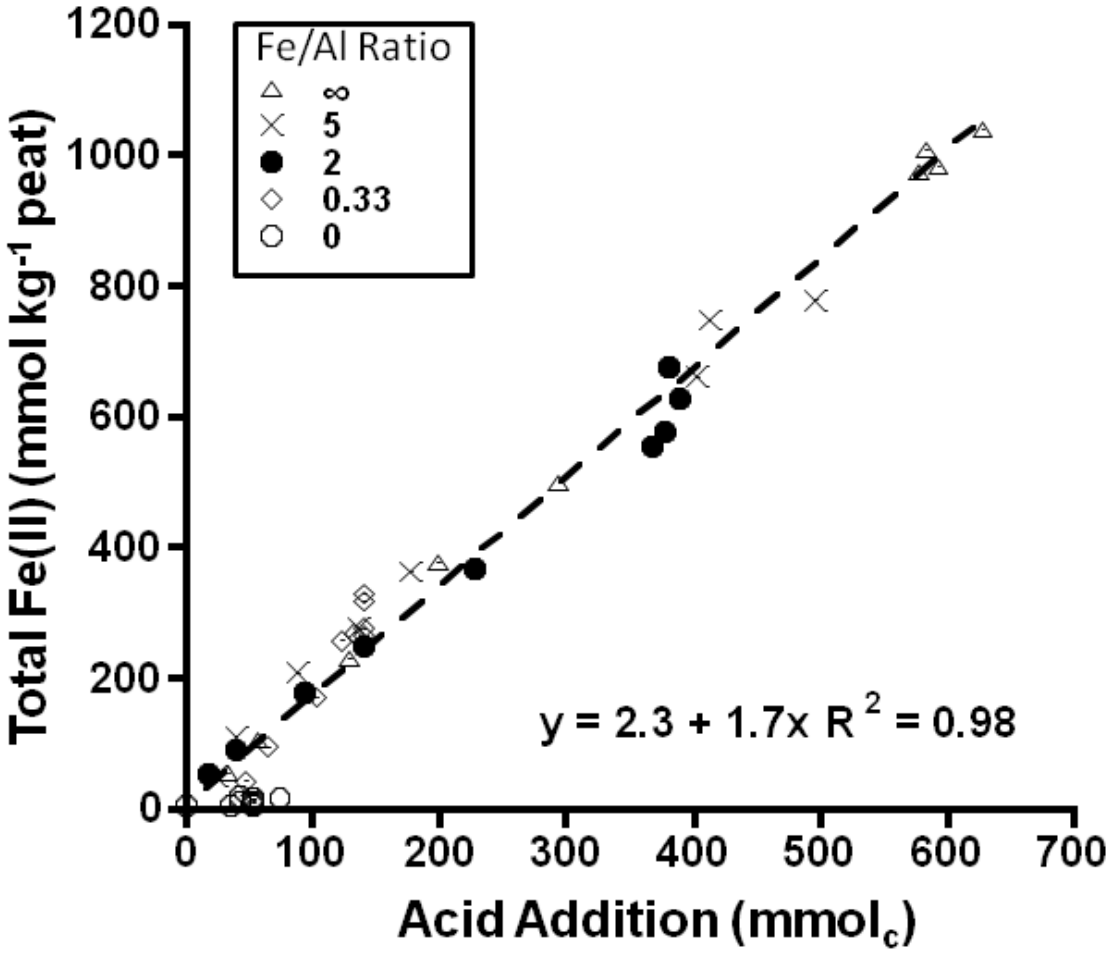

Figure 6.4. Addition of 0.05 M HCl was linearly correlated with total Fe(II) production for Fe/Al ratios of ∞, 5, 2, and 0.33, and Al only (mmol Fe kg^{-1} peat / mmol Al kg^{-1}peat).

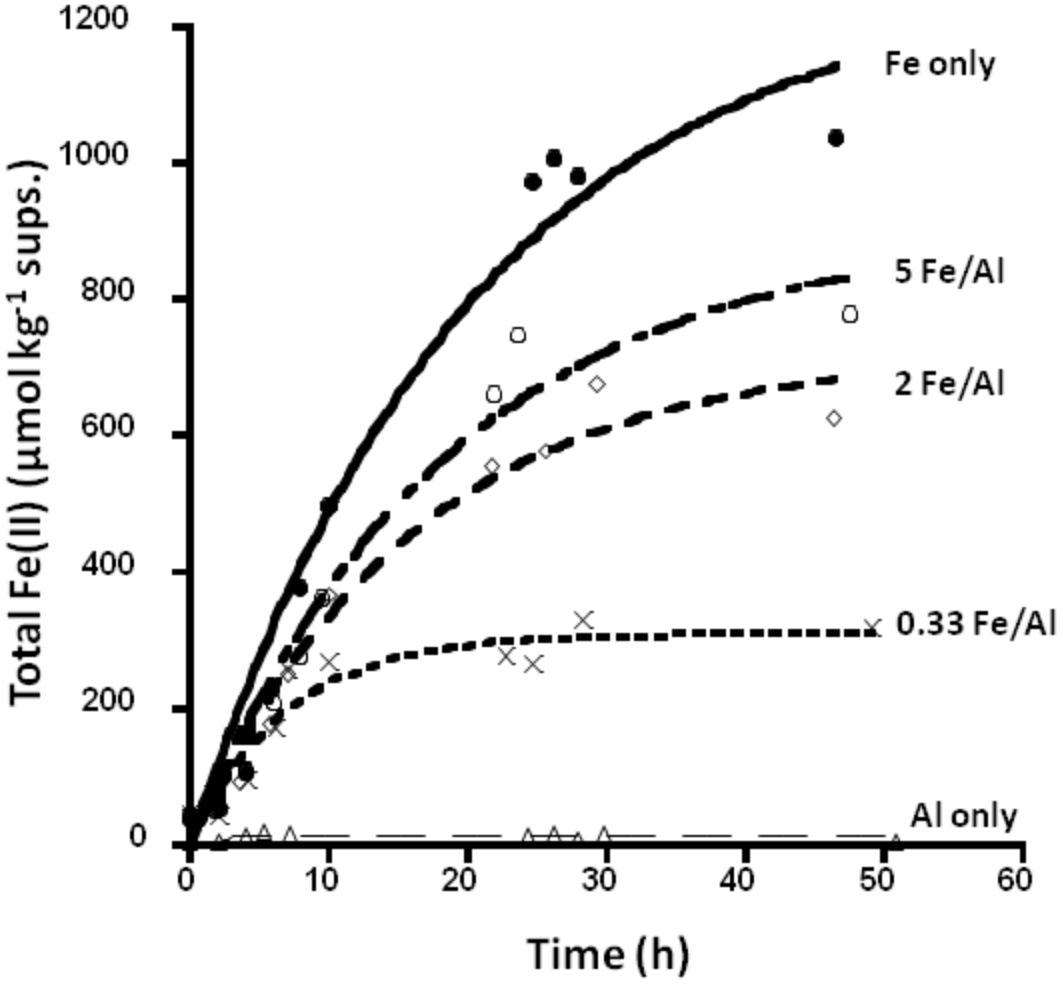

Figure 6.5. Increase in total Fe(II) (mmol kg^{-1} suspension) during microbial reduction over 48 h for Fe only, Al only, and Fe/Al ratio treatments of 5, 2, and 0.33.

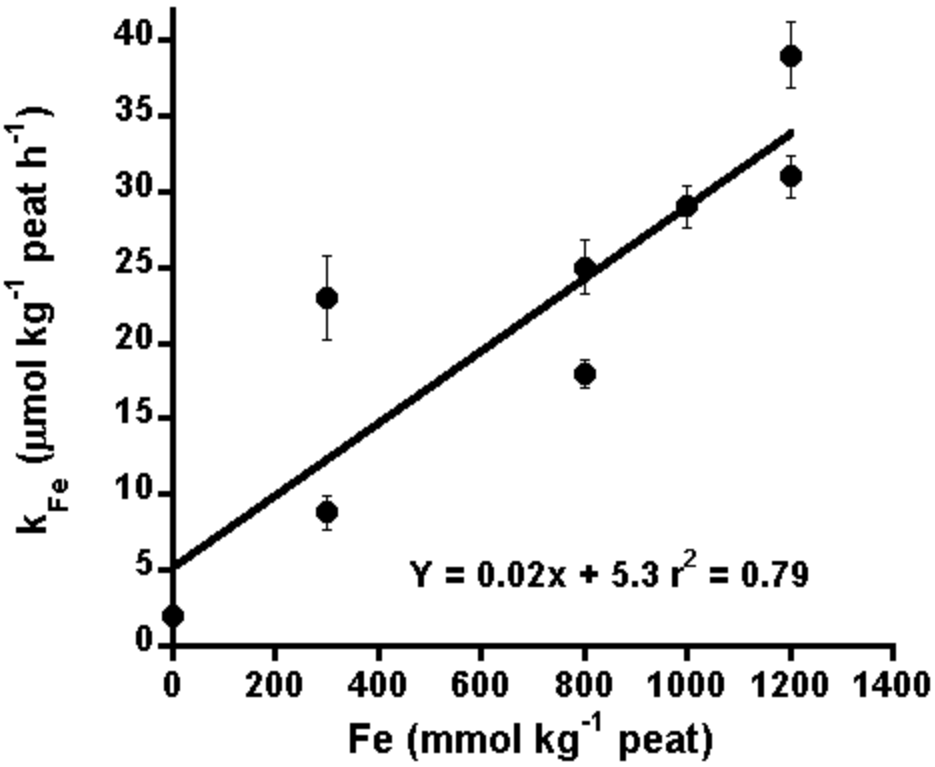

Figure 6.6. Zero-order Fe(III) reduction rate coefficients (k_{Fe}) across Fe addition treatments. Initial Fe(II) was subtracted from total Fe(II) at any given time and y-intercepts were set to 0 in order to determine k_{Fe}.

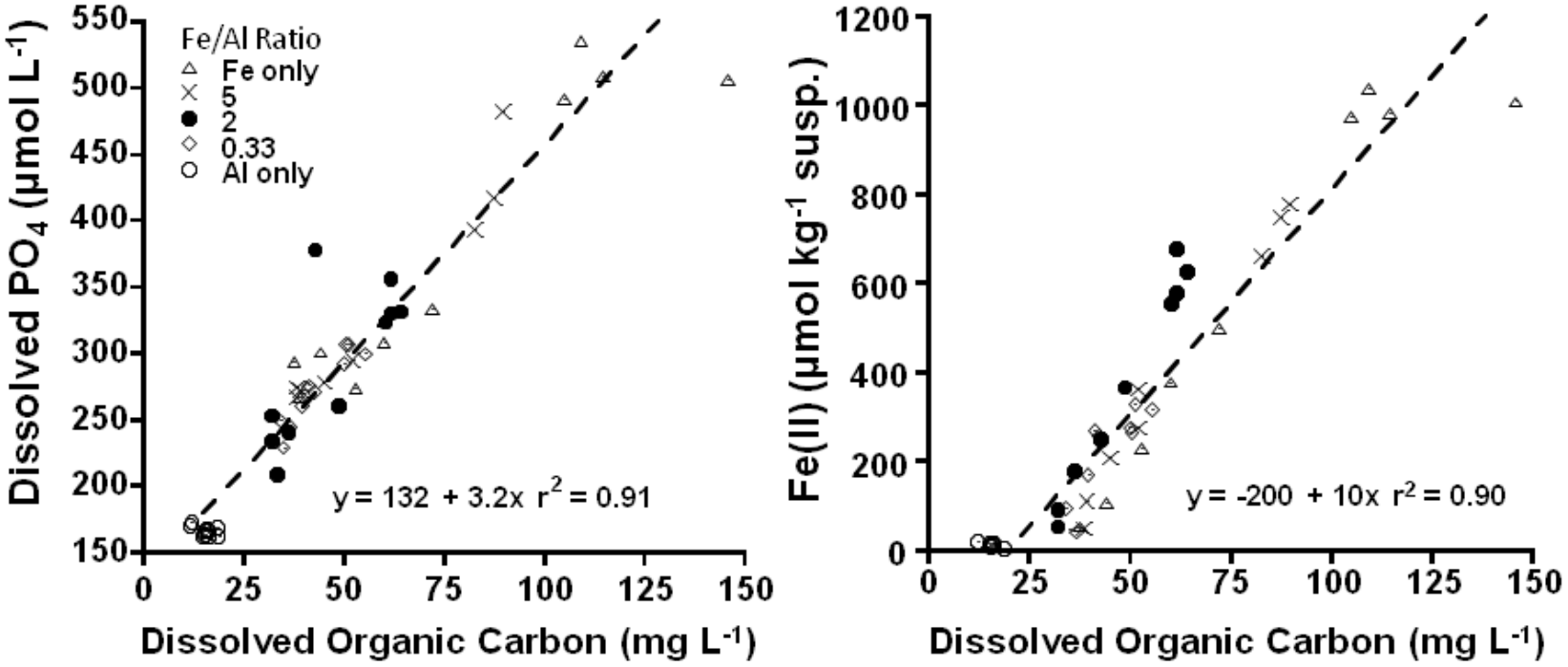

Figure 6.7. Dissolved PO_4 increased linearly with dissolved organic carbon (DOC) (left) and total Fe(II) production increased linearly with increasing dissolved organic carbon (right) for Fe only, Al only, and Fe/Al ratios of 5, 2, and 0.33 (left). Linear regressions were significant with $P < 0.0001$.

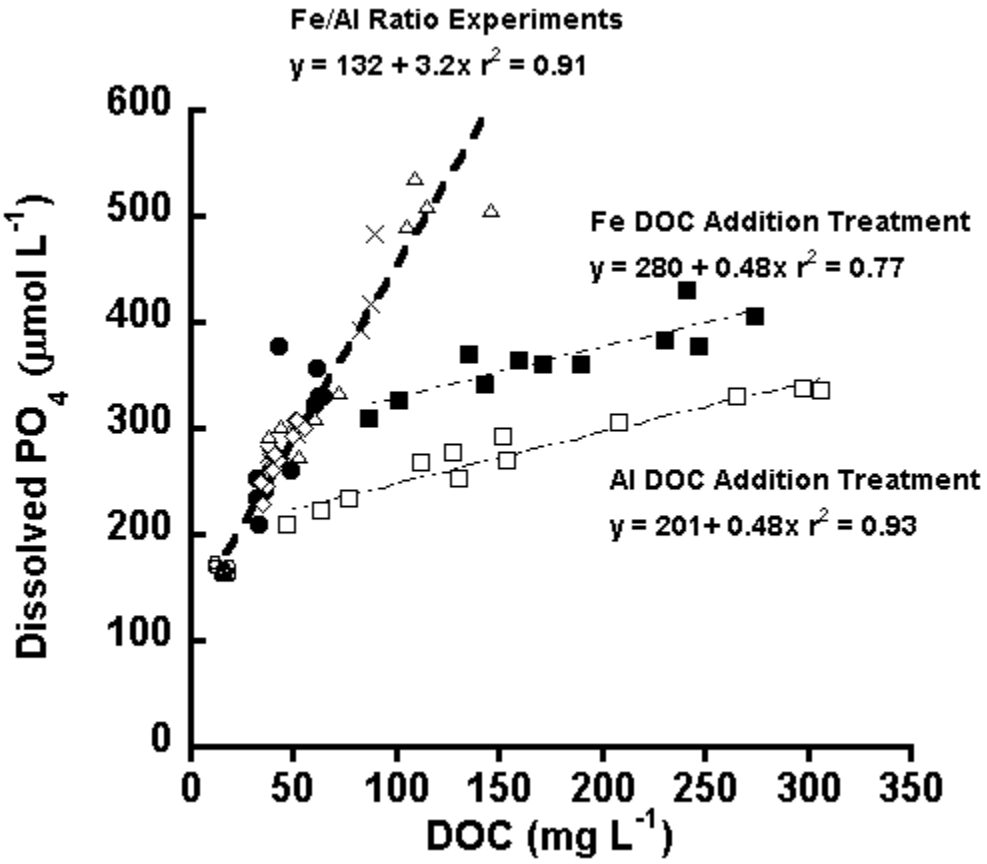

Figure 6.8. Dissolved PO_4 increased linearly with increasing dissolved organic carbon in microbial reduction incubations, and DOC addition experiments with 1200 mmol Fe or Al kg^{-1} peat. Phosphorus was added at 600 mmol P kg^{-1} peat and pH was held constant at 6.0.

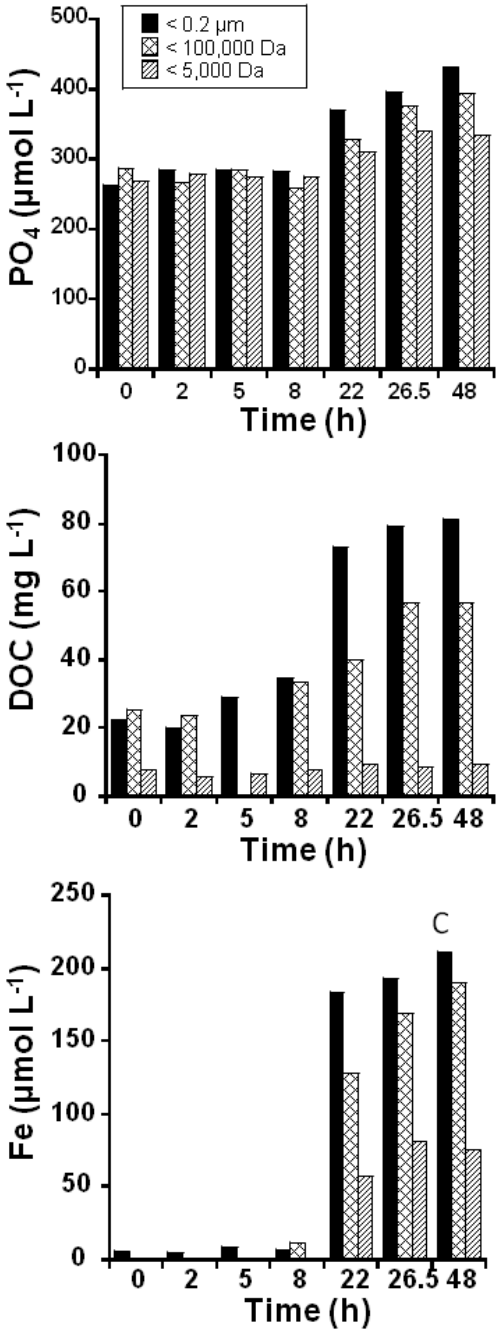

Figure 6.9. Solution concentrations of dissolved P (µmol L^{-1}), DOC (mg L^{-1}), and dissolved Fe (µmol L^{-1}) filtered through 0.2 µm 100,000 Da, and 5,000 Da molecular weight cut-off filters.

CHAPTER 7. OVERALL CONCLUSIONS AND IMPLICATIONS

PO_4 Sorption to Soil Organic Matter

Eutrophication remains a significant threat to water quality and ecosystem health. Traditionally, PO_4 binding in acidic soils has been attributed primarily to the amount and form of Fe and Al oxides. Although the impacts of soil organic matter (OM) and dissolved organic carbon (DOC) on PO_4 dissolution from mineral soils have been widely researched, little research has been conducted regarding the potential for PO_4 sorption directly to organic matter in either organic or mineral soils. My research addressed this knowledge gap and found that PO_4 sorption to organic matter can occur, and depends directly on pH, bound Fe and Al, and DOC.

Because PO_4 sorption in mineral soils depends in part on the amount and form of Fe- and Al- oxides, the form of Fe- and Al- in organic matter was expected to influence PO_4 sorption to OM as well. In this research, the presence of mononuclear Fe(III) bound to organic matter (OM), and/or polynuclear Fe(III)-OM clusters were identified using XANES and EXAFS analysis. As Fe(III)-OM cluster size decreases, the accessibility of Fe(III) for PO_4 sorption potentially increases. Thus, even low concentrations of bound Fe and Al in OM would potentially impact PO_4 sorption in organic soils. For example, here we observed that 560 mmol PO_4 kg^{-1} peat was bound to peat containing 1200 mmol Fe or Al kg^{-1} peat.

Three mechanisms contributed to changes in PO_4 sorption with increasing pH: (i) changes in Fe, Al, and PO_4 protonation and binding affinity (ii) changes in bound Fe and Al concentration, and (iii) pH induced DOC production at pH > 5.0. The dominant mechanism

responsible for PO_4 sorption was the changing binding affinity of Fe, Al, and PO_4 due to protonation, and as such, pH should be considered first when attempting to prevent PO_4 dissolution from organic soils. Maximum PO_4 sorption in all cases was observed between pH 4.0 and 5.0, which suggested that organic soils should be maintained between pH 4.0 and 5.0 in order to maximize PO_4 sorption. In agricultural soils Al toxicity to plants becomes a threat as pH decreases < 5.0. In organic soils, however, Al toxicity is typically not observed because dissolved Al concentrations are generally low (as evidenced by my data), and Al sorption to OM is maximized between pH 4 and 5.

Once optimum pH is obtained, the influence of DOC on PO_4 dissolution becomes more important. In a separate experiment at pH 6.0, the addition of DOC enhanced PO_4 dissolution. Two proposed mechanisms of PO_4 mobilization by DOC are; (i) formation of mobile complexes such as PO_4-Fe/Al-OM or Fe/Al-PO_4, and (ii) competitive sorption of DOC and PO_4 for sorption sites. Distinguishing between these PO_4 mobilization mechanisms is important, because the formation of mobile PO_4-Fe/Al-OM or Fe/Al-PO_4 colloids < 2 µm may facilitate the movement of PO_4 through soils to open water bodies. Results suggested that in the presence of DOC at pH $\geq$ 6.0, the formation of mobile colloidal PO_4 < 0.2 µm occurs, which potentially enhances PO_4 mobilization.

A model that predicts PO_4 sorption and dissolution in soils could be used to predict and potentially prevent PO_4 mobilization from soils. Here, the CD-MUSIC surface complexation model in Visual MINTEQ was used to model PO_4 sorption to OM across pH. This model accurately predicted PO_4 sorption to Fe bound to OM across pH, but was less successful in the Al bound to OM system. Although further work is needed to optimize the

model, (particularly in the case of Al) results indicated that modeling PO_4 sorption to OM is possible using a surface complexation model in Visual MINTEQ. Despite the models over-simplification of the complex PO_4-Fe/Al-OM systems, predicting PO_4 sorption to Fe-OM is a critical step toward understanding the mechanisms of PO_4 sorption and dissolution in organic soils. With further calibration (including the use of several different organic soils) this model could serve as an accurate estimator for the PO_4 sorption capacity in organic soils.

Mobilization of PO_4 Due to Fe(III) Reduction

Mobilization of PO_4 from mineral soils subjected to anaerobic conditions can occur by as Fe(III) with co-dissolution of Fe(II) and PO_4. Previous research has indicated that the mobilization of PO_4 during Fe(III) reduction depends in part on soil properties such as Fe, Al, and DOC concentrations and pH. Similarly, both Fe(III) reduction and DOC production simultaneously enhanced PO_4 mobilization, and the addition of Al decreased the rate of Fe(III) reduction and associated PO_4 mobilization. These results indicate that PO_4 sorption in anaerobic organic soils would increase as Al(III) concentration increases, and that in organic wetland soils frequently subjected to microbial Fe(III) reduction, the ratio of Fe(III) to Al(III) bound with OM would potentially impact the mobilization of PO_4. The ratio of Fe(III) to Al(III), however, may decrease as soils are subjected to reduction-oxidation cycles. When Fe(III) becomes reduced to Fe(II) it can be mobilized and translocated, resulting in Fe depletions and concentrations depending on the redox state of any given area of soil. Based on my results, these changes would potentially alter both PO_4 sorption, and the likelihood for PO_4 mobilization due to Fe(III) reduction.

In previous research it was not clear to what extent each variable played in the mobilization of PO_4 during microbial reduction. Here, although DOC contributed to the dissolution of PO_4, the rate of PO_4 mobilization due to Fe(III) reduction was 6.7 x the rate of PO_4 dissolution due to increasing DOC. It remains important to consider DOC impacts, however, because as Fe(III) reduction occurs, DOC can increase. In addition, results suggested that the translocation of reduced Fe(III) depends on DOC. Consequently, the sorption and mobility of PO_4 from soil to surface waters potentially is closely associated with changes in both Fe(III) redox state and DOC concentrations.

Summary of Conclusions

My results filled a critical knowledge gap regarding the role of pH, DOC, redox potential, and Fe(III) and Al(III) concentrations on the sorption and dissolution of PO_4 from oil OM. My data showed that maximum PO_4 sorption to OM with bound Fe(III) and Al(III) occurs between pH 4.0 and 5.0. This pH range should be conducive for maximal retention of inorganic PO_4 in organic soils. In addition, organic soils that contain a high ratio of Fe(III) to Al(III) should be maintained under aerobic conditions when possible to prevent the mobilization of PO_4. If anaerobic conditions are unavoidable, then the concentrations of Fe, Al, and DOC should be considered carefully to determine the potential for PO_4 sorption and mobilization. Although my results give one example of the impacts of bound Fe and Al on PO_4 sorption across pH, research that details the impacts of OM type and Fe/Al:PO_4 loading ratios on PO_4 sorption would significantly contribute to the understanding of PO_4 sorption to OM. Additionally, the impacts of bound Fe(III) and Al(III) on PO_4 mobilization may vary

depending on the type of OM and Fe/Al:PO_4 loading rate. Overall, my results provide a clear example of the impacts of pH, bound Fe and Al, and DOC on PO_4 sorption to organic matter.

APPENDICES

APPENDIX 1: SUPPLEMENTAL FIGURES TO CHAPTER 2

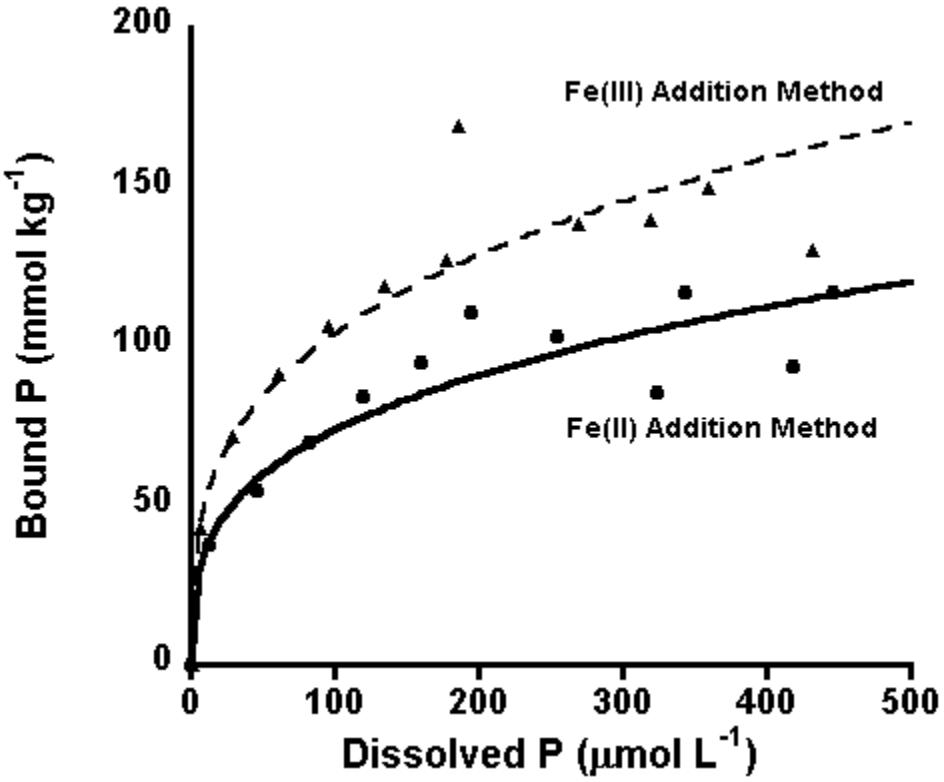

Figure A1.1. PO_4 sorption isotherms conducted at pH 6.8 and 25°C for Fe(II) and Fe(III) addition methods. Data were fit using the Freundlich model with linearlized models of $y = 0.30x + 1.3$ $r^2 = 0.87$ and $y = 0.3x + 1.4$ $r^2 = 0.90$ for the Fe(II) and Fe(III) addition methods, respectively. Because the logarithm of any positive number < 1.0 is negative, the bound PO_4 to bound Fe ratios were multiplied by 100 prior to log transformation and divided by 100 following back-transformation.

APPENDIX 2: FTIR ANALYSIS OF METAL BINDING TO OM ACROSS pH

OBCECTIVE

The objective was to determine if Fe and Al were bound to peat carboxylic functional groups, and if addition of PO_4 altered Fe and Al binding to peat.

MATERIALS AND METHODS

The freeze-dried M-OM and PO_4–M-OM complexes (Chapter 3) were prepared for Fourier transformed infrared spectroscopy (FTIR) spectroscopy by mixing 0.2 mg sample with 500 mg of KBr dried for 2 h. at 70˚C, and pressing the mixture into a pellet. Infrared spectra (32 scans) were recorded on pellets with a Nicolet Nexus 470 FTIR spectrometer over the 4000 – 400 cm^{-1} range.

RESULTS AND CONCLUSIONS

Infrared active vibrations of carboxylate groups are sensitive to metal binding environment (Nakamoto 1986), and have been used extensively to probe the binding of organic molecules to metals (Al-Mustafa, 2003; Clausen et al., 2003; Lemercier et al., 2004; Kato et al., 1995) and surfaces (Nilsson, 1996; Rosenqvist et al., 2003; Parikh and Chorover, 2006; Borer et al., 2009; Lindegren et al., 2009). Vibrational bands corresponding to asymmetric (ν_{asym}) and symmetric (ν_{sym}) stretches of carboxylate groups in OM appear at 1624-1633 cm^{-1} and 1385-1383 cm^{-1}, respectively, and depend on protonation, metal binding

mode, and metal/ligand concentrations (Baigorri et al., 2007; Guardado, 2008; Hay and Myneni, 2007).

In these OM system, ν_{asym} decreased by 41cm^{-1} from pH 3.0-3.5 prior to metal addition (Figure A2.1). In the Fe-OM and PO_4-Fe-OM systems respectively, ν_{asym} increased by 27.2 and 2.6 cm^{-1} from pH 3.0 to 3.5 (Table A2.1, Figure A2.2A). In the Al-OM and the PO_4-Al-OM systems, ν_{asym} decreased by 6 to 9 nm respectively and was stabilized between pH 4.5 and 6.0 (Figure A2.2 C). The ν_{sym} stretch decreased by 5 cm^{-1} as pH increased from 3.0 to 8.5 in OM and the Fe-OM and PO_4-Fe-OM systems, however no significant increase was noticeable in the Al system. In both Fe and Al systems, increasing bound Fe/Al concentrations led to increased ν_{asym}, indicating a possible interrelated dependence of ν_{asym} on bound metal concentration and pH (Figure A2.2 D). No comparable increase in ν_{sym} was determined in the Al systems, although a distinct increase in ν_{asym} occurring at pH $\leq$ 3.5 was present (Figure A2.2 C). Generally, results indicated that Fe and Al were bound to carboxylic groups in the OM and that the addition of PO_4 did not significantly alter the metal binding mode.

An additional tool that has been used to examine metal binding is the wavenumber separation between symmetric and asymmetric stretches (Figure A2.1) (Deacon and Phillips 1980; Nakamoto, 1986; Baigorri et al., 2007). These shifts are caused by vibrational coupling of carboxylate stretching frequencies. Metal binding modes including unidentate (UD), bidentate (BD) and bidentate-bridging (BD-BG) have been previously hypothesized based on frequency shifts. Although this approach was developed for small molecules (Deacon and Phillips, 1980) it has been applied to more complicated polymers and humic substances

(Baigorri et al., 2007; Guardado et al., 2008). Generally, the UD structure will display C=O and single C-O band while BD and BD-BG structures have equivalent C-O bands (Baigorri et al., 2007). As separate peaks develop, the frequency shift is higher than that from the corresponding OM indicating UD structure. Although separate peaks for C=O and C-O stretching were not resolved within this study on complicated OM systems, information about binding conformation may still be obtained by focusing on peak shifts. For example, a decrease in the frequency shift can be attributed to BD structure while little to no change in the shift can be attributed to a BD-BG structure (Guardado et al., 2008).

Here, analysis of the ν_{asym} - ν_{sym} shift resulted in predominantly bidentate (BD) binding conformation with a transition to unidentate (UD) at pH 6.5-7.0 and bidentate-bridging (BD-BG) at pH 7.5 in all systems. All FTIR based assignment of binding mode should be considered tentative, however, for a number of reasons. First, frequency shifts alone provide a frame work for interpretation, but do not allow for an unambiguous assignment of coordination structure. Secondly, the natural OM used is this study is a complicated mixture that potentially contains many chemically distinct carboxylate moieties. Because FTIR samples all of these moieties and gives a number-weighted average of the vibration frequencies, an assignment is at best an average of many distinct sites that may interact differently with metals. Thirdly, changes in ν_{asym} directly corresponded to bound metal concentrations (Figure A2.2D) which could eclipse changes resulting from binding mode alone. Lastly, drying may significantly affect metal-ligand interactions, and thus complexation structures (Hug, 1997). An unambiguous assignment of structure requires a multi-technique perspective (e.g., FTIR in conjunction with complementary techniques, such

as X-ray spectroscopy or ab initio calculations). Despite these limitations, an analysis of frequency shifts is useful for a comparison of binding similar systems and allows for tentative assignment of dominant binding modes.

The shifting of ν_{asym} following addition of metal clearly indicated that metal-carboxylic bonding existed in PO_4-Fe/Al-OM and Fe/Al-OM systems (Table A2.1). Although ternary complexes in the solid phase potentially existed, differences in either ν_{asym} or ν_{sym} between Fe/Al-OM and PO_4-Fe/Al-OM could not be attributed to PO_4 addition alone. It is difficult to quantify the extent of bonding based on these shifts. Overlapping bands that stem from unbound carboxylates as well as bound metals in multiple coordination states are convoluted to produce these spectra, making interpretation difficult.

Guardado et al. (2008) analyzed ν_{asym} - ν_{sym} shifts of OM with bound Fe, Al and PO_4 and found that BD complexes were present in all Fe treatments while BD-BG complexes were present in Al treatments at pH 4 and 8 and UD complexes were present at pH 6. Jones et al. (1998) found that at pH 7.0 an UD binding conformation between hematite and polyacrylate existed while at higher pH BD-BG occurred. Similar to their work, my data suggests UD binding at pH 6.5-7.0 in Fe/Al-OM, PO_4-Fe-OM, and PO_4-Al-OM systems, with predominantly BD or BG binding at pH < 6 and > 7.0 in the Fe and Al systems. Separating the impacts of bound metal concentration from potential changes in binding mode was not accomplished in this study. Therefore, conclusions regarding metal binding mode were not made. Instead, FTIR spectra indicated that at least part of the added Fe and Al was bound to carboxylic functional groups in the peat.

Phosphate Binding in OM

Infrared absorption of inorganic and organic phosphates are mainly characterized by strong P-O-(H) stretching and bending vibrations in the 1250 to 750 cm^{-1} spectral range (Kizewski et al., 2011). Generally, bands between 1150 and 1000 cm^{-1} have been attributed to PO_4 distortions and used to determine the protonation state of PO_4 (He et al., 2006). Table A2.2 shows the position of the P-O vibrational band near 1030 cm^{-1}. The position of the P-O band was in the same region as a C-O stretching band, making interpretation of results based on peak position difficult. In all cases, however, the intensity of the peat near 1030 cm^{-1} increased following PO_4 addition. For example, Figure A2.3 compares the Fe-OM and PO_4-Fe-OM spectra. Here, the peak at 1033 cm^{-1} is consistent with the ν_{as} in the P-O bond of PO_3^{2-}. This peak around 1033 is present in all the data, and becomes larger following P addition in most cases. In addition, Figure A2.4 shows the PO_4-Fe-OM spectra subtracted from the Fe-OM spectra at pH 5.0. In this example, the peak at 1020 cm^{-1} is consistent with the ν_{as} in the P-O bond of PO_3^{2-}, and the ν_{as} of P-O bound in a bidentate complex formed between orthophosphate and goethite (1023 cm^{-1}) (Tejedor-Tejedor and Anderson, 1990). Since the dominant form of PO_4 is predicted to be $H_2PO_4^-$ at pH 5.0 (See Figure A4.1), it is likely that the peak at 1020 cm^{-1} is a direct result of the formation of Fe-PO_4 complexes.

Overall Summary of FTIR Results

Overall, FTIR spectra indicated that (1) Fe and Al binding to carboxylic functional groups occurred, and (2) that PO_4 binding to Fe and Al occurred. The occurrence of both of these indicates that the formation of ternary PO_4-Fe/Al-OM complexes is possible. However, at maximum only 50% of the total Fe or Al sites were potentially saturated by PO_4 based on

stoichiometry. In addition, Fe and Al bound to carboxylic groups potentially only represented a small fraction of total bound Fe and Al in OM. The formation of Fe(III)-OM polynuclear clusters was found at pH 6.8 (Chapter 2), which were likely a significant component of these systems across pH. In conclusion, although a portion of Fe and Al were bound to carboxylic functional groups in OM, and a portion of PO_4 was bound to Fe and Al, proof for the formation of ternary PO_4-Fe/Al-OM was not obtained in this study.

Table A2.1. Fourier Transformed Infrared Spectra (FTIR) collected from freeze dried envelope samples.

Compound	Asymmetric	Symmetric	Δ (asym-sym)	Binding Mode
OM pH 3.0	1633.02	1373.01	260.01	
OM pH 3.5	1633.30	1372.82	260.48	
OM pH 4.0	1633.39	1372.51	260.88	
OM pH 4.5	1627.22	1374.58	252.64	
OM pH 5.5	1627.26	1373.98	253.28	
OM pH 6.0	1627.23	1376.55	250.68	
OM pH 6.5	1597.01	1376.90	220.11	
OM pH 7.0	1593.64	1377.12	216.52	
OM pH 7.5	1593.45	1377.77	215.68	
OM pH 8.0	1593.64	1377.12	216.52	
OM pH 8.5	1592.71	1378.10	214.61	
Fe-OM pH 3.0	1594.55	1375.47	219.08	BD
Fe-OM pH 3.5	1621.72	1372.63	249.09	BD
Fe-OM pH 4.0	1621.81	1372.94	248.87	BD
Fe-OM pH 4.5	1624.01	1375.56	248.45	BD
Fe-OM pH 5.5	1614.57	1372.64	241.93	BD
Fe-OM pH 6.0	1620.45	1375.92	244.53	BD
Fe-OM pH 6.5	1597.22	1374.45	222.77	UD
Fe-OM pH 7.0	1596.48	1375.88	220.6	UD
Fe-OM pH 7.5	1594.47	1375.47	219.00	BD-BG
Fe-OM pH 8.0	1592.72	1372.86	219.86	BD-BG
Fe-OM pH 8.5	1592.31	1372.94	219.37	BD-BG
PO_4-Fe-OM pH 3.0	1621.82	1373.18	248.64	BD
PO_4-Fe-OM pH 3.5	1624.38	1376.04	248.34	BD
PO_4-Fe-OM pH 4.0	1621.64	1372.83	248.81	BD
PO_4-Fe-OM pH 4.5	1624.17	1376.16	248.01	BD
PO_4-Fe-OM pH 5.5	1614.45	1373.13	241.32	BD
PO_4-Fe-OM pH 6.0	1600.99	1376.21	224.78	BD
PO_4-Fe-OM pH 6.5	1600.28	1377.58	222.7	UD
PO_4-Fe-OM pH 7.0	1600.23	1377.43	222.8	UD
PO_4-Fe-OM pH 7.5	1593.45	1376.96	216.49	BD-BG
PO_4-Fe-OM pH 8.0	1595.84	1384.27	211.57	BD-BG
PO_4-Fe-OM pH 8.5	1592.89	1384.06	208.83	BD
Al-OM pH 3.0	1627.32	1383.96	243.36	BD
Al-OM pH 3.5	1621.90	1384.28	237.62	BD
Al-OM pH 4.0	1633.30	1384.63	248.67	BD
Al-OM pH 4.5	1621.66	1384.11	237.55	BD
Al-OM pH 5.5	1621.88	1384.13	237.75	BD
Al-OM pH 6.0	1621.75	1384.22	237.53	BD
Al-OM pH 6.5	1614.61	1384.33	237.7	UD
Al-OM pH 7.5	1597.13	1384.23	212.9	BD-BG
Al-OM pH 8.0	1593.35	1384.25	209.1	BD
Al-OM pH 8.5	1592.89	1384.06	208.83	BD
PO_4-Al-OM pH 3.0	1633.31	1384.43	248.88	BD
PO_4-Al-OM pH 3.5	1627.00	1401.66	225.34	BD
PO_4-Al-OM pH 4.0	1624.73	1383.99	240.74	BD
PO_4-Al-OM pH 4.5	1624.43	1384.31	240.12	BD
PO_4-Al-OM pH 5.5	1623.80	1384.20	239.6	BD
PO_4-Al-OM pH 6.0	1623.96	1384.25	239.71	BD
PO_4-Al-OM pH 6.5	1621.90	1384.20	237.7	UD
PO_4-Al-OM pH 7.0	1641.63	1384.29	257.34	UD
PO_4-Al-OM pH 7.5	1600.80	1384.12	216.68	BD-BG
PO_4-Al-OM pH 8.0	1595.84	1384.27	211.57	BD
PO_4-Al-OM pH 8.5	1593.47	1384.04	209.43	BD

Table A2.2. Fourier Transformed Infrared Spectra (FTIR) collected from freeze dried envelope samples. Here the ν_{as} of P-O is shown for all samples.

Compound	ν_{as} P-O
OM pH 3.0	1036.60
OM pH 3.5	1034.28
OM pH 4.0	1033.33
OM pH 4.5	1033.61
OM pH 5.5	1033.44
OM pH 6.0	1032.92
OM pH 6.5	1033.31
OM pH 7.0	1034.08
OM pH 7.5	1033.87
OM pH 8.0	1034.08
OM pH 8.5	1033.31
Fe-OM pH 3.0	1032.41
Fe-OM pH 3.5	1080.30
Fe-OM pH 4.0	1034.11
Fe-OM pH 4.5	1036.87
Fe-OM pH 5.5	1034.92
Fe-OM pH 6.0	1034.16
Fe-OM pH 6.5	1089.38
Fe-OM pH 7.0	1078.43
Fe-OM pH 7.5	1032.41
Fe-OM pH 8.0	1034.05
Fe-OM pH 8.5	1078.86
PO_4-Fe-OM pH 3.0	1036.09
PO_4-Fe-OM pH 3.5	1035.80
PO_4-Fe-OM pH 4.0	1033.87
PO_4-Fe-OM pH 4.5	1034.74
PO_4-Fe-OM pH 5.5	1035.12
PO_4-Fe-OM pH 6.0	1034.39
PO_4-Fe-OM pH 6.5	1035.28
PO_4-Fe-OM pH 7.0	1035.69
PO_4-Fe-OM pH 7.5	1034.45
PO_4-Fe-OM pH 8.0	1032.36
PO_4-Fe-OM pH 8.5	1034.99
Al-OM pH 3.0	1033.84
Al-OM pH 3.5	1034.06
Al-OM pH 4.0	1034.88
Al-OM pH 4.5	1035.72
Al-OM pH 5.5	1034.85
Al-OM pH 6.0	1034.28
Al-OM pH 6.5	1034.13
Al-OM pH 7.0	1038.36
Al-OM pH 7.5	1034.77
Al-OM pH 8.0	1034.60
Al-OM pH 8.5	1033.75
PO_4-Al-OM pH 3.0	1095.06
PO_4-Al-OM pH 3.5	1076.46
PO_4-Al-OM pH 4.0	1082.34
PO_4-Al-OM pH 4.5	1079.95
PO_4-Al-OM pH 5.5	1041.38
PO_4-Al-OM pH 6.0	1083.29
PO_4-Al-OM pH 6.5	1076.88
PO_4-Al-OM pH 7.0	1084.88
PO_4-Al-OM pH 7.5	1080.61

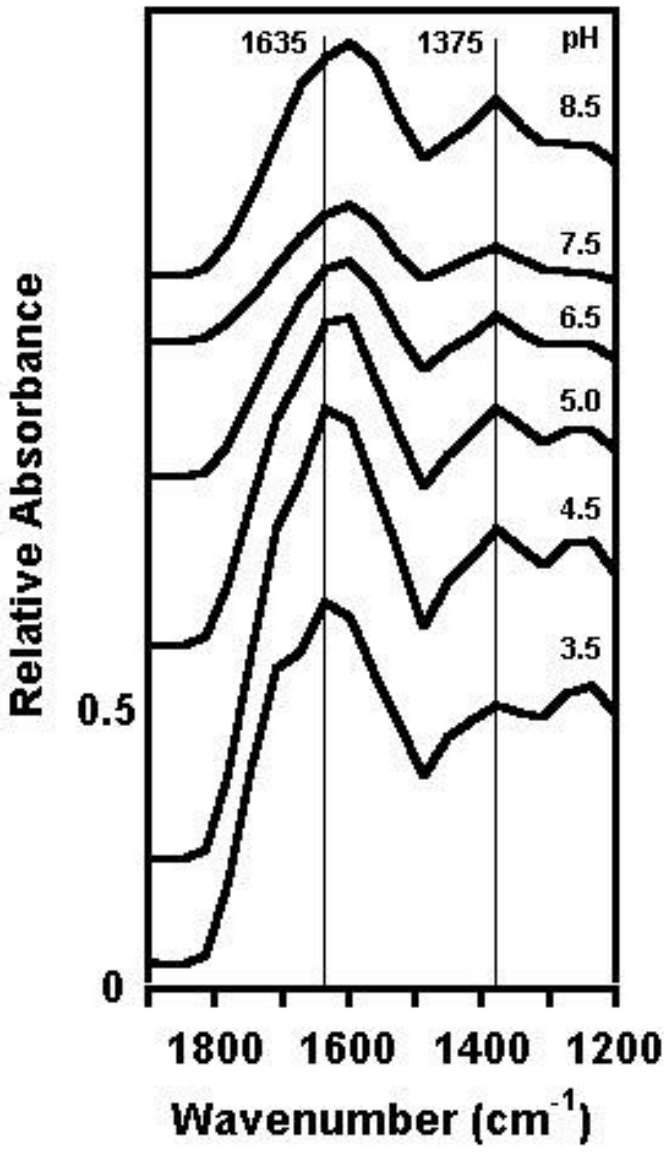

Figure A2.1. Selected FTIR spectra of hydrated peat across pH. Note the shift in ν_{asym} and the resulting decrease in frequency shift with increasing pH.

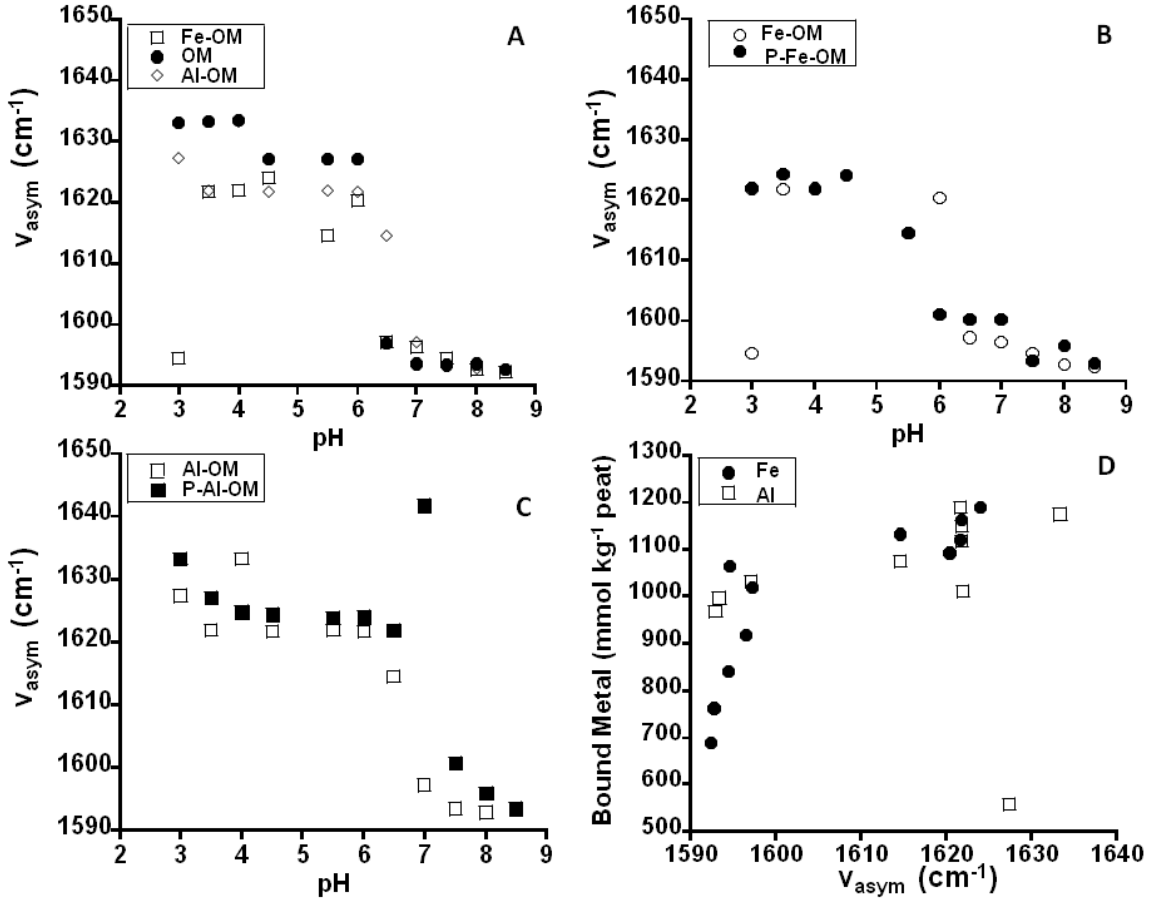

Figure A2.2. The asymmetric peak position decreased with increasing pH in the Fe-OM (○), PO_4-Fe-OM, Al-OM, and PO_4-Al-OM systems. Few differences appeared between the Fe/Al-OM and PO_4-Fe/Al-OM treatments (B and C) indicating that either PO_4 did not bind in PO_4-M-carboxyl ternary complexes, or that differences were masked by the large number of carboxylic groups. Shifts in v_{asym} also corresponded to increasing bound metal concentration in both Fe and Al-OM (D).

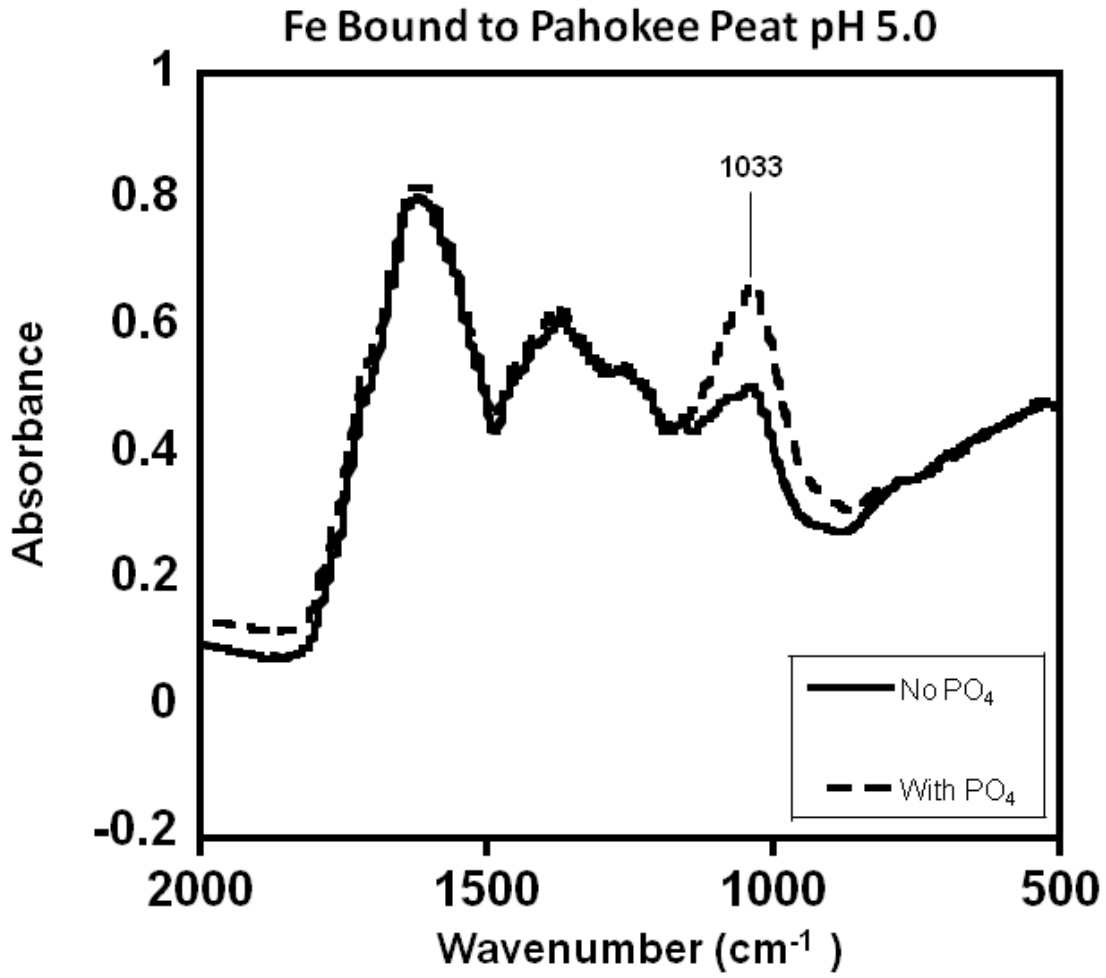

Figure A2.3. FTIR spectra of Fe bound to Pahokee peat with (dashed line) and without (solid line) PO_4 at pH 5.0. The peak at 1033 cm^{-1} is consistent with the ν_{as} in the P-O bond of PO_3^{2-}. This peak around 1033 is present in all the data, and becomes larger following P addition in most cases.

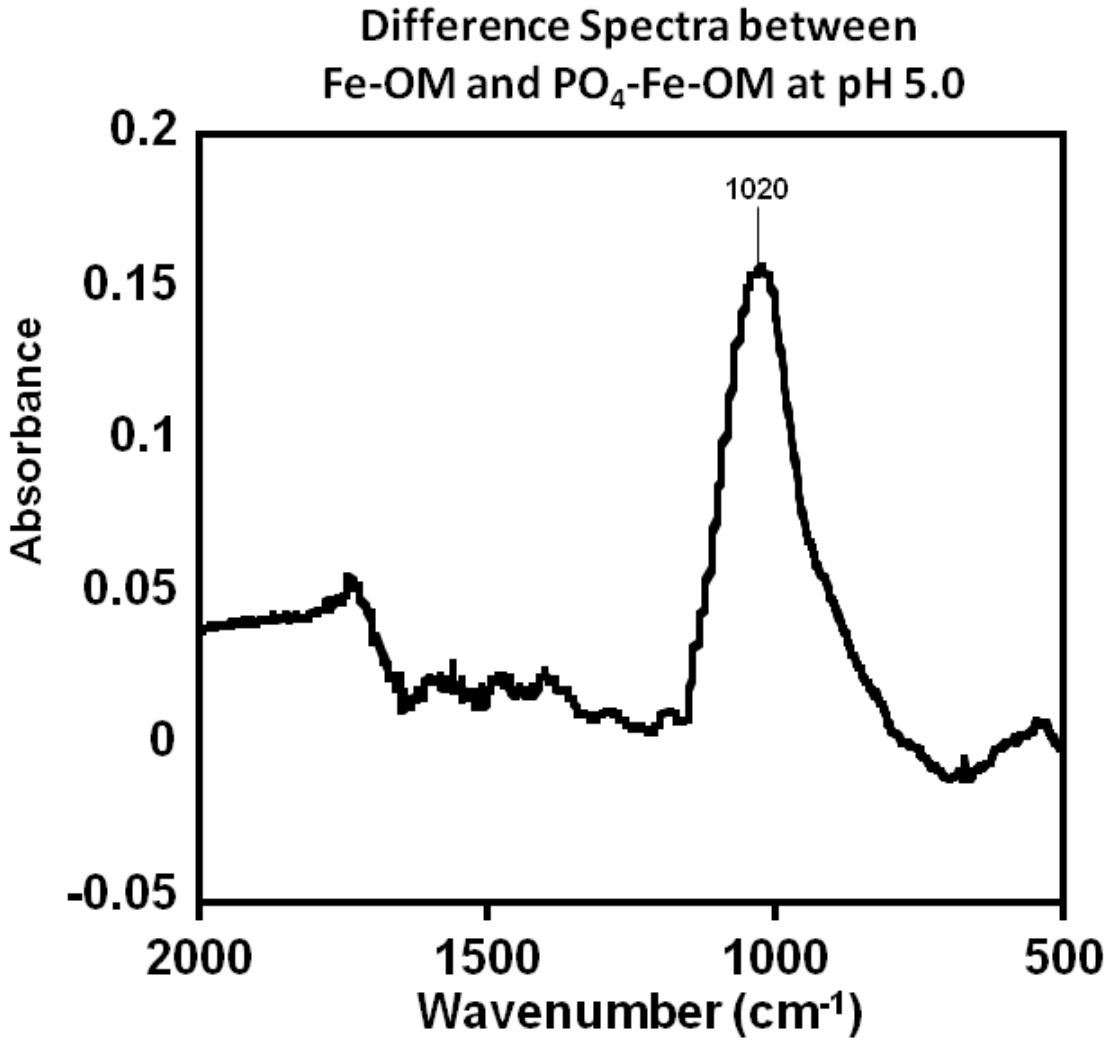

Figure A2.4. Subtracted FTIR spectra of PO_4 bound to Fe in Pahokee peat from Fe bound in Pahokee peat without PO_4 at pH 5.0. The peak at 1020 cm^{-1} is consistent with the ν_{as} in the P-O bond of PO_3^{2-}, and the ν_{as} of P-O bound in a bidentate complex formed between orthophosphate and goethite (1023 cm^{-1}) (Tejedor-Tejedor and Anderson, 1990).

Bibliography

Al-Mustafa J., and B. Tashtoush. 2003. Iron(II) and iron(III) perchlorate complexes of ciprofloxacin and norfloxacin. J. Coord. Chem. 56, 113-124.

Baigorri R., J.M. Garcia-Mina, and B. Gonzalez-Gaitano. 2007. Supramolecular association induced by Fe(III) in low molecular weight sodium polyacrylate. Colloids Surf., A. 292:212-216.

Borer P., Hug S.J., Sulzberger B., Kraemer S.M., Kretzschmar R., 2009. ATR-FTIR spectroscopic study of the adsorption of desferrioxamine B and aerobactin to the surface of lepidocrocite (gamma-FeOOH). Geochim. Cosmochim. Acta. 73, 4661-4672.

Clausen M., L.O.Ohman, K. Axe, and P. Persson, 2003. Spectroscopic studies of aluminum and gallium complexes with oxalate and malonate in aqueous solution. J. Mol. Struct. 648, 225-235.

Deacon, G.B. and R.J. Phillips. 1980. Relationships between the carbon-oxygen stretching frequencies of carboxylato complexes and the type of carboxylate coordination. Coord. Chem. Rev. 33:227-250.

Guardado I., O. Urrutia, and J.M. Garcia-Mina. 2008. Some structural and electronic features of the interactions of phosphate with Metal-humic Complexes. J. Agric. Food. Chem. 56:1035-1042.

Hay M.B., and S.C.B. Myneni. 2007. Structrual environments of carboxyl groups in natural organic molecules from terrestrial systems. Part 1. Infrared spectroscopy. Geochim. Cosmochim. Acta. 71:3518-3532.

He, Z.Q., C.W. Honeycutt, T.Q. Zhang, and P.M. Bertsch. 2006. Preparation and FT-IR characterization of metal phytate compounds. J. Environ. Qual. 35:1319-1328.

Hug S.J., 1997. In situ Fourier transform infrared measurements of sulfate adsorption on hematite in aqueous solutions. J. Colloid Interface Sci. 188, 415-422.

Jones F., J.B. Farrow, and W. van Bronswikjk. 1998. An infrared study of a polyacrylate flocculant adsorbed on hematite. Langmuir 14:6512-6517.

Kato M., Yamada Y., Inagaki T., Mori W., Sakai K., Tsubomura T., Sato M., Yano S., 1995. Structures and magnetic-properties of iron(III) dinuclear complexes with alkoxo and caboxlato bridges. Inorg. Chem. 34, 2645-2651.

Kizewski, F., Y. Liu, A. Morris, and D. Hesterberg. 2011. Spectroscopic approaches for phosphorus speciation in soils and other enveironmental systems. J. Environ. Qual. In Press.

Lemercier G., E. Mulliez, C. Brouca-Cabarrecq, F. Dahan, and J.P. Tuchagues, 2004. Iron(II) carboxylate complexes based on a tetraimidazole ligand as models of the photosynthetic non-heme ferrous sites: Synthesis, crystal structure, and Mossbauer and magnetic studies. Inorg. Chem. 43, 2105-2113.

Lindegren M., J.S. Loring, and P. Persson. 2009. Molecular Structures of Citrate and Tricarballylate Adsorbed on alpha-FeOOH Particles in Aqueous Suspensions. Langmuir 25, 10639-10647.

Nakamoto, K. 1986. Infrared and Raman spectra of inorganic and coordination compounds. John Wiley & Sons, New York.

Nilsson, N., P. Persson, L. Lovgren, and S. Sjoberg. 1996. Competative surface complexation of o-phthalate and phosphate on goethite (alpha-FeOOH) particles. Geochim. Cosmochim. Acta. 60:4385-4395.

Parikh S.J., Chorover J., 2006. ATR-FTIR spectroscopy reveals bond formation during bacterial adhesion to iron oxide. Langmuir 22, 8492-8500.

Rosenqvist J., Axe K., Sjoberg S., Persson P., 2003. Adsorption of dicarboxylates on nano-sized gibbsite particles: effects of ligand structure on bonding mechanisms. Colloids Surf., A. 220, 91-104.

Tejedor-Tejedor, M.I., and M.A. Anderson. 1990. Protonation of phosphate on the surface of goethite as studied by CIR-FTIR and electrophoretic mobility. Langmuir. 6:602-611.

APPENDIX 3: SUPPLEMENTAL FIGURES TO CHAPTER 3

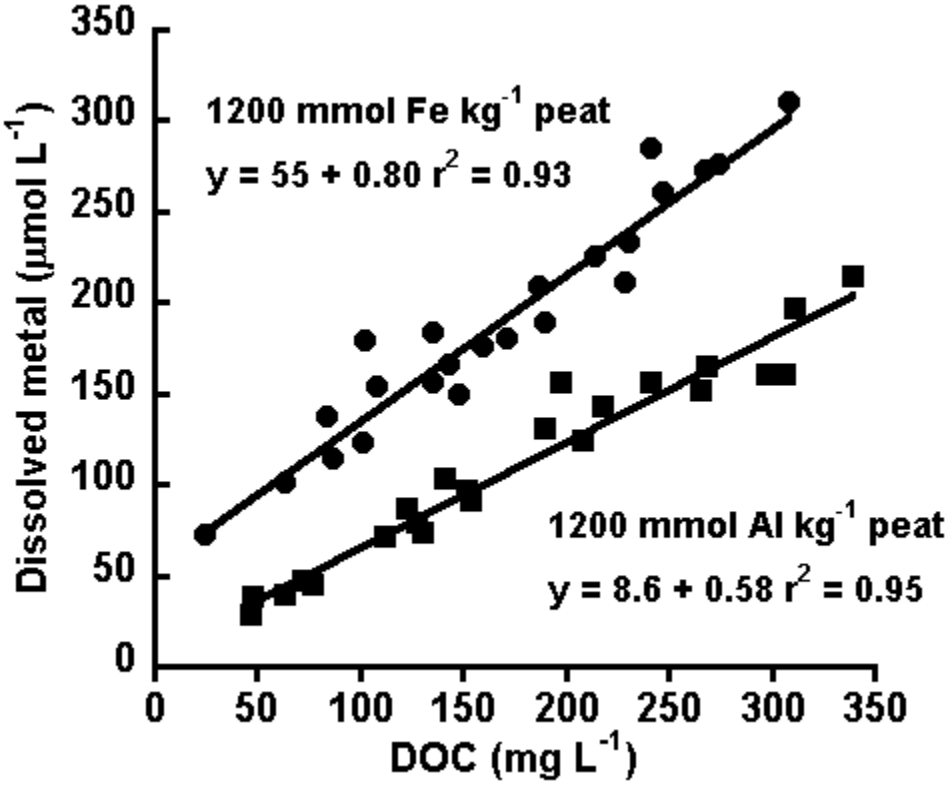

Figure A3.1. Dissolved Fe and Al increased with increasing dissolved organic carbon (DOC) in the DOC addition experiment at pH 6.0.

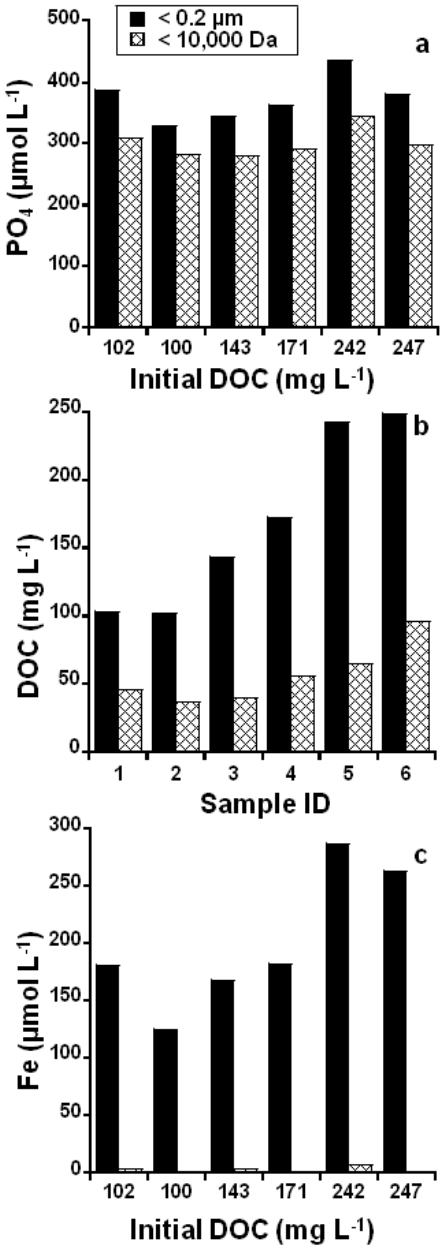

Figure A3.2. MWC filtration results from DOC addition experiment at pH 6.0. Filtration indicated that < 25% of dissolved P was potentially present as colloidal PO_4-Fe-OM complexes (> 10,000 Da). Furthermore, dissolved Fe(III) increased with increasing DOC suggesting complexation between DOC and Fe increased Fe solubility.

APPENDIX 4: SUPPLEMENTAL FIGURES TO CHAPTER 4

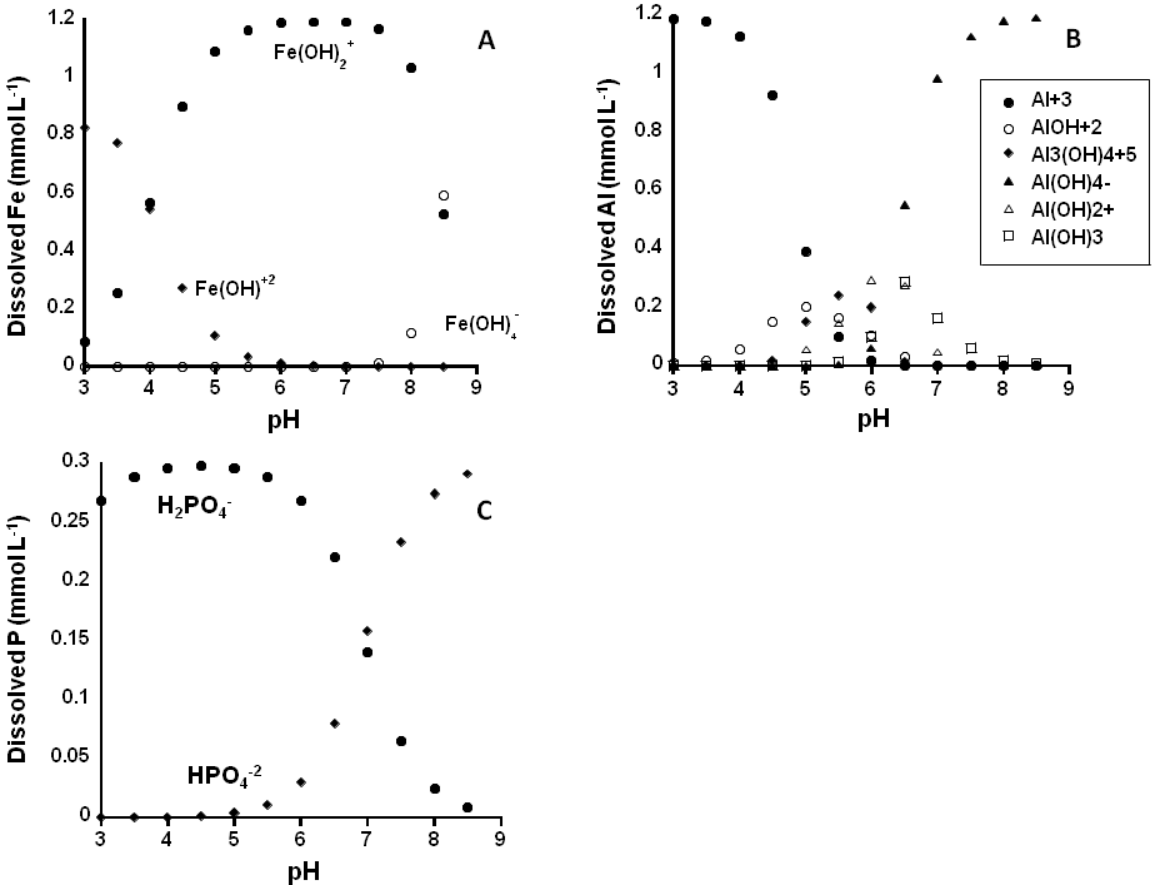

Figure A4.1. Predicted Fe (A), Al (B) and PO_4 (C) species across pH. Speciation calculations were performed in Visual MINTEQ with input parameters of 1200 µmol $FeCl_3$ L^{-1}, 1200 µmol $AlCl_3$ L^{-1}, and 600 µmol KH_2PO_4 L^{-1} respectively in 0.05 M KCl backgrounds.

APPENDIX 5: SUPPLEMENTAL FIGURES TO CHAPTER 5

Table A5.1. Pseudo-first-order fits for dissolved Fe(II) production. Rate coefficients ($k_{2(dis)}$) were calculated over the course of the first 48 h of microbial Fe reduction for all experiments.

Treatment ID	Added Fe (mmol kg^{-1} peat)	Added Peat (g L^{-1})	With or without CN32	Equation	Max Fe	$K_{2(dis)}$
300	300	4	With	$Y=518(1-\exp(-0.11x))$ $r^2=0.63$	518	0.11
300(II)	300	4	With	$Y=470(1-\exp(0.17x))$ $r^2=0.09$	470	0.17
600	600	2	With	$Y=373(1-\exp(0.12x))$ $r^2=0.84$	373	0.12
1200	1200	1	With	$Y=568(1-\exp(0.06x))$ $r^2=0.94$	568	0.06
1200(II)	1200	1	With	$Y=657(1-\exp(0.02x))$ $r^2=0.97$	657	0.02
1200(III)	1200	1	With	$Y=653(1-\exp(0.02x))$ $r^2=0.97$	653	0.02
2400	2400	0.5	With	$Y=983(1-\exp(0.04x))$ $r^2=0.92$	983	0.04
3600	3600	0.33	With	$Y=1005(1-\exp(0.05x))$ $r^2=0.94$	1005	0.05
3600(II)	3600	0.33	With	undetermined	-	-
Control 1	2400	0.5	Without	undetermined	-	-
Control 2	∞	0	With	$Y=1559(1-\exp(0.02x))$ $r^2=0.99$	1559	0.02
Control 3	0	4	With	$Y=245(1-\exp(0.37x))$ (ns)	245	0.37
Control 4	300	4	With	$Y=6400(1-\exp(0.002x))$ $r^2 = 0.79$	6400	0.002
Ferrihydrite	∞	0	With	$Y=73(1-\exp(0.08x))$ $r^2=0.74$	73	0.08

Table A5.2. Pseudo-first-order fits for total Fe(II) reduction. Rates ($k_{2(tot)}$) were calculated over the course of the first 48 h of microbial Fe reduction for all experiments.

Treatment ID	Added Fe (mmol Fe kg^{-1} peat)	Added Peat (g L^{-1})	With or without CN32	Equation	Max Fe	$K_{2(tot)}$
300	300	4	With	$Y=1308(1-\exp(-0.12x))$ $r^2=0.91$	1308	0.12
300(II)	300	4	With	$Y=1156(1-\exp(0.11x))$ $r^2=0.79$	1156	0.11
600	600	2	With	$Y=967(1-\exp(0.13x))$ $r^2=0.84$	966.6	0.13
1200	1200	1	With	$Y=988(1-\exp(0.12x))$ $r^2=0.95$	988	0.12
1200(II)	1200	1	With	$Y=1011(1-\exp(0.07x))$ $r^2=0.90$	1011	0.07
1200(III)	1200	1	With	$Y=1010(1-\exp(0.06x))$ $r^2=0.98$	1010	0.06
2400	2400	0.5	With	$Y=1182(1-\exp(0.06x))$ $r^2=0.98$	1182	0.06
3600	3600	0.33	With	$Y=1167(1-\exp(0.07x))$ $r^2=0.95$	1167	0.07
3600(II)	3600	0.33	With	Undetermined	-	-
Control 1	2400	0.5	Without	Undetermined	-	-
Control 2	∞	0	With	$Y=1345(1-\exp(0.03x))$ $r^2=0.99$	1345	0.03
Control 3	0	4	With	$Y = 282(1-\exp(0.45x))$ (ns)		
Control 4	300	4	With	$Y = 5600(1-\exp(0.01x))$ $r^2 = 0.93$	5600	0.01
Ferrihydrite	∞	0	With	$Y=123(1-\exp(0.09x))$	123	0.09

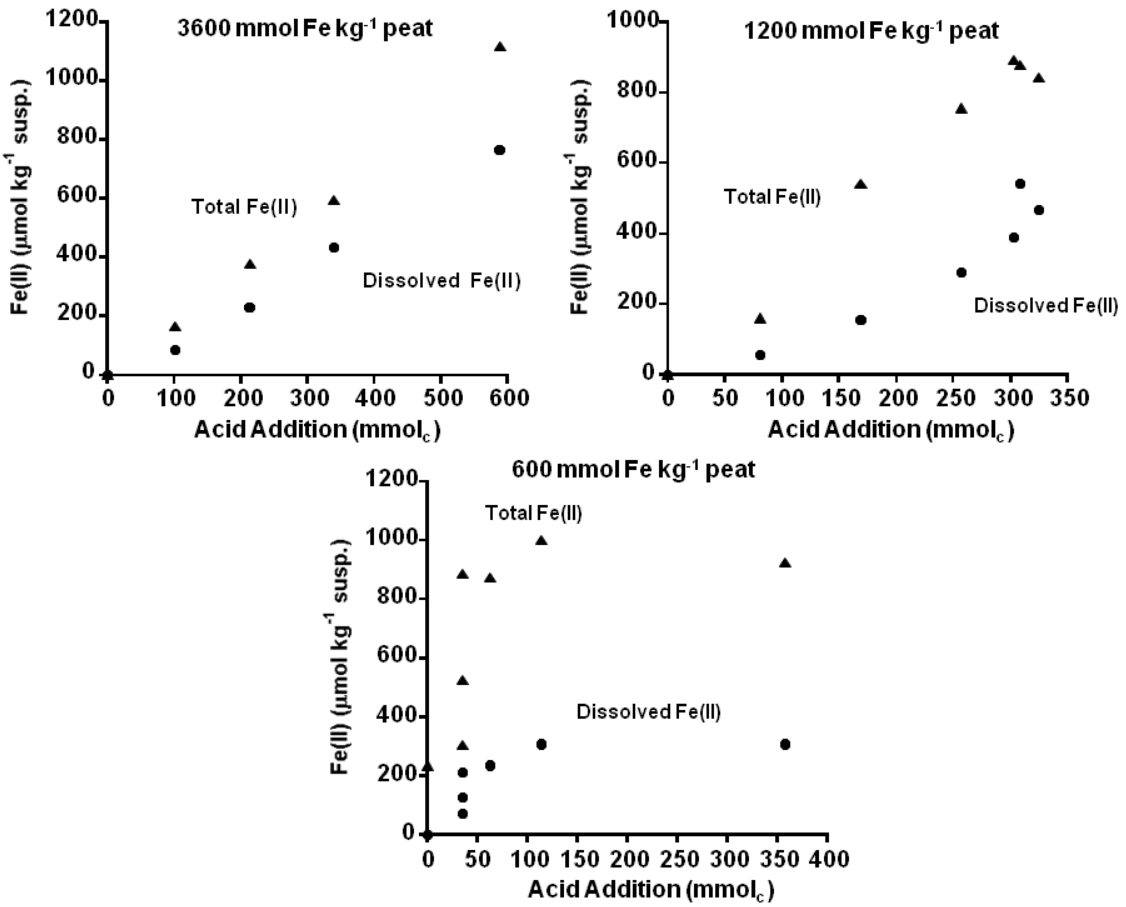

Figure A5.1. Total Fe(II) and dissolved Fe(II) across Acid addition during microbial reduction of 3600, 1200, and 600 mmol Fe kg^{-1} peat treatments.

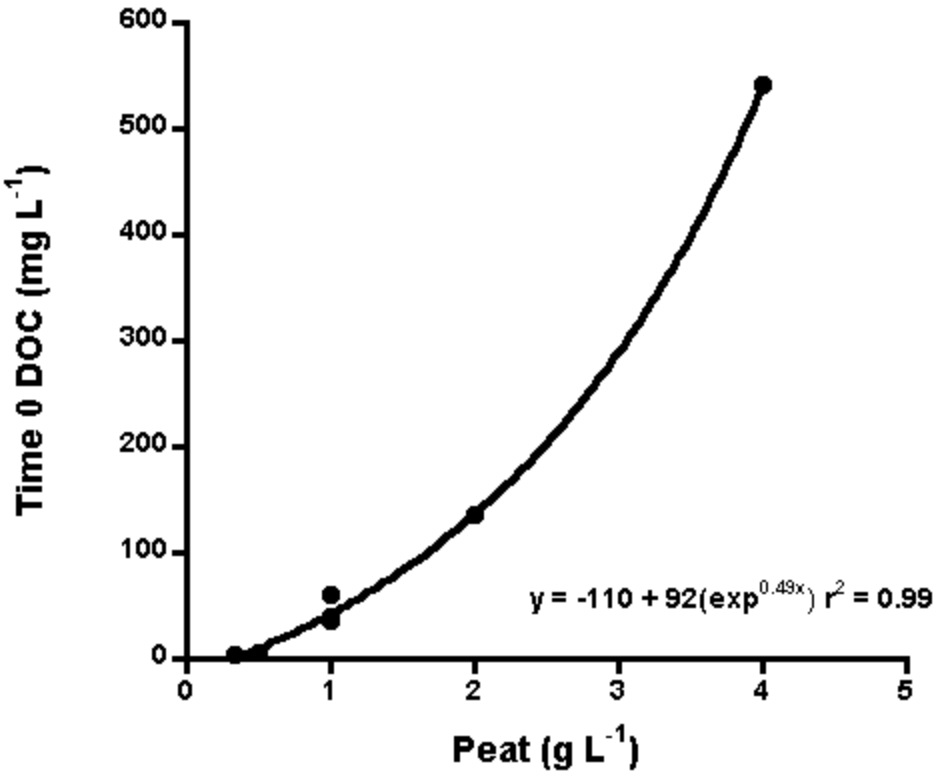

Figure A5.2. Initial DOC was higher as peat addition increased from 3600 to 300 mmol Fe kg^{-1} peat.

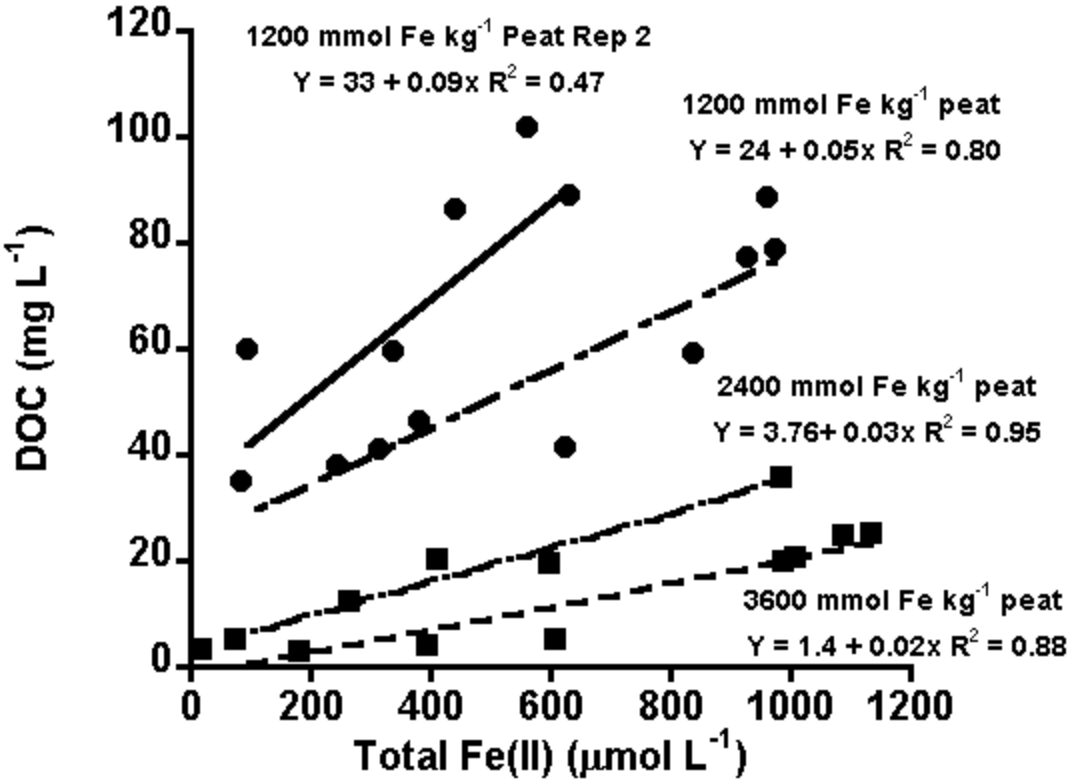

Figure A5.3. DOC production compared to total Fe(II) for 1200, 2400, and 2600 mmol Fe kg^{-1} peat treatments.

APPENDIX 6: SUPPLEMENTAL FIGURES TO CHAPTER 6

Table A6.1. List of microbial reduction experiments performed with different Fe/Al ratios.

Fe/Al Ratio (mmol kg^{-1} peat)	Added Fe (mmol kg^{-1} peat)	Added Al (mmol kg^{-1} peat)	Peat (g L^{-1})	PO_4 (mmol kg^{-1}peat)
Fe only (300 P)	1200	0	1	300
Fe only (600 P)	1200	0	1	600
5	1000	200	1	600
2	800	400	1	600
0.33	300	900	1	600
Al only	0	1200	1	600

Table A6.2. Total and dissolved Fe(II) with time compared with total dissolved Fe determined by atomic absorption spectroscopy (AA) in the 100,000 and 5,000 molecular weight cut off filtration fractions. An AA detection limit of 0.92 µmol Fe L^{-1} was estimated from the mean of the blank solutions.

Time (h)	Initial Dissolved Fe(II) (µmol L^{-1})	Initial Total Fe(II) (µmol kg^{-1} peat)	Initial total dissolved Fe (µmol L^{-1})	100,000 D dissolved Fe (µmol L^{-1})	5,000 D dissolved Fe (µmol L^{-1})
0	3.6	33	5.5	0	0
2.15	3.2	45	4.7	0	0
5.28	12	110	8.6	0	0
7.65	24	240	7.5	12	0
22.1	220	700	180	130	58
26.4	240	630	190	170	81
47.6	300	820	211	190	76

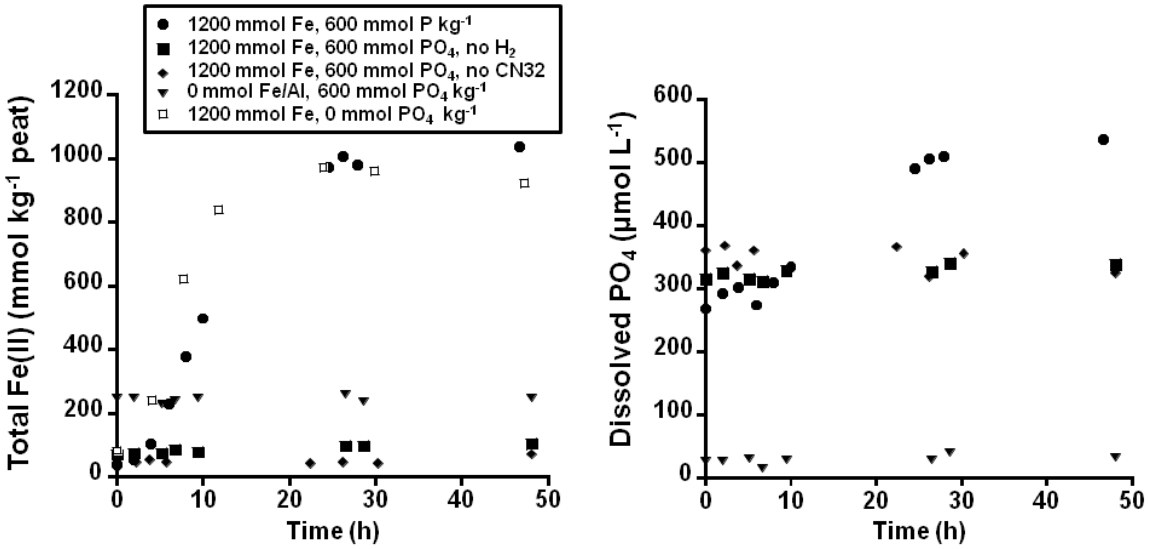

Figure A6.1. Total Fe(II) and dissolved PO_4 measured in several control experiments including 0 P addition, 0 Fe and Al input, abiotic 0 CN32, and 0 H_2.

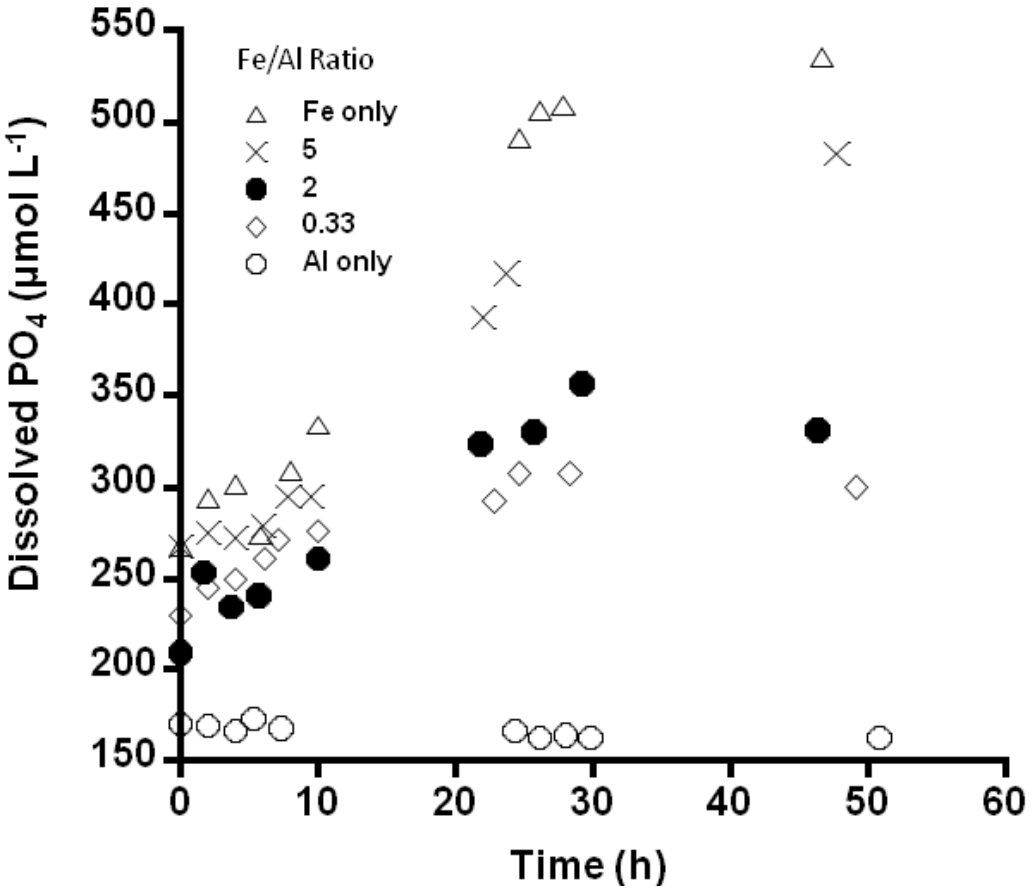

Figure A6.2. Dissolved PO_4 increased during 50 h of microbial reduction in the Fe only, and Fe/Al ratio treatments of 5, 2, and 0.33. Dissolved PO_4 did not increase during microbial reduction of the Al only treatment.

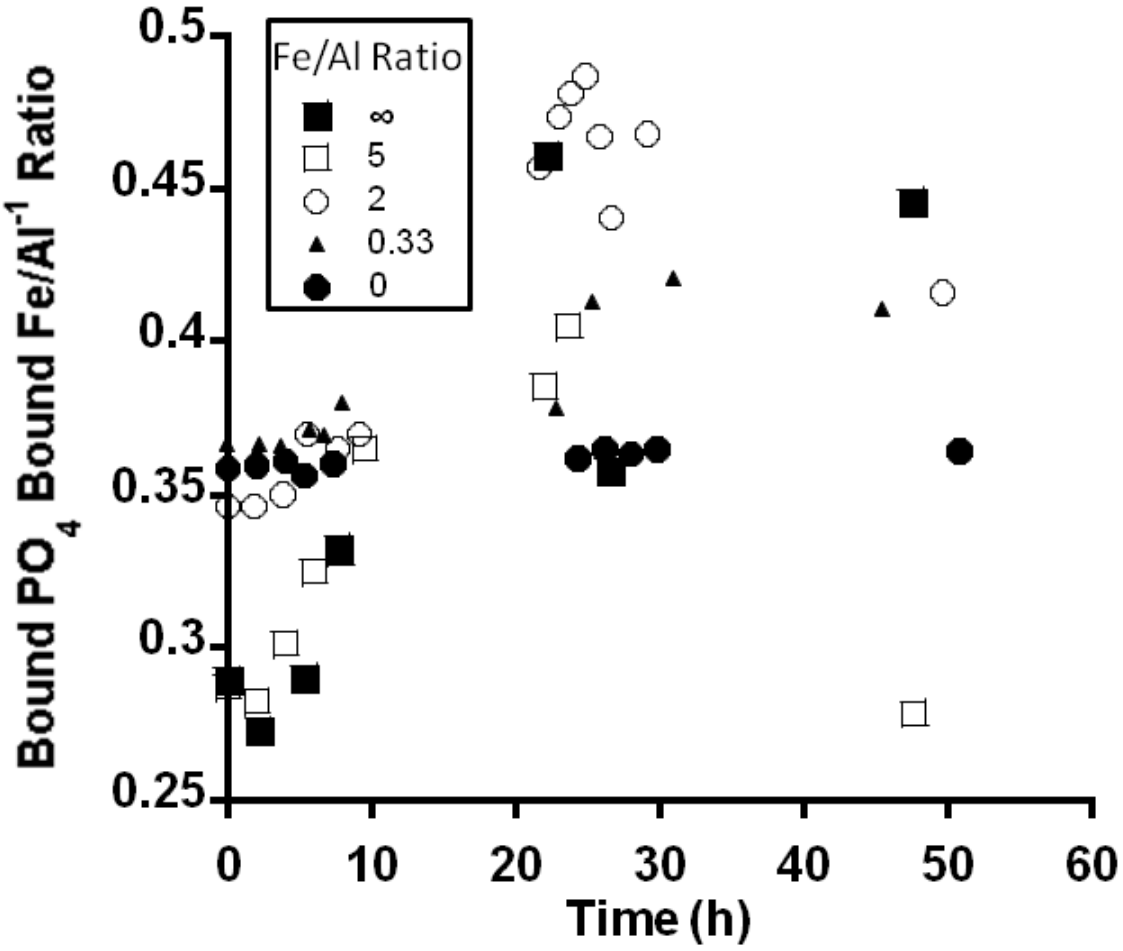

Figure A6.3. Bound PO_4 to bound Fe/Al ratio with time during microbial reduction incubations.

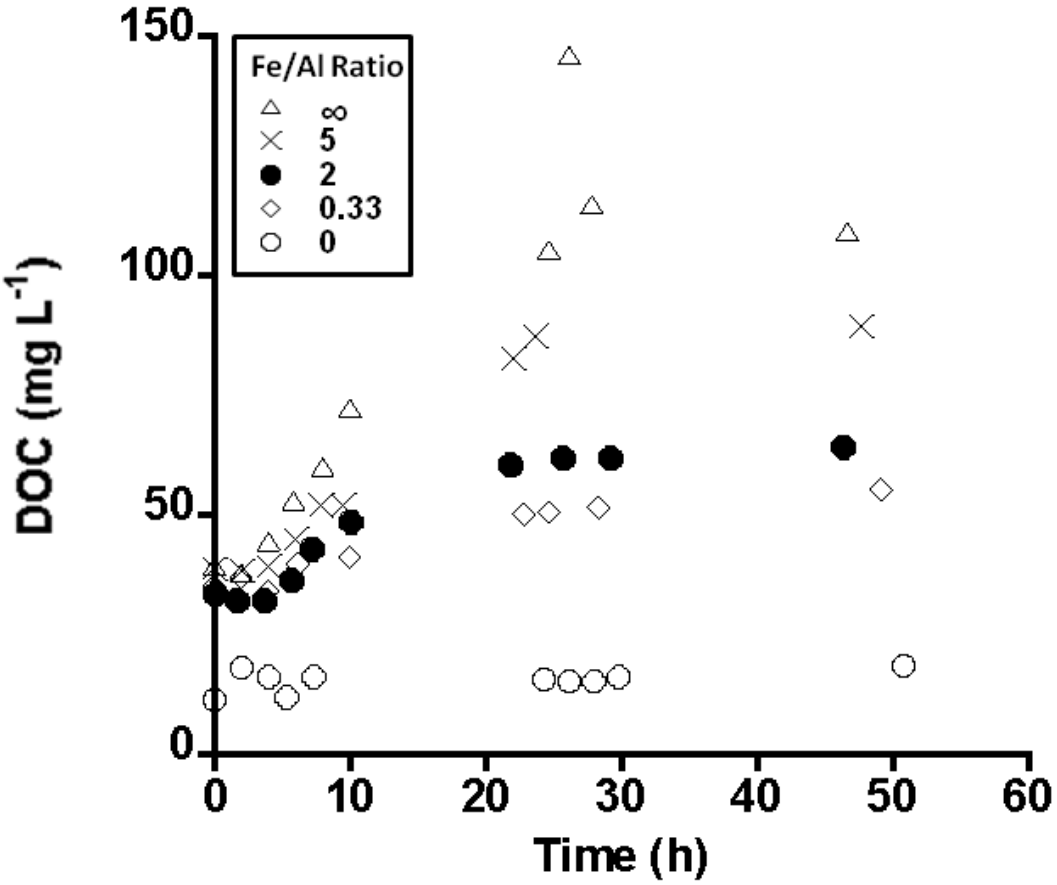

Figure A6.4. Dissolved organic carbon (DOC) with time during microbial reduction incubations for Fe/Al ratios of 0 to ∞.

APPENDIX 7: REPRODUCIBILITY OF MICROBIAL REDUCTION TREATMENTS

Replications indicated that general trends in Fe(III) reduction and PO_4 dissolution were similar, despite quantitative variation (Figure A6.5). Total Fe(II) production was similar between the 300 and 800 mmol Fe kg^1 peat treatments (Figures A6.5 A and C) but varied considerable between the 1200 mmol Fe kg^{-1} peat treatments (Figure A6.5 E). Dissolved PO_4 varied between treatments with a difference of as much as 100 µmol P L^{-1} between replicates (Figure A6.5 B, D, and F). Several variables may have accounted for differences between replicates, such as variability in the input hydrogen concentration (e.g. tanks had 0.5% $\pm$ 1 – 2 % H_2), variation in peat hydration, and variation in CN32 inputs. Specifically, the potential impact of H_2 input concentration is illustrated in Figure 6.10 which shows the impact of varying hydrogen concentration on Fe(III) production rates. Here the input concentration of $H_{2(g)}$ used was varied between 0.5 and 0.8 %, well within the variation between different $H_{2(g)}$ tanks supplied by National Welders ($\pm$ 2%). For all experiments only two different H_2 tanks were utilized. The first tank was used for all Fe/Al ratio treatments in the first replicate (except for the Al only, 0 H_2, and no microbial input controls), while the remaining experiments were conducted with the second H_2 tank. Thus, a comparison of PO_4 dissolution rates between experiments was useful despite variation between replicates.

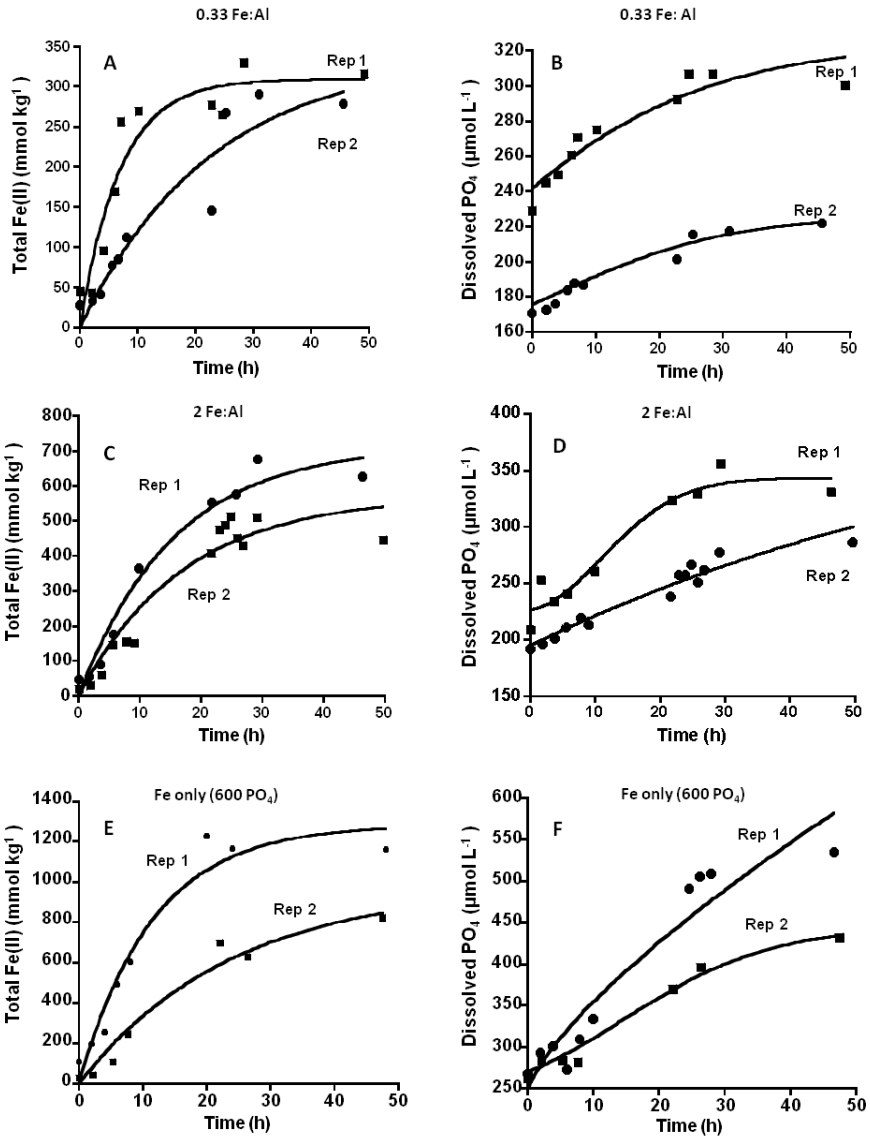

Figure A7.1 Replicate comparisons of total Fe(II) and PO_4 during microbial reduction for 0.33 (A and B), 2 (C and D) and Fe only (E and F) Fe/Al ratio treatments. Phosphate was added at 600 mmol P kg^{-1} peat and pH was held constant at 6.0.

Table A7.2. Reduction rates of Fe(III) resulting from the use of two different H_2 concentrations.

% $H_{2(g)}$ in $N_{2(g)}$	Fe(III) Reduction Rate	Fe(II) Dissolution Rate
0.5	20.6	9.3
0.8	125.0	51.2